



Technische Universität München

# TECHNISCHE UNIVERSITÄT MÜNCHEN

TUM School of Life Sciences

## Hydro-, Alco- and Aerogels from Potato and Whey Proteins

Correlation between Protein Interactions and Rheological Properties

David Julian Andlinger

Vollständiger Abdruck der von der TUM School of Life Sciences der Technischen Universität München zur Erlangung des akademischen Grades eines

Doktors der Ingenieurwissenschaften (Dr.-Ing.)

genehmigten Dissertation.

Vorsitz: Prof. Dr. rer. nat. Michael Rychlik

Prüfer\*innen der  
Dissertation:

1. Prof. Dr.-Ing. Ulrich Kulozik
2. Prof. Dr.-Ing. Irina Smirnova
3. apl. Prof. Dr.-Ing. Petra Först

Die Dissertation wurde am 20.12.2021 bei der Technischen Universität München eingereicht und durch die TUM School of Life Sciences am 01.06.2022 angenommen.



*“Nobody ever figures out what life is all about, and it doesn't matter. Explore the world!”*

*Nearly everything is really interesting if you go into it deeply enough . . . even potatoes. ”*

*Richard P. Feynman (. . . more or less)*





## Acknowledgments

First of all, I want to thank Prof. Dr.-Ing. Ulrich Kulozik for giving me the opportunity to do my doctoral thesis at the Chair of Food and Bioprocess Engineering. Thank you for giving me a second chance after I sacrificed my first opportunity. I never regretted my decision to do my Doctoral study at your chair. The academic freedom in combination with an abundance of resources is truly something unique and despite some lows, I enjoyed my time at your chair to the fullest. Also, I want to thank my mentor and friend Alan Wolfschoon-Pombo, whose passion for dairy science led me to the path of becoming a Dr.-Ing.

However, a good chair is not just built by the Professor, it is formed by the people that work there. I want to thank all employees who made my time at the chair so enjoyable. Especially Sabine Becker and Friederike Schöpflin for their administrative work, without you I would probably still wait for my travel reimbursements... Sabine Grabbe for her help with all the IT problems, especially during Lockdown you were truly the lifeline of everything. Annette Brümmer-Rolf and Claudia Hengst are especially thanked for their grit and support in developing brand new analytical methods. Without you two this thesis would not have been possible in the here presented depth. The "Werkstatt" is thanked for providing a place where you find solutions, not problems.

All fellow doctoral candidates are thanked for their camaraderie. Some of you I want to thank especially. Simon Schiffer and Roland Schopf for all the heart they put into the organization of social events. Martin Hartinger for his mentoring of the "Prüfstelle". Marius Reiter and Maria Weinberger for making the office a place I enjoyed working AND living. Caren Tanger for motivating me to bring my best in work and life, you defined my life during this thesis more than anyone else.

Furthermore, I want to thank my colleagues over at the Technical University of Hamburg without whom this project would have never been finished: Thank you Baldur Schröter, Isabella Jung and Prof. Irina Smirnova

Further, I want to thank all students that worked under my guidance. The people who did internships: Jiashu Li, Zhe Que, Miray Kurt, Lorenz Thurin, Paola Quintana Ramos, and Jolie Miller, as well as Bachelor and Master thesis by Nora Biesenthal and Melania Pilz. Special thanks to Lena Rampp, Lisa Schlemmer, Pauline Röscheisen, and Ulrich Schrempl whose Bachelor's and Master's thesis laid the groundwork for the here presented papers.

Also, thanks to all the friends who stayed with me since high school (or even pre-school !), you will always have a special place in my heart. And my friends from university with whom I never thought we could keep in contact so long after graduation. All of you were a counterweight to experiments, data curation, and paper writing. Thank you very much! Last but not least I want to thank my family. Thanks to my Grandpa, who showed me how to be interested in the world, without a college degree or wild travel plans. Thanks to my parents and my brother, who supported me through all the ups and downs of this thesis.



# Contents

<b>ACKNOWLEDGMENTS .....</b>	<b>V</b>
<b>CONTENTS.....</b>	<b>VII</b>
<b>ABBREVIATIONS AND SYMBOLS .....</b>	<b>XI</b>
<b>1 GENERAL INTRODUCTION.....</b>	<b>1</b>
<b>1.1 Molecular structure and properties of food proteins .....</b>	<b>2</b>
1.1.1 General features of proteins .....	2
1.1.2 Whey proteins .....	4
1.1.3 Potato proteins.....	6
<b>1.2 Unfolding and Aggregation of proteins .....</b>	<b>7</b>
1.2.1 Heat-induced denaturation and aggregation .....	7
1.2.2 Solvent induced denaturation and aggregation .....	10
1.2.3 Kinetic description of protein aggregation .....	11
1.2.4 Changes in aggregate morphology in dependence of the milieu .....	13
<b>1.3 Hydrogel formation from protein solutions.....</b>	<b>15</b>
1.3.1 General gelation mechanism.....	16
1.3.2 Change in gelation behavior in dependence of pH .....	18
1.3.3 Change in aggregation and gelation behavior in dependence of salt addition .....	20
1.3.4 Rheological characterization of hydrogels.....	24
<b>1.4 Alco- and Aerogels .....</b>	<b>27</b>
1.4.1 Alco- gels: Structural changes upon solvent exchange .....	27
1.4.2 Aerogels: Porous gel structures through supercritical drying .....	29
<b>2 OBJECTIVE AND OUTLINE.....</b>	<b>33</b>
<b>3 RESULTS .....</b>	<b>35</b>
<b>3.1 Quantification of protein-protein interactions in highly denatured whey and potato protein gels .....</b>	<b>35</b>
3.1.1 Background information and applicability of the method .....	38
3.1.2 Explanation on changes made .....	40
3.1.3 Description of modified protein interaction assay .....	42
3.1.3.1 Materials.....	42
3.1.3.2 Preparation of buffer systems .....	42
3.1.3.3 Dissolution of gel in buffer system .....	42
3.1.3.4 Mixing.....	42
3.1.3.5 Determination of soluble nitrogen content .....	43
3.1.3.6 Quantification of protein interactions.....	43
3.1.4 Method validation.....	44
3.1.4.1 Reproducibility of method .....	44
3.1.4.2 Limitation of the method.....	47

3.1.5	Conclusion .....	48
<b>3.2</b>	<b>Influence of pH, temperature and protease inhibitors on kinetics and mechanism of thermally induced aggregation of potato proteins .....</b>	<b>49</b>
3.2.1	Introduction .....	51
3.2.2	Materials and Methods.....	53
3.2.2.1	Materials and Sample preparation .....	53
3.2.2.2	Modulated differential scanning calorimetry (mDSC).....	54
3.2.2.3	Heating experiments .....	54
3.2.2.4	Size-exclusion chromatography coupled with fluorescence intensity detection .....	55
3.2.2.5	Determination of free thiol groups in heated PPI solutions .....	55
3.2.2.6	Blocking of protein interactions .....	56
3.2.2.7	Gel electrophoretic analysis .....	57
3.2.2.8	Determination of exposed hydrophobicity .....	57
3.2.2.9	data evaluation and kinetic data fit .....	58
3.2.3	Results and Discussion.....	59
3.2.3.1	Heat-induced denaturation and aggregation in PPI solutions.....	59
3.2.3.2	Kinetic parameters of patatin denaturation and aggregation .....	60
3.2.3.3	Protein-protein interactions within PPI aggregates measured by SDS-PAGE .....	63
3.2.3.4	Reduction of free thiol groups in PPI solutions and formation of disulfide bonds during heat-induced aggregation .....	66
3.2.3.5	Change in the hydrophobic character of PPI aggregates during heat-induced aggregation .....	68
3.2.4	Conclusion .....	70
3.2.5	Supporting information.....	72
<b>3.3</b>	<b>Heat-induced aggregation kinetics of potato protein - Investigated by reversed phase high pressure liquid chromatography, differential scanning calorimetry, and dynamic light scattering.....</b>	<b>77</b>
3.3.1	Introduction .....	79
3.3.2	Materials and methods.....	81
3.3.2.1	Materials and sample preparation .....	81
3.3.2.2	Modulated differential scanning calorimetry (mDSC).....	81
3.3.2.3	Heating experiments .....	82
3.3.2.4	Purification of patatin from PPI for use as a standard in RP-HPLC calibration and protein quantification .....	82
3.3.2.5	Determination of native patatin by RP-HPLC.....	83
3.3.2.6	Particle size measurement by dynamic light scattering .....	83
3.3.2.7	Determination of free thiol-groups in heated PPI solutions.....	84
3.3.2.8	Evaluation of Kinetic Parameters .....	85
3.3.3	Results and discussion .....	85
3.3.3.1	Relation between the thermal unfolding of patatin and the thermal reaction kinetic parameters of protein aggregation.....	85
3.3.3.2	Change in reaction behavior of patatin in dependence of the heating temperature ....	87
3.3.3.3	Disulfide formation during heat-induced protein aggregation .....	89
3.3.3.4	Size of PPI aggregates measured by dynamic light scattering .....	90
3.3.4	Conclusion .....	92
3.3.5	Supporting Information.....	93
<b>3.4</b>	<b>Microstructures of potato protein hydrogels and aerogels produced by thermal crosslinking and supercritical drying .....</b>	<b>97</b>
3.4.1	Introduction .....	99
3.4.2	Materials and methods.....	101

3.4.2.1	Materials.....	101
3.4.2.2	Modulated differential scanning calorimetry (mDSC) .....	102
3.4.2.3	Rheological characterization of the hydrogels .....	102
3.4.2.4	Hydrogel capsule preparation .....	102
3.4.2.5	Solvent exchange and alcogel characterization .....	103
3.4.2.6	Supercritical drying.....	103
3.4.2.7	Aerogel characterization .....	103
3.4.2.8	Statistical methods .....	104
3.4.3	Results and discussion .....	104
3.4.3.1	Influence of protein concentration on potato protein gelation and stability after solvent exchange .....	104
3.4.3.2	Impact of pH on hydrogel, alcogel and aerogel structure .....	108
3.4.3.3	Relationship between hydrogel rheology and aerogel microstructure .....	116
3.4.4	Conclusion .....	121
<b>3.5</b>	<b>Viscoelasticity and protein interactions of hybrid gels produced from potato and whey protein isolates.....</b>	<b>123</b>
3.5.1	Introduction .....	125
3.5.2	Materials and methods .....	127
3.5.2.1	Materials.....	127
3.5.2.2	Rheological characterization of the hydrogels .....	127
3.5.2.3	Texture profile analysis .....	127
3.5.2.4	Protein interaction assay.....	128
3.5.2.5	SDS polyacrylamide gel electrophoreses .....	129
3.5.2.6	Determination of exposed hydrophobicity.....	129
3.5.2.7	Experimental design.....	130
3.5.3	Results and discussion .....	130
3.5.3.1	Visual appearance of PPI/WPI hybrid gels .....	130
3.5.3.2	Protein interactions of heat-induced PPI/WPI hybrid gels .....	131
3.5.3.3	Rheological characteristics of heat-induced PPI/ WPI hybrid gels .....	135
3.5.3.4	Textural properties of heat-induced PPI/WPI hybrid gels .....	140
3.5.3.5	Influence of salt on heat-induced PPI/WPI hybrid gels.....	141
3.5.4	Conclusion: Relationship between gelation mechanism and textural properties in PPI/WPI hybrid gels .....	143
<b>3.6</b>	<b>Hydro- and aerogels from ethanolic potato and whey protein solutions: Influence of temperature and ethanol concentration on viscoelastic properties, protein interactions, and microstructure .....</b>	<b>145</b>
3.6.1	Introduction .....	147
3.6.2	Materials and Methods .....	149
3.6.2.1	Preparation of protein mixtures with variable EtOH content.....	149
3.6.2.2	Modulated differential scanning calorimetry (mDSC) .....	150
3.6.2.3	Rheological characterization of the hydrogels .....	150
3.6.2.4	Hydrogel capsule preparation .....	151
3.6.2.5	Protein interaction assay.....	151
3.6.2.6	Solvent exchange to obtain alcogels .....	152
3.6.2.7	Textural characterization of alcogels .....	152
3.6.2.8	Supercritical drying.....	152
3.6.2.9	Aerogel characterization .....	153
3.6.2.10	Gel nomenclature.....	153
3.6.2.11	Statistical methods .....	153
3.6.3	Results and discussion .....	153
3.6.3.1	Thermal properties of ethanolic protein mixtures measured by DSC .....	153

---

3.6.3.2	Rheological properties of hydrogels gelled in the presence of ethanol .....	155
3.6.3.3	Protein interactions in protein hydrogels gelled in the presence of ethanol.....	157
3.6.3.4	Textural properties of gel beads before and after complete solvent exchange with EtOH .....	160
3.6.3.5	Aerogel characterization.....	162
3.6.3.6	Scheme of the proposed gelation mechanism influenced by EtOH in concentrated protein systems.....	165
3.6.4	Conclusion .....	166
3.6.5	Supporting Information.....	167
<b>4</b>	<b>OVERALL DISCUSSION AND MAIN FINDINGS.....</b>	<b>169</b>
4.1	Aggregation behavior of potato proteins.....	170
4.2	Influence of milieu conditions on potato- and animal-derived protein gels .....	173
4.3	Correlation between rheological properties and the type of protein-protein interactions in protein gels .....	176
<b>5</b>	<b>SUMMARY &amp; ZUSAMMENFASSUNG .....</b>	<b>185</b>
5.1	Summary .....	185
5.2	Zusammenfassung.....	188
<b>6</b>	<b>REFERENCES.....</b>	<b>193</b>
<b>7</b>	<b>APPENDIX.....</b>	<b>213</b>
7.1	Peer reviewed publications (included in this thesis).....	213
7.2	Peer reviewed publications (not included in this thesis).....	213
7.3	Oral & poster presentations .....	213

## Abbreviations and symbols

Abbreviations	Unit	Meaning
BET		inner surface area determined by the Brunauer-Emmett-Teller method
Cys		cystein
EWP		egg white protein
G'	Pa	storage modulus
G''	Pa	loss modulus
IEP		isoelectric point
k <sub>app</sub>	s <sup>-1</sup>	apparent reaction rate
kDa		kilo-Dalton
LVE		linear viscoelastic range
n	[-]	reaction order
NaCas		sodium caseinate
NEM		N-Ethylmaleimide
PPI		potato protein isolate
RP-HPLC		reversed-phase high-performance liquid chromatography
scCO <sub>2</sub>		supercritical CO <sub>2</sub>
SDS-PAGE		sodium dodecyl sulphate–polyacrylamide gel electrophoresis
SEC		size exclusion chromatography
SEM		scanning electron microscopy
T	K	temperature
t	s	time
tan δ	[-]	loss factor
T <sub>d</sub>	°C	temperature of denaturation peak
Tgase		transglutaminase
T <sub>onset</sub>	°C	temperature of denaturation onset
WPI		whey protein isolate
α-La		alpha-Lactalbumin
β-Lg		beta-Lactoglobulin
γ	%	strain





## 1 General introduction

Proteins are one of the most important components of food systems. Under certain conditions protein solutions can form gels, thereby turning the liquid solution into a solid structure. Although a lot of knowledge exists on the gelation of whey and egg proteins, two of the most widely used protein systems, for newer protein sources this knowledge is more scarce. One such novel food protein is potato protein obtained from waste streams in the potato starch industry. As the main focus of this thesis is to understand the gelation behavior of potato proteins and compare these to well-researched whey proteins the different steps in the protein gelation will be explained in the following.

The process of gelation is a multistep process and understanding each step is crucial in developing new protein systems. First, the molecular structure of proteins in general, and whey and potato proteins, in particular, will be explained (see section 1.1). Thereby the different aspects that influence protein functionality should be explained. Then, the mechanism that can induce the unfolding and aggregation of protein structures will be explained (see section 1.2). Depending on the milieu and the protein structure of the native molecule very different reaction mechanisms can occur in protein systems. The protein can follow different reaction kinetics and can form aggregates of different structures and sizes. From these aggregates, macromolecular hydrogel structures can be formed. The mechanism of this gelation phenomenon will be explained in section 1.3. The gel structure can be influenced by changes in milieu conditions and the general principles of changes in milieu on protein gelation are explained as well. The section is concluded with an overview of how the viscoelastic properties of hydrogels can be analyzed with a rheometer.

Hydrogels can be further processed into aerogels, a novel class of protein gels with unique properties. Aerogels from biopolymers such as protein were already used for application as encapsulation materials, oleogelators, and in biomedical applications such as tissue engineering scaffolds. Furthermore, the gentle drying step in the aerogel process preserves the original hydrogel structure very well. Therefore, investigations into the aerogel microstructure do directly correlate with the hydrogel structure and give a unique insight into gelation phenomena. Therefore, the general introduction is closed by explanations on how these aerogel structures are formed from hydrogels via the solvent exchange route involving alcogels (see section 1.4).

## 1.1 Molecular structure and properties of food proteins

### 1.1.1 General features of proteins

In the following chapter, the general structure of proteins will be explained in order to understand how these structures differ between protein sources, and how they can be influenced. Proteins are biological macromolecules that consist of amino acids. They are often described as biological catalysts as they facilitate all sorts of reactions in the biological tissues of plants and animals. To fulfill these biological functions the proteins need to be folded into very specific structures. Only when they are folded correctly they form reactive sites where the catalyzed reaction can occur. They derive their three-dimensional fold from a certain hierarchy of structures. These structures are shown in Figure 1-1 and are described in more detail in the following.

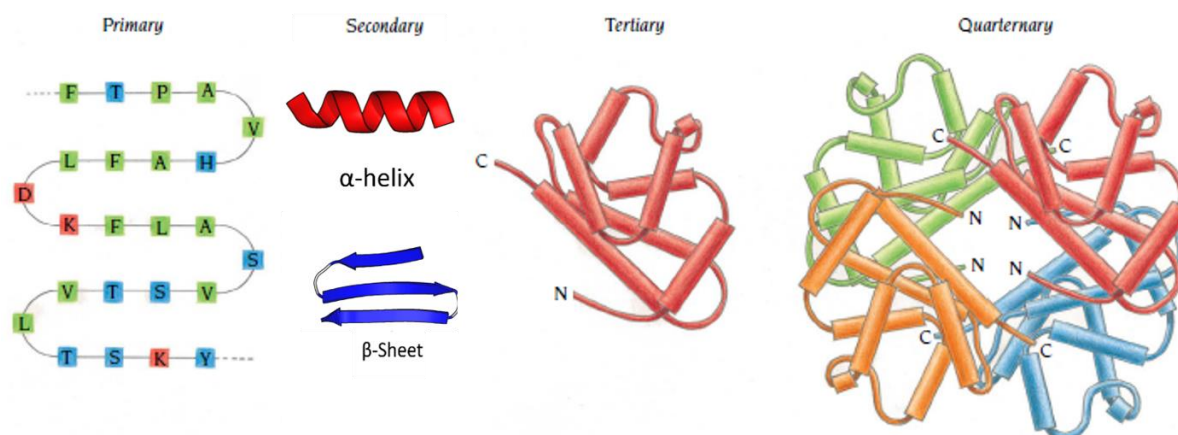


Figure 1-1 Schematic representation of protein structures, modified from Branden & Tooze, (2012), page 3, figure 1.1. Rights granted by Informa UK Ltd.

The first level is the primary structure. This describes the amino acids that form the protein as well as their connection, indicating which amino acid follows on which amino acid in a string like structure

The secondary structure describes how the one-dimensional amino-acid strings fold into three-dimensional structures. Depending on the orientation of the hydrogen bonds that form between the amino acids, spiral-like  $\alpha$ -helices or plane  $\beta$ -sheets emerge. The elements of the secondary structure can arrange in a higher three-dimensional level, the so-called tertiary structure.

The tertiary structure of the native protein is what is commonly described as the correctly folded state. Changes in the tertiary structure are called unfolding and can severely change the protein function, as will be shown later. The arrangement of secondary structure elements into the tertiary structure is mainly determined through a variety of protein interactions. Depending on the amino acid type, different interactions between the side chains can occur. An overview can be seen in Figure 1-2.

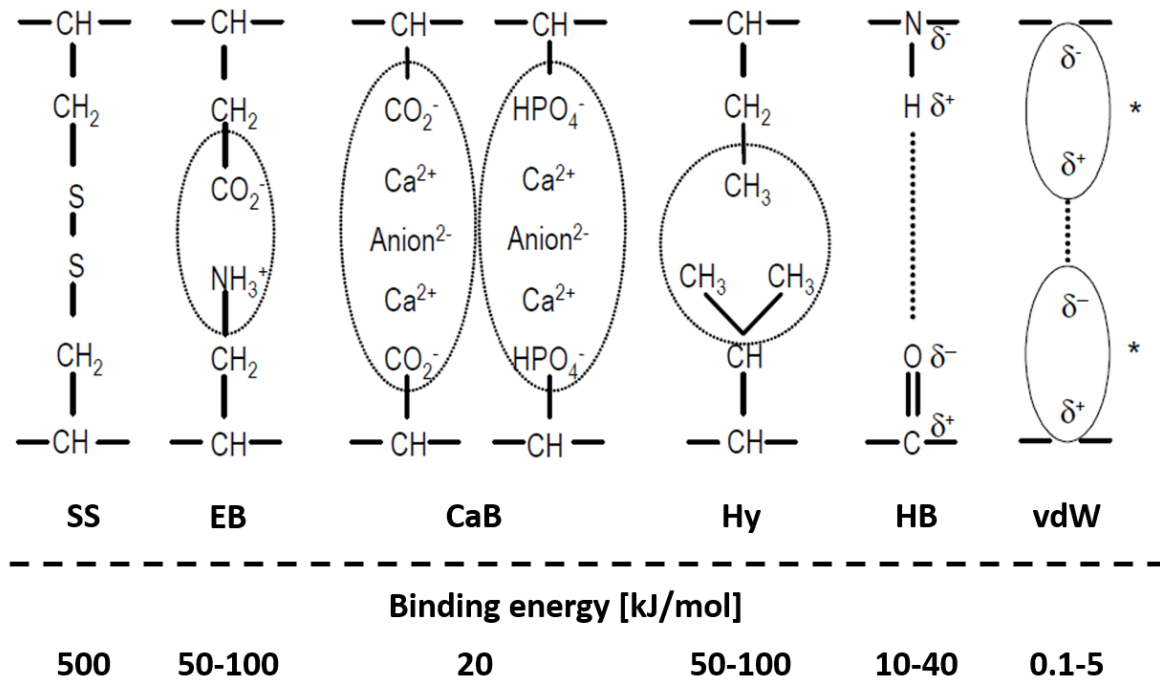


Figure 1-2 Overview of different protein interactions occurring between amino acid side chains. Disulfide bonds (SS), electrostatic interactions (EB), Calcium bridges (CaB), Hydrophobic interactions (Hy), hydrogen bonds (HB), and van der Waals interactions (vdW) are depicted. Adapted from Toro Sierra, (2016), page 26, table 1.3 and Keim, (2004), page 3, figure 2.1. Binding energies are reported by Li-Chan, (1996) and Le Meste et al., (2006)

Some proteins also show higher levels of order, the so-called quaternary structure. Single protein monomers arrange in certain ways to form these supramolecular structures. Examples in food proteins are the dimeric structure of the whey protein  $\beta$ -lactoglobulin or the arrangements occurring in seed storage proteins of pea and soy containing up to 4 subunits (Rasheed et al., 2020). Therefore, although there are only 21 amino acids that form the primary structure of proteins the functionalities of proteins that can derive from this are nearly infinite due to different secondary, tertiary, and quaternary structures.

Globular proteins describe a wide variety of proteins that are characterized by their spherical structure. These proteins are especially important for food applications as the major proteins of whey, egg white, pea, potato, and other food sources all belong to this class of proteins. Their structure stems from the fact that hydrophobic amino acids turn inwards to the protein core and hydrophilic proteins turn outward to the protein surface. This way globular proteins obtain some sort of solubility in water. Depending on the amino acid composition they are differently charged. Changes in the pH of the solution change the overall charge of the protein. The pH value at which positively and negatively charged amino acids in a protein neutralize each other is called the isoelectric point (IEP) of the protein. At the IEP the overall charge of the protein is zero and no electrostatic repulsion between protein monomers occurs.

To conclude, protein structure and protein interactions are fundamental to understanding how proteins behave. Therefore there will be a special focus on structure and interactions for the two protein systems that shall be investigated in more detail. One

protein source is whey protein isolate (WPI), which is detailed in section 1.1.2 as it contains some of the extensively researched food proteins. Another source is potato protein isolate (PPI) as a class of new, plant-based proteins, detailed in section 1.1.3. The different structural features of the proteins will help to explain differences in their respective unfolding and aggregation behavior (section 1.2) the resulting protein interactions and subsequently the different gel structures that result from these protein types (section 1.2.3).

### 1.1.2 Whey proteins

Among the best-researched proteins in food science are whey proteins. As these proteins will be the reference system throughout the thesis, these milk-derived proteins are explained in more detail in the following. Milk contains around 3-4% protein, comprised of two major protein fractions: caseins and whey proteins. Casein represents 80% of total milk protein, and whey proteins the remaining 20%. Whey proteins are a heterogeneous group of proteins that vary greatly in their biological function and protein chemical properties. The two most abundant proteins are  $\beta$ -lactoglobulin ( $\beta$ -lg) and  $\alpha$ -lactalbumin ( $\alpha$ -la), representing nearly ~60 and 15% of the whey proteins, respectively. However, depending on the isolation process the amount of  $\beta$ -lg can rise to 80% of total protein (Elgar et al., 2000). The remaining few percent are lactoferrin, bovine serum albumin (BSA), and immunoglobulins such as Immunoglobulin G. The techno-functional properties of WPI such as gelation, emulsification, and foamability however can easily be understood if one focuses on the properties of  $\beta$ -lg and to a smaller extent on  $\alpha$ -la. Therefore, these two proteins shall be characterized in more detail in the following.

$\beta$ -lg is a globular protein with a size of 18.3 kDa, which occurs as a dimer in the neutral pH range and consists of 162 amino acids. Two genetic variants are known,  $\beta$ -lg A and  $\beta$ -lg B. These two variants only differ in amino acid composition in two positions (position 64 and 118) where aspartic acid and valine of variant B is replaced by glycine and alanine in variant B. Although some differences in the techno-functional properties of these variants exist (Boye et al., 1997), these will not be addressed in more detail. The isoelectric point (IEP) of  $\beta$ -lg is around 4.8.

The structure of  $\beta$ -lg is given in Figure 1-3. The secondary structure is characterized by a  $\beta$ -barrel which is stabilized by two disulfide bonds and one  $\alpha$ -helix. Behind the  $\alpha$ -helix, the cysteine group at position 121 provides a free thiol group which plays a crucial role in the aggregation and gelation mechanism of  $\beta$ -lg (Qi et al., 1997). It could be shown, that dimer dissociation was a necessary step for reaction with sulfhydryl agents (Iametti et al., 1996). Therefore, the dissociation of  $\beta$ -lg dimers into monomeric  $\beta$ -lg is the first step in the heat-induced reaction of  $\beta$ -lg.

For  $\beta$ -lg, temperatures of unfolding are reported between 75-80 °C (Delahaije et al., 2015; Creusot et al., 2011; Tolkach & Kulozik, 2007). Upon unfolding the tertiary protein structure is disrupted and an intermediate state of unfolding is reached. This reversibly unfolded state is often described as a molten globule-like state. However, a classical molten globule state only shows a loss in tertiary and not secondary structure

(Judy & Kishore, 2019). As loss of secondary structure is also occurring in  $\beta$ -lg upon heating, therefore the classic definition of molten globule state does not apply (Qi et al., 1997).

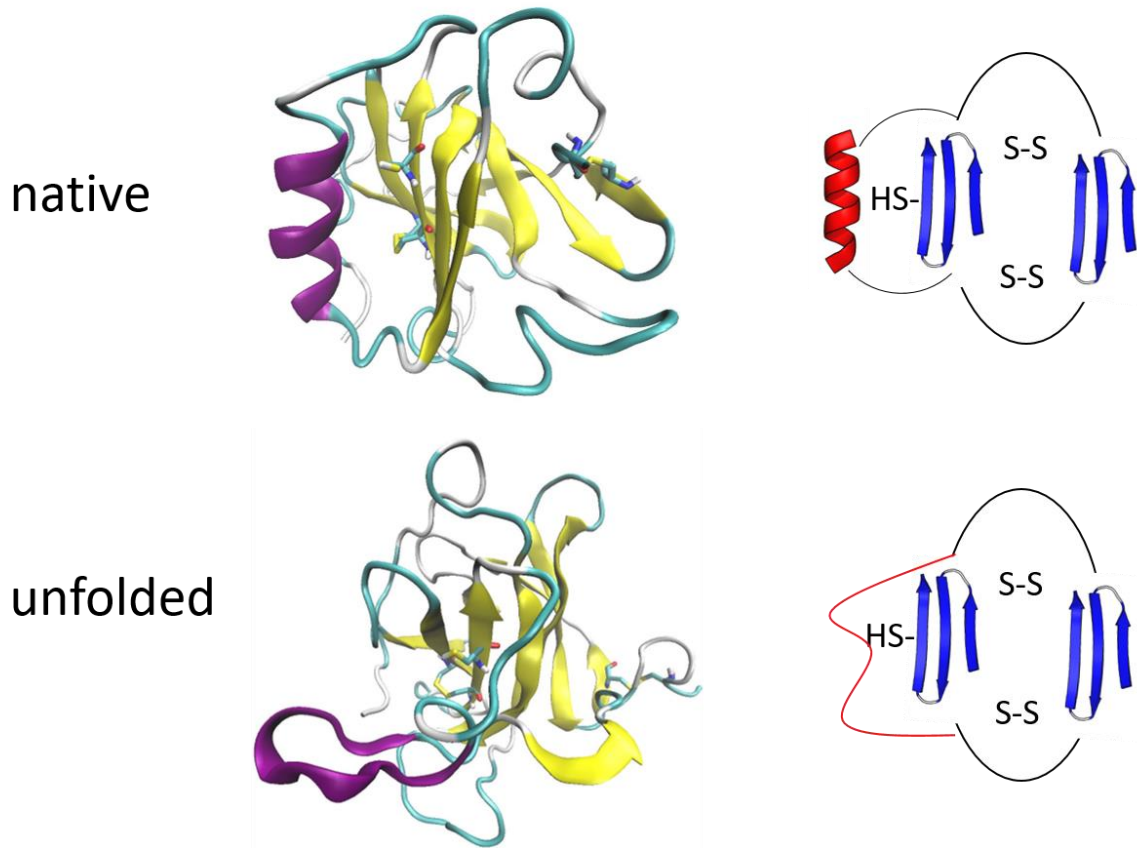


Figure 1-3 Schematic representation of  $\beta$ -Lg in its native and unfolded state. The 3D model was created by the author with the program Visual Molecular Dynamics (VMD) from protein data bank (PDB) entry 3BLG, according to the method by Euston, (2013). Under heat denaturing conditions the  $\alpha$ -helix unfolds and the cysteine group (SH) is exposed. The remaining  $\beta$ -barrel structure is stabilized by disulfide bonds (S-S).

The second major whey protein is  $\alpha$ -la which has a size of 14.2 kDa and consists of 123 amino acids. Two genetic variants (A and B) are known where glycine at position 10 is exchanged with arginine.  $\alpha$ -la contains four internal disulfide bonds and no free thiol groups. It consists of two sub-domains, a bigger  $\alpha$ , and a smaller  $\beta$  domain. Sub-domain  $\alpha$  consists of three  $\alpha$ -helices and sub-domain  $\beta$  consist of two anti-parallel  $\beta$ -sheets, a small  $3_{10}$ -helix and irregular structures (Pike et al., 1996).  $\alpha$ -La can bind calcium ( $\text{Ca}^{2+}$ ) in a region between the two sub-domains. The calcium-binding *holo*-form has higher thermal stability than the  $\text{Ca}^{2+}$  free *apo*-form, with denaturation temperatures of 60 and 30  $^{\circ}\text{C}$ , respectively (Relkin et al., 1992). As the protein solutions investigated in this thesis contain little  $\text{Ca}^{2+}$ , apo- $\alpha$ -la denaturation is expected to occur already at low temperatures.

Due to the lack of free thiol groups,  $\alpha$ -La monomers cannot directly form disulfide-linked aggregates. However, in the presence of  $\beta$ -lg, it could be shown that hybrid

aggregates of  $\beta$ -lg and  $\alpha$ -La could be formed. Furthermore, rearrangements of the disulfide links within these aggregates could be observed which led to the release of disulfide-linked dimeric  $\alpha$ -La from these aggregates (Schokker et al., 2000). Furthermore, it could be shown that the presence of  $\beta$ -lg increases the gelation rate of  $\alpha$ -la (Hines & Foegeding, 1993). However, the rheological properties of these gels were very similar indicating the importance of  $\beta$ -lg in building up the gel network.

### 1.1.3 Potato proteins

Besides whey proteins, other globular proteins are researched in more detail in the last decade, among them potato proteins. Potato protein isolate (PPI) is obtained from the aqueous residue processing stream of starch production, which is called potato fruit juice (PFJ). PFJ contains ~2% protein with the following protein fractions: The most important fraction is patatin representing 35-40% of total protein. The second dominant fraction is the protease inhibitor fraction a heterogeneous group of proteins of different sizes, representing 25-50% of total protein. The rest belongs to higher molecular weight fractions (Løkra et al., 2008).

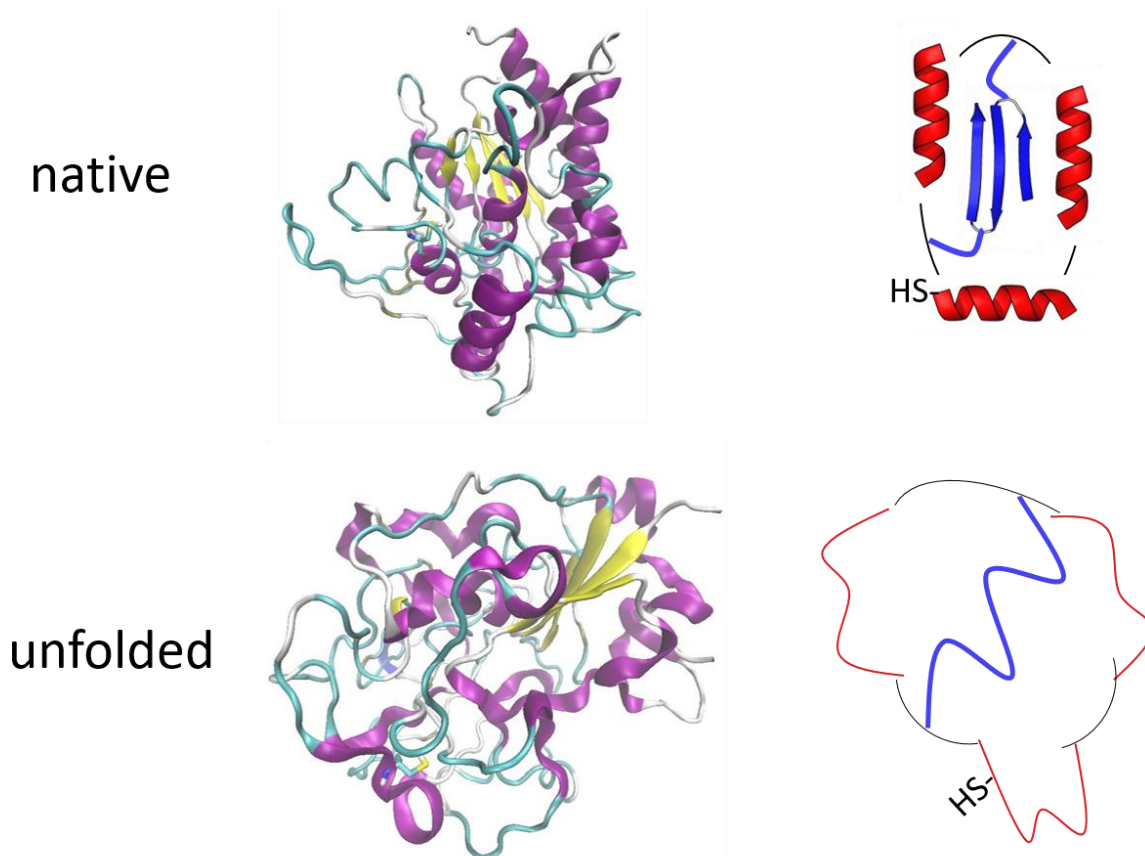


Figure 1-4 Schematic representation of Patatin in its native and unfolded state. The 3D model was created by the author with the program Visual Molecular Dynamics (VMD) from protein data bank (PDB) entry 1OXW, according to the method by Euston, (2013). Patatin has no internal disulfide bonds. Therefore, upon heating, no areas in the structure are specifically stabilized.

Patatin has a high amount of lysine, which is unusual for plant proteins. This makes patatin a very nutritive protein with a well-balanced amino acid profile (Bártová & Bárta, 2009). Although different isoforms of patatin are known they are very homogenous and



exhibit similar behavior under heat treatment (Pots et al., 1999b). Patatin has a molecular mass of around 40-42 kDa and an IEP around 5.0 (Racusen & Weller, 1984). Although it is considered a storage protein, it also exhibits lipid-acyl hydrolase activity (Andrews et al., 1988) allowing it to cleave fatty acids. In contrast to other enzymes that interact with hydrophobic substances, like lipases, it lacks a flexible lid structure that shields the active site (Rydel et al., 2003). Instead, it has hydrophobic patches on its surface to interact with hydrophobic structures. The occurrence of these patches explains the high hydrophobicity of native patatin when compared to other food proteins, like  $\beta$ -lg (Creusot et al., 2011).

Contrary to patatin, the PI are a very heterogeneous group with IEPs between 5-8 and molecular weights ranging from 7 to 21 kDa (Løkra et al., 2008; Pouvreau et al., 2001). They play an important part in the defense mechanism of the potato tuber by inactivating proteolytic enzymes of microorganisms and insects (Jongsma & Bolter, 1997).

The first and second most abundant PI are potato serine protease inhibitors (Pouvreau et al., 2005a) and potato cysteine protease inhibitors (Pouvreau et al., 2005b), respectively. The thermal stability of both these PI is higher than patatin's, indicated by a higher temperature of unfolding. PIs were shown to form gels. However, at neutral or mildly acidic pH, the gels were very brittle compared to patatin (Schmidt et al., 2019). Although interactions between patatin and PI are likely no results are published. Besides gelation, PI can also be used to stabilize foams (Dachmann et al., 2020).

## 1.2 Unfolding and Aggregation of proteins

As it could be shown in section 1.1.1 the correct folding of a protein is dependent on a very delicate balance of repulsive and attractive forces within the protein. Therefore, disturbance of this balance by changes in the milieu conditions around the protein will lead to changes in the protein conformation. These changes will lead to the protein losing its native folding and becoming unfolded. This unfolded state is called denatured, in contrast to the correctly folded native state (Tanford, 1968). Conditions that induce unfolding include changes in temperature, ion content, and pH milieu as well as the addition of organic solvents. These effects will be explained in more detail in the following.

### 1.2.1 Heat-induced denaturation and aggregation

For food technology applications the occurrence of temperature-induced denaturation is often the most important form of denaturation. Although there is also denaturation by cold temperatures and especially freezing we will focus in this work on denaturation occurring at elevated temperatures. From a thermodynamic perspective, the native conformation represents a minimum of the energy landscape funnel (see Figure 1-5). From all possible conformations of the protein, the protein will fold to the one conformation with the lowest free energy.

When kinetic energy in the form of elevated temperatures is transferred onto the protein the protein conformation can exhibit an intermediary or even completely unfolded state with higher free energy. This energy transfer can be interpreted as a lift of the protein from a state of lowest possible energy to a state of higher energy in the energy

landscape given in Figure 1-5. The unfolding is often reversible upon cooling as the protein wants to achieve a state of minimum free energy, again. For patatin (Pots et al., 1998a),  $\alpha$ -la and  $\beta$ -lg (Tolkach & Kulozik, 2007), refolding to a high degree could be observed. However, the refolding can also result in a natively folded state, but more likely by partial refolding into a new non-native state.

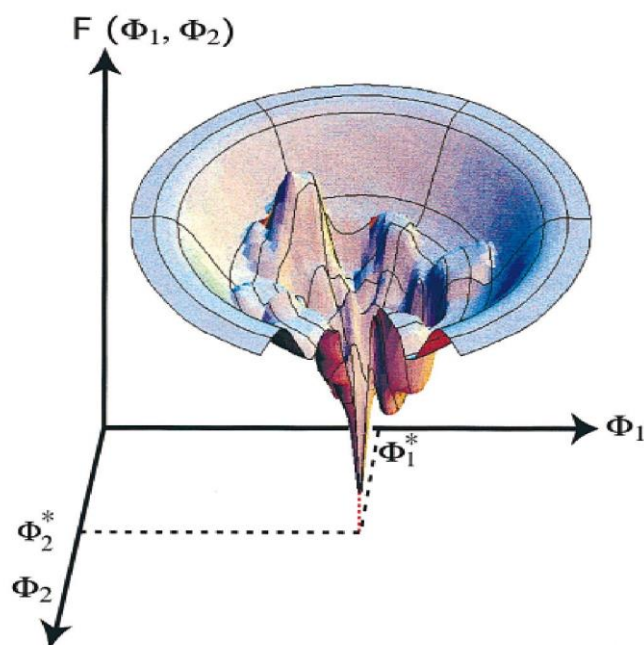


Figure 1-5 Energy landscape of a protein as a function of the degrees of freedom  $\phi_1$  and  $\phi_2$ . The degrees of freedom for a protein can be bond torsion angles of the backbone and side-chain taken from Dill, (1999), page 1172, figure 4. Only a very specific conformation of the protein will thus yield the lowest free energy, representing the bottom of the funnel.

The unfolding process leads to amino acids being exposed to the surrounding, which would normally reside within the protein core. A lot of research on this was done on  $\beta$ -lg (Cairolì et al., 1994; Qi et al., 1997), but other globular proteins, such as patatin were shown to exhibit similar behavior (Pots et al., 1998a). The exposed amino acids led to the development of new protein interactions between amino acids of different molecules. These protein monomers then form oligomers of a few monomers and even aggregates with several dozens of monomers.

Depending on the protein source, the aggregates can form in many different ways. For  $\beta$ -lg, a three-step reaction mechanism is proposed (see Figure 1-6). First, the dimeric  $\beta$ -lg dissociates into monomers. Then the protein monomers unfold and amino acids from the protein core are exposed. For  $\beta$ -lg, the reactive Cys-121 group is of high importance for the aggregation process (Croguennec et al., 2004). This group can only readily interact after the  $\alpha$ -helix, shielding the Cys-121 group, has unfolded (also visible in Figure 1-3). The free thiol group can react with disulfide bonds in  $\beta$ -lg. This way the intermolecular disulfide bonds are broken up and a new disulfide bridge between two  $\beta$ -lg monomers is formed. During this process, a thiol group, which was bound in a disulfide bond before the reaction, is exposed. This thiol group can then react with another disulfide bond, inducing the polymerization of  $\beta$ -lg monomers.



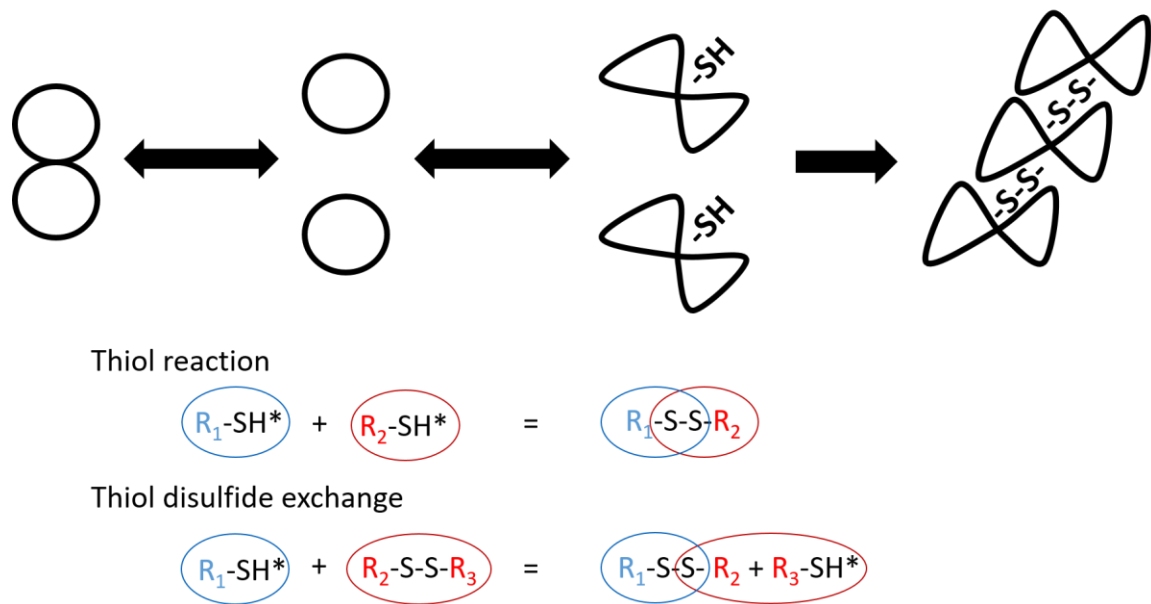


Figure 1-6 Schematic representation of the reaction pathway of  $\beta$ -Ig. The different possibilities on how the thiol groups can react in the presence of oxygen are depicted on the bottom. SH\* indicates a reactive thiol group.

For patatin, less research was done so far, but some notable differences, as well as similarities, are described. Patatin has a thermal denaturation temperature ( $T_d$ ), determined by DSC, of around 60 °C (Creusot et al., 2011; Delahaije et al., 2015) which is considerably lower than  $\beta$ -Ig's  $T_d$  of 75-80 °C (Delahaije et al., 2015; Creusot et al., 2011; Tolkach & Kulozik, 2007). The difference can be explained by the different structures of patatin and  $\beta$ -Ig. The higher amount of internal disulfide bonds in  $\beta$ -Ig compared to patatin results in a stronger stabilization of the protein against unfolding. Nevertheless, the unfolding behavior of patatin resembles that of  $\beta$ -Ig in some way. For patatin, a two-step unfolding and aggregation process was proposed, where the first native protein reversibly unfolds. This is then followed by the formation of a reactive particle which forms irreversible aggregates (Pots et al., 1999c). As patatin also occurs in a dimeric form, a dissociation similar to  $\beta$ -Ig dissociation, before aggregation is likely.

Although this basic principle is similar to the reaction mechanism proposed for  $\beta$ -Ig, the interactions occurring between the proteins are very different. As patatin contains only one free-thiol group, a polymerization of patatin monomers into aggregates via thiol-disulfide exchange seems unlikely. However, one study reported the formation of trimeric patatin structures, which showed sensitivity towards reducing buffers indicating the formation of disulfide links (Pots et al., 1999a). How exactly these trimeric structures can be formed, although a thiol-disulfide exchange is unlikely, could not be explained so far. When a recent comparative study investigated the aggregation behavior of three major food proteins, ovalbumin,  $\beta$ -Ig, and patatin, notable differences between the reaction speeds were observed (Delahaije et al., 2015). However, these differences between the reaction rates could not be attributed to one specific attribute of the native protein, such as exposed hydrophobicity, amount of free thiol, or net surface charge. This highlights the importance to investigate protein denaturation separately

for each protein. Furthermore, special emphasis should be put on the molecular interactions that are occurring during aggregation (see Figure 1-2).

### **1.2.2 Solvent induced denaturation and aggregation**

Next to heat-induced denaturation, solvent-induced denaturation is a widely studied subject in protein chemistry. Similar to heat-induced unfolding the presence of an organic solvent, such as ethanol (EtOH), leads to changes in the preferred protein interactions of the amino acid side chains. By studying the denaturing effect of solvents on protein solutions, this study aims to understand differences between the unfolding behavior of potato and whey proteins in a holistic way rather than by focusing on heat-induced denaturation alone. Furthermore, as EtOH is a necessary ingredient in the creation of aerogels, the presence of this solvent prior to the alco- and aerogel process might be beneficial (see chapter 1.4 for background on alco- and aerogels). These changes will lead to changes in the proteins' tertiary structure and therefore to unfolding. The changes occurring for proteins in the presence of alcohols can be explained as follows. When  $\beta$ -lg was investigated in different organic solvents the protein denatured when a certain solvent concentration was surpassed (Uversky et al., 1997). It could be shown that denaturation occurred at lower protein concentrations when the polarity of the medium was lower (i.e. the hydrophobicity was higher). Instead of solvent concentration, the main property of the solution that predicted the unfolding of the protein was the dielectric constant ( $\epsilon$ ) of the solution. When the mixture of solvent and water was below a dielectric constant of  $\sim 62$  the protein  $\beta$ -lg unfolded. This was especially remarkable as a wide range of organic solvents in different mixtures was tested. The unfolded state exhibited a high exposed hydrophobicity and was described as molten-globule-like. Similar to the molten globule state induced by elevated temperatures, the solvent-induced molten globule state leads to aggregation of the unfolded proteins (Yoshida et al., 2014). Besides the changes in protein conformation, the lower  $\epsilon$  of the solution leads to stronger interactions through electrostatic interactions. In addition to being a denaturant on its own, organic solvents such as ethanol lower the thermal resistance of proteins and therefore lead to denaturation at lower temperatures (Nikolaidis & Moschakis, 2018).

Similar to the denaturation by heat, the unfolding through solvents is due to changes in the protein tertiary structure. When organic solvents are present in a solution, the preferred interactions of the amino acids changes. Organic solvents such as alcohols contain hydrophobic parts, for example, the ethyl chain in EtOH. With these hydrophobic parts, no hydrogen bonds can be formed. Therefore, rather than forming hydrogen bonds with the solution, the proteins prefer the formation of intermolecular hydrogen bonds. This leads to the formation of  $\alpha$ -helices rather than  $\beta$ -sheets (Yoshida et al., 2010). In addition, the presence of hydrophobic solvents allows the hydrophobic proteins from the protein core to unfold and interact with the solutions. The exposure of hydrophobic groups leads to aggregation into short worm-like fibrils (Gosal et al., 2004a). Details on changes in the aggregate morphology are given in chapter 1.2.4.

### 1.2.3 Kinetic description of protein aggregation

To compare different unfolding and aggregation reactions their kinetic parameters have to be obtained. To describe chemical reactions two kinetic parameters are commonly used. One is the reaction order  $n$  and the other is the reaction rate  $k$ . The reaction rate is indicating how much molecules react per second. It is temperature-dependent as higher temperatures will result in more collisions of the molecules and thus more reactions. The reaction order in formal kinetics is dependent on how many different reactants are participating in a reaction. If a reaction is independent of the concentration of reactants it follows 0<sup>th</sup> order kinetics. However, if it is dependent on the concentration of one, two, or three reactants it follows 1<sup>st</sup>, 2<sup>nd</sup>, or 3<sup>rd</sup> order kinetics, respectively. If multiple reactions are involved in an overall reaction the reaction order of this overall reaction can differ. For example, the unfolding of  $\beta$ -lg follows 1<sup>st</sup> order kinetics, while the aggregation reaction from two unfolded species follows 2<sup>nd</sup> order (Mounsey & O'Kennedy, 2007). Therefore, the overall reaction can be approximated with a reaction order of 1.5 (Loveday, 2016). For a given reaction the reaction order is temperature independent. Increasing the temperature only increases the collisions and therefore the reaction opportunities but not the reaction itself.

On a fundamental level denaturation and aggregation are chemical reactions between reactive molecules. For  $\beta$ -lg and patatin, these were abstracted to the following equations (Pots et al., 1999c; Roefs & Kruif, 1994).



With N being the native protein, U the unfolded, and R\* the protein in a reactive state. How these states can be interpreted from a protein chemical viewpoint was already discussed in section 1.2.1. These reactive particles (R\*) then can react further into bigger aggregates.



To obtain  $k$  and  $n$  from denaturation data the reaction can be abstracted to a single-species reaction, only dependent on native protein (C). The time-dependent change of C is described in Equation (1-3).

$$-\frac{dC}{dt} = kC^n \quad (1-3)$$

To obtain kinetic parameters from this equation one has to measure the concentration of unreacted protein (C) after a certain time (t) in relation to the initial protein concentration ( $C_0$ ). The integrated form of Equation (1-3) is given in Equation (1-4).

$$C = [(n-1)kt + C_0^{1-n}]^{\frac{1}{1-n}} \quad (1-4)$$

Equation (1-4) can be rearranged into

$$\frac{C}{C_0} = [(n-1)tkC_0^{1-n} + 1]^{\frac{1}{1-n}} \quad (1-5)$$

If  $C_0$  is kept constant throughout the experiments  $kC_0^{1-n}$  can be shortened to the apparent rate constant  $k_{app}$  (Loveday, 2016).

$$\frac{C}{C_0} = [(n - 1)k_{app}t + 1]^{\frac{1}{1-n}} \quad (1-6)$$

The classical approach transforms Equation (1-6) as described below

$$\left(\frac{C}{C_0}\right)^{1-n} = (n - 1)k_{app}t + 1 \quad (1-7)$$

Then  $(C/C_0)^{1-n}$  is plotted against  $t$  and  $n$  is chosen in a way that a linear relation can be obtained. For the denaturation of  $\beta$ -lg this linearization was often obtained for  $n = 1.5$  (Leeb et al., 2018; Tolkach & Kulozik, 2007).

However, this linearization of non-linear data is inadvisable and other methods are proposed to be more suitable to fit the data (van Boekel, 1996). Another method to obtain the kinetic parameters from Equation (1-6) is fitting the denaturation data by non-linear regression. For this approach, a computer program fits Equation (1-6) iteratively onto denaturation data until a combination of  $n$  and  $k_{app}$  is found which fits the data well.

Through this approach, data of the denaturation of  $\beta$ -lg was reevaluated and new insights into the reaction mechanism could be gained (Loveday, 2016). It could be shown that  $n$  varied in dependence of the temperature and also of protein concentration. This change in reaction order can be interpreted as a change in the underlying reaction. When the reaction changes, e.g. more or fewer reactants are contributing to the reaction,  $n$  will increase or decrease as well. Furthermore, the overall reaction is dependent on two successive reactions, the unfolding and aggregation step each of which follows its own reaction order. A change in  $n$  can therefore be interpreted as a change in which of these reactions limit the overall reaction (Mounsey & O'Kennedy, 2007). A change in reaction mechanism is described in detail for  $\beta$ -lg (Tolkach & Kulozik, 2007). It could be shown that the aggregation had a higher temperature dependence in the range from 60 to 90 °C and a lower between 90 and 120 °C. A schematic representation of this finding can be seen in Figure 1-7. The change in the reaction mechanism can be explained as follows.

In the first regime,  $\beta$ -lg unfolds gradually, some proteins are still in native conformation, and unfolded protein does also refold. In this environment not every collision between two protein monomers leads to aggregation. Increasing the temperature in this range has two effects. First, the kinetic energy in the protein mixture is increased and leads to more collisions. Second, the ratio of unfolded protein is increased. The ratio of unfolded protein was investigated through DSC measurements. As the unfolding is the rate-limiting step, this regime is called unfolding limited or reaction limited.

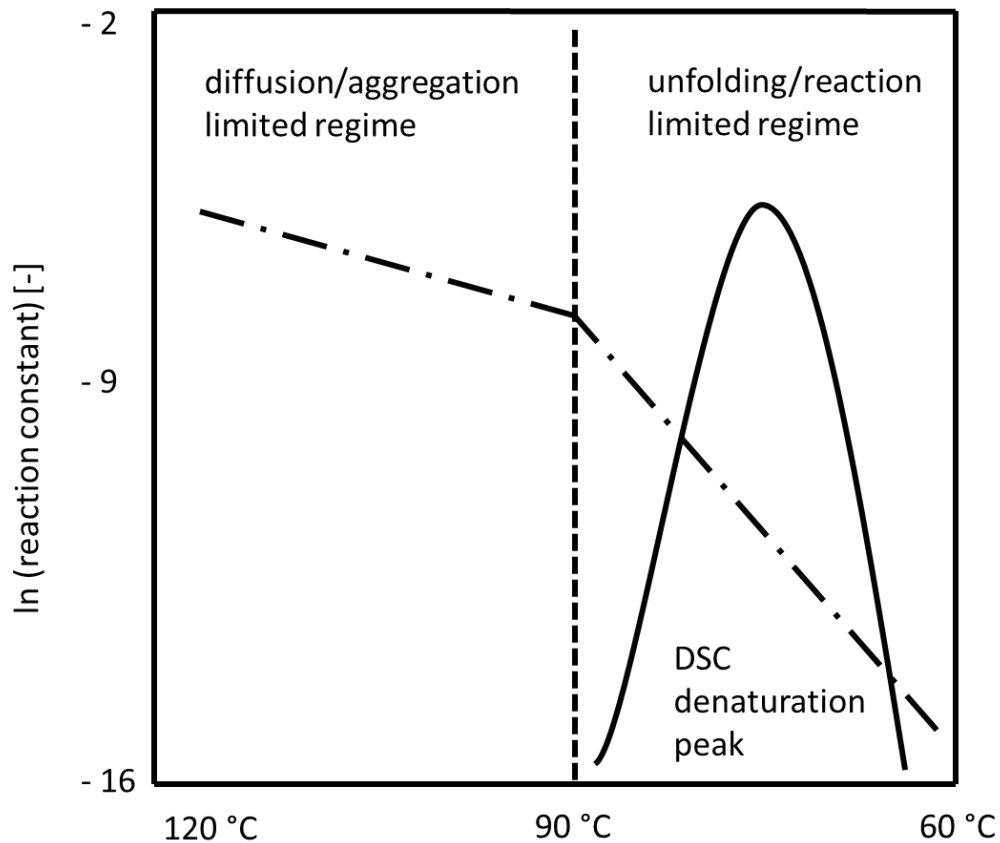


Figure 1-7 Dependence of the reaction rate of  $\beta$ -lg denaturation in dependence of the heating temperature combined with the DSC thermogram of the  $\beta$ -Lg solution, adapted from Tolkach & Kulozik, (2007), page 312, figure 6.

When the temperature exceeds 90 °C the temperature dependence is lower. This can be explained by the fact that nearly all protein is unfolded at this temperature. Therefore, the temperature dependence of unfolding, which contributed to the overall temperature dependence of the reaction can be neglected. As all protein is unfolded, every collision of two monomers can lead to aggregation. Therefore, the aggregation is only limited by the diffusion of two monomers towards each other and this regime is called aggregation limited or diffusion-limited.

#### 1.2.4 Changes in aggregate morphology in dependence of the milieu

In order to design protein structures, not only the kinetics of aggregate formation but also the morphology such as size, form, the density of these aggregates have to be understood. Changes in the interactions between protein monomers will lead to very different morphologies of the aggregate. In Figure 1-8 three distinct morphologies of  $\beta$ -lg aggregates are depicted. The different aggregates were produced through the application of heat at different pH values.

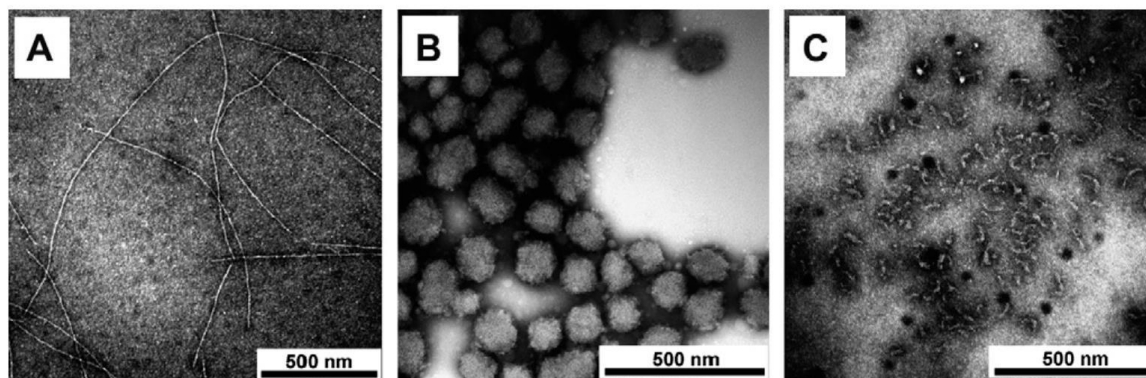


Figure 1-8 TEM micrographs of  $\beta$ -lg aggregates in a 1 % (w/w) protein solution heated at different pH values: (A) rod-like aggregates at pH 2.0; (B) spherical aggregates at pH 5.8; (C) worm-like primary aggregates at pH 7.0. Reprinted with permission from Jung et al., (2008), page 2480, figure 1. Copyright 2008 American Chemical Society.

The most common morphologies are elongated rod-like or fibrillary aggregates, spherical or particulate aggregates as well as short worm-like fibrils. The formation of these aggregate structures can be influenced by changes in pH during heat-induced aggregation.

In Figure 1-8 B the particulate aggregates are formed at pH 5.8 which is very close to the IEP of  $\beta$ -lg of 5.2 (Reithel & Kelly, 1971). These primary aggregates are nearly spherical with radii up to 150 nm (Nicolai et al., 2011). At IEP the charges of the amino acid side chains cancel each other out and the protein monomer has a neutral overall charge. Therefore, the electrostatic repulsion between the proteins is very low and proteins can aggregate easily.

Depending on the side chains interactions through hydrophobic interactions, hydrogen bonds but also oppositely charged electrostatic interactions are possible. The fact that a protein with a net charge of zero can have substantially localized charge patches can be seen for  $\beta$ -lg in Figure 1-9.

This explains how native  $\beta$ -lg can aggregate at these pH conditions. Of course, the reaction gets more complex when aggregation is induced under heating, as the increased temperature will not only result in more collisions but will also lead to a higher degree of unfolding with the exposure of further reactive groups. The charges around the protein monomers are also very important to explain the formation of long fibrils at low pH and the shorter worm-like fibrils at neutral and alkaline pH values.

At low pH levels and und low ionic strength as well as heating for a long time, fibrils with several  $\mu$ m in length but with diameters of only 4-5 nm are formed (Nicolai et al., 2011). It could be shown that these fibrils are formed in a multi-step process. First, the protein unfolds and  $\beta$ -sheets can come into contact with each other, connecting the unfolded proteins. The high electrostatic repulsion between the monomers inhibits random aggregation events and the formation can take several hours. The formation of these fibrils exhibits a certain lag time as first a nucleus has to be formed before more protein  $\beta$ -sheets can attach to this structure. It should be noted that these fibrils can also form in different solvents over several days (Gosal et al., 2004a). The second

important step is the partial hydrolysis of certain loops in the fibrils and the formation of “shaved” fibrils. Due to their very regular structure, these aggregates are also often described as “strings of beads”.

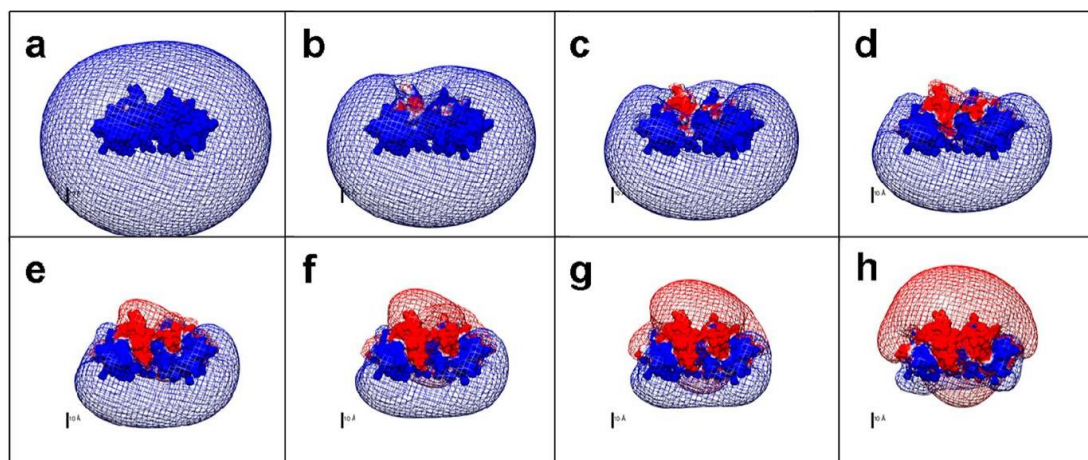


Figure 1-9 Simulation of electrostatic potential contours around a  $\beta$ -lg dimer at ionic strength 0.0045 M. pH values and corresponding net charges (blue positive charge, red negative charge): (a) 4.0, +12 mV, (b) 4.4, +7 mV (c) 4.6, +6 mV, (d) 4.8, +5 mV, (e) 5.0, +3 mV, (f) 5.2, 0, (g) 5.4, -2 mV, and (h) 5.8, -3 mV. Calculation was based on pdb ID 1BEB. Reprinted with permission from Yan et al., (2013), page 4590, figure 9. Copyright 2013 American Chemical Society.

Close relatives of these long rod-like fibrils are shorter worm-like fibrils formed at neutral or alkaline pH values. It could be shown that these fibrils have a lower amount of  $\beta$ -sheets compared to the long rod-like structures (van den Akker et al., 2011). They have a diameter of around 10 nm and a length of 100 nm. These worm-like fibrils have also been found at very acidic pH conditions in the presence of salt (Loveday et al., 2010).

To conclude, it could be shown that the morphology, especially the size and form, of protein aggregates can be greatly influenced by changes in pH and salt milieu. As an approximation, conditions of high electrostatic repulsion lead to elongated aggregate structures (amyloid fibrils as well as worm-like fibrils) and conditions of low electrostatic repulsion lead to particulate structures (Nicolai & Durand, 2013). After primary aggregation, these particulate or fibrillary aggregates form higher-ordered gel structures. These gels can be soft and opaque or hard and transparent depending on the morphology of the primary aggregates. How gels are formed and how their structure can be influenced is explained in more detail in the following section.

### 1.3 Hydrogel formation from protein solutions

Gelation describes the formation of a solid continuous network, in which pores are filled with a solvent. In the case of hydrogels, this solvent is water. These hydrogels are basic food structures. In order to understand why whey and potato proteins form different gel structures, the fundamental mechanism of gelation from proteins will be explained in the following.



### 1.3.1 General gelation mechanism

Gelation can occur in a wide range of colloidal systems ranging from inorganic silica particles to biopolymers such as starch. All have in common that after a critical parameter is surpassed the liquid turns into a viscoelastic solid, often irreversibly.

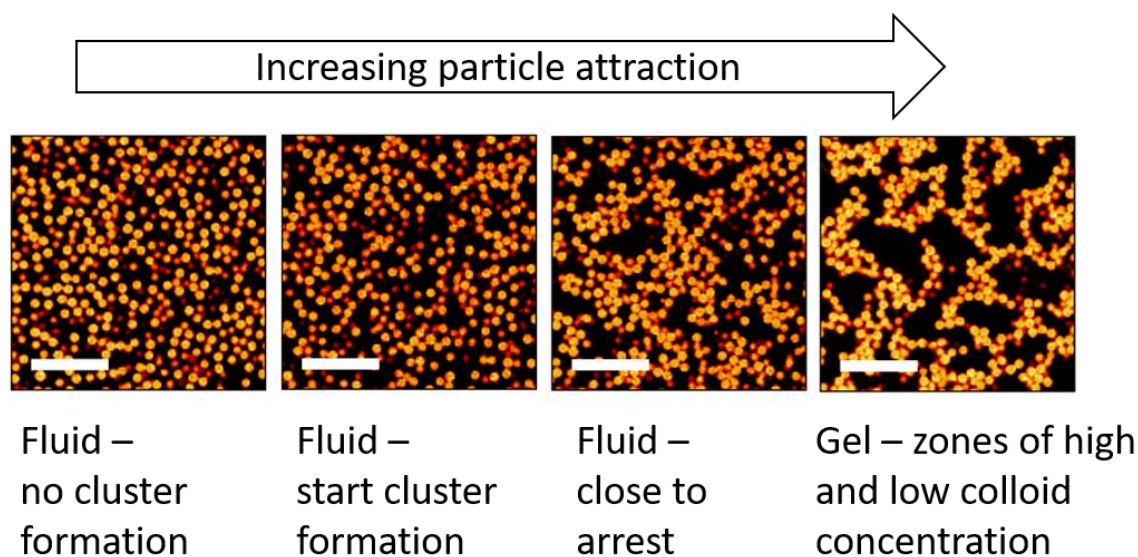


Figure 1-10 Changes in a colloidal particle suspension, consisting of polystyrene chains and polymethyl methacrylate spheres, in dependence on the attractive forces. The white scale bar represents 20  $\mu\text{m}$ . Adapted from Richard et al., (2018), page 5557, figure 2,

As the polymers vary considerably in their shape and properties different gelation mechanisms are proposed. However, as globular protein monomers resemble spherical particles the gelation mechanism is often approximated as gelation of sticky spheres (Nicolai & Durand, 2007). How colloidal particles can turn a liquid sol into a solid gel is depicted in Figure 1-10.

The attractive forces between the inert colloidal particles were increased by the addition of a polymer (Richard et al., 2018). It can be seen that with increasing particle attraction colloidal clusters form within the fluid. The fluid remains liquid until a critical point of attraction is reached. Above this point, the solution arrests, and areas with dense colloid clusters as well as areas completely devoid of protein form.

These results obtained for inorganic particles can be transferred to protein gelation. When the protein concentration in a solution exceeds a certain concentration, denaturation of proteins will not only result in the formation of aggregates but will lead to gelation (Foegeding, 2006). Depending on the dominance of long-range repulsive or attractive forces, very different aggregate shapes and structures can be induced. These different aggregate architectures will lead to very different microstructures in the hydrogel. An overview of different structures ranging from particulate and spherical to linear and fibrillary aggregates is given in Figure 1-11.

A helpful concept for describing the structure of hydrogels is the fractal dimension ( $d_f$ ). The concept was first described by the mathematician Benoit Mandelbrot (Mandelbrot, 1983) and describes the “roughness” or “self-similarity” of geometrical objects. For example, a simple straight line will have a  $d_f$  of 1 whereas more branched structures



(fractals) will have higher  $d_f$ . Another important property of these fractals is their self-similarity over different length scales. In the classic example, Mandelbrot describes a measurement of the coastline of England. When zooming in, the measured length is increased every time. Therefore the length was not deemed a suitable description of these structures. However, the “roughness” of the coastline was the same on every length scale. This roughness was described as the fractal dimension. In the same way, colloidal particles were shown to form fractal-like structures with a high degree of self-similarity, described by  $d_f$ , over different length scales. There are different methods described in the literature to determine the fractal dimension of protein aggregates and gels, ranging from light, x-ray, and neutron scattering measurements (Bushell et al., 2002). The scattering methods are helpful in deriving  $d_f$  as they measure structural elements over different length scales. The self-similarity over different length scales is an important premise in deriving  $d_f$ .

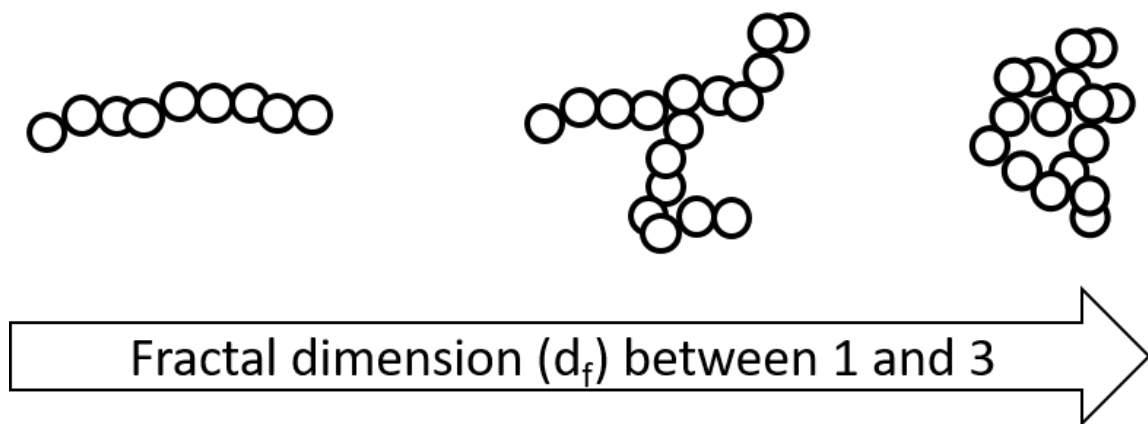


Figure 1-11 Schematic overview of how fractal dimension ( $d_f$ ) can change in aggregate systems

Depending on the mode of aggregation, the  $d_f$  of an aggregate can be influenced. Under diffusion-limited aggregation, where every contact between two particles results in aggregation of these particles, the  $d_f$  is lower than under reaction limited aggregation, where not every contact results in aggregation (Weitz et al., 1985). Therefore, denser, more branched aggregate structures are expected under reaction limited aggregation (see chapter 1.2.3 for different reaction regimes occurring in food proteins).

Besides scattering methods, different rheological models exist to derive  $d_f$  from rheological properties such as storage modulus ( $G'$ ) or limit of linear viscoelasticity (see also section 1.3.4 for more on rheological characterization) (Shih et al., 1990; Wu & Morbidelli, 2001). However, the method of deriving  $d_f$  from rheological properties in dependence protein concentrations can be disputed as the gel structure is not investigated over several length scales (Kavanagh et al., 2000).

The main takeaways with regard to this thesis should be: Gels are built by smaller primary structures such as aggregates. There exists a certain self-similarity between the aggregates and the overarching macrostructure of the gel. Furthermore, microstructural changes lead to changes in rheological properties, and microstructure can be influenced through different reaction conditions and reaction mechanisms. How the

microstructure of hydrogels can be influenced through different milieu conditions during gelation is described in the following section.

### 1.3.2 Change in gelation behavior in dependence of pH

The different primary aggregates described in section 1.2.3 form gels, provided a certain critical concentration is exceeded. It was already described that different aggregate shapes can be induced in dependence on the electrostatic interactions. As this thesis aims to understand gel structure from novel protein sources under different milieu conditions, the general influence of these milieu conditions is described in the following. How changes in aggregate morphology affect the gelation of  $\beta$ -lg is depicted in Figure 1-12.

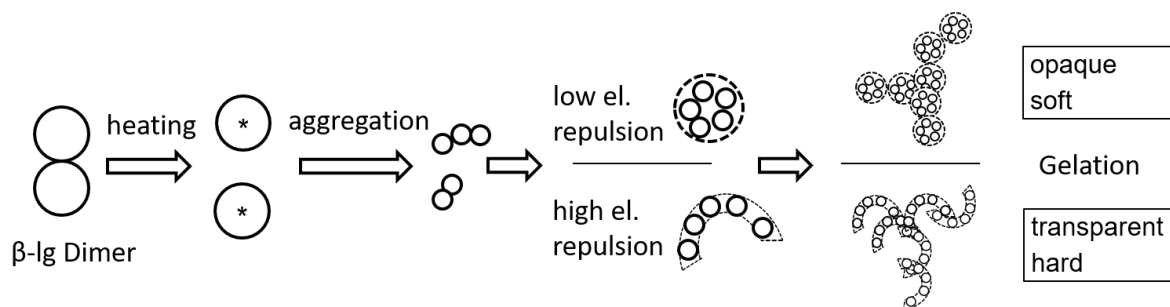


Figure 1-12 Schematic representation of the heat-induced aggregation processes occurring in  $\beta$ -lg solutions under conditions of high and low electrostatic repulsion. First,  $\beta$ -lg dimers dissociate into monomers, which then react further into different aggregate and gel structures. Adapted from Nicolai & Durand, (2013), page 254, figure 2.

Depending on the structure of the primary aggregates, the resulting microstructure of the hydrogels can vary considerably. The short worm-like aggregates form very homogeneous networks, whereas the particulate aggregates form structures with considerable phase separation, visible in areas devoid of protein. This change in microstructure can be seen for WPI gels in Figure 1-13.

The gelation mechanism can be described as follows: At higher electrostatic repulsion, branched fractal-like aggregates are formed that form homogeneous gels. Under conditions of low electrostatic repulsion, spherical aggregates, sometimes referred to as microgels, are formed. The resulting macrostructure exhibits a very porous network. How all these mechanisms can be utilized to fine-tune the properties of protein systems is discussed in the following.

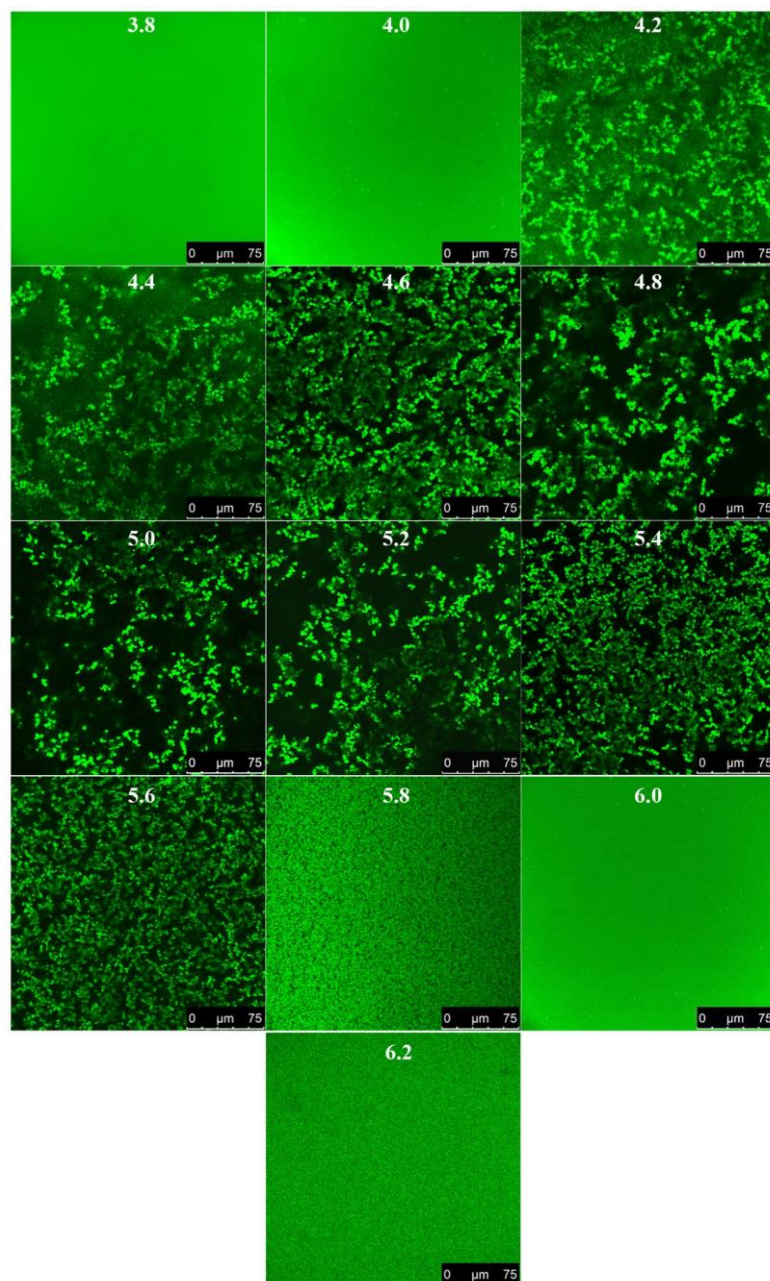


Figure 1-13 CLSM images of 10% WPI gels. Numbers indicate the pH values. The green color indicates protein structures. Taken from Homer et al., (2018)

A detailed investigation into pea protein aggregation revealed that the system can form very different structures depending on the pH and heating conditions (Cochereau et al., 2019). First, it could be shown that the protein suspension showed microphase separation into protein-rich and protein-depleted domains after the pH is lowered (see chapter 1.2.4 for background on this phenomenon). Upon heating, these protein-rich domains redispersed, leading to a homogenous suspension rather than a phase separation. However, aggregation also occurred. Depending on the relation of the aggregation and redispersion rate three distinct structures could be obtained (see Figure 1-14).

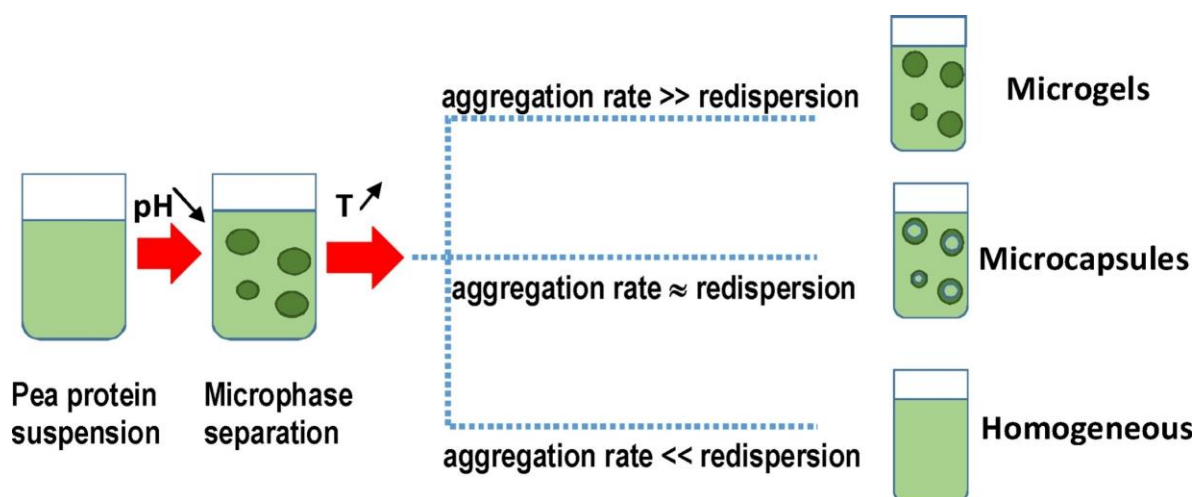


Figure 1-14 Dependence of aggregate structure on aggregation and redispersion rate of a pea protein solution. Taken from Cochereau et al., (2019), graphical abstract.

If the aggregation rate was higher than the redispersion rate, the microphase separated domains formed microgels. However, if the redispersion rate was much higher than the aggregation rate, the microdomains dissolved and a homogeneous aggregate mixture could be obtained. A special case is when aggregation and redispersion rates were similar. In this case, microcapsules formed with a gelled hull and liquid core. The authors postulated that this behavior should not be unique to pea proteins but rather a property of globular proteins.

One can conclude that in dependence on the electrostatic interactions between protein monomers, very different aggregate structures could be obtained. Particulate aggregates, created under low electrostatic repulsion resulted in the creation of heterogeneous gels with big voids. Fine stranded aggregates, created under high electrostatic repulsion resulted in very homogenous gels.

However, thus far only the gelation in dependence on the pH was described. As the electrostatic interaction between the proteins can be also influenced by salts the influence of ions on the gel properties will be explained in the following.

### 1.3.3 Change in aggregation and gelation behavior in dependence of salt addition

Similar to changes in pH, changes in the ion milieu of a solution can considerably influence the microstructure of protein gels. One important influence of salt addition is the shielding of charges of the protein monomers by counter ions of the salt. This shielding of charges leads to lower electrostatic repulsion between the protein monomers and thus changes the aggregate structure from fine-stranded to coarse, particulate structures. This change in optical appearance and microstructure can be seen in Figure 1-15.

Another influence of salt on the gelating properties of globular proteins is the change of minimum gelation concentration. Increasing the amount of NaCl in protein solutions reduced the protein concentration necessary for gelation for soy glycinin, patatin, ovalbumin, and  $\beta$ -lg (Creusot et al., 2011). Clear differences between the protein sources

regarding the minimum gelation concentration and the dependence on the ionic strength could be observed. These differences could be explained by differences in the exposed hydrophobicity. For proteins with a higher exposed hydrophobicity, such as patatin, a small increase in ionic strength led to considerable increases in aggregation which explains the low minimum gelation concentration. For proteins with a lower exposed hydrophobicity, an increase of solubility is observed with a small increase in ionic strength.

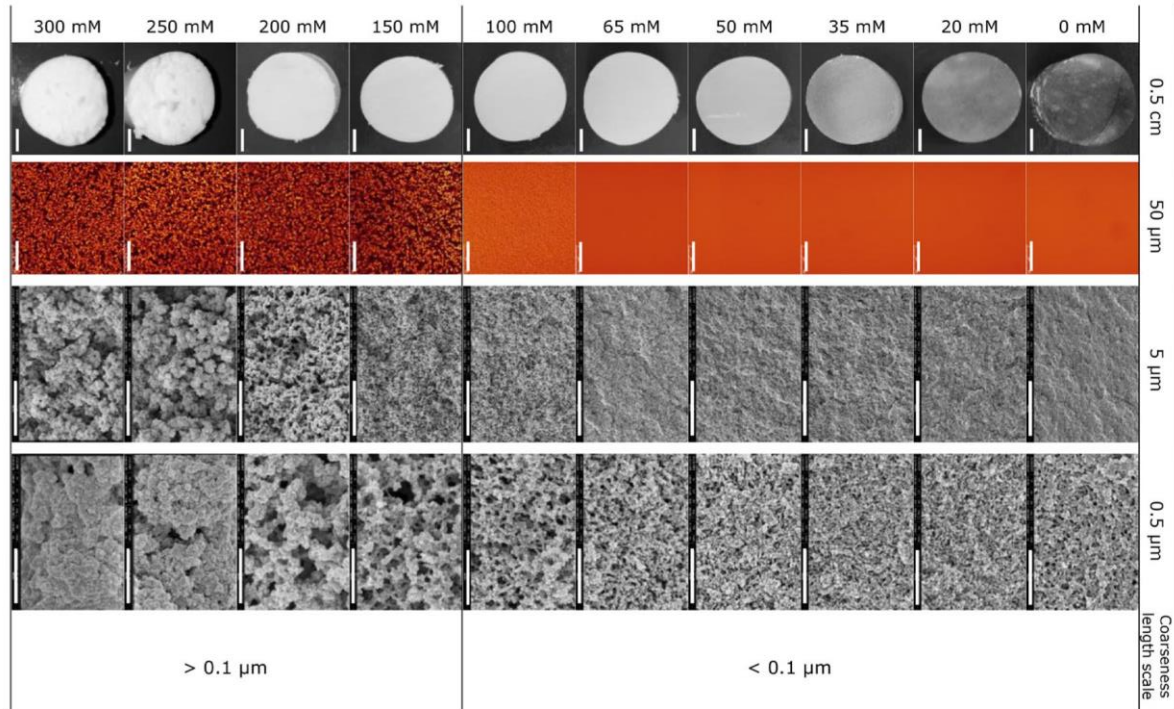


Figure 1-15 Microstructure of WPI gels in dependence of the NaCl content, determined by CLSM and SEM, taken from Urbonaite et al., (2016), page 337, figure 1.

Therefore, it could be shown that ions can increase as well as decrease the solubility of proteins. These opposite effects of salting in (increasing solubility) and salting-out (decreasing solubility) are best described in the Hofmeister series of cations and anions (see Figure 1-16).

Depending on the kind of anions and cations used, proteins are affected differently (an overview is given by Okur et al., (2017)). Kosmotropic ions such as potassium and hydrogen phosphate decrease the solubility of proteins by increasing the tendency of proteins to form aggregates. At the same time, the tertiary structure is stabilized and therefore protein denaturation is low. Chaotropic ions such as calcium ( $\text{Ca}^{2+}$ ), guanidium (Gu), and thiocyanate (SCN) induce the opposite effects. In the presence of these salts, the protein structure is destabilized and proteins denature. At the same time, these denatured proteins are kept in solution. To determine the chaotropic/kosmotropic character of a salt, anions and cations have to be investigated in combination. For example,  $\text{NaPO}_4$  will have a more kosmotropic effect than  $\text{NaCl}$ , as  $\text{PO}_4^-$  is more kosmotropic than  $\text{Cl}^-$ . An overview of different salt systems is given by Melander & Horváth, (1977).



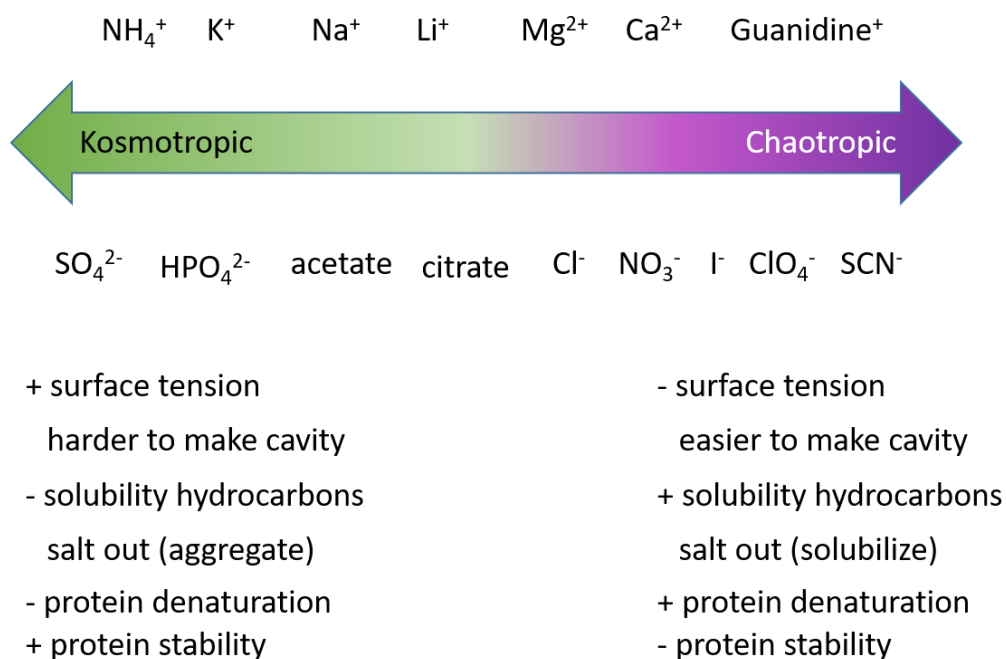


Figure 1-16 Overview on the effect of anions and cations according to the Hofmeister series, adapted from Okur et al., (2017), page 1998, figure 2.

The destabilizing and solubilizing effect of Gu and SCN is best explained in light of the hydrophobic effect, which will be explained in the following. First of all, strictly polar and non-polar substances do not mix. This is the reason oil and water interfaces separate in absence of emulsifiers. This also plays a role in protein folding as the hydrophobic amino acids orient themselves towards each other. They cluster in the protein core, away from the polar water that surrounds the protein monomers. To expose these hydrophobic side chains into the water phase, first, a cavity has to be formed in which the non-polar residue can be exposed, followed by a structuring effect of the water around the residue. A schematic representation of this effect is given in Figure 1-17.

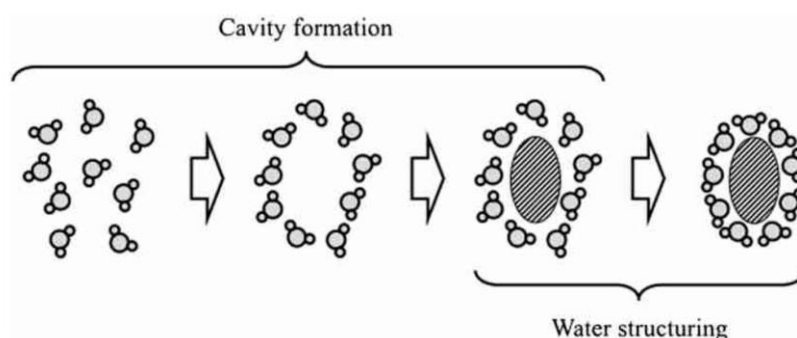


Figure 1-17 Transfers of hydrophobic component (shaded oval) into water. Taken from Kronberg, (2016), page 17, figure 4.

Chaotropic ions facilitate the transfer of hydrophobic components by influencing the structure of water in two ways. First they “break” the water structure, which is evident in the reduced surface tension of water in presence of these salts (Melander & Horváth,

1977). This “breakage” allows for the easier formation of a cavity and the lack of hydrogen bonding that occurs with these salts facilitates the insertion of hydrophobic molecules in these cavities.

The effect of kosmotropic and chaotropic ions on the gelation of WPI was investigated in two studies, which shall be reviewed in the following. Increasing the ion concentration in WPI lead to a transition from a fine stranded to a particulate microstructure, with a mixed structure in between. A general relationship between textural properties and microstructure could be found (Bowland & Foegeding, 1995), depicted in Figure 1-18.

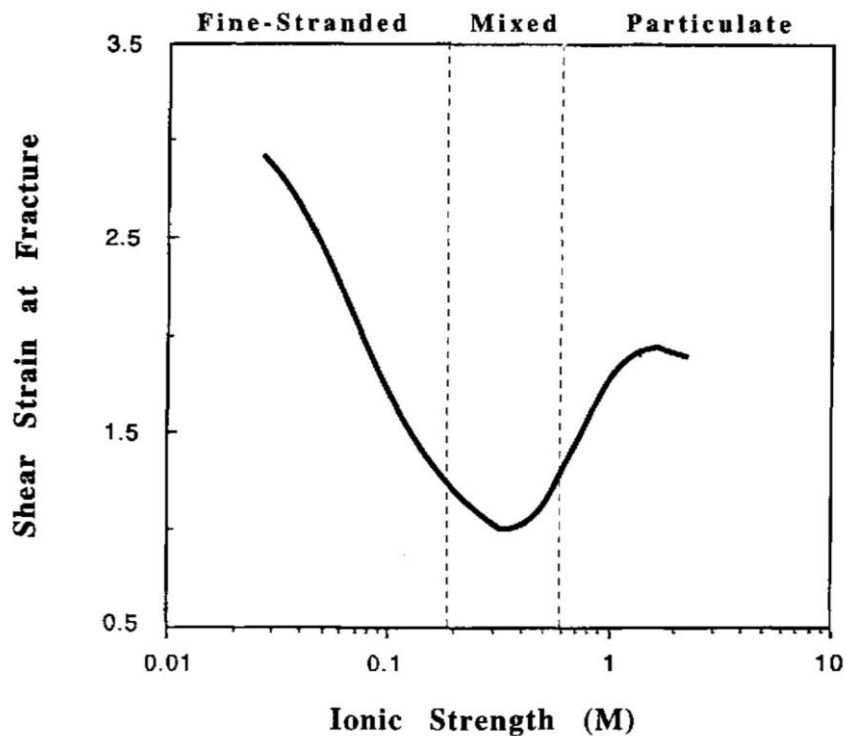


Figure 1-18 General relationship between shear strain at fracture and microstructure (fine, mixed or particulate) of WPI gels in dependence of the ionic strength, taken from Bowland & Foegeding, (1995), *Effects of anions on thermally induced whey protein isolate gels*, page 52, figure 4.

It can be seen that increasing the ionic strength led to changes in the gel microstructure from a fine-stranded to a particulate microstructure. In between those two extremes a mixed structure can be observed, which exhibited the lowest resistance against fracture. Particulate structures exhibited lower shear strain at fracture which is due to changes in the protein interactions that stabilize the proteins, from covalent to non-covalent bonds.

Although the general trend between all tested salts was the same, there were notable differences between the ions depending on their position in the Hofmeister series. Kosmotropic ions facilitated the change from fine-stranded to particulate matrices, whereas chaotropic SCN anions inhibited the transition.

In a follow-up study, the rheological properties of these different gels were investigated. For this, the relation between the storage modulus of the gel at gelation temperature

( $G'_{hot}$ ) was related to the storage modulus of the protein after gelation and cooled down to ambient temperatures ( $G'_{cool}$ ) (Bowland et al., 1995).

It could be seen that the proteins gels reacted differently to the temperature change. Particulate gels had higher  $G'_{cool}/G'_{hot}$  values than fine-stranded or mixed structures. Furthermore, there were clear differences between chaotropic and kosmotropic ions at higher ionic strength. Kosmotropic ions led to structures that increased  $G'$  upon cooling ( $G'_{cool} > G'_{hot}$ ). Chaotropic SCN, on the other hand, led to structures with higher  $G'$  values at high temperatures compared to low temperatures ( $G'_{hot} > G'_{cool}$ ). Bowland et al., (1995) hypothesized that the increase was due to increased hydrophobic interactions at elevated temperatures. The presence of SCN promotes the exposure of hydrophobic amino acids and thus the structure should be stabilized more through hydrophobic interactions, rather than other protein interactions.

It should be noted that most of the known effects were described for monovalent ions. However, there are also divalent ions such as Calcium ( $Ca^{2+}$ ) which can induce calcium bridges between proteins chains, by binding to two negatively charged amino acid side chains from two protein monomers, thereby introducing another way to connect proteins. As these interactions are not relevant for the here presented study they are not further considered.

#### **1.3.4 Rheological characterization of hydrogels**

To characterize hydrogels, rheological measurements are one of the most used and most important tools. These measurements are performed in rheometers. In a rheometer, a sample is sheared between two “plates”. It should be noted that a lot of different geometries for these “plates” exist. However, in the here presented study, we will focus on two concentric cylinders with a small gap between them. The shearing can be done either rotational or oscillating. The focus will be put on the oscillatory deformation as this can be used to determine the viscoelastic properties of gels without destroying their structures (Mezger, 2006).

For this, samples are sheared to a certain degree of deformation in one direction followed by deformation by the same degree in the other direction. The frequency of this deformation can be varied but is often around 1 Hz or 10 rad/s. The applied strain ( $\gamma$ ) follows a sinusoidal deformation and the resulting stress response ( $\tau$ ) can be measured. Depending on the behavior of the sample, the strain and stress function is either in-phase or a certain phase angle can be observed ( $\delta$ ). A schematic representation of this process is given in Figure 1-19.

Hydrogel samples exhibit viscoelastic behavior, a response which is between purely viscous samples (such as Newtonian fluids) and purely elastic samples (such as springs according to Hooke's law). To understand how viscoelastic behavior can be characterized by oscillatory rheology, one has to consider these two extremes.

A purely viscous response is measured in Newtonian fluids. It is modeled with the response of a damper where the stress response is offset to the applied strain ( $\delta = 90^\circ$ ). After a full strain cycle ( $\gamma = 0$  to  $\gamma = 0$ ) the fluid remains deformed ( $\tau = +/-$ ). On the other hand, a sample with a purely elastic stress response can be abstracted as a spring. In



this case stress and strain move in tandem ( $\delta = 0^\circ$ ). The highest strain is measured when the spring exhibits the highest deformation. Therefore, viscoelastic samples, such as protein gels, exhibit phase angles between these two extrema ( $0 < \delta < 90^\circ$ ).

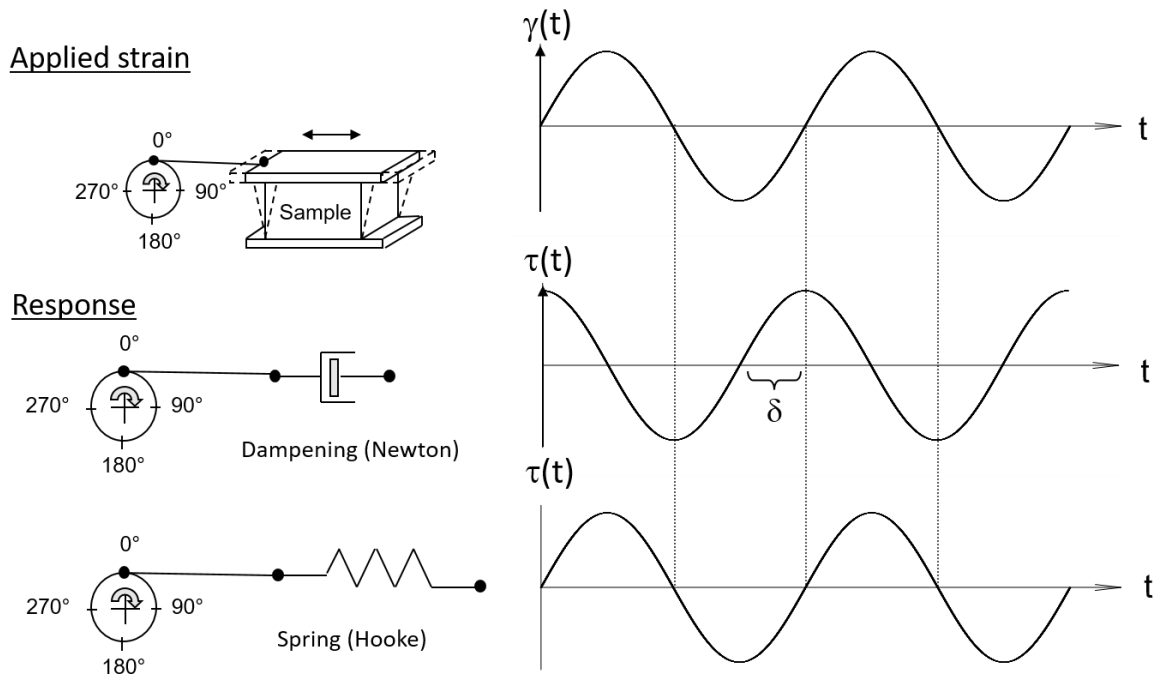


Figure 1-19 Correlation between applied stress and response of the sample. Adapted from Mezger, (2006), with permission from publisher "Vincentz Network".

From these strain-stress responses, the storage ( $G'$ ) and loss ( $G''$ ) modulus can be obtained.  $G'$  represents the elastic and  $G''$  the viscous behavior of a sample. As shown before,  $\gamma$  and  $\tau$  should move in tandem in a purely elastic sample. Therefore, the function of  $\delta$  should yield 1. For  $\delta = 0^\circ$  this function has to be a cosinoidal function and the corresponding correlation is given in Equation (1-8).

$$G' = \frac{\tau}{\gamma} * \cos(\delta) \quad (1-8)$$

As mentioned above, the stress response is offset in a purely viscous sample. Therefore, for  $\delta = 90^\circ$  the function has to be a sinus function. The viscous response is described in Equation (1-9).

$$G'' = \frac{\tau}{\gamma} * \sin(\delta) \quad (1-9)$$

From  $G'$  and  $G''$  the loss factor ( $\tan \delta$ ) can be obtained.

$$\tan(\delta) = \frac{G''}{G'} \quad (1-10)$$

The loss factor gives information on whether elastic or viscous behavior dominates the rheological behavior of the sample. A  $\tan(\delta) > 1$  can be measured for viscoelastic fluids,  $\tan(\delta) < 1$  for viscoelastic solids, such as gels. When trying to identify gelation

phenomena where a viscoelastic liquid, such as a protein solution, turns into a viscoelastic solid, such as a hydrogel, the point in time where  $\tan(\delta) = 1$  is often referred to as the gelation point.

Besides these basic oscillatory measurements, certain tests are frequently used to investigate the rheological characteristics of gels. These are temperature, frequency, and strain sweeps and are explained in the following. Schematic drawings that represent the fundamental relationship of these tests are depicted in Figure 1-20.

Temperature sweeps refer to oscillatory experiments where the temperature is changed over a certain time frame. Depending on the sample, cooling or heating can induce gelation and the change from a fluid ( $G'' > G'$ ) to a solid ( $G' > G''$ ) can be observed.

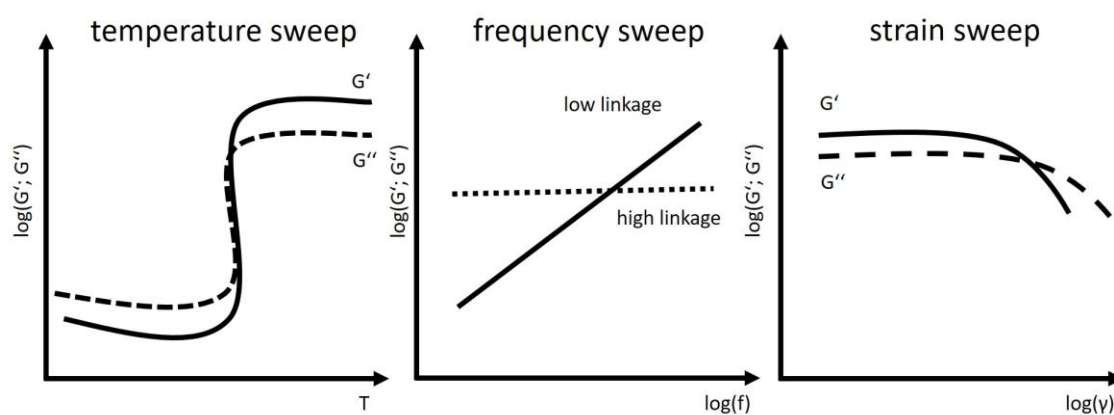


Figure 1-20 Schematic representation of temperature, frequency, and strain sweep

For frequency sweeps, the strain amplitude is kept constant and the frequency is increased logarithmically. As the frequency is the inverse function of time the frequency sweep is used to simulate the time stability of a sample. This can be used to simulate the shelf stability of emulsions, for example (Schmidt et al., 2018). When gels are subjected to frequency sweeps, the change in  $G'$  and  $G''$  in dependence of the frequency can be used to estimate the types of links stabilizing the gel network (Egelandsdal et al., 1986). Covalently linked gels show a low dependency of  $G'$  and  $G''$  on the frequency. This is because real covalent bonds are very stable over a long time frame. Non-covalent linked gels, or sometimes referred to as physical gels, exhibit a high dependency on time. Electrostatic and hydrophobic interactions are less stable over time, which explains the higher frequency dependence.

The third test is the strain sweep, sometimes referred to as amplitude sweep. Here the frequency is kept constant, but the strain is increased logarithmically. Up to a certain strain amplitude  $G'$  and  $G''$  remain constant. This is called the linear viscoelastic range (LVE). In this range, the deformation does not induce any changes in the gel structure. This is the reason why the strain sweep is often used on unknown samples to obtain the LVE at which oscillatory measurements can be conducted without destroying the microstructure. Although only a decrease of  $G'$  and  $G''$  is depicted in dependence of  $\gamma$ , also increases in  $G'$  and/or  $G''$  can occur. Although this is not typical for globular protein

gels, some bigger molecules such as collagen can “jam” into each other upon high shearing and increase  $G'/G''$  of the sample (Hyun et al., 2011). For gels, however, when the strain is increased above the LVE range  $G'$  and  $G''$  usually drop in value. This can be explained by the breakage of bonds or some sort of strain thinning. If the LVE spans a wider or smaller range is also dependent on the bonds in the gel. For example, protein gels from patatin and the green leaf protein ‘RuBisco’, both of which are stabilized through non-covalent bonds, were shown to have smaller LVE ranges when compared to covalently linked gels from  $\beta$ -lg or other whey proteins (Martin et al., 2014; Creusot et al., 2011). As oscillatory measurements are usually performed at low deformation, a strain sweep can help to characterize gels under high shear conditions. Conditions of high strain under which the sample fractures are often more predictive of the textural and sensory properties of food during chewing (Bourne, 2002). However, after the strain sweep, the structure of the gel is irreversibly deformed and thus these tests should be performed after the others.

#### 1.4 Alco- and Aerogels

In the previous chapters, the focus was on the creation of hydrogels from proteins as these structures are the best researched. However, gels, in general, describe two-component systems and the pores can be filled not only with water but also with other solvents such as alcohols or even just with air. These two special forms are discussed in the following section. Alcolgels are created by the washing of hydrogels in organic solvents, such as ethanol (EtOH), thus gradually replacing the aqueous phase. These EtOH-filled structures can be dried by the extraction of EtOH from the pores through supercritical carbon dioxide (scCO<sub>2</sub>) drying. These dried gels are then called aerogels. The drying step by scCO<sub>2</sub> is only possible when the solvent has sufficient solubility in scCO<sub>2</sub>, which is not the case for water. This explains why the solvent exchange from water to an organic solvent is a necessary premise for the creation of aerogels.

Protein-based aerogels were shown to be potent encapsulation systems for hydrophobic substances, such as fish oil (Selmer et al., 2019), and their use for targeted release of the oil in the intestine was shown (Kleemann et al., 2020a). Because of this interesting field of application and the possibilities to investigate the microstructure of protein gels further, alco- and aerogels will be explained in more detail in the following. For these systems few data is published on protein gels, therefore conclusions have to be drawn from other organic but also inorganic materials.

##### 1.4.1 Alcolgels: Structural changes upon solvent exchange

The exchange of the solvent filling the pores of a gel network has profound effects on its structure. These solvent exchanges result in organogels, sometimes also referred to as alcolgels if the organic solvent is an alcohol. Upon solvent exchange, shrinkage can be observed in the gel structure. Depending on the solvent, this shrinkage can be very different in extent. An overview of the effect of different solvents on the shrinkage behavior of alginate gels is given in Figure 1-21.

It can be seen that the shrinkage occurring in the organogels varies greatly across the investigated solvents. One important factor was the solubility of alginate in the different

solvents. At low solubility, the shrinkage was very high. Lower shrinkage was observed when the solubility was increased. Especially the amount of hydrogen bonding was important to determine the amount of shrinkage (Subrahmanyam et al., 2015). From all these different solvents, ethanol (EtOH) is the most suitable for applications in the food sector.



Figure 1-21 Shrinkage of alginate hydrogels in dependence of the solvent. (a) methyl ethyl ketone (MEK); (b) isopropanol (IPA); (c) acetone; (d) 1-butanol; (e) methanol (MeOH); (f) dimethyl sulfoxide (DMSO); (g) glycerol; (h) propylene glycol; (i) ethylene glycol; (j) ethanol; (k) 1,4-dioxane; (l) propylene carbonate; (m) furfuryl alcohol; (n) N,N-dimethylformamide (DMF) and (o) acetonitrile. Taken from Subrahmanyam et al., (2015)

Therefore, the influence of EtOH on the structure of egg white protein (EWP) and WPI hydrogel capsules was assessed (Kleemann et al., 2020b). Up to 60% EtOH, no measurable changes in gel properties could be observed. The proteins shrank down to 40% of initial volume when EtOH content in the pores was increased to 80%. Between 80 and 100% EtOH the volume stayed constant. Simultaneously the hardness of the gel capsules increased up to 30 fold. Especially between 80% and 100% EtOH the hardness increased from ~ 20 N to 90 N for WPI gels at pH 10 and up to 60 N for WPI at pH 7. This led to the observation that shrinkage and increase in hardness were more pronounced in alkaline hydrogels, compared to gels at lower pH levels. These effects are schematically depicted in Figure 1-22.

Furthermore, it could be shown, that the highest increase in hardness occurred between 80-100% EtOH, while the relative volume due to shrinkage did not change any further. Therefore shrinkage and hardness did not correlate and Kleemann et al., (2020b) concluded that shrinkage cannot be the main factor to explain the increase in hardness.

The characterization through compression further revealed that in the range where hardness increased also a strong decrease in elasticity in the capsules could be observed. It seems reasonable to assume that the interactions stabilizing the protein network are probably influenced by the change of the solvent.

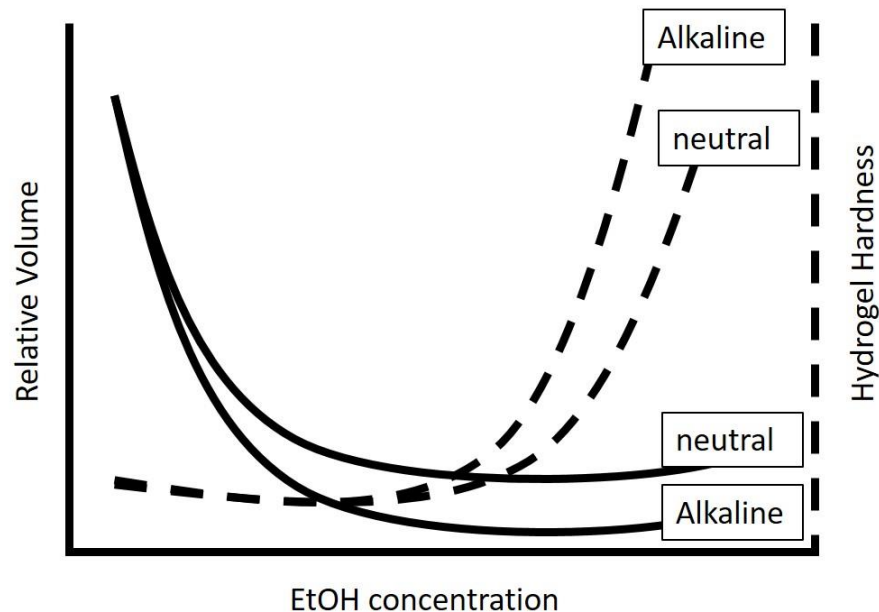


Figure 1-22 Influence of EtOH concentration on protein hydrogels. Schematic representation of findings by Kleemann et al., (2020b). Hardness increases substantially at high EtOH content, whereas shrinkage occurs especially during the beginning of the solvent exchange.

First, the electrostatic repulsion between protein amino acid side chains is reduced as EtOH has a lower permittivity than water, an effect which was already discussed for the influence of solvents on protein interactions in chapter 1.2.2. The same effects that led to the aggregation of protein allow the strands forming the gel to get in closer contact with each other, thereby increasing the resistance against deformation.

Furthermore, investigations on the ion content of the solutions revealed that the interactions with ions and the proteins increased and fewer ions were soluble in EtOH. This could further enhance the effect of the reduced permittivity by reducing the charges on protein side chains. Both effects will lead to a dominance of hydrophobic interactions and other non-covalent bonds over the covalent bonds, explaining the shift from soft but elastic hydrogels to hard and brittle alcogels.

After explaining the structural changes occurring during the exchange from water to EtOH we will explain the structural changes occurring during the extraction of EtOH through  $\text{scCO}_2$ .

#### 1.4.2 Aerogels: Porous gel structures through supercritical drying

Although the nomenclature differs across publications, the term aerogel will only be used for gels dried by  $\text{scCO}_2$  extraction. These gels were first created from inorganic materials such as silica (Yokogawa & Yokoyama, 1995) and carbon (Job et al., 2005). For these systems, it could be shown that the drying through  $\text{scCO}_2$  led structures

without pore collapse. This porous structure makes aerogels some of the lowest density solids with very good insulation thermal properties (Baetens et al., 2011). The high porosity is also coupled with high inner surface areas of a couple hundred  $\text{m}^2/\text{g}$  aerogel. This makes aerogels also excellent absorbers with possible applications in the clean-up of oil spills (Reynolds et al., 2001).

To understand the effect  $\text{scCO}_2$  drying and its advantages over other drying methods, such as freeze-drying, one has to consider the extraction of solvent from the pores. The changes occurring within the pores for the three most important drying methods are depicted in Figure 1-23.

The simplest form of drying is drying under ambient pressure due to evaporation. Gels dried in this way are called Xerogels. At the interface between air and solvent in the pore, the surface tension of the solvent exerts a force on the pores. During the drying process, the evaporating water pulls the pores closer together resulting in pores collapse and shrinkage. The solvent undergoes a phase transition from liquid to gaseous.

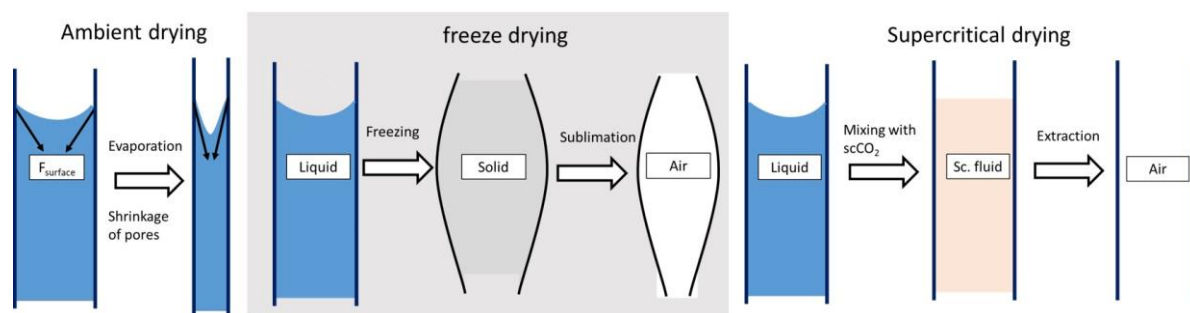


Figure 1-23 schematic process of three most common drying methods and their influence on the pore structure.

During freeze-drying, liquid water is first frozen and then extracted through sublimation. Although this process is more gentle on the product and a certain amount of pore structure can be kept intact, the process is very sensitive towards the freezing step. To keep the pores intact, water has to be frozen rapidly to keep ice crystal growth low. Nevertheless, the expansion of water upon freezing will always damage pores to some extent. This will leave damaged pores after the ice is sublimated. The water undergoes a phase transition from liquid to solid to gaseous. Gels dried in this way are sometimes referred to as cryogels.

The third process is the extraction of the solvent via  $\text{scCO}_2$  extraction. The solvent and  $\text{scCO}_2$  mix within the pores under high pressure and medium temperature conditions in a high-pressure autoclave. This way a supercritical fluid consisting of  $\text{CO}_2$  and the solvent is formed. Therefore no phase transition occurs. This supercritical fluid can be extracted by careful depressurization which leaves the pores intact. That pores are exceptionally well preserved can be seen in the high amount of pores in the micro ( $< 2 \text{ nm}$ ) and meso (2-50 nm) range.

This high inner surface area and pore volume allow for interesting applications in food and biosciences. Aerogels from biopolymers have been successfully used as delivery systems for hydrophobic drugs like Ibuprofen (Mehling et al., 2009) or neutraceuticals

such as fish oil (Selmer et al., 2019). In-vitro digestion of protein aerogels loaded with fish oil revealed that the protein matrix was resistant against digestion in the oral and gastric phases (Kleemann et al., 2020a). However, under simulated intestinal conditions, the capsules did dissolve and released the encapsulated fish oil. This showed the feasibility of the aerogel protein capsules as a novel encapsulation system.

Other promising applications are in the field of oleogelation. Oleogelation describes the structuring of oil to obtain solid fats that do not melt at room temperature. These structures can be obtained through different waxes and sterolic acids (Fayaz et al., 2020). However, proteins also found applications as oleogelator, either through the addition of aggregates to oil (Vries et al., 2017) or through a stepwise solvent exchange (Vries et al., 2015). The aggregates formed a gel-like network when the interactions between the aggregates were stronger than the interactions with the oil. The solvent route changed the liquid in the gel network from water to solvent to oil. This solvent route is similar to the solvent exchange steps during the aerogel process, this is why aerogels were also investigated as oleogelators by other research groups. WPI aerogels were shown to structure sunflower oil to achieve similar rheological and textural properties as commercial shortenings (Plazzotta et al., 2020). At the same time, freeze-dried gels were not able to induce these structures when mixed with oil. This is a clear indication that the porous structure of aerogels is beneficial for oleogelation.





## 2 Objective and outline

Proteins are one of the most important ingredients in food. With the advent of new protein sources, especially plant-based ones, the need to understand how their techno-functionality can be influenced grew in recent years. As a lot of research in the past was done on whey proteins, especially  $\beta$ -lactoglobulin, what is known about protein unfolding, aggregation and gelation should be re-evaluated, extended, and modified for these new proteins.

Therefore, structure formation from plant proteins in comparison to animal-derived proteins will be the focus of this thesis. A water-soluble patatin rich potato protein isolate (PPI) will be used as one example of novel plant-based proteins. Its reaction mechanism will be investigated on a micro-scale during aggregation to a higher scale by investigating its gelation behavior. By creating aerogels from these hydrogels the microstructure that is created under different gelation mechanisms will be investigated.

First, a method should be adapted from the literature to quantify the protein interactions stabilizing protein hydrogels. This method will be used in other chapters throughout the thesis to understand the different interactions occurring in dependence on milieu conditions and protein sources.

To understand how PPI forms gel structures, first, the aggregation mechanism was to be investigated. For this, the influences of milieu conditions such as temperature, pH, and also the presence of minor components were investigated. This was accompanied by an in-depth investigation into unfolding and aggregation behavior to determine changes in the aggregation mechanism in dependence of the temperature.

How these PPI aggregates form gel structures was investigated afterward. By supercritical CO<sub>2</sub> drying (scCO<sub>2</sub>) of the hydrogels, aerogels were produced. The gentle drying mechanism kept the pore structure of the gel network intact. Therefore, the investigation of the aerogel structure allowed to determine changes in microstructure during gelation. By comparing the rheological properties of the hydrogels with structural parameters of the aerogel new ways to predict structural parameters from rheology were assessed.

The relation between protein interactions, rheological properties, and microstructure was also investigated for other gel systems. Mixtures of WPI and PPI were gelled to create hybrid gels of both protein systems. Depending on pH and ion milieu very different rheological and textural properties could be created. The differences should be explained, possibly by differences in the protein interactions.

WPI and PPI gels were also compared when gelled in the presence of ethanol (EtOH). EtOH is a powerful denaturant and very different gel structures could be induced through the combination of EtOH and increased temperature.

Overall, the expected results and their interpretation were aimed at yielding a mechanistic understanding of how protein gels are formed and how molecular features of the protein source influence gel formation. Further to that, it should be analyzed how and

why different protein sources respond differently to changes in milieu and heating conditions and how rheological measurements can be utilized to investigate changes in protein interactions. The results will provide the base for a targeted modification of compositional and processing variables to achieve techno-functionally optimized plant-derived proteins similar in understanding to animal-based proteins. Furthermore, the result will help to create completely novel structures from plant-based protein sources.

### 3 Results

#### 3.1 Quantification of protein-protein interactions in highly denatured whey and potato protein gels

##### Summary and contribution of the doctoral candidate

Denatured proteins can form self-standing gels. The texture and structure of these gels can vary strongly depending on protein type, mode of denaturation, and other milieu conditions. Although some methods exist in the literature to determine the protein interactions in a protein gel, most of them are not suitable given the specific objectives of this thesis. Therefore, an assay was developed that gives a quantitative contribution of the major protein interactions and is able to determine it in highly denatured whey and potato protein gels.

A buffer system was developed that can selectively cleave electrostatic, hydrophobic, and disulfide bonds in protein gels. Three sample protein gels were produced to determine the efficiency of the buffer system. WPI gels at pH 7 were mainly stabilized through disulfide bonds, PPI gels by hydrophobic interactions, and WPI gels at pH 5 by electrostatic interactions. These results were as expected from literature reports on the main protein interactions. Hence, the assay produced reasonable results.

The major contributions of the doctoral candidate were as follows: First literature was reviewed to determine what buffer systems might be feasible for highly denatured plant and whey proteins. Based on this, buffer systems were adapted and results were checked for plausibility. Sample preparation was altered to ensure high reproducibility. Other contributions included conceptualization of the experiments, writing of the original draft, responding to reviewer comments as well as data curation and statistical analysis.

The publication was done under a shared first-authorship from the doctoral candidate and his colleague Caren Tanger. Both first authors contributed equally to the work. The doctoral candidate was mostly involved in literature review and method development. The other first author was more involved in method improvement, statistical data analysis, and interpretation. Both contributed to writing the original draft and including feedback from revision. Other Co-authors contributed to experimental work and/or discussion.

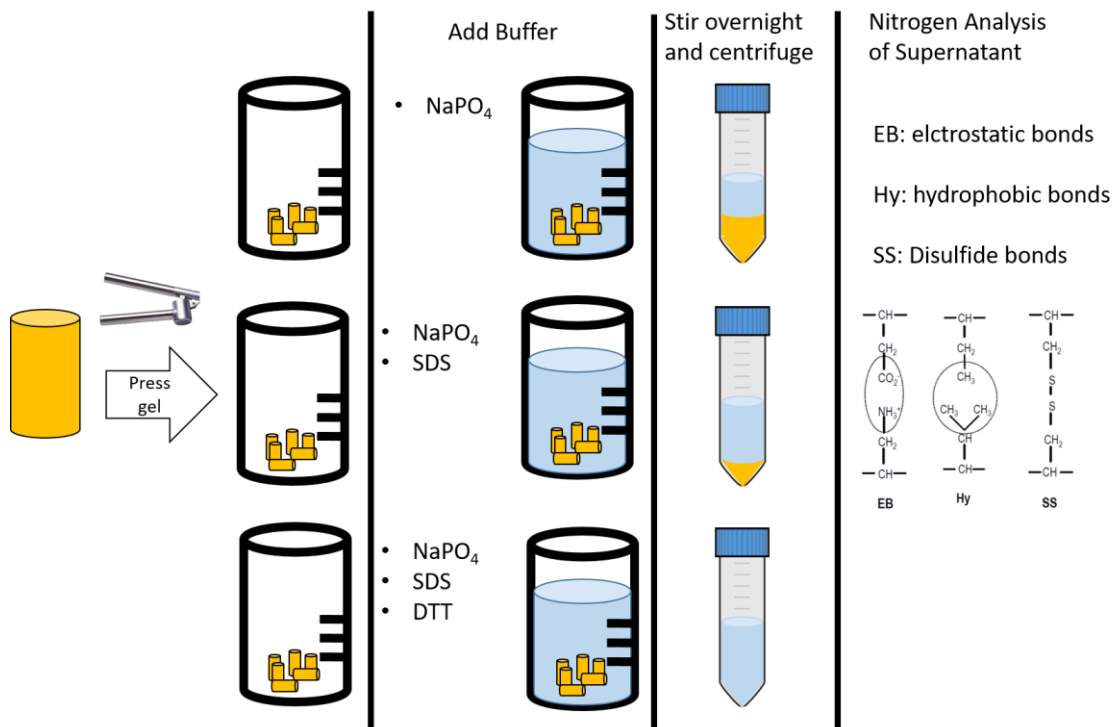
*Adapted original manuscript<sup>1</sup>*

## Quantification of protein-protein interactions in highly denatured whey and potato protein gels

Caren Tanger\*, David Andlinger\*, Annette Brümmer-Rolf, Julia Engel, Ulrich Kulozik

Chair of Food and Bioprocess Engineering, TUM School of Life Science, Technical University of Munich, Weihenstephaner Berg 1, 85354, Freising, Germany

### Graphical Abstract



<sup>1</sup> (Adaptions refer to formatting issues: e.g., numbering of sections, figures, tables and equations, abbreviations, axis labeling, figure captions and style of citation. Reference lists of all publication based chapters were merged at the end of this thesis to avoid duplications.

Original publication: Tanger, Caren; Andlinger, David; Brümmer-Rolf, Annette; Engel, Julia; Kulozik, Ulrich (2021): Quantification of protein-protein interactions in highly denatured whey and potato protein gels. In: MethodsX, S. 101243. DOI: 10.1016/j.mex.2021.101243.

## Abstract

Understanding the stabilizing protein interactions in protein gels is of high importance for food- and biotechnology. Protein interactions in protein gels can help to predict hardness, deformability and other gel parameters. Currently there are two types methods used. One is to use protein interaction blocking agents and the other is to dissolve the gel in different buffer systems, which cleave the interactions. The first method alters the gelling mechanism, which is why the second method is the preferred one. However, currently published methods are often only suitable for specific gel systems as for example weakly bound protein gels. In this paper, a method is introduced, which is suitable for highly denatured whey and plant protein.

- Suitable for strongly cross-linked whey protein and plant protein gels
- Stronger buffer system to ensure cleavage of all protein interactions
- More reproducible and simplified crushing of the gel without the introduction of uncontrolled shear stress excessively affecting the analysis of chemical bonds

## SPECIFICATIONS TABLE

<b>Subject Area</b>	Chemistry
<b>More specific subject area</b>	<i>Protein analysis</i>
<b>Method name</b>	<i>Protein interaction assay</i>
<b>Name and reference of original method</b>	Keim and Hinrichs (Keim & Hinrichs, 2004) Influence of stabilizing bonds on the texture properties of high-pressure-induced whey protein gels. In: International Dairy Journal 14, S. 355-363
<b>Resource availability</b>	<ul style="list-style-type: none"> <li>• Sodium phosphate</li> <li>• Sodium dodecyl sulfate</li> <li>• Dithiothreitol</li> <li>• Shaker or magnetic stirring plate</li> <li>• Garlic press</li> <li>• Centrifuge</li> <li>• Nitrogen analysis according to Dumas</li> </ul>

### 3.1.1 Background information and applicability of the method

Elevated temperature, pressure, organic solvents and other conditions are known to denature proteins. Usually, this is accompanied by unfolding of the protein. During unfolding the hydrophobic core and buried reactive amino acid groups as well as buried thiol groups get exposed and proteins can react with each other. This leads to the formation of aggregates and gels. The interactions can be non-covalent (hydrophobic, electrostatic interactions) or covalent (disulfide bonds). The type of interaction determines the textural properties of a protein gel. By controlling the protein interaction by pH and other process parameters the structural properties gels from dairy and plant proteins can be manipulated (Nicolai et al., 2011; Nicolai & Chassenieux, 2019). This is of great importance in the food industry, where proteins are used as structuring agents, next to increasing the nutritional value. One can change the process parameters and analyze the outcome by texture and rheological measurements.

However, this approach does not provide in depth information about the types of bonds stabilizing the gel. This additional information is of increasing interest with the advance of plant proteins in the food industry. Animal protein are progressively substituted by plant proteins as structuring agents. However, animal and plant proteins differ greatly in their molecular structure. Examples are amount of free thiol groups, intramolecular disulfide bonds, molecular weight and surface hydrophobicity (Creusot et al., 2011; Delahaije et al., 2015). Therefore, they also react differently on triggers inducing gelation and the resulting gels show large differences in textural properties (Martin et al., 2014). With this in mind, it is necessary to have a method available for analyzing the stabilizing bond interactions in animal protein gels and plant protein gels to tailor gel properties. This will allow more insights in the gelation behavior and gelation mechanisms of animal and plant protein and provides the option to modify processing parameters to obtain desired gel structures in a targeted way.

In literature, there are two main methods to determine the stabilizing protein interactions in a gel: Blocking of protein interactions during gelation and analyze resulting textural properties (1) and measuring the protein/nitrogen solubility of the produced gel in different buffers cleaving specific stabilizing protein interactions (2).

The use of blocking substances can seriously alter the gelation mechanism. For example N-Ethylmaleimide (NEM) is used to inhibit the reaction of thiol groups (Mounsey & O'Kennedy, 2007; Sun & Arntfield, 2012).

However, NEM was also shown to promote hydrophobic interactions in soy bean globulins (Hua et al., 2005) and  $\beta$ -lactoglobulin (Xiong et al., 1993). To determine stabilizing protein interactions in a gel, it is therefore preferred to determine the protein/nitrogen solubility in different buffer systems cleaving specific stabilizing protein interactions after gel formation has occurred. The salient buffer systems applied so far include cleaving agents such as sodium dodecyl sulfate (SDS) (Keim & Hinrichs, 2004; Martin et al., 2014; Shimada & Cheftel, 1988), urea (Felix et al., 2017; Gómez-Guillén et al., 1997; Martin et al., 2014; Shimada & Cheftel, 1988),  $\beta$ -mercaptoethanol (Shimada & Cheftel, 1988; Gómez-Guillén et al., 1997; Martin et al., 2014) and dithiothreitol (DTT) (Keim & Hinrichs, 2004; Shimada & Cheftel, 1988). These substances are known to disrupt

hydrophobic (SDS and urea) and disulfide bonds (DTT and  $\beta$ -mercaptoethanol). This approach is reported in literature as suitable for different protein system such as egg protein gels (Martin et al., 2014), sardine muscle gels (Gómez-Guillén et al., 1997), pea protein gels (Felix et al., 2017), whey protein gels (Shimada & Cheftel, 1988; Martin et al., 2014), lupine protein gels, soy protein gels and leaf protein (RuBisCO) gels (Martin et al., 2014). Different cleaving agents were used by the different authors.

However, differences in the properties of the cleaving agents have to be considered.  $\beta$ -mercaptoethanol is toxic and its disulfide reduction potential is lower compared to DTT (Lukesh et al., 2012). Urea contains high amount of nitrogen, which can interfere in nitrogen content determination. Because of this, SDS and DTT are preferred as cleaving agents. The evaluation of the solubility can be either binary (Martin et al., 2014) (did the gel dissolve or not) or the amount of solubilized nitrogen can be used to provide semi-quantitative information on the contribution of each type of protein interaction (Gómez-Guillén et al., 1997; Felix et al., 2017; Keim & Hinrichs, 2004; Shimada & Cheftel, 1988). The semi-quantitative approach is preferred, because it offers the possibility of setting the individual protein interactions in relation. For example, it could be shown that an increase in protein stabilized through disulfide bonds correlated with an increase in gel strength and other rheological parameters of pressure induced whey protein gels (Keim & Hinrichs, 2004). This was possible as the changes from protein stabilized through disulfide bonds from 20% to 90% could be measured. With the binary approach, such fine differences could not have been detected.

Several methods are available for quantification of solubilized nitrogen/protein content as a base for determining the soluble protein content in the serum after cleavage of certain types of bonds. Three of these methods were recently used for quantification of stabilizing bonds, the Lowry method (Felix et al., 2017; Gómez-Guillén et al., 1997), absorbance at 280 nm (spectrophotometric) (Shimada & Cheftel, 1988) and the Dumas method (Keim & Hinrichs, 2004). It has to be considered that the cleaving agents chosen have an effect on the nitrogen/protein content determination and vice versa. The Lowry protein assay is a biochemical assay using colorimetric techniques. The biggest disadvantages of the Lowry method are the interferences of buffer and protein with the reactive agent. This can lead to inaccuracies (physico-chemical effects, sorption) (Shimada & Cheftel, 1988). Physical interference refers to macroscopic particles. They interfere in the light scattering during photometrical absorption measurement. Physical interference also plays a role in spectrophotometric measurements. In case of DTT as the cleaving agent, the oxidized form of DTT has the same absorption maximum as the one of protein (Cleland, 1964). This makes the method unnecessarily prone to experimental error. For two of these methods, Lowry and spectrophotometric measurement, a calibration curve is needed and this is highly labor intensive. The third method mentioned was the Dumas method. There, the nitrogen content in the buffer system is determined by controlled combustion of a sample. Therefore, there is no interference of a chemical reagent with the protein or buffer. An additional advantage is the reproducibility and the high throughput. This is the reason why the Dumas method is the method of choice of many laboratories to determine nitrogen/protein

content. A disadvantage of the Dumas method, however, is that the total nitrogen content of the sample is determined. This means that nitrogen containing substances in the buffer are also measured as protein. This would be the case for urea and the common buffer substance 2-Amino-2-(hydroxymethyl)propane-1,3-diol (TRIS) leading to a high background noise. However, the method of Dumas can be considered advantageous. However, buffers with nitrogen containing substances should be avoided.

The Dumas method was utilized by Keim and Hinrichs for the determination of pressure induced whey protein gels (Keim & Hinrichs, 2004) and acid, rennet and pressure induced milk protein gels (Keim et al., 2006) with some limitations or even restrictions regarding highly thermally denatured protein.

The aim of this work was to modify a protein interaction assay, which can be applied to both highly denatured animal derived proteins (especially whey proteins) and plant proteins. The determination of protein interactions should be semi-quantitative. Furthermore, a high reproducibility and high throughput were aimed at.

Concluding from this, the method of Keim and Hinrichs (Keim & Hinrichs, 2004) was the most suitable for modification. It is a semi-quantitative method using the Dumas method for nitrogen quantification and the buffer system contains SDS and DTT as cleaving agents. The method was used for whey protein with a low degree of denaturation (Keim & Hinrichs, 2004; Keim, 2004), where protein interaction was weak. In order to extend the method and to make it suitable for highly denatured whey and plant protein with strong protein interactions, adjustments to the buffer systems, dissolving method and dissolving parameters had to be made. The proposed and validated changes are discussed in detail below.

### **3.1.2 Explanation on changes made**

The following buffer system was used by Keim and Hinrichs. Buffer S1 was composed to cleave all hydrophobic and electrostatic interactions and contained a TRIS-Acetate buffer with SDS. Buffer S2 was composed to cleave all hydrophobic and electrostatic interactions and disulfide bonds and contained a TRIS-Acetate buffer, SDS and DTT. In theory, the gel should completely dissolve in buffer S2. Buffer S3 was composed to cleave all electrostatic interactions and contained a sodium phosphate buffer with NaCl. In later works the authors added two new buffers, which were able to cleave calcium bridges (D) and non-specific bonds (H) (Keim et al., 2006). This addition made the method suitable for pressure-induced, heat-induced and rennet-induced milk protein gels. TRIS contains nitrogen, which leads to a high background noise during nitrogen measurement. The authors probably used a TRIS-Acetate buffer, because it does not interact with casein micelles. Casein micelles are present in milk protein gels. Phosphate buffers, on the other hand, are known to severely influence the casein equilibrium and alter micelle structure and composition (Udabage et al., 2000). However, caseins are not present in whey protein or plant protein. In order to reduce the background noise, the TRIS-Acetate buffer was substituted by a phosphate buffer. No differences were found between the usage of TRIS-Acetate and phosphate buffer for



whey and plant protein gels. The buffers S1 and S2 were not able to cleave all hydrophobic interactions and disulfide bonds in highly denatured whey and plant proteins. Therefore, the concentration of SDS and DTT had to be increased. Additionally, the pH was increased to pH 7.5 to increase the reducing ability of DTT. Furthermore, stirring time was increased to a minimum of 16 h. These were found to be optimal condition for DTT and SDS to cleave all protein interactions. Stirring temperature was set to room temperature to avoid crystallization of SDS at low temperatures.

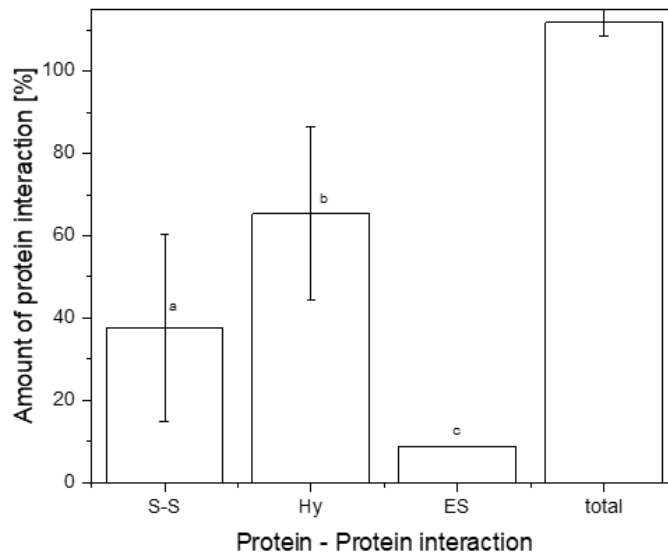


Figure 3-1 Protein interactions of a WPI gel prepared at pH 7 at 85°C crushed with an ultra-turrax, determined in six-fold. Error bars depict standard deviation. a-c different letters indicate significant differences between samples ( $P < 0.05$ ).

The cleaving agents can only work on the exposed surface of the gel. They cannot penetrate into the inside of the gel. In order to increase the exposed surface of the gel Keim and Hinrichs (Keim & Hinrichs, 2004) as well as Gómez-Guillén et al. (Gómez-Guillén et al., 1997), Felix et al. (Felix et al., 2017) and Shimada and Cheftel (Shimada & Cheftel, 1988) used an ultra-turrax to crush the gel in the buffer. The ultra-turrax can shear the gel in small particles, which increases the exposed surface. However, it also induced an uncontrollable shear stress destroying bonds prior to the analysis in an uncontrolled or excessive way. This can lead to misconceptions regarding the types of bonds stabilizing a gel. Whey protein gels produced at pH 7 and 15 % protein concentration heated for 30 min above denaturation temperature led to very hard gels. The gel either got partially stuck in the case of the ultra-turrax or was not comminuted at all, thus not allowing the buffer systems to enter the gel sample. This leads to a low reproducibility. The result of a six-fold measurement of such a gel using an ultra-turrax is shown in Figure 3-1.

### 3.1.3 Description of modified protein interaction assay

#### 3.1.3.1 Materials

For the method development, heat set protein gels at different pH values from patatin rich potato protein isolate and whey protein isolate were created. Commercial patatin rich potato protein isolate (PPI) powder (Solanic 200), was kindly provided by AVEBE (Veendam, The Netherlands). The protein powder had a protein content of 88.6% (w/w). Commercial WPI (BiPROTM) powder from Agropur Dairy Cooperative (Saint-Hubert, Longueuil, Canada) was obtained. The protein powder had a protein content of 90.9 % (w/w). The protein content was determined using the method of Dumas with an accuracy of  $\pm 0.1\%$  (w/w) (Vario MAX CUBE, Elementar Analysensysteme GmbH, Hanau, Germany). The Dumas factor was 6.38 and 6.25 for WPI and PPI, respectively. However, the Dumas factors are not necessary to determine soluble nitrogen.

#### 3.1.3.2 Preparation of buffer systems

Three buffers were prepared. The detailed composition of the three buffers can be found in Table 3-1.

Table 3-1 Composition of the three different buffers used in this study.

Buffer system	NaH <sub>2</sub> PO <sub>4</sub> /Na <sub>2</sub> HPO <sub>4</sub> [mol/L]	SDS [g/L]	DTT [g/L]	pH
B1	0.05	-	-	7.5
B2	0.05	2	-	7.5
B3	0.05	2	15	7.5

Note: Higher concentration of DTT and SDS, compared to Keim & Hinrichs (Keim & Hinrichs, 2004), were chosen to fully dissolve strongly bound globular proteins. Even higher concentrations of SDS were also tested (up to 10 g/L). However, this resulted in the formation of filaments of some covalent linked protein gels, which could not be separated through centrifugation.

#### 3.1.3.3 Dissolution of gel in buffer system

1. Press gel through a garlic press, for homogenization and size reduction
2. Weigh 0.5 g of crushed gel in each of three 50 ml glass beakers
3. Label the glass beakers B1, B2, B3
4. Pour 20 g buffer of the respective buffer in each in beaker

Note: 0.5 g gel does refer to a gel with 10 % - 15 % protein content. Thus, the protein to buffer ratio is 0.01-0.015: 4. If the nitrogen content gets too high, the buffer is not able to cleave all protein – protein interactions in the gel.

#### 3.1.3.4 Mixing

Stir overnight at room temperature with a magnetic stirrer

Note: Dissolving in centrifuge tubes and using a shaker instead of a beaker and a magnetic stirrer does also work and allows dissolving and centrifuging in the same tube increasing the reproducibility of the process.

### 3.1.3.5 Determination of soluble nitrogen content

1. Centrifuge stirred samples at 10 000 g at 20°C for 20 min
2. Separate supernatant from pellet. The pellet can be discarded.
3. Determine % nitrogen content in supernatant by the Dumas method
4. Determine also the % nitrogen content of the original gel by the Dumas method

Note: An SDS-PAGE of the supernatants of the gel dissolved in the three buffers can give an indication of which proteins are engaged in the different protein – protein interactions. Some pellets were very soft and the supernatant had to be removed with a pipette to avoid mixing between pellet and supernatant.

### 3.1.3.6 Quantification of protein interactions

First, the concentration of protein bonds that are cleaved by the different buffer systems ( $C_{n,bond,Bx}$ ) has to be calculated. This is shown in Eq. (3-1):

$$C_{n,bond,Bx} = \frac{(m_S + m_{gel})}{m_{gel}} * C_{n,sup,Bx} \quad (3-1)$$

With  $m_S$  being the initial mass of the buffer (20 g),  $m_{gel}$  being the mass of the gel (0.5 g) and  $C_{n,sup,Si}$  being dissolved nitrogen in the supernatant in [%], determined by the method of Dumas.

Buffer B1 cleaves electrostatic protein-protein interactions and hydrogen bonds[P(ES)]:

$$\frac{C_{n,bond,B1}}{C_{n,gel}} = P(ES) \quad (3-2)$$

With  $C_{n,gel}$  being the nitrogen content in [%] of the analyzed gel. P describing the relative amount of protein bound by this protein interaction. ES is abbreviated for electrostatic bonds including hydrogen bonds

Buffer B2 cleaves all electrostatic [P(ES)] and hydrophobic protein-protein interactions [P(Hy)]. Therefore, it can be said that:

$$\frac{C_{n,bond,B2}}{C_{n,gel}} = P(ES) + P(Hy) \quad (3-3)$$

with Hy being short for hydrophobic interactions.

Buffer B3 cleaves all protein-protein interactions, including disulfide bonds [P(SS)]. Therefore, it can be said that:

$$\frac{C_{n,bond,B3}}{C_{n,gel}} = P(ES) + P(Hy) + P(SS) \quad (3-4)$$

With SS being short for disulfide bonds.

From Equation (3-1) to (3-4) we can deduce following equations to calculate the amount of protein bound by the different protein interactions.

The quantity of electrostatic interactions including hydrogen bonds is given by the concentration of solubilized protein nitrogen in Buffer C divided by the protein nitrogen content of the analyzed gel:

$$P(ES) = \frac{C_{n,bond,B1}}{C_{n,gel}} \quad (3-5)$$

The amount of protein nitrogen bound by hydrophobic interactions can be calculated by the difference of solubilized protein nitrogen in buffer B2 and B1:

$$P(Hy) = \frac{C_{n,bond,B2}}{C_{n,gel}} - \frac{C_{n,bond,B1}}{C_{n,gel}} \quad (3-6)$$

The amount of protein nitrogen bound by disulfide bonds can be calculated by the difference of concentration of solubilized protein nitrogen in buffer B3 and B2:

$$P(SS) = \frac{C_{n,bond,B3}}{C_{n,gel}} - \frac{C_{n,bond,B2}}{C_{n,gel}} \quad (3-7)$$

### 3.1.4 Method validation

#### 3.1.4.1 Reproducibility of method

In order to validate the method and to test the buffer system, three different types of gels were tested six-fold. For each gel type samples for six-fold measurement were taken from the same gel. This was done to test the reproducibility of the method and not of the gel formation. The chosen test gels should be different in their dominant protein interactions. Therefore, two different whey protein gels and a potato protein gel were tested. One whey protein gel was made by heating a 15 % whey protein solution 30 min at 85°C at pH 7. The second whey protein gel was made by heating a 15 % whey protein solution at pH 5 30 min at 70°C. The potato protein gel was made by heating a 10 % potato protein solution at pH 7 for 30 min at 70°C. Differences in protein type, heating and milieu conditions will lead to different protein interactions being dominant within the gels. First the reproducibility of the nitrogen solubilization will be examined. Afterwards, the results of this will be discussed with literature findings.

The soluble nitrogen content in the different buffers with standard deviation are shown in Figure 3-2. The soluble nitrogen content already indicates which protein interaction is dominant in the gel. For PPI only a 10 % (w/w) protein gel was used therefore less nitrogen can be solubilized. This explains the low soluble nitrogen content in buffer B3 of the PPI gel.

Most important in Figure 3-2 is the standard deviation. In contrast to Figure 3-1 the standard deviation is acceptably small (below 5 %). This implies that the changes made to the initial method of Keim and Hinrichs (Keim & Hinrichs, 2004) led to a reproducible method for highly denatured whey and plant proteins.

In the following the ability of the buffers to cleave all protein interactions is determined. For this, Equations (3-1) to (3-6) were applied to the measured nitrogen solubility in each buffer. For calculation the average of the six-fold nitrogen determination was used. From this the relative amount of each protein interaction within the gels were obtained. This is shown in Figure 3-3.

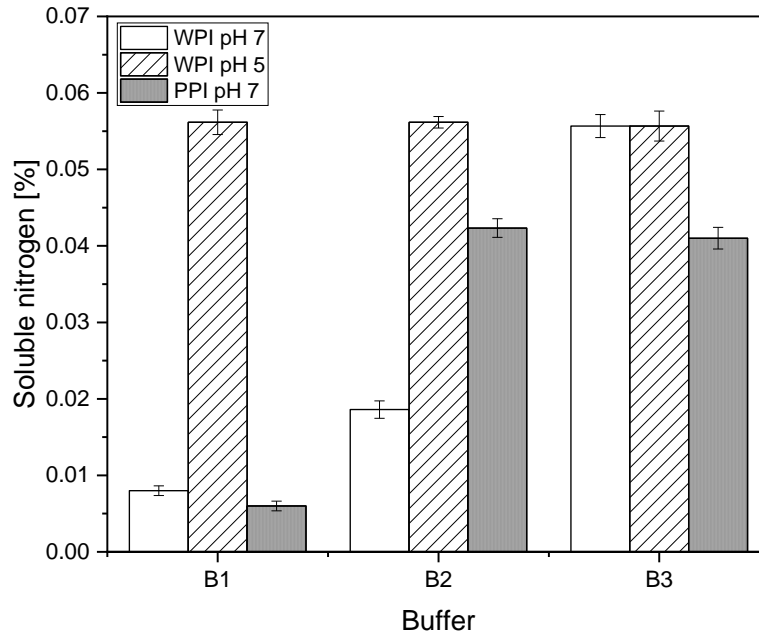


Figure 3-2 Soluble nitrogen content of the supernatant of the three gels dispersed in the three buffers (see Table 3-1 for composition of the buffers) and centrifuged at 10000 g for 20 min. The three gels were: a WPI gel at pH 7 heated 85 °C, a WPI gel at pH 5 heated at 70 °C and a PPI gel at pH 7 heated at 70 °C. All gels were heated for 30 min.

It should be noted that the highest amount of nitrogen is dissolved in buffer B3 as this buffer cleaves all protein interactions. The total amount of protein interactions was found to be around 100 % for the WPI gels. For PPI a total amount of around 110% interactions was found. This indicates that more nitrogen is determined than could be theoretical dissolved in buffer B3. The origins of this is not clear but can be found in published data, as well (Keim & Hinrichs, 2004; Keim et al., 2006). However, the method should be seen to determine trends regarding the main protein interactions. More importantly all bonds were cleaved and there is no remaining undissolved protein, as seen in other methods (Felix et al., 2017). Below, the results obtained with this method were compared to literature findings using other methods.

As expected, the main protein interaction in whey protein gels, heated well above their temperature of denaturation and at pH 7, was by disulfide bonds (66 %) followed by hydrophobic interactions (19 %) and electrostatic interactions. The formation of disulfide linked whey protein gels and the effect of pH and temperature on the gelation are described in detail elsewhere (Monahan et al., 1995; Sava et al., 2005). Monahan et al. and Sava et al. also found that disulfide bonds were the dominant protein interaction

in heated whey protein and  $\beta$ -lactoglobulin by measuring the sulfhydryl group content using Ellmann reagent.

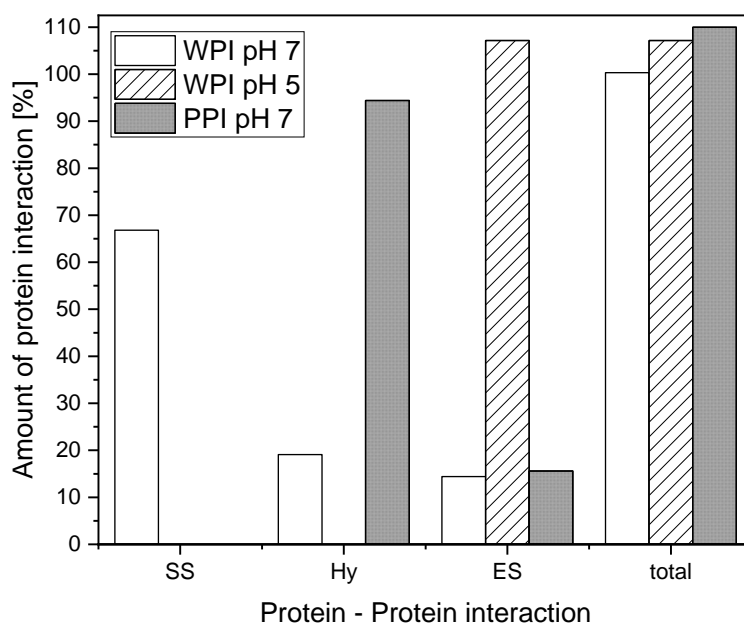


Figure 3-3 Protein interactions of a WPI gel at pH 7 heated 85 °C, a WPI gel at pH 5 heated at 70 °C and a PPI gel at pH 7 heated at 70 °C. All gels were heated for 30 min. The protein interactions are: disulfide bonds (SS), hydrophobic interactions (Hy) and electrostatic interactions (ES).

In contrast, protein interactions in the whey protein gel heated at pH 5 below denaturation temperature were mainly found to be of electrostatic nature. For these type of gels, the low electrostatic repulsion of protein monomers led to electrostatic interactions without the formation of disulfide bonds. This is in line with the finding of Sava et al.

The potato protein gel was formed mainly by hydrophobic interactions. Patatin, the main potato protein, contains one free thiol group. Because of this, only two proteins can be bound together by a disulfide bridge. No larger networks can in this case be formed by disulfide bonds as compared to whey proteins which create multilateral networks by a thiol-disulfide exchange mechanism (Creusot et al., 2011; Pots et al., 1999a). The lack of internal disulfide bonds in patatin leads to an extensive unfolding upon heating (Pots et al., 1998a). Upon unfolding, the hydrophobic core gets exposed and hydrophobic residues can react with each other. Several proteins can react with each other via hydrophobic interactions building a gel network. Gelation of potato protein is not dependent on the formation of disulfide bonds. This explains the dominant hydrophobic interactions in the potato protein gel.

Summarizing, the method was found to be reproducible and all protein interactions were cleaved by SDS and DTT. The dominant protein interactions of the three gels were in line with what was expected from the literature.

### 3.1.4.2 Limitation of the method

The method is based on the centrifugal separation. Cleaved particles became soluble and uncleaved gel particles remained insoluble. Disulfide linked dimers or small oligomers cannot be cleaved by buffer B2. However, these protein particles are small enough to stay soluble in buffer B2. They contribute to the calculated hydrophobic interactions even though they are cross-linked by disulfide bonds. To investigate those small oligomers, an SDS-PAGE with the supernatant of buffer B2 was performed. The SDS-PAGE of the three gels in buffer B2 can be seen in Figure 3-4.

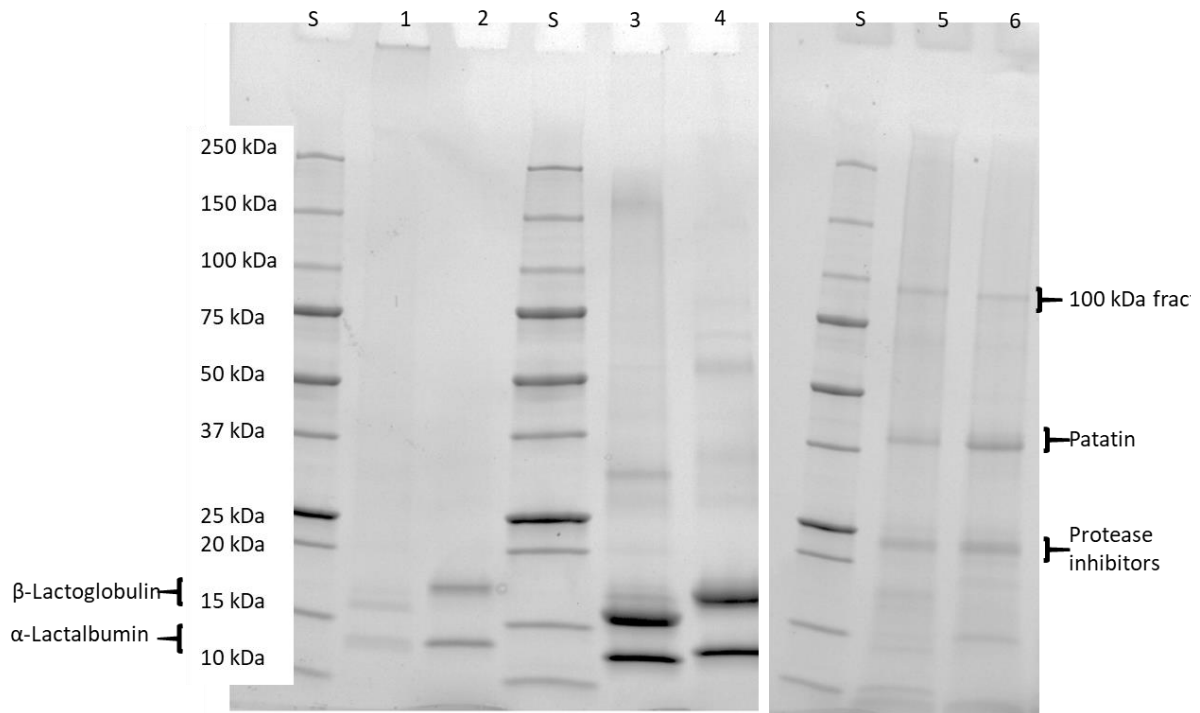


Figure 3-4 SDS-PAGE of supernatant of buffer B2 of the two WPI gels and the PPI gel. S marks the standard lane. Lane 1 and 2 are WPI gels at pH 7, non-reducing and reducing. Lane 3 and 4 are WPI pH 5, non-reducing and reducing. Lane 5 and 6 are PPI gels at pH 7, non-reducing and reducing.

Uncleaved oligomers can be found in the pocket of the SDS-PAGE. This is the case for whey protein gel prepared at pH 7 at 85°C for 30 min (Lane 1). Thus, there are aggregates bound via disulfide bonds, which are larger than 250 kDa, but small enough to stay soluble during centrifugation. The two other bands (around 18 and 14 kDa) in lane 1 are monomeric  $\beta$ -Lg and  $\alpha$ -La. No dimers were found. With this it can be said that there are monomeric proteins, which are bound together by hydrophobic interactions. It can also be said that there are small oligomers cross-linked by disulfide bonds. These small oligomers are connected by hydrophobic interactions forming a gel network. No bands were found for proteins above 250 kDa in the whey protein gel prepared at pH 5, with heating below denaturation temperature. Thus, no disulfide bonds were formed. In the potato protein gel, no bands above 250 kDa could be found. The band at 95 kDa could be attributed to lipoxygenase and does not disappear in a reducing SDS-PAGE. Therefore, it can be said that this gel solely relies on hydrophobic interactions. The addition of performing an SDS-PAGE with the supernatant of the three buffers provides even more information to the protein interaction assay. It gives the opportunity to separate between the protein interaction between big particles and

between the proteins itself. The SDS-PAGE gel also shows a limitation of the method presented in this paper. Separation of cleaved and uncleaved proteins and particles by the buffers is based on centrifugation. Therefore, smaller aggregates, such as dimers and trimer, bound together by disulfide bonds, stay soluble in buffer B2 and add to the calculated hydrophobic interactions. They can only be made visible by non-reducing SDS-PAGE.

Note: If not all protein is dissolved in buffer B3 an investigation into the pellet by SDS-PAGE could hint at the formation of isopeptide bonds, as described elsewhere (Rom-bouts et al., 2011). However, dissolution of the pellet in the SDS-PAGE buffer indicates that the buffer B3 is not strong enough to cleave all disulfide bonds. This was the case when WPI gels heated at pH 7 and 85 °C were investigated and the DTT concentration was below 15 g/L and the protein to buffer ratio was higher than described here.

### 3.1.5 Conclusion

In this paper a method for the determination of stabilizing protein bonds in a protein gel is presented. The method was based on an existing method for weakly bound milk protein gels and adapted. Changes to the composition of the buffer system, the crushing method of gel and dissolution parameters had to be made. It could be shown that the presented method is reproducible and suitable for highly denatured whey and potato protein gels. A limitation is that stabilizing protein bonds of small aggregates such as dimers and small oligomers could not be determined. Although this method was only validated for highly denatured whey and potato protein gels it is likely to also be suitable for other food protein gels. From this, it can be anticipated that the presented method is of interest for further research in strongly bound protein gels from both animal and plant proteins. Especially for plant proteins, there is still a lot to be learned about the type of protein interactions forming aggregates and gels.

### Acknowledgements:

We would like to acknowledge the help of Christine Haas for Elementar measurement and Heidi Wohlschläger and Claudia Hengst for experimental idea generation. Maria Weinberger and Marius Reiter are thanked for valuable discussion. Prof. Dr. Jörg Hinrichs and Dr. Susanne Keim are thanked for giving insight into their methodology on which this work is based on. We would like to thank Marc Laus from AVEBE, Veendam, The Netherlands, for providing the potato protein isolate.

This work was funded by IGF Projects of the FEI (AiF 20197 N and 19712 N) and supported via AiF within the program for promoting the Industrial Collective Research (IGF) of the German Ministry of Economic Affairs and Energy (BMWi), based on a resolution of the German Parliament.



### **3.2 Influence of pH, temperature and protease inhibitors on kinetics and mechanism of thermally induced aggregation of potato proteins**

#### Summary and contribution of the doctoral candidate

Protein denaturation leads to aggregation and then subsequently to gelation. Therefore, to understand how potato proteins form gels we investigated the underlying aggregation mechanism. In this chapter, the influence of pH and temperature on heating kinetics and the underlying aggregation mechanism was investigated. Furthermore, the influence of minor protein components, namely the protease inhibitors, that are present in the protein isolate was investigated.

Protein aggregation was influenced by the adjustment of the pH. It could be shown that increases in pH lowered the temperature of unfolding. Similar kinetics of aggregation could be observed if the temperature was set in relation to the determined temperature of unfolding. Furthermore, it could be shown that covalent links are formed in PPI aggregates and that protease inhibitors are not involved in the aggregation reaction. One should notice however that covalent bonds play a subordinated role behind hydrophobic interactions, especially under conditions of rapid unfolding, e.g. high temperatures. Aggregates were shown to expose hydrophobic amino acids from the protein core. The exposed hydrophobicity could be altered by the pH during aggregation with less hydrophobic groups being exposed at higher pH and vice versa. The study helps to understand what protein interactions occur in PPI aggregates. This will be important in understanding how hydrogels can be formed from PPI and where the differences are compared to WPI.

The doctoral candidate designed the experiments based on extensive literature research. Another major contribution was the establishment of the chromatography method for kinetic investigations. The interpretation of the data to derive kinetic parameters was also done by the candidate. Furthermore, different methods to investigate protein interactions occurring during PPI aggregation were utilized. The doctoral candidate was responsible for the establishment of all methods for the PPI system. The interpretation of different methods, such as SDS-PAGE, utilization of blocking substances, and fluorescence spectroscopy to derive one reaction mechanism was one of the main tasks of the candidate. Other contributions included the writing of the original draft, responding to reviewer comments as well as data curation and statistical analysis.

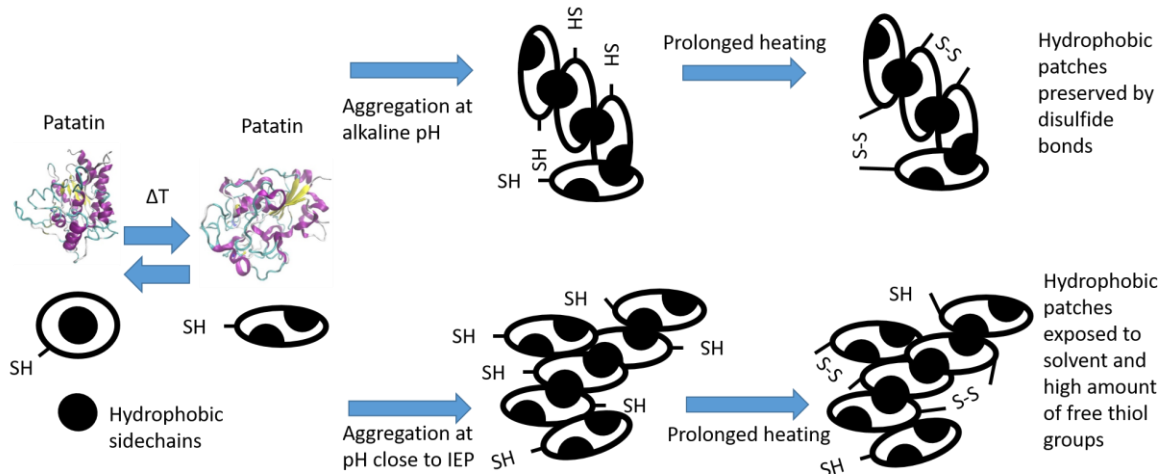
*Adapted original manuscript<sup>2</sup>*

## Influence of pH, temperature and protease inhibitors on kinetics and mechanism of thermally induced aggregation of potato proteins

David J. Andlinger\*, Pauline Röscheisen, Claudia Hengst, Ulrich Kulozik

Chair of Food and Bioprocess Engineering, TUM School of Life Science, Technical University of Munich, Weihenstephaner Berg 1, 85354, Freising, Germany

### Graphical Abstract



<sup>2</sup> (Adaptions refer to formatting issues: e.g., numbering of sections, figures, tables and equations, abbreviations, axis labeling, figure captions and style of citation). Reference lists of all publication based chapters were merged at the end of this thesis to avoid duplications.

Original publication: Andlinger, D. J., Röscheisen, P., Hengst, C., & Kulozik, U. (2021). Influence of pH, Temperature and Protease Inhibitors on Kinetics and Mechanism of Thermally Induced Aggregation of Potato Proteins. *Foods*, 10(4), 796. <https://doi.org/10.3390/foods10040796>

## Abstract

Understanding aggregation in food protein systems is essential to control processes ranging from the stabilization of colloidal dispersions to the formation of macroscopic gels. Patatin rich potato protein isolates (PPI) have promising techno-functionality as alternatives to established proteins from egg white or milk. In this work, the influence of pH and temperature on the kinetics of PPI denaturation and aggregation was investigated as an option for targeted functionalization. At slightly acidic pH, rates of denaturation and aggregation of the globular patatin in PPI were fast. These aggregates were shown to possess a low amount of disulfide bonds and a high amount of exposed hydrophobic amino acids ( $S_0$ ). Gradually increasing the pH slowed down the rate of denaturation and aggregation and alkaline pH levels led to an increased formation of disulfide bonds within these aggregates, whereas  $S_0$  was reduced. Aggregation below denaturation temperature ( $T_d$ ) favored aggregation driven by disulfide bridge formation. Aggregation above  $T_d$  led to fast unfolding, and initial aggregation was less determined by disulfide bridge formation. Inter-molecular disulfide formation occurred during extended heating times. Blocking different protein interactions revealed that the formation of disulfide bond linked aggregation is preceded by the formation of non-covalent bonds. Overall, the results help to control the kinetics, morphology, and interactions of potato protein aggregation for potential applications in food systems.

### 3.2.1 Introduction

Protein aggregates can be used as functional ingredients in different food formulations (Nicolai & Durand, 2013). The formation of these aggregates can be induced by unfolding of the globular molecular structure at elevated temperatures. Upon unfolding, proteins lose their tertiary and secondary structure, and reactive amino-acid groups get exposed, and the proteins thus can interact with each other to form aggregates. These interactions can be of covalent or non-covalent nature. The most important covalent bonds are disulfide bonds, which can be formed by the reaction of two thiol-groups or by the reaction of a thiol group with an intramolecular disulfide bond leading to a chain reaction, the thiol-disulfide interchange (Monahan et al., 1995). Non-covalent interactions comprise hydrophobic interactions and electrostatic interactions. These interactions are weaker than disulfide bonds. The type of protein interaction influences the morphology of the aggregates and is pH and ionic-strength dependent (Nicolai et al., 2011).

In comparison to other globular proteins, in particular  $\beta$ -lactoglobulin ( $\beta$ -lg), the major whey protein from bovine milk, the aggregation mechanism has been much less well studied and understood for plant proteins, including patatin, the main protein from the potato tuber. Patatin has a molecular mass of around 40-42 kDa, and 4 different isoforms are known (Pots et al., 1999b). The isoelectric point (IEP) of patatin is between a pH of 4.5-5.1 (Racusen & Foote, 1980). It comprises around 40 % of the total potato protein (Singh & Kaur, 2016). The heat-induced unfolding of patatin at pH 8 was shown to be partly reversible (Pots et al., 1998a). It was shown that initial unfolding occurs at temperatures as low as 28 °C.  $\alpha$ -helices unfold between 45-55 °C followed by  $\beta$ -strands between 50-90 °C. This unfolding was accompanied by precipitation.

Like for other globular proteins, heat-induced patatin aggregation was shown to follow a two-step aggregation scheme where the native protein first reversibly unfolds and then irreversibly forms a reactive species, which can form larger aggregates (Pots et al., 1999c). At temperatures at and above 60 °C, no unfolding reaction rate constant could be determined, probably because it happened too fast. The authors concluded that detailed insights into this physical reaction step that preceded aggregation could not be deduced. Another study found that heating of patatin resulted in the formation of dimers and trimers (Pots et al., 1999a). The disintegration of these structures following the addition of  $\beta$ -mercaptoethanol indicated that the aggregates were stabilized by disulfide bonds. However, these aggregates also formed in the presence of the thiol blocking agent NEM. The authors postulated that the formation of disulfide links might play a secondary role and hypothesized that disulfide formation might only occur after aggregation through interactions further along the thermal process. However, no time-resolved analysis on the reactivity of the thiol groups was performed.

Another study compared the aggregation kinetics of patatin to two other major food proteins, i.e. ovalbumin from egg white and  $\beta$ -lg from whey (Delahaije et al., 2015). Higher aggregation rates were found for ovalbumin and patatin in comparison to  $\beta$ -lg. However, this order of aggregation rates could not be explained by simple molecular differences such as exposed hydrophobicity, free sulfhydryl groups, or net surface charge density. Furthermore, the kinetic data showed differences between  $\beta$ -lg and patatin. In contrast to  $\beta$ -lg, different heating conditions could not be combined in a simple denaturation scheme for patatin. Certain heating conditions clearly deviated from the averaged denaturation curve, a fact that could not be fully explained by the data. There was a clear distinction between conditions of rapid denaturation above  $T_d$  and slow denaturation below  $T_d$ . Furthermore, there were differences between the electrostatic repulsion at neutral pH and at reduced pH, closer to the IEP. Therefore, more research appears to be required to better understand the aggregation mechanism under a wider range of heating conditions.

Aggregation and gelation of patatin were described by several studies as driven by hydrophobic interactions. Although the hydrophobicity of unheated patatin has been compared to  $\beta$ -lg and ovalbumin, the results are not conclusive. Patatin was found to be more hydrophobic than  $\beta$ -lg when investigated by hydrophobic interaction chromatography (Creusot et al., 2011) and less hydrophobic when investigated by the fluorescence dye ANS (1-anilinonaphthalene-8-sulfonic acid) (Delahaije et al., 2015). Furthermore, the hydrophobicity of aggregated patatin has not been assessed so far.

After patatin, the second most abundant group of potato proteins are protease inhibitors (PI). PI are a heterogeneous group of proteins with IEPs between 5-8 and molecular weights between 7-21 kDa (Pouvreau et al., 2001; Løkra et al., 2008). The first and second most abundant protease inhibitors are potato serine protease inhibitors (Pouvreau et al., 2005a) and potato cysteine protease inhibitors (Pouvreau et al., 2005b), respectively. From both of these PI, it is known that their thermal stability is higher than patatin's, indicated by a higher temperature of unfolding. PIs were shown

to form gels, although, at neutral or mildly acidic pH, the gels were very brittle compared to patatin (Schmidt et al., 2019). Besides this, little is known about their techno-functionality. To the best of our knowledge, there is no study investigating if protease inhibitors interact with patatin upon heating.

Although there were already some investigations reported on the aggregation of patatin, the mechanism behind the aggregation, especially in regard to protein interactions, remains unclear. In this study, commercial patatin enriched potato protein isolate (PPI) was used to investigate the heat-induced aggregation of the potato protein patatin and possible interactions with PI. The following approach was chosen: The formation of covalent disulfide bonds was investigated by SDS-PAGE. Certain blocking substances were used to differentiate between the roles of hydrogen, hydrophobic, and thiol interactions in the aggregation of PPI. Blockers, such as sodium dodecyl sulfate (SDS) and N-Ethylmaleimide (NEM), Urea, and Tween 20 disrupt interactions with proteins in different ways and block the formation of certain protein interactions (Disanayake et al., 2013).

Potato protein denaturation and aggregation were investigated over a broad range of pH values. Changes in pH were applied to change the interactions between the protein monomers during unfolding and aggregation. Protein interactions closer to the isoelectric point (IEP), i.e. at less intense electrostatic interaction between patatin monomers, were studied to assess aggregation by short-ranged bonds. Higher pH values were established to favor the formation of disulfide bonds.

The influence of pH will lead to different properties of the aggregates, such as exposed hydrophobicity and stabilization through disulfide bonds. Such aggregates can be used to stabilize foams (Dombrowski et al., 2017) and emulsions (Delahaije et al., 2013) or as oil-structuring agents (Vries et al., 2017). Furthermore, aggregates are considered the building block of protein gels. Depending on the aggregate properties, the properties of the gels can be severely influenced. Such gels can be used as fat replacers (Wolz & Kulozik, 2017) and encapsulation systems (Betz et al., 2012; Selmer et al., 2019), among others. To predict how PPI will behave in these applications, a deeper understanding of the denaturation and aggregation mechanism should be established. Therefore, the aim of this study is to understand these mechanisms in dependence of different heating conditions.

## **3.2.2 Materials and Methods**

### **3.2.2.1 Materials and Sample preparation**

All weight ratios are given as weight percentage (gram protein per 100 gram solution) abbreviated as % (w/w).

Commercial PPI powder (Solanic 200®) with a high content of patatin, was obtained from AVEBE (Veendam, The Netherlands). The protein powder had a protein content of 88.6% (w/w). The protein content was determined using the method of Dumas with an accuracy of  $\pm 0.1\%$  (w/w) and a Dumas factor of 6.25 (Vario MAX CUBE, Elementar Analysen-Systeme GmbH, Hanau, Germany). This conversion factor was already used

by other researchers for PPI (Schmidt et al., 2019; Dachmann et al., 2020) The patatin content, measured by the relative band intensity (RBI) in a reducing SDS-PAGE, was found to be around 60% RBI. A similar patatin concentration for this PPI was reported by others (Katzav et al., 2020). Other protein components were Protease inhibitors (25% RBI) and a higher molecular weight fraction with 100 kDa (15% RBI).

The powder was solubilized in deionized water and stirred overnight, to ensure complete dissolution of the protein powder. To limit bacterial growth stirring was done at 4°C. The water was deionized in a two-step process. Water was softened by removing calcium carbonate followed by a deionization by an ion exchange gel. The solution was then centrifuged at 6000 g for 15 min to eliminate insoluble components, around 5% of the total protein. The protein concentration of the final solution was determined by using the method of Dumas, similar to the determination for the protein powder. The protein concentration of the final solutions was around 1% (w/w) (Accuracy from a triplicate  $0.97 \pm 0.04$  (w/w)). In order to investigate the influence of pH on aggregation, the solutions were adjusted with 1 mol/L HCl and 1 mol/L NaOH (Merck, Darmstadt, Germany) to pH 6.0, 7.0, 8.0, 9.0, and 10.0. pH values were checked with a pH meter a deviation of  $\pm 0.01$  from the target value was deemed sufficient.

### **3.2.2.2 Modulated differential scanning calorimetry (mDSC)**

The denaturation temperatures ( $T_d$ ) of PPI solutions at pH 6.0, 7.0, 8.0, 9.0, and 10.0 were measured using Tzero-calibrated modulated differential scanning calorimetry (mDSC Q1000, TA Instruments, New Castle, United Kingdom). To measure each solution with an individual pH, 20  $\mu$ L of the solution was filled into a hermetically sealed aluminum pan. As a reference, an empty aluminum pan was used. The temperature was gradually heated from 25 to 90 °C with a modulated heating rate of 2 °C/min. The respective  $T_d$  for each pH level was used to determine heating temperatures (see Table 3-2). One example of an mDSC thermogram is given under Figure S5

### **3.2.2.3 Heating experiments**

3.14 mL of the protein solution was filled into stainless steel tubes, with a length of 240 mm, an inner diameter of 5 mm, and an outer diameter of 6 mm, closed with a screw cap. Several tubes were prepared this way, transferred into a water bath, and removed from the water bath after a certain heating time intervals to obtain time-resolved information about the aggregation process (see Appendix Table A1 for an Overview of the time intervals). After the heating step, the tubes were immediately put into ice water to stop the heat-induced reaction. The heating temperature chosen was dependent on  $T_d$  determined by modulated differential scanning calorimetry (mDSC). The denaturation temperature results for pH 6 to 10 are summarized in Table 3-2. Four temperatures were investigated per pH value. Temperatures for the heating trials were set 5 and 10 °C above and below the determined  $T_d$ . By using this heating regime, similar unfolding kinetics should be achieved. This approach was already used for the comparison of the aggregation behavior of different protein sources (Delahaije et al., 2015). The samples were heated for a maximum of 30 min above denaturation temperature and for 45 min below denaturation temperature.

Table 3-2 Values of the peak maximum of denaturation peaks obtained through mDSC experiments. PPI samples were heated with 2 °C/min. The values are given as the average of two independent runs, and ± indicates the range of this double measurement. pH values from 6-9 are taken from somewhere else (Andlinger et al., 2021a).

pH value	6	7	8	9	10
peak maximum (T <sub>d</sub> )	64.5 ± 0.2	60.8 ± 0.4	57.7 ± 0.6	54.8 ± 0.1	51.5 ± 0.6

#### 3.2.2.4 Size-exclusion chromatography coupled with fluorescence intensity detection

The denaturation of patatin and the formation of aggregates, as well as the interaction with protease inhibitors during the heating experiments, were investigated by size exclusion chromatography (SEC). The separation was performed on an Agilent 1100 Series chromatograph (Agilent Technologies, Waldbronn, Germany) equipped with a quaternary pump. The system was controlled by Agilent ChemStation software (Rev. C.01.08). An analytical guard cartridge (GFC 4000 4 x 3.0 mm) was used. The SEC column used was a “Yarra 3 µm 7.8\*300 mm SEC 4000” column (Phenomenex Torrance, California, United States). For eluting the protein from the column, a 100 mM sodium phosphate buffer decontaminated with dimethyl dicarbonate (DMDC) with a flow of 1 mL/min was used. The protein solution was mixed 1:1 with the elution buffer, filtered through a 0.45 µm syringe filter (Chromafil Xtra RC), and injected onto the column. The elution signal was determined at 214 nm with a diode array detector (DAD). To calibrate the retention times to certain molecular weights, a commercial SEC calibration standard (Phenomenex Torrance, California, United States) with proteins ranging from 0.214 – 900 kDa was used. Monomeric patatin has a molecular mass of around 40 kDa (Pots et al., 1998a) to 43 kDa (Racusen & Weller, 1984). Native dimers (Racusen & Weller, 1984) and trimers (Rydel et al., 2003), with 80 and 120 kDa, are described in the literature. Therefore, the UV signal between 44 and 150 kDa was described to the patatin fraction in the protein solution. The fraction with a molecular weight below 44 kDa was ascribed to the protease inhibitor (PI) fraction. The molecular weights of these proteins are typically 25 kDa and below (Katzav et al., 2020). To investigate the intrinsic fluorescence of protease inhibitors, patatin, and the formed aggregates, a fluorescence detector (FLD) was added after the diode array detector. Samples were excited at 280 nm, and the emission spectrum in the range of 300 – 400 nm was recorded. By injecting different aliquots of a solution prepared with the patatin standard described above, the area of the elution signal obtained by SEC could be attributed to a certain amount of protein. A sample Chromatogram can be found in the Appendix Figure S1

#### 3.2.2.5 Determination of free thiol groups in heated PPI solutions

The loss of free thiol groups during the heat-induced aggregation of patatin was measured through the reaction of thiol groups with the reagent 4,4'-Dithiodipyridine (DTDP). Free thiol groups crosslink in the presence of the dye and result in the conversion of DTDP into 4-thiopyridine (4-TP). 4-TP has an absorption maximum at 324 nm and can

be quantified on a reversed-phase high-pressure liquid chromatography system (RP-HPLC) coupled with a DAD. The amount of 4-TP formed is directly related to the amount of free thiols in a sample. The absorption signal was calibrated through calibration with cysteine in different concentrations. A detailed description of sample preparation, evaluation, and method validation can be found elsewhere (Kurz et al., 2020).

To calculate the theoretical amount of free thiols in the aggregates, Equation (3-8) was used

$$\frac{C_{Pat,SEC}}{M_{Pat}} = n_{Thiol,Pat} \quad (3-8)$$

With  $C_{Pat,SEC}$  being the concentration of native sized patatin obtained by SEC in g/L,  $M_{Pat}$  the molecular weight of Patatin (40 kDa) and  $n_{Thiol,Pat}$  the molar concentration of free thiols in the solution in mol/L. The molar concentration is calculated under the assumption that each native sized patatin molecule only contains 1 free thiol group (Creusot et al., 2011; Delahaije et al., 2015).

This thiol concentration ( $n_{Thiol,Pat}$ ) can be subtracted from the total amount of thiols determined by the RP-HPLC method ( $n_{total,Thiols}$ ) (see Equation (3-9)). This way an excess amount of thiols is obtained ( $n_{Thiols,excess}$ )

$$n_{total,Thiols} - n_{Thiol,Pat} = n_{Thiols,excess} = n_{Thiol,Aggregates} \quad (3-9)$$

An excess of thiols indicates that more thiols are measured in the solution than would be predicted by the amount of native sized patatin. Therefore, changes in  $n_{Thiols,excess}$  must occur within the protease inhibitor or the aggregate fraction. As will be shown in this study the interaction of protease inhibitors with the patatin is low. Therefore, we assume that excess thiols are mainly measured due to the fact that reactive thiols reside within the aggregate fraction ( $n_{Thiol,Aggregates}$ ).

However, the calculated amount should not be viewed as a quantitative measurement. It is rather a qualitative description of how the protein denaturation, measured by SEC, correlates with the loss of free thiol groups. If the loss of free thiols moves in tandem with the denaturation and subsequent aggregation of patatin, the value will not change much. If denaturation and aggregation are much faster than the loss of free thiols, the calculated amount of free thiols in the aggregates will increase.

### 3.2.2.6 Blocking of protein interactions

To investigate the contribution of different protein interactions on the aggregation behavior of PPI, protein solutions were heated in the presence of sodium dodecyl sulfate (SDS), N-Ethylmaleimide (NEM), Urea and Tween 20. Each of these are able to block certain protein interactions (Dissanayake et al., 2013). For this, 2.2% PPI solutions were prepared in distilled water and stirred overnight. After stirring, the solution was centrifuged at 6000 g for 15 min to eliminate undissolved particles. The protein concentration of the supernatant was around 2%. The 2% solution was mixed in a 1:1 ratio with the blocker substances to obtain final concentrations of 1% (w/w) SDS, 20 mmol/L NEM, 3 mol/L Urea, and 0.5% (w/w) Tween 20. The solutions were heated for 30 min in a heated shaker (HLC – Haep Labor Consult, Bovenden, Germany) at 10 °C above



denaturation temperature to ensure total denaturation of the proteins. The solutions were then analyzed by gel electrophoretic analysis as described below.

### **3.2.2.7 Gel electrophoretic analysis**

To investigate the formation of covalently linked aggregates and the loss of patatin during heat-ing, polyacrylamide gel electrophoresis (PAGE) was utilized. Therefore, the protein solution was diluted to 2 mg/mL protein in two types of buffers. One buffer containing 10% SDS, 0.5 M Tris-HCl, and 0.5% bromophenol blue pH 6.8 for non-reducing condition and another buffer containing 10% SDS, 0.5 M Tris-HCl, 0.5% bromophenol blue, and 15 mg/mL dithiothreitol (DTT) pH 6.8 for reducing condition. Samples were heated at 100 °C for 5 min to allow for complete interaction with SDS. For analysis, a prepacked, stain-free TGX gradient gel (4–20%) (Bio-Rad Lab., Hercules, CA, USA) was used. Each well of the gel was loaded with 10 µL of sample dissolved in buffer. A standard marker Precision Plus Protein™ Standard (Bio-Rad Lab., Hercules, CA, USA) was loaded on a separate well. Protein separation was run at 300 V, 50 mA/gel, and 35 W for approximately 35 min. Protein bands were made visible at 300 nm and scanned using Molecular Imager Gel Doc™ XR system (Bio-Rad Lab., Hercules, CA, USA) controlled with ImageLab (v 6.0) software. The protein bands were assigned as follows:

The band intensity around 40 kDa, was ascribed to monomeric patatin in the sample. A second band around 100 kDa could be some residual enzyme-like lipoxygenase present in PFJ (Singh & Kaur, 2016). The bands at 25 kDa and below were ascribed to the protease inhibitors present in the protein solution. Under non-reducing conditions, the 100 kDa band can also consist of dimeric patatin. Prolonged heating can lead to an increase in band intensity above 100 kDa, due to the formation of bigger aggregates.

### **3.2.2.8 Determination of exposed hydrophobicity**

A 1.41 mM N,N-dimethyl-6-propionyl-2-naphthylamine (PRODAN) solution was prepared by dissolving PRODAN in pure methanol to ensure complete dissolution of the fluorescence probe. The solution was kept at – 40 °C under the exclusion of light. For each measurement, small aliquots of the sample were taken from the freezer. Aluminum foil ensured the exclusion of light from the solution, and it was kept over ice for the whole time. Protein solutions were diluted to 1 mg/mL. 1 mL of the diluted solution was transferred into a deep well plate. The PRODAN solution was added in amounts of 0, 5, 10, 15, 20, 25, 30, 40, and 50 µL. Afterward, the solution was thoroughly mixed with a pipette. 100 µL of the mixed solutions were transferred to a black 96-well plate (Greiner chimney flat back 96 well), and the mixture was incubated for 30 min at room temperature in the dark. All solutions were transferred in triplicate onto the plate. After incubation, the solutions were excited at 365 nm in a Tecan Spark microplate reader (Tecan Group Ltd., Männedorf, Switzerland). The emission spectra between 400 and 650 nm were recorded. A maximum was detected at 440 nm, and the absorption value at this wavelength was plotted against the amount of PRODAN added. For most solutions, 30 µL marked the beginning of a plateau in the fluorescence intensity indicating saturation of all hydrophobic binding sites. The fluorescence intensity over the amount

of PRODAN in the linear region before the plateau was fitted by linear regression, and the slope of regression was taken as a measure of the exposed surface hydrophobicity ( $S_0$ ).

### **3.2.2.9 data evaluation and kinetic data fit**

Experiments were done in duplicate from two independently prepared solutions. If not described otherwise, the depicted data points describe the average of two measurements and error bars the min/max range of the measurements. As only experiments were only done in duplicate no standard deviations could be obtained. The kinetic data of the loss of native patatin during heating was obtained from the SEC experiments described above. To derive kinetic parameters from the SEC data, the loss of native patatin at every point in time ( $C_t$ ) in relation to native patatin in the unheated sample ( $C_0$ ) was fitted by non-linear regression (see Equation (3-10)).

$$\frac{C_t}{C_0} = [(n - 1)k_{app} * t + 1]^{\frac{1}{1-n}} \text{ for } n \neq 1 \quad (3-10)$$

Where  $n$  is the reaction order and  $k_{app}$  is the apparent rate constant. The formula was already used by other research groups (Delahaije et al., 2015; Loveday, 2016) for the fitting of kinetic data.

### 3.2.3 Results and Discussion

#### 3.2.3.1 Heat-induced denaturation and aggregation in PPI solutions

Heating a protein solution for a prolonged time results in the unfolding of the proteins and subsequent formation of higher molecular aggregates. The denaturation of a pH 7 PPI solution can be seen in Figure Figure 3-5. The biggest changes occurring during heating relate to the loss of native size patatin and the increase of the aggregate fraction (> 670 kDa). Smaller aggregates are also present in the protein solution. However, these readily react into bigger aggregates (> 670 kDa) as was already observed by others (Pots et al., 1999c).

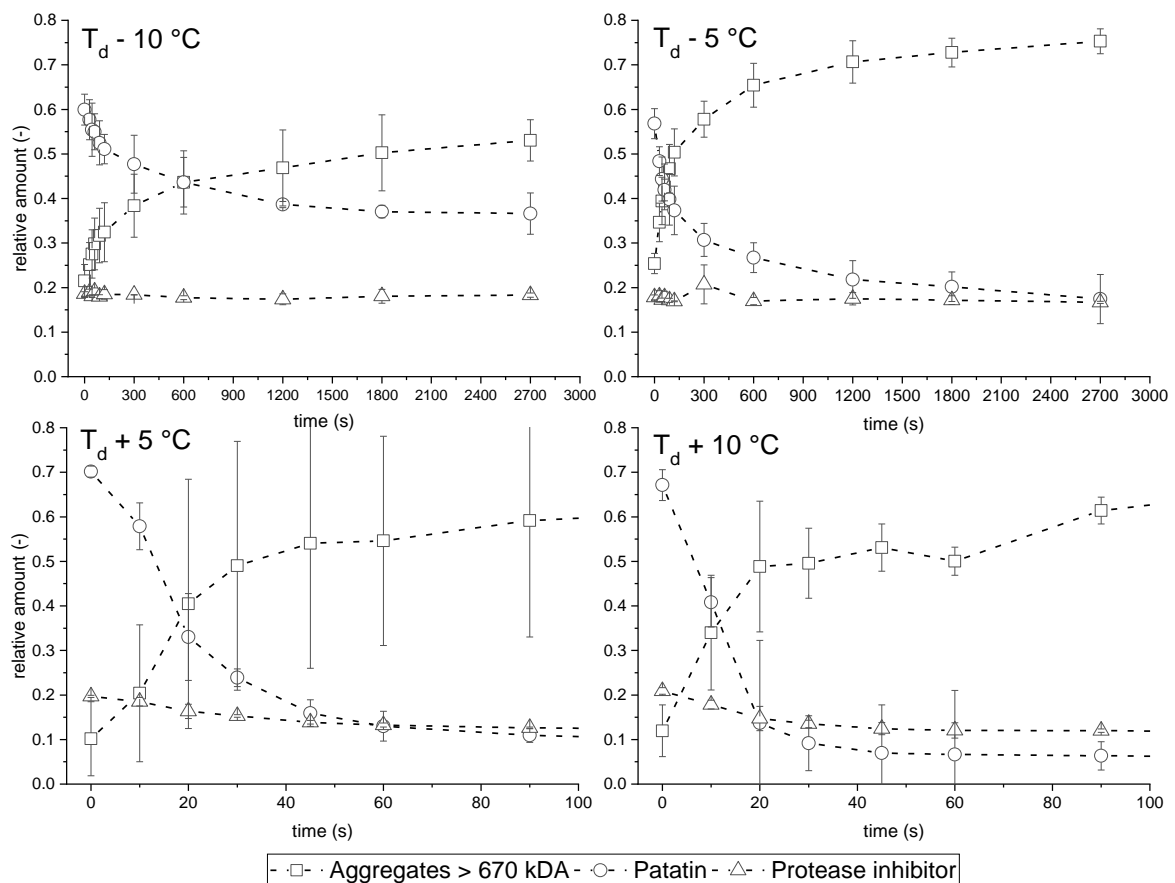


Figure 3-5 Change of absorbance area measured by SEC of the different protein fractions, exemplarily shown for a 1% PPI pH 7 solution after heating for different durations. As denaturation above  $T_d$  happens very fast, only the first 100 s of are depicted.

It can be seen that the loss of native patatin goes in parallel with the increase of the large aggregate fraction. It is, therefore, reasonable to assume that the formed aggregates mainly consist of aggregated patatin. Furthermore, it can be seen that the PI fraction is unaffected by the heat treatment. Although PI were shown to unfold and form gels at temperatures around 70 °C (Schmidt et al., 2019), nearly no interaction between PI and patatin could be seen. Small decreases in the protease inhibitor fraction were observed for the higher temperatures investigated, which will be explained later when the intrinsic fluorescence spectra of the solution are discussed.

### 3.2.3.2 Kinetic parameters of patatin denaturation and aggregation

Prolonged heating of the PPI solutions resulted in the loss of native-sized patatin due to unfolding and aggregation (Figure 3-6). When heating was done above  $T_d$ , the loss of patatin was fast, and residual native-sized protein was below 20% within 200 s. When heating was done below  $T_d$ , the loss of native patatin was much slower; however quite similar for pH 7, 8, and 9. The most pronounced differences between the denaturation curves were found at the extremes of the investigated pH range. The fastest denaturation occurred for PPI solutions at pH 6, and the slowest denaturation was observed for pH 10. This showed that electrostatic repulsion has an important influence on the aggregation behavior of patatin. The reduced electrostatic repulsion at pH 6 increases the likelihood of the unfolded protein monomers aggregating, whereas the increased electrostatic repulsion at pH 10 decreases aggregation. Because of this, the aggregation is slowed for alkaline conditions.

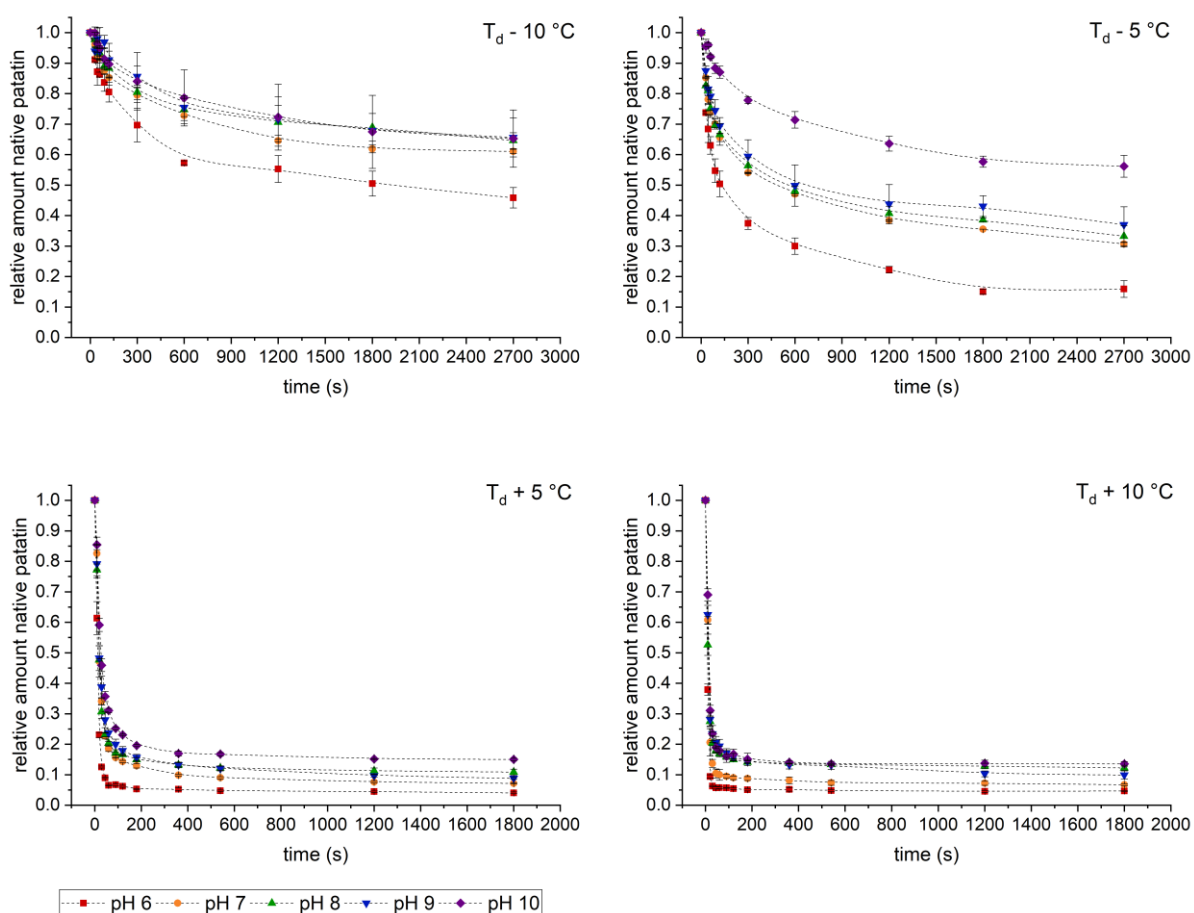


Figure 3-6 Decrease of native sized patatin in relation to the unheated sample during heating, determined by SEC.

Furthermore, the loss of native protein in a solution can be used to derive reaction parameters of the underlying chemical reaction. One simple method for fitting kinetic data is through non-linear regression, demonstrated for a variety of  $\beta$ -lg data (Loveday, 2016) as well as for aggregation kinetics of ovalbumin and patatin (Delahaije et al., 2015).

From the denaturation described in Figure 3-6, the apparent reaction rate ( $k_{app}$ ) can be derived through non-linear regression. From the reaction rate, the Arrhenius diagram of the reaction can be obtained, as shown in Figure 3-7. The reaction orders of the PPI aggregation in dependence of the denaturation temperature and the pH are given in Table 3-1. For all pH values, a decline in reaction order was observed with increasing temperatures. For comparison, data on patatin denaturation at pH 7 (Pots et al., 1999c) was fitted with the same non-linear regression, and a similar trend could be seen. At 50 °C, a high reaction order of  $8.78 \pm 2.44$  was found, which decreased to  $2.39 \pm 0.14$  at 65 °C. Another study reported a reaction order of 2.9 when fitting the average of patatin denaturation data under different heating conditions (Delahaije et al., 2015). However, in this study, certain conditions clearly deviate from the averaged trend line, something which was not observed for the other proteins ( $\beta$ -lactoglobulin and ovalbumin) in the study. For example, denaturation at low temperature and/or low electrostatic repulsion behaved very differently from denaturation at higher temperatures and at neutral pH. Therefore, changes in the reaction order appear to be more pronounced for patatin than for  $\beta$ -lg.

Table 3-3 Reaction order of the denaturation of a PPI solution in dependence of temperature and pH. The temperature is given in relation to the determined denaturation temperature  $T_d$ . The standard error obtained from fitting Eq. 3 to the Data shown in Figure 2.

	pH 6	pH 7	pH 8	pH 9	pH 10
$T_d - 10 \text{ }^\circ\text{C}$	$6.09 \pm 0.30$	$8.33 \pm 0.39$	$9.57 \pm 0.58$	$7.75 \pm 0.98$	$8.27 \pm 0.57$
$T_d - 5 \text{ }^\circ\text{C}$	$3.45 \pm 0.10$	$4.96 \pm 0.11$	$5.37 \pm 0.13$	$5.55 \pm 0.16$	$6.49 \pm 0.28$
$T_d + 5 \text{ }^\circ\text{C}$	$1.10 \pm 0.24$	$1.89 \pm 0.32$	$2.19 \pm 0.30$	$2.42 \pm 0.31$	$2.32 \pm 0.31$
$T_d + 10 \text{ }^\circ\text{C}$	$1.48 \pm 0.27$	$1.69 \pm 0.36$	$2.29 \pm 0.40$	$3.02 \pm 0.46$	$2.60 \pm 0.37$

Figure 3-7 shows the Arrhenius diagram of the denaturation kinetics of PPI. A change in reaction rate in dependence of the temperature of unfolding can be seen. The  $k_{app}$  of the three highest temperatures investigated for each pH value, with the exception of pH 10, are on a straight line. The lowest investigated temperature exhibited the lowest  $k_{app}$  and deviated clearly from the trend line of the other three data points. This could indicate two different ways on how the proteins unfold and aggregate.

For  $\beta$ -lg, a bend in the Arrhenius diagram was already observed for purified protein (Tolkach & Kulozik, 2007) and in different milk milieus (Anema et al., 2006). The reaction at lower temperatures was described as rate limited by the unfolding step and for higher temperatures as rate limited by aggregation. Under unfolding limited conditions, not every protein monomer is unfolded and therefore reactive. Therefore, not each collision of two proteins results in aggregation. Furthermore, when the temperature was not too high and irreversible aggregation not likely, proteins can also refold. The fact that patatin is able to refold was already observed by others (Pots et al., 1998a). Contrary to this, the protein collisions result in high rates of irreversible aggregation in case most proteins are already unfolded. For  $\beta$ -lg, this is the case when the temperature is sufficiently high so that all proteins in a solution are unfolded. This was found to

be the case around 90 °C, as analytically determined by DSC (Tolkach & Kulozik, 2007).

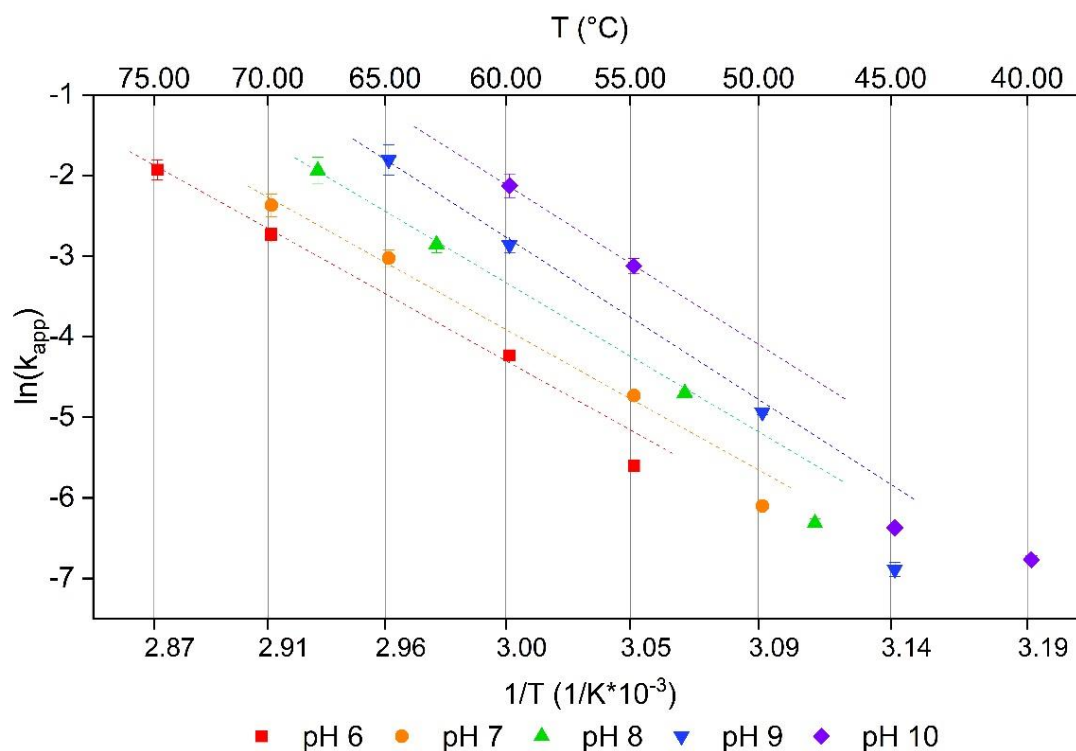


Figure 3-7 Arrhenius diagram of the PPI denaturation reaction rate. The reaction rate is obtained by fitting Equation (3-10) to the data presented in Figure 3-6. For temperatures 10 °C below the respective denaturation temperature, a deviation from the linear behavior is observed. The dashed line is meant as a guide for the eye.

This is a clear difference from what was found in this study for patatin. The bend in the Arrhenius diagram for patatin occurs somewhere between  $T_d - 10$  °C and  $T_d - 5$  °C. At  $T_d - 5$  °C, less than 20% of protein is unfolded according to the DSC data (data not shown). This indicates that already small amounts of unfolded or partially unfolded protein are enough to change the aggregation kinetics towards diffusion rate-limited kinetic behavior. This might also explain why aggregation of patatin is much faster than  $\beta$ -lg (Delahaije et al., 2015). Due to the lack of internal disulfide bonds, patatin's tertiary structure is less stabilized than  $\beta$ -lg. Therefore, unfolding in patatin should happen at a higher degree and the exposure of hydrophobic groups is more pronounced.

The fact that native patatin already develops considerable interactions with hydrophobic interaction columns (Creusot et al., 2011) gives an indication that this protein, even in its native state, might be more readily prone to aggregation driven by hydrophobic interactions. As the aggregation should be mainly initiated through exposed hydrophobic groups, these groups might initiate aggregation even with native proteins, allowing for diffusion-limited aggregation despite not all proteins being unfolded. The reason why pH 10 deviates from this trend is probably due to the low temperatures used for denaturation. Furthermore, the high negative charge at such elevated pH levels might lead to the unfolding of proteins independent of heat application, influencing the overall aggregation mechanism. In addition, aggregates could dissolve and form denatured

monomeric proteins in extreme alkaline conditions. For example, whey protein aggregates at pH levels of 11 and above were shown to dissolve (Mercadé-Prieto et al., 2007).

At a given temperature, decreasing the pH resulted in decreases in the reaction rate, and increases in pH resulted in increases in the reaction rate (Delahaije et al., 2015). However, it is known that lowering the pH towards the IEP of a protein results in an increase in heat-resistance of the protein, seen in increased  $T_d$ . The reason for this are stronger intramolecular interactions between the amino-acid residues due to a reduced electrostatic repulsion between the chains (Haug et al., 2009). Therefore, when heating temperatures are set in relation to the  $T_d$ , the lower electrostatic repulsion between the proteins facilitates protein aggregation.

### 3.2.3.3 Protein-protein interactions within PPI aggregates measured by SDS-PAGE

By applying reducing and non-reducing SDS-PAGE, the formation of covalently linked protein aggregates can be investigated. To determine how the formation of covalent bonds changes during thermal aggregation, a PPI solution with pH 7 was heated at 70 °C, and samples were taken at different time steps, see Figure 3-8. Under non-reducing conditions, a decrease in monomeric patatin and an increase in di- and trimers and larger aggregates were detected. This showed that prolonged heating of patatin results in more disulfide bond formation between the monomers. When the heated solutions under reducing conditions were investigated, the native-sized patatin fraction had a similar band intensity as in the unheated sample (data not shown).

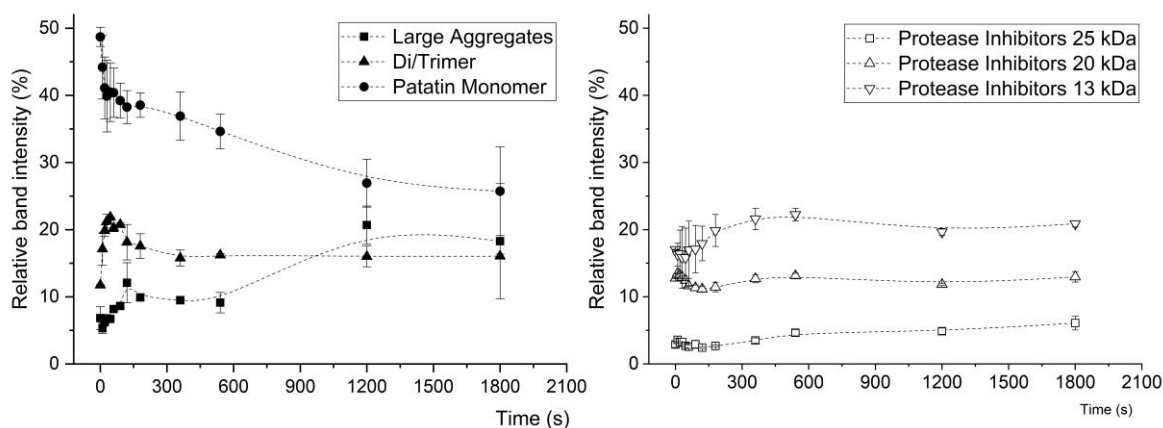


Figure 3-8 Change in protein amount of the patatin and aggregate fractions of a 1% PPI solution at pH 7 in dependence of the time heated at 70 °C. The band intensity was averaged from two SDS-PAGE gels under non-reducing conditions, and the range is indicated by the error bars.

Furthermore, the protease inhibitor fraction showed no pronounced changes in band intensity over the heating time. This led to the conclusion that the protease inhibitor fraction does not participate in aggregate formation via covalent bonds. For other protein systems, like whey and egg proteins, alkaline pH levels led to increased reactivity of thiol groups and subsequently to more disulfide bond formation (Monahan et al., 1995; Leeb et al., 2018; Handa et al., 1998). The main difference between these pro-

tein systems and the patatin system is that patatin lacks internal disulfide bonds. Therefore, a thiol-disulfide exchange reaction is not likely to occur. Nevertheless, disulfide-linked trimeric structures were described for very diluted PPI solutions heated at neutral pH (Pots et al., 1999a). The aggregation mechanism behind these trimeric structures remained unclear. In Figure 3-9, it can be seen that the amount of monomeric patatin decreased for all pH values upon heating.

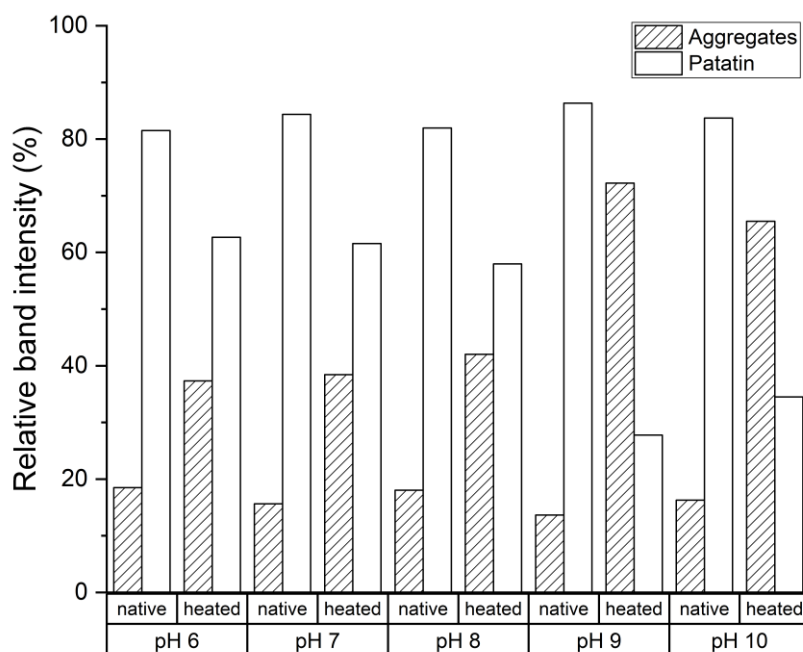


Figure 3-9 Influence of pH on the amount of native sized and aggregated patatin in dependence of the pH in a non-reducing SDS-PAGE. The heating was done 10°C above  $T_d$  for 30 min. The band intensity was taken from one SDS-PAGE gel under non-reducing conditions.

Furthermore, increasing the pH value to alkaline levels resulted in patatin forming more covalently linked aggregates. This is a clear indication that patatin is able to form disulfide-linked aggregates and that the reactivity of the thiol group is increased with alkaline pH values. At first the increased aggregate formation at alkaline pH levels seems like a contradiction to what was described for the SEC results where lower amounts of aggregates were found at alkaline levels. However, one has to consider that the SEC measures the protein solution in an aqueous phosphate buffer. Therefore aggregates linked through non covalent bounds are intact. In the SDS buffer only covalent linked aggregates are shown. It can be concluded, that at alkaline pH values aggregation in PPI is slowed down compared to neutral or slightly acidic pH. However, the aggregates that do form are rather formed through disulfide bonds than non-covalent bonds. The reactivity of the free thiol groups will be described in detail further below.

For a better understanding of the protein interactions forming the aggregates, PPI solutions were mixed with the blocking substances sodium dodecyl sulfate (SDS), N-Ethylmaleimide (NEM), Urea and Tween 20. Upon heating, the relative intensity of the



patatin and aggregate fraction under non-reducing conditions changed (see Figure 3-10). The reduction in patatin indicated the formation of covalently linked aggregates from this protein. The formation of covalent linked aggregates can be also seen when the aggregate fraction is increased upon heating. Non-covalently linked proteins is dissociated by the SDS-PAGE buffer and can therefore, not be detected.

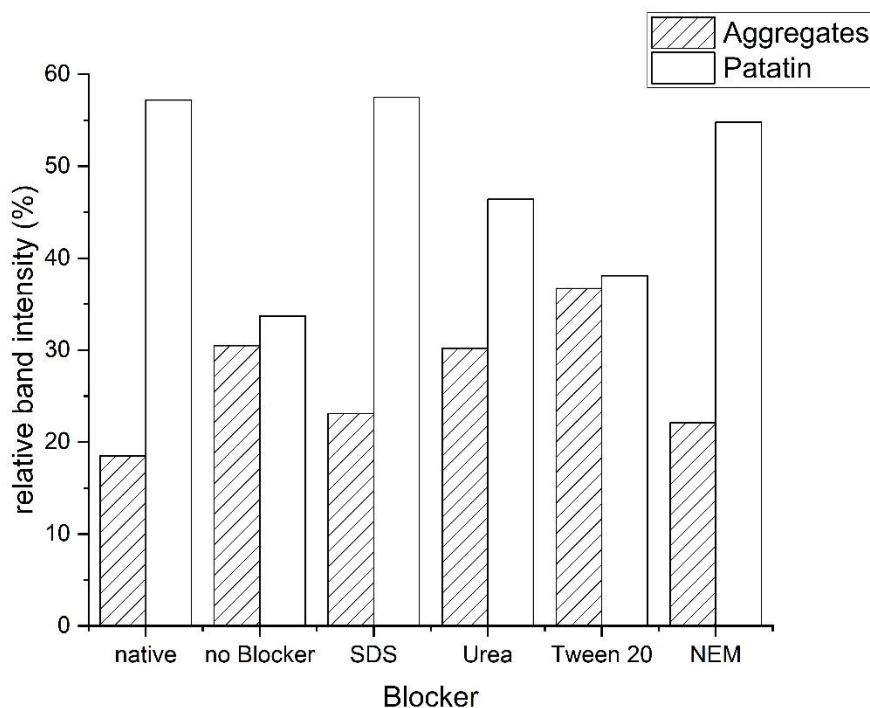


Figure 3-10 relative amount of protein in the aggregate and patatin fraction under non-reducing conditions in the presence of different blocking substances. The heating was done 10°C above  $T_d$  for 30 min. The band intensity was taken from one SDS-PAGE gel under non-reducing conditions. The solution heated in the presence of NEM formed a weak gel. This indicated a strong influence of the thiol groups on the aggregation behavior of PPI.

Tween, with its large non-polar structure, is expected to disrupt hydrophobic protein interactions (Baldwin, 2010). Urea is described as a blocker of hydrogen bonds (Martin et al., 2014) as well as a blocker of hydrophobic interactions (Gómez-Guillén et al., 1997; Messens et al., 2000; Lupano, 2000). For both systems, the band intensity of the aggregate peak was reduced, and patatin was increased compared to the heated sample without added blocker. This indicates that if the non-covalent interactions are inhibited to a certain degree, the formation of covalent disulfide bonds is reduced as well.

That initial interactions through hydrophobic interactions are necessary for the formation of disulfide bonds is even more apparent when SDS is used as a blocker. SDS binding to proteins correlates very well with the hydrophobicity of the protein (Takenaka et al., 1972; Kato et al., 1984; Reynolds & Tanford, 1970). Therefore it is used to investigate the contribution of hydrophobic interactions in the aggregation and gelation of protein systems (Martin et al., 2014; Keim & Hinrichs, 2004; Havea et al., 2009; Dissanayake et al., 2013). SDS prevented the formation of disulfide-linked aggregates, as indicated by a similar band intensity of the heated patatin band as in the unheated

sample.. This indicates that at first, a hydrophobic interaction between protein monomers has to occur before disulfide links can be formed. This was also proposed by other researchers investigating the aggregation of  $\beta$ -lg (Carrotta et al., 2001; Bauer et al., 2000).

The fact that disulfide bridges were indeed involved in the formation of aggregates was additionally shown through the addition of NEM. NEM binds to the free thiol groups available in the protein solution and should therefore inhibit any disulfide formation. This led to the smallest measured aggregate fraction and the same amount of native-sized patatin measured as in the unheated reference.

It can be concluded that patatin rich potato protein isolate can form aggregates that are intermolecularly linked by disulfide bonds. However, these disulfide-linked aggregates are around 250 kDa and smaller, in the presence of SDS. This is considerably smaller than the size of aggregates measured by SEC. The aggregates in the SEC had a size of over 1.500 kDa, which is the size exclusion limit of the used SEC column. Therefore it can be concluded that smaller disulfide linked aggregates (around 250 kDa) interact through non-covalent interactions to form bigger aggregates of over 1.500 kDa.

Based on these results, the importance of disulfide links within the aggregates is apparent when taking a closer look at the aggregation in the presence of NEM. The 1 % PPI solution in 20 mM NEM gelled upon heating. This behavior was not observed for any of the other solutions in the presence or absence of blocking substances. Gelation at 1% protein concentration is considerably lower than the 6% minimum gelling concentration reported before for patatin (Creusot et al., 2011). The blocking of the thiol group might lead to more exposure of hydrophobic groups that induce the gelation, something which was observed for  $\beta$ -lg and soybean protein heated in the presence of NEM (Hua et al., 2005; Xiong et al., 1993; Boye & Alli, 2000).

To sum up, disulfide links were not shown to induce polymerization in patatin, the same way as reported for  $\beta$ -lg. Nevertheless, blocking of thiols seriously altered the techno-functional properties of the aggregates. Therefore, the reaction of thiols during heat-induced aggregation of PPI will be investigated in more detail in the following.

#### ***3.2.3.4 Reduction of free thiol groups in PPI solutions and formation of disulfide bonds during heat-induced aggregation***

The loss of free thiols during heating was correlated with the denaturation of the native-sized patatin fraction. The data was processed according to Equation (3-8) and (3-9) to obtain the theoretical amount of thiols in the aggregate fraction. The results of this comparison are shown in Figure 3-11. Higher pH values resulted in more disulfide formation, thus lowering the amount of free thiols within the aggregates. Negative values indicate that less thiol groups are measured than could be expected from the amount of native sized patatin. As SEC measures also dimers as native sized patatin disulfide bonds that links dimer without being incorporated in bigger aggregates will lead to a negative value.

For all investigated temperatures, the solutions at pH 6 exhibited the highest amount of free SH groups within the aggregates. This can be explained by the electrostatic interactions influenced by the pH level. At reduced electrostatic repulsion, protein molecules can interact with each other more readily. Furthermore, the formation of short-ranged non-covalent bonds like hydrogen bonds is increased. In a study on PPI gels, it was shown that closer to the IEP, the relative contribution of electrostatic and hydrogen bonds to the gel network was higher than for neutral or alkaline pH (Andlinger et al., 2021a). When patatin aggregates at low electrostatic repulsion, the aggregation is fast. Furthermore, aggregates grow in size, turning the solution turbid. The proteins interact mainly through non-covalent bonds, and there is a low amount of disulfide formation.

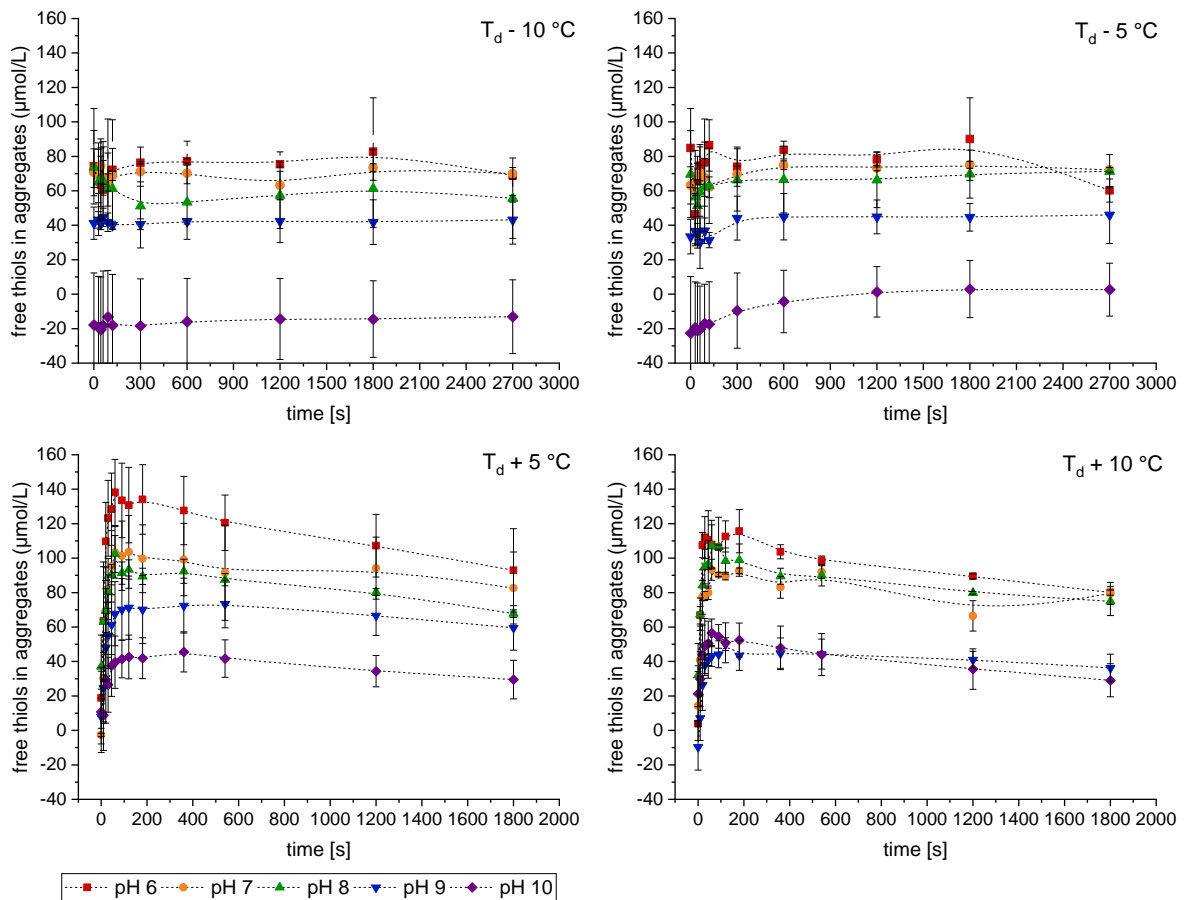


Figure 3-11 Amount of free thiol groups in the aggregate fraction during heating of a PPI solution in dependence of temperature and pH. Error bars represent the range of two independent heating trials.

The temperature also has a strong influence on the formation of disulfide bonds. Below  $T_d$ , the aggregation is slow and limited by the unfolding of the proteins. At the lowest investigated temperatures ( $T_d - 10\text{ °C}$ ) patatin denaturation and loss of free thiols move in tandem. Under these conditions, each patatin molecule that unfolds and aggregates forms a disulfide bridge. Therefore, no excess free thiols in the aggregates are measured, and the calculated amount of free thiols in the aggregate fraction remained constant. With temperatures above  $T_d$ , the aggregation process changes. Above  $T_d$ , most monomers are unfolded and can readily interact through exposed hydrophobic groups. The aggregation is fast and only limited by the diffusion of the proteins towards each

other. For patatin heated above  $T_d$ , a high amount of free thiols within the aggregates was detected. Therefore, an increase in reaction rate favors the formation of non-covalent bonds over disulfide bonds. However, with prolonged heating at higher temperatures, the amount of free thiols decreases, indicating that after initial aggregation through non-covalent bonds, disulfide bridges are formed. This two-step process, which involves initial aggregation via non-covalent bonds, followed by stabilization through internal disulfide bonds, was also proposed for ovalbumin (Broersen et al., 2006). Ovalbumin was shown to have similar reaction rates as patatin (Delahaije et al., 2015) which might be explained by a similar reaction mechanism. Besides the formation of disulfide bonds, the accessibility of hydrophobic amino acids also plays an important part in the aggregation of patatin. Therefore, the hydrophobic character of PPI during heat treatment shall be accessed in the following.

### 3.2.3.5 Change in the hydrophobic character of PPI aggregates during heat-induced aggregation

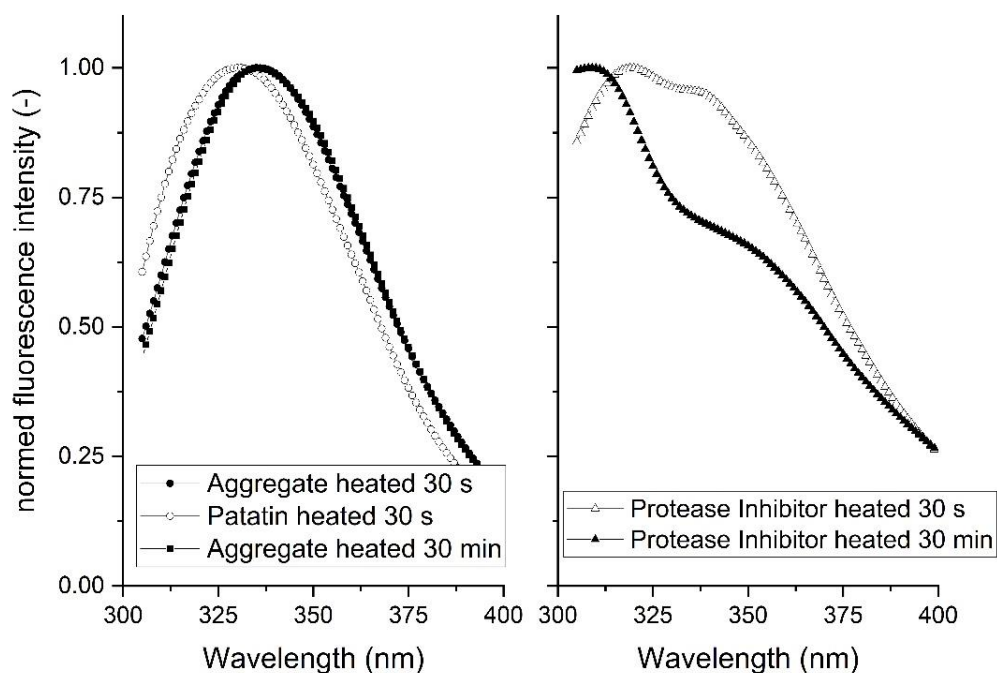


Figure 3-12 Fluorescence spectra of the patatin, aggregate (> 670 kDa), and protease inhibitor fraction, determined by coupled SEC and FLD. Spectra were normed on the maximum detected emission value. Excitation of the sample was done at 280 nm.

The SEC coupled with FLD was used to investigate the local environment of aromatic amino acid groups in the different protein fractions. In Figure 3-12, the emission spectra of the patatin and the > 670 kDa aggregate fraction are displayed. The native patatin fraction exhibited an emission maximum at around 331 nm, whereas for the aggregate fraction, a maximum was found at 341 nm. At 280 nm, both aromatic residues, tryptophan (trp) and tyrosine (tyr) can be excited. After falling back to the unexcited state, photons of a higher wavelength are emitted. The measured emission spectrum, especially the maximum, is dependent on the local environment of the excited aromatic

amino acid. When the proteins are in their native state, the aromatic amino acids reside within the protein core, and the environment is mostly apolar. Upon unfolding, the amino acids are exposed to the polar water environment resulting in a shift of the emission spectrum towards higher wavelengths. This behavior has been reported for  $\beta$ -Ig (Cairoli et al., 1994) and patatin (Pots et al., 1998a). The investigation of thermally induced aggregation of patatin showed a substantial refolding of the tryptophan residues when the hot solution was cooled down to ambient temperature. However, a partial shift suggested that the local environment did not fully fold back into the native state or that not all proteins did refold. Unheated patatin as well as heated patatin samples exhibited no difference in the fluorescence spectra (data not shown). Therefore, it can be assumed that the native –sized patatin in heated samples is either not unfolded or is refolded upon cooling. A difference between the aggregates heated for 30 s or 30 min could not be observed. Therefore increased unfolding after longer heating times could not be detected.

From SEC and SDS-PAGE results, it could be shown that the protease inhibitor fraction does not decrease considerably for the investigated temperature and pH conditions. However, a small decrease could be observed for samples heated at high temperatures, indicating the aggregation of certain protease inhibitors. The protease inhibitor, which is the least affected by the heat treatment, had a retention time of around 11.7 min, and the fluorescence spectrum is given in Figure 3-12. The described protease inhibitor shows a clear fluorescence maximum around 310 nm. It is reasonable to assume that this protease inhibitor is the potato cysteine protease inhibitor (PCPI). PCPI is the second most abundant protease inhibitor and possesses trp and tyr fluorescence with a peak maximum around 310 nm (Pouvreau et al., 2005b). With a determined unfolding peak temperature of 67 °C, PCPI should be more heat resistant than patatin, which would explain why PI aggregation plays a minor role in the investigated PPI system.

Although the unfolding of patatin aggregates was shown by the intrinsic fluorescence tests, no changes between the pH levels could be observed by this method. To investigate the influence of pH on the extent of unfolding and accessibility of hydrophobic groups, a fluorescence test with the uncharged PRODAN dye was conducted.

PRODAN binds to hydrophobic amino acid residues and forms a fluorescent complex. Contrary to other fluorescence dyes, PRODAN contains no charge- Therefore, interactions between the dye and the protein should be only hydrophobic in nature. The dye was already used to measure exposed hydrophobicity in succinylated patatin samples (Delahaije et al., 2014). Independent of the pH value, all unheated protein solutions exhibited a similar exposed hydrophobicity ( $S_0$ ) (see Figure 3-13).

Heat treatment changed the affinity of the protein solutions towards the fluorescence probe PRODAN. The higher the pH value of a solution, the lower  $S_0$  of the solution. This indicates that hydrophobic groups are less accessible at higher pH values. A similar dependence of PRODAN- $S_0$  on the pH value was recently described for BSA (Lan et al., 2020). At high pH values, alkaline side chains are deprotonated, which will lead to the formation of hydrophobic interactions of these side chains (Dyson et al., 2006).

These newly formed hydrophobic regions can be stabilized via disulfide bonds, similar to what was shown for WPI gels (Betz et al., 2012). At pH 6, patatin monomers exhibit a lower overall charge as this pH value is closer to the protein's IEP. However, the charge is more evenly distributed across the protein surface, allowing for more electrostatic interactions between positively and negatively charged amino acid residues (Yan et al., 2013). Therefore, pH values closer to the IEP allow for more non-hydrophobic protein interactions. This leads to more of the hydrophobic groups exposed into the solution and increased accessibility for the fluorescence probe.

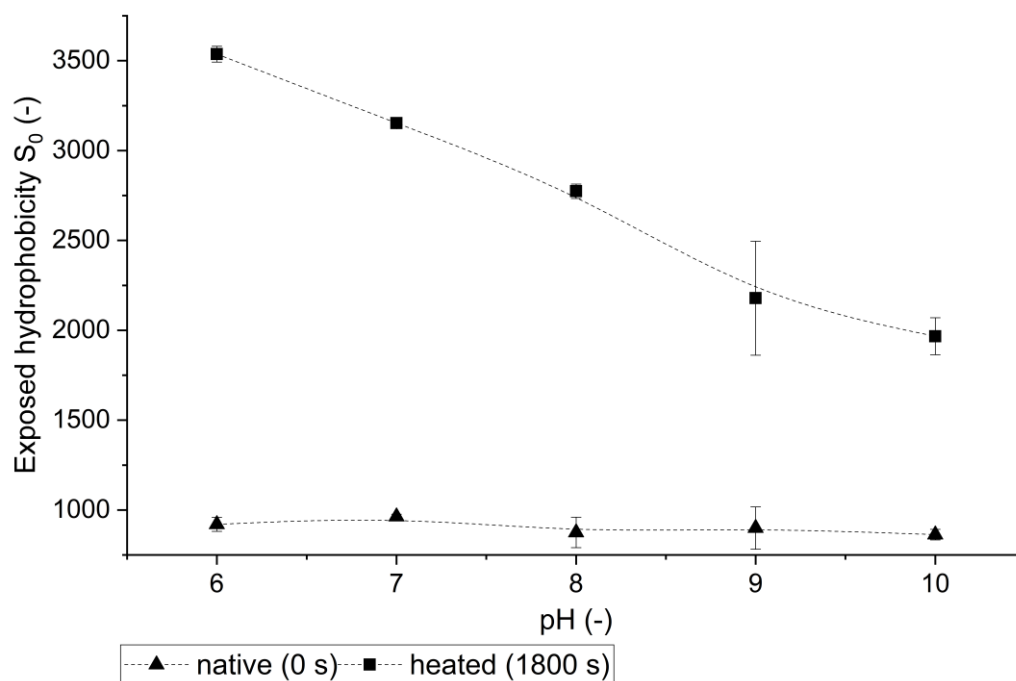


Figure 3-13 Exposed hydrophobicity of a 1% PPI solution native (unheated) and heated for 1800 s above  $T_d$ , in dependence of the pH

### 3.2.4 Conclusion

The influence of protein interactions on the aggregation mechanism of patatin rich potato protein isolate (PPI) has been evaluated for different heating conditions. It could be shown that disulfide-linked aggregates can be formed when initial aggregation through non-covalent bonds is possible. At low pH, aggregates grew in size, had a high amount of exposed hydrophobic groups, and low stabilization through disulfide bonds. Increasing the pH reduced the exposure of hydrophobic residues and increased the formation of disulfide bonds. Therefore, disulfide bond formation plays an important role in stabilizing hydrophobic patches within the patatin aggregates.

This knowledge can be used to alter techno-functional properties of PPI aggregates through different heating conditions and pH milieus. For example, aggregates with a high exposed hydrophobicity will be beneficial for the stabilization of air/water (Dombrowski et al., 2017) and oil/water interfaces (Delahaije et al., 2013). However, for the application as an oleogelator, more hydrophilic particles are preferred (Vries et al., 2017). Furthermore, the aggregates can be considered building blocks of hydrogels. The different kinetics and protein interactions that happen in PPI in dependence of the

pH explain why the microstructure of PPI gels differ considerably in dependence of the pH (Andlinger et al., 2021a). Unordered, particulate gels are formed under conditions where the aggregation is fast and a high amount of exposed hydrophobicity is present. Under conditions of high disulfide bond formation and low exposed hydrophobicity, the resulting gels are finely stranded.

**Author Contributions:**

D.J.A.: writing—original draft preparation, data curation; investigation, conceptualization; project administration, validation, methodology, formal analysis

P.R.: formal analysis, validation, investigation,

C.H.: validation, investigation, methodology, resources

U.K.: writing - Review & Editing; funding acquisition; Supervision

**Funding:** This IGF Project AiF 19712 N of the FEI was supported via AiF within the program for promoting the Industrial Collective Research (IGF) of the German Ministry of Economic Affairs and Energy (BMWi), based on a resolution of the German Parliament.

**Acknowledgments:** We would like to thank Marc Laus from AVEBE, Veendam, The Netherlands, for providing the potato protein isolate. Furthermore, we would like to thank Melania Pilz for her experimental contributions during method development. Annette Brümmer-Rolf and Paola Quintana-Ramos are thanked for their help in establishing the PRODAN fluorescence test.

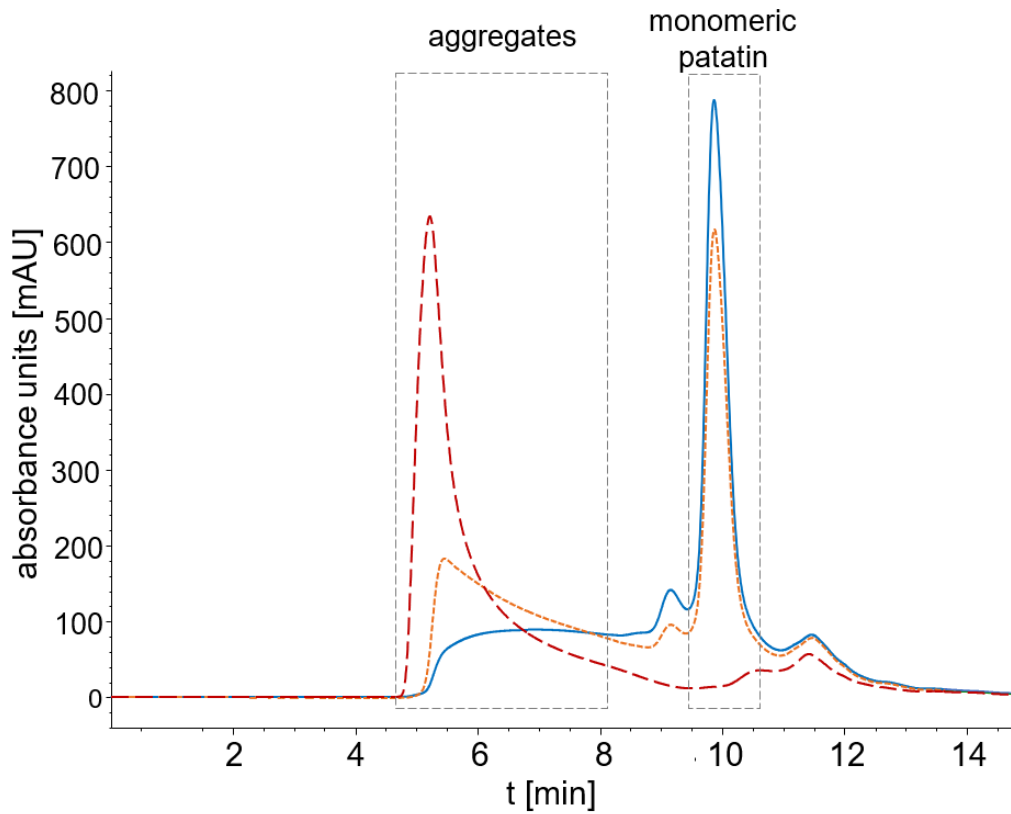
**Conflicts of Interest:** The authors declare that they have no known competing financial interests or personal relationships that could have appeared to influence the work reported in this paper.

### 3.2.5 Supporting information

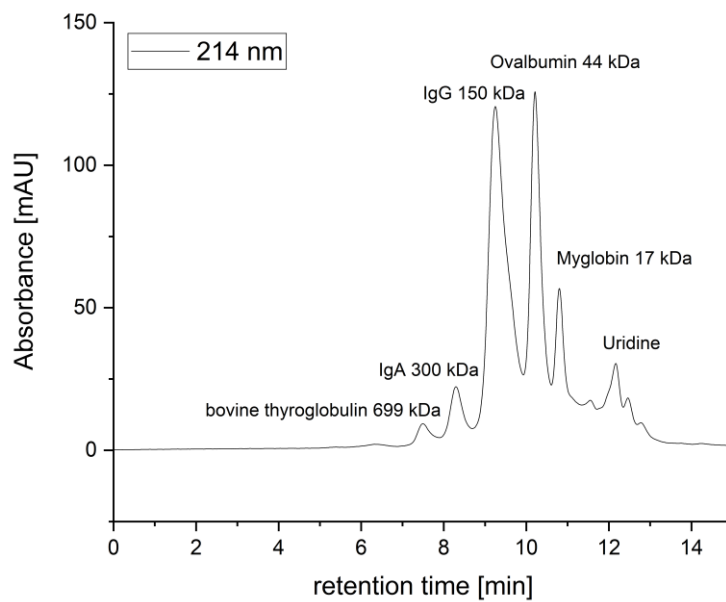
**Table S1.** Time intervals at which heating was stopped for further analysis.

<b>Heating time for temperatures below <math>T_d</math> (s)</b>	<b>Heating time for temperatures above <math>T_d</math> (s)</b>
0	0
30	10
45	20
60	30
90	45
120	60
300	90
600	120
1200	180
1800	360
2700	540
	1200
	1800

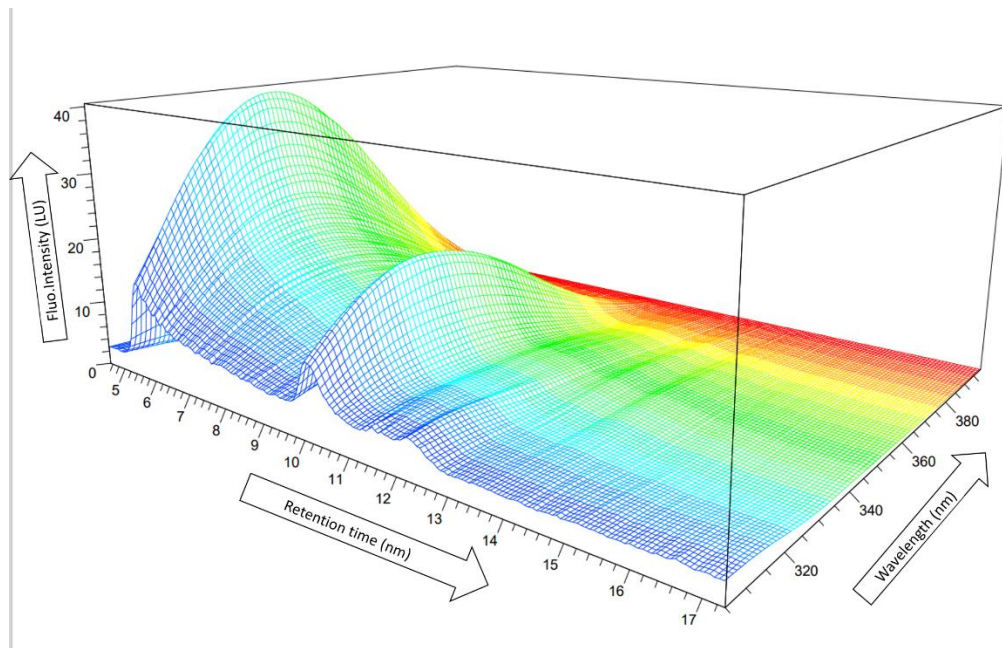




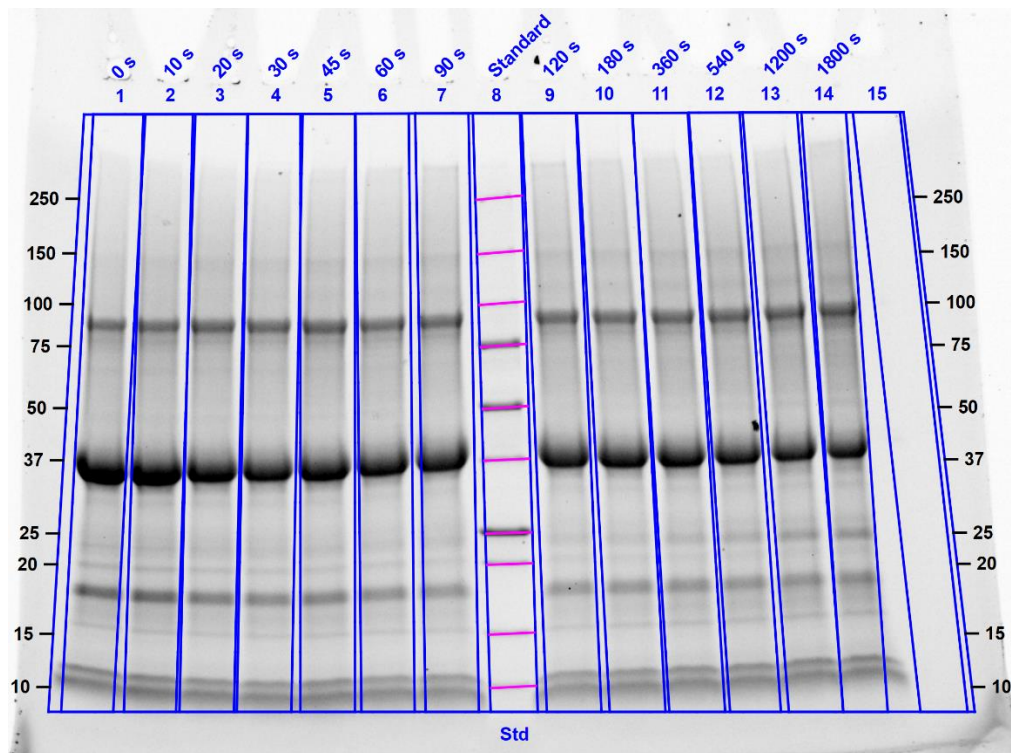
**Figure S1.** Chromatograms demonstrating the shift of size fractions in SEC analysis upon heating of PPI solutions. Exemplary data shown is for 1 % PPI solutions adjusted to pH 7 and heated at 65 °C (Td + 5 °C). Chromatograms shown are for PPI unheated (blue, solid), heated for 10 s (orange, narrow dashes) and heated for 30 min (red, wide dashes). Absorbance was measured at 214 nm.



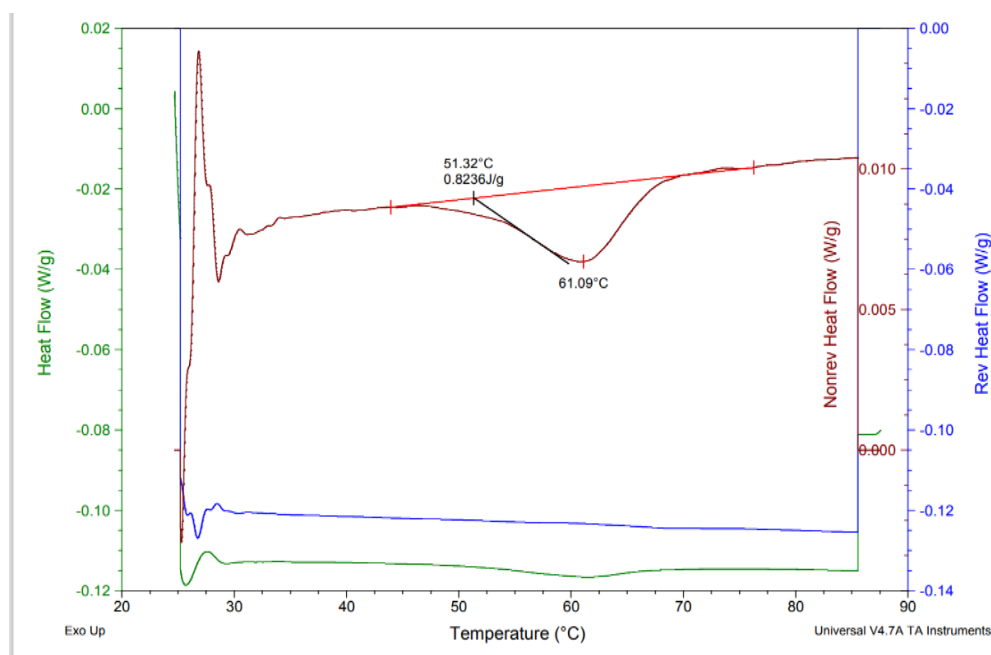
**Figure S2.** Chromatogram of the SEC standard. The commercial standard was applied on every test day to check the performance of the column. Absorbance was measured at 214 nm.



**Figure S3.** 3D-FLID Chromatogram a heated PPI sample. For every peak determined through the retention time the whole fluorescence spectra was recorded.



**Figure S4.** SDS-PAGE of a PPI solution heated for different time intervals. Protein bands at 13, 20 and 25 kDa are protease inhibitors, 40 kDa is patatin, the band around 100 kDa is containing dimers, trimers as well as a non-patatin 100 kDa fraction, 150 kDa and above is considered higher molecular aggregates. The time intervals are given on top.



**Figure S5.** Heat flow recorded during a mDSC measurement of a PPI sample at pH 7. The heating ramp was set to 2°C/min. peak temperature was obtained by analyzing the non-reversed heatflow.



### **3.3 Heat-induced aggregation kinetics of potato protein – Investigated by chromatography, calorimetry, and light scattering**

#### Summary and contribution of the doctoral candidate

In the previous chapter, it could be shown that the aggregation mechanism of PPI could be influenced by changes in the pH conditions. Furthermore, the data suggested that the kinetics of the reaction changed in dependence on the temperature, but not enough temperature levels were investigated to describe this phenom further. Changes in the aggregation kinetics in dependence of the temperature were already described for whey proteins, such as  $\beta$ -lactoglobulin ( $\beta$ -lg). For this a RP-HPLC method for the determination of patatin was adapted from  $\beta$ -lg analytics. Three distinct aggregation regimes could be found. At temperature levels where no unfolding occurred, patatin showed aggregation. In temperature regions where unfolding was detected the temperature dependence was lower. Not every collision between two monomers results in aggregation, hence the reaction was described as reaction-limited. The third and final reaction regime was found for high temperatures where > 90% of protein is unfolded. At these temperatures, every collision of monomers results in aggregation and thus the reaction is described as diffusion-limited. The comparison between pH 6 and 7 showed that the changes in the reaction mechanism occurred at temperature levels that were dependent on the unfolding behavior measured by DSC. Although the kinetics were similar for both pH values and only dependent on the unfolding behavior, the size of the aggregates was very different for both pH values. At pH 6 bigger aggregates were obtained than at pH 7. Furthermore, at low temperatures at pH 6 aggregates were bigger by an order of magnitude compared to higher temperatures.

The doctoral candidate was main responsible for the development of all utilized methods as well as the method validation. The comparison of the patatin aggregation data and the comparison with literature data on  $\beta$ -lg aggregation was done by the candidate to derive the mechanistic understanding of the here presented protein aggregation. Further contributions included conceptualization of the experiments, writing of the original draft, responding to reviewer comments as well as data curation and statistical analysis.

*Adapted original manuscript*<sup>3</sup>

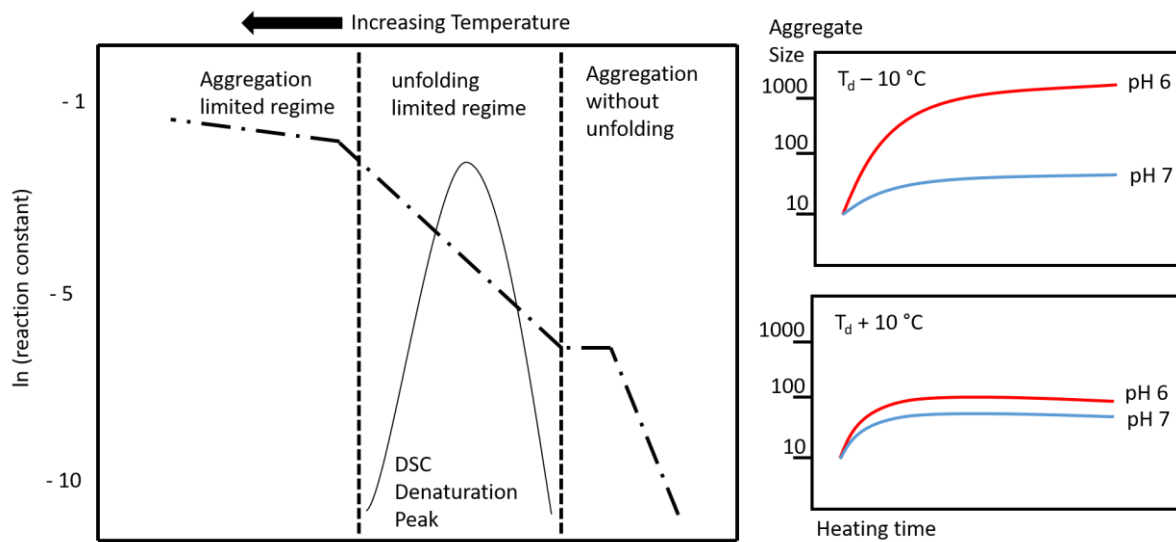
## Heat-induced aggregation kinetics of potato protein – Investigated by chromatography, calorimetry, and light scattering

David J. Andlinger\*, Ulrich Schrempl, Claudia Hengst, Ulrich Kulozik

Chair of Food and Bioprocess Engineering, TUM School of Life Sciences,

Technical University of Munich, Weihenstephaner Berg 1, 85354, Freising, Germany

### Graphical Abstract



<sup>3</sup> (Adaptions refer to formatting issues: e.g., numbering of sections, figures, tables and equations, abbreviations, axis labeling, figure captions and style of citation). Reference lists of all publication based chapters were merged at the end of this thesis to avoid duplications.

Original publication: Andlinger, D. J., Schrempl, U., Hengst, C., Kulozik, U. (2022). Heat-induced aggregation kinetics of potato protein – Investigated by chromatography, calorimetry, and light scattering. *Food Chemistry*, 389, 133114. <https://doi.org/10.1016/j.foodchem.2022.133114>

Permission for the reuse of the article is granted by Elsevier Limited.

## Abstract

In this study, the heat-induced aggregation behavior of patatin rich potato protein isolate (PPI) was investigated by reversed-phase high-pressure liquid chromatography (RP-HPLC), differential scanning calorimetry (DSC), and dynamic light scattering. It could be shown that aggregation already occurs at low temperatures, despite low degrees of unfolding. The unfolding temperature, determined by DSC, coincided with a change in the reaction kinetics, which is determined by the unfolding step below a critical temperature up to the point, where the proteins are completely unfolded. The reaction rate  $k$  as a function of the absolute temperature  $T$  is then determined by diffusion of unfolded proteins forming aggregates. This change can be visualized in the Arrhenius diagram by a change of the slope of the relationship  $k \sim 1/T$ . A change in pH from 7 to 6 shifted the critical temperature towards higher values and resulted in larger aggregate sizes, due to reduced electrostatic repulsion.

### 3.3.1 Introduction

In general, the application of heat on globular proteins, induces unfolding of these proteins, thus exposing hydrophobic amino acid side chains or other hidden reactive groups from the protein's core. This step is then followed by the aggregation of the protein molecules through these side chains. This aggregation can be accompanied by the formation of covalent disulfide bonds in case that reactive thiol (SH) groups get exposed (Roefs & Kruif, 1994). These protein aggregates can act as building blocks forming protein gels (Nicolai & Durand, 2007), or oleogels (Vries et al., 2017), and they can stabilize gas bubble interfaces (Kurz et al., 2021). However, they can also be undesirable, as they might negatively impact storage stability and textural properties in food products.

In the past, most investigations of protein denaturation and aggregation were conducted with whey proteins as a research subject, especially  $\beta$ -lactoglobulin ( $\beta$ -lg), which has thus become one of the best-characterized proteins (Wagner et al., 2020b). However, comparing the aggregation behavior of proteins from different sources revealed that their aggregation behavior could be very different and difficult to predict by generalizing or transferring observations from one protein to another one, even if the molecular structure appears to be similar (Delahaije et al., 2015). The current trend of using plant proteins for food products texture design is not based on an equally deep knowledge of the reaction kinetics, compared to milk proteins for instance. Due to this gap in fundamental knowledge, these proteins should be characterized in their specific unfolding and aggregation characteristics. This way, thermal processing conditions can be selected to induce structure building effects in a targeted manner.

One of the still emerging plant proteins is patatin, the main protein obtained from potato fruit juice as a by-product of starch production (Waglay et al., 2014). Patatin is the major potato protein with around 40% of total potato protein content (Singh & Kaur, 2016). Patatin is a globular protein with a mass of about 40-42 kDa and an isoelectric point of around 4.8-5.2 (Løkra & Strætkevorn, 2009). It has one free thiol group and no internal disulfide bonds. Although different isomers are known, they behave similarly

upon heating (Pots et al., 1999b). Like other heat-sensitive globular proteins, patatin unfolds upon heating. A partial unfolding of patatin can already occur at low temperatures of around 28 °C, followed by a loss of secondary structural elements, i.e.  $\alpha$ -helices between 45 - 55 °C and  $\beta$ -strands between 50 - 90 °C (Pots et al., 1998a). The kinetics of aggregation was investigated in another study for diluted (0.33-1.5 mg/mL) patatin solutions at pH 7 by size exclusion chromatography (SEC), and a two-step aggregation process was proposed (Pots et al., 1999c). At first, patatin reversibly unfolds. The unfolded monomer forms a reactive particle, which can further react to irreversibly crosslinked aggregates. When heating was performed at temperatures of 60 °C or above, the unfolding step was determined to be nearly instantaneous.

When interpreting literature data, one has to consider that potato protein isolates (PPI) enriched in patatin can still contain considerable amounts of protease inhibitors (PI) (Schmidt et al., 2019; Ralet & Guéguen, 2000). However, a recent study showed that the reactivity of this PI fraction is low, and aggregates are almost exclusively formed by the patatin fraction, although the patatin content in commercially available PPI generally does not exceed 60% (Andlinger et al., 2021c).

Furthermore, in this study, it was shown that stabilizing bonds of the aggregates, i.e. hydrophobic interaction and the amount of disulfide bonds, could be modified by a change in pH. At any of the pH levels studied so far, the aggregation speed at the lowest heating temperature (10 °C below the determined temperature of unfolding) was lower than at the higher temperatures.

Such temperature-dependent changes in aggregation behavior were also described for  $\beta$ -Ig (Zúñiga et al., 2010). At lower temperatures, not every collision of two proteins results in aggregation, as some proteins are still in their native state. Increasing the temperature led to a higher degree of unfolding and higher kinetic mobility and, therefore, to more frequent collisions. At higher temperatures, nearly all proteins are considered unfolded and reactive. Therefore, the aggregation rate of these reactive proteins is only dependent on the diffusion of two proteins towards each other. These two reaction rate regimes are called unfolding-limited and diffusion-limited, respectively (Tolkach & Kulozik, 2007).

For potato proteins, previous studies found evidence that the aggregation kinetics change in dependence of the temperature (Andlinger et al., 2021c; Pots et al., 1999c). However, the kinetics were never set in relation to the foregoing unfolding step, determined by the endothermic heat flux of unfolding by DSC. Therefore, a clear correlation between unfolding and aggregation, as was shown by Tolkach et al. (2007) for  $\beta$ -Ig, could not be established so far.

This study aims at investigating the thermal aggregation behavior of patatin in dependence of the heating temperature and pH. These findings shall be correlated with data on unfolding of the proteins. This will give new insights related to the formation of patatin aggregates as a way of functionalization for applications in food structure engineering.



The experimental methodology was based on determining the effects of aggregation kinetics and protein interactions on the aggregate size. By reducing the pH from 7 to 6 and heating at temperatures below and above the respective unfolding temperatures the effect of protein-protein interactions was influenced. The related hypothesis claims that different reaction mechanisms can be induced in patatin aggregation and these aggregation mechanisms can influence the aggregation kinetics and aggregate structure.

### 3.3.2 Materials and methods

#### 3.3.2.1 Materials and sample preparation

All weight ratios are given as weight percentage (gram protein per 100 g solution) abbreviated as % (w/w). Commercial patatin rich potato protein (PPI) powder (Solanic 200®), was obtained from AVEBE (Veendam, The Netherlands). The protein content was 88.6% (w/w), determined using the method of Dumas with an accuracy of  $\pm 0.1\%$  (w/w) and a nitrogen conversion factor of 6.25 (Schmidt et al., 2019; Dachmann et al., 2020) (Vario MAX CUBE, Elementar Analysen Systeme GmbH, Hanau, Germany). The patatin content, measured by the relative band intensity (RBI) in a reducing SDS-PAGE, was found to be around 60%. A similar patatin concentration for this PPI was reported by Katzav et al. (2020). Other protein components were so-called protease inhibitors (25% RBI) and a higher molecular weight fraction with 100 kDa (15% RBI).

The powder was solubilized in deionized water and stirred overnight at 4°C to limit bacterial growth. The protein concentration was 2.8% (w/w). In order to remove insoluble and aggregated components, the solution was adjusted to pH 5, with 1 mol/L HCl (Merck, Darmstadt, Germany), and centrifuged at 6000  $\times g$  for 15 min. The supernatant was re-adjusted to the final pH of either 6 or 7 with 1 mol/L NaOH (Merck, Darmstadt, Germany). The protein concentrations of the final solutions were determined to be around 1% (w/w). The protein distribution was similar to the start solution with 60% Patatin, as determined by SDS-PAGE (see Supporting information Fig. 2). This solution with 1% (w/w) protein is called PPI solution throughout the paper.

#### 3.3.2.2 Modulated differential scanning calorimetry (mDSC)

The denaturation behavior of the protein solutions was measured by using  $T_{\text{zero}}$ -calibrated modulated differential scanning calorimetry (mDSC Q1000, TA Instruments, New Castle, United Kingdom).

For both investigated pH values, a protein solution was prepared as described above. To obtain a clear DSC signal, the protein concentration in the solution was increased by a factor of ten by a 10 kDa centrifugal filter (Chromafil Xtra RC, Düren, Germany). From each solution, 25  $\mu\text{L}$  were filled into a hermetically sealed aluminum pan. As a reference, an empty aluminum pan was used. The temperature was gradually increased from 30 to 80 °C with a rate of 2 K/min and an overlaid sinusoidal modulation of  $\pm 0.5$  K/min. The modulation allowed for both high sensitivity and selectivity as described by (Badkar et al., 2006). The denaturation temperature ( $T_d$ ) was determined as the peak temperature in the DSC thermogram. The integral of the peak area can be

correlated with the degree of unfolding (Tolkach & Kulozik, 2007) with 0% unfolding at the onset of the peak and 100% at the end of the peak.

#### **3.3.2.3 Heating experiments**

3.14 mL of the protein solution were filled into stainless steel tubes (L = 240 mm, wall thickness 1 mm) and closed with a screw cap. The samples were preheated in a water bath to 34 °C for 2 min, low enough to prevent pre-term aggregation, to shorten the heating-up ramp to the target temperature. The final heat treatment to target temperature was performed in a water bath at intervals ranging from 0 s to 45 min. The samples were heated for a maximum of 30 min for 5 and 10 °C above denaturation temperature and for 45 min 5 and 10 °C below denaturation temperature, which was determined by DSC. The heating was performed at temperatures from 45° to 70°C. At temperatures below 45 °C, no denaturation could be observed in the investigated time frame, and at temperatures above 70 °C, the denaturation occurred too fast to obtain reasonable fits. The temperature was monitored with an external thermometer. After the heating step, the tubes were immediately transferred into ice water to rapidly stop the heat-induced reaction.

#### **3.3.2.4 Purification of patatin from PPI for use as a standard in RP-HPLC calibration and protein quantification**

To quantify the patatin content in the heat-denatured PPI samples, first an analytical standard for the determination via RP-HPLC had to be obtained. For this, patatin was purified from the commercial powder as described in the following. PPI solutions with a protein concentration of 7.3% (w/w) were prepared by dissolving the PPI powder in deionized water overnight. The protein solution was centrifuged at 6000 x g for 15 min to remove any insoluble parts. A second centrifugation step was conducted after adjusting pH 5, close to the IEP of patatin. This precipitated any aggregates and insoluble components, resulting in a final concentration of 2.4 % (w/w). The solution was re-adjusted to pH 7 and separated by a preparative Superdex 200/pg column in an ÄKTA Pure 25 system (Cytiva, Freiburg im Breisgau, Germany). A 100 mM sodium phosphate buffer pH 7 was used for elution of the sample. Then, the patatin fraction (around 40 kDa) was collected, concentrated, and dialyzed with a 30 kDa centrifuge filter (Amicon Ultracel, Merck, Darmstadt). This way the patatin fraction could be separated from the protease inhibitor fraction with a smaller size.

After four complete solvent exchange steps against deionized water, the sample was deionized, confirmed by conductivity measurements (SevenMulti™ dual meter pH/conductivity, Mettler Toledo, Gießen, Germany). The deionized solution was shock-frosted in a round-bottomed flask by rotating the flask in a cooled ethanol bath (-40 °C). The frozen solution was lyophilized by connecting the glass flasks with the frozen protein to a freeze dryer Delta 1-24 LSC (Martin Christ, Osterode am Harz, Germany) at ambient temperatures at 0.370 mbar for 48 h. Analysis by SDS-PAGE determined a patatin purity of 86.3 % (see Figure 1 of supplementary information).

Nitrogen analysis by the method of Dumas determined a protein concentration of 86.0 %, with the remaining portion being mostly salts as the deionized water was not

completely salt free. This isolate was used as analytical standard in the RP-HPLC method.

### 3.3.2.5 Determination of native patatin by RP-HPLC

The native patatin in the solution was quantified. The in-house generated patatin standard, described above, was used for calibration. Before analysis, the aggregated protein was separated from the native and soluble protein. By adding between 50 - 140  $\mu\text{L}$ , of a 0.01 mol HCl solution to 500  $\mu\text{L}$  of PPI solution, a pH of 5.55 was obtained. The amount of HCl was dependent on the degree of denaturation, as native protein exhibited a higher buffer capacity than denatured. At pH 5.55, the denatured protein formed larger aggregates that could be filtered from the native protein using a 1 mL syringe with a 0.45  $\mu\text{m}$  pore size syringe filter (Chromafil Xtra RC, Düren, Germany) (see Fig. 3 of Supporting Information for the pH dependent solubility of PPI Aggregates).

To ensure complete unfolding of the protein, 200  $\mu\text{L}$  of each filtered solution was mixed with 800  $\mu\text{L}$  of a BisTris-guanidine hydrochloride (GuHCl) with dithiothreitol (DTT) (0.1 M Bis Tris, 6 M GuHCl, 21.5 mM Trisodiumcitrate, 19.5 mM DTT). The protein-buffer mixture reaction time was 30 min at room temperature. For the HPLC analysis, an Agilent PLRP-S 300A 8 $\mu\text{m}$  150\*4,6mm with guard column (5\*3mm) was used in an Agilent 1100er Series chromatography system equipped with a binary pump. The analysis temperature was set to 40 °C. 100% gradient grade water with trifluoroacetic acid (TFA) (c = 0.1 %) was used as eluent A. 80% acetonitrile gradient grade containing 0.055% TFA served as eluent B. The flow rate was 1.0 mL/min. The injection volume was 10 $\mu\text{l}$  for the non-heated sample and 20  $\mu\text{l}$  for the heat-treated samples, depending on the expected native protein content. Following Gradient was used (Table 3-4)

The chromatographic process was controlled by Agilent OpenLab CDS ChemStation Edition software. Signals were quantified by the detection of UV absorbance by a diode array detector (DAD) at a wavelength of 226 nm. By injecting the patatin standard, see “Purification of patatin” as described above, with known protein content the amount of protein could be quantified and assigned to the patatin fraction. Results were analyzed using Agilent OpenLab CDS ChemStation Edition software.

Table 3-4 Continuous phase gradients used for RP-HPLC analysis

0 – 2 min	2 – 17 min	17 – 19 min	19 – 19.5 min	19.5 – 24 min
A: 55%	A: 0%	A: 0%	A: 55%	A: 55%
B: 45%	B: 100%	B: 100%	B: 45%	B: 45%

### 3.3.2.6 Particle size measurement by dynamic light scattering

Data on particle size were obtained by dynamic light scattering (DLS). The solution was measured in a micro-cuvette (Brand GmbH & Co. KG, Wertheim, Germany) in a Zetasizer Nano System (Malvern Panalytical Ltd, Malvern, United Kingdom). The sample was analyzed in backscattering mode at an angle of 173 °. The system correlates the scattering intensity over time. From this auto-correlation function, a weighted mean hydrodynamic size, the so-called z-Average of the particles could be obtained. The z-

average was already used to characterize a wide range of food protein systems (Sarkar et al., 2010; Liu & Tang, 2014; Donato et al., 2011).

### 3.3.2.7 Determination of free thiol-groups in heated PPI solutions

The loss of free thiol-groups during the heat-induced aggregation of patatin was measured through the reaction of the remaining thiol-groups not involved in disulfide bonds with the reagent 4,4'-Dithiodipyridine (DTDP). Free thiol-groups crosslink in the presence of the dye and result in the conversion of DTDP to 4-thiopyridine (4-TP). 4-TP has an absorption maximum at 324 nm and can be quantified on a reversed-phase high-pressure liquid chromatography system (RP-HPLC) coupled with a DAD detector. The amount of 4-TP formed is directly related to the amount of free thiols in a sample. The absorption signal was calibrated with cysteine as standard material in different concentrations. A detailed description of materials, sample preparation, evaluation, and method of validation was reported recently by our group (Kurz et al., 2020).

Under the assumption that each native patatin molecule only contains one free thiol-group (Delahaije et al., 2015; Creusot et al., 2011) the amount of free thiols can be calculated by Equation (3-11).

$$\frac{C_{Pat,HPLC}}{M_{Pat}} = n_{Thiol,Pat} \quad (3-11)$$

with  $C_{Pat,HPLC}$  as the concentration of native patatin obtained by HPLC in g/L,  $M_{Pat}$  the molecular weight of patatin (40 kDa) and  $n_{Thiol,Pat}$  the molar concentration of free thiols in the solution in mol/L.

This thiol concentration ( $n_{Thiol,Pat}$ ) can be subtracted from the total amount of thiols determined by the dye-coupled RP-HPLC method ( $n_{total,Thiols}$ ) (see Equation (3-12)). This way, an excess amount of thiols ( $n_{Thiols,excess}$ ) was obtained

$$n_{total,Thiols} - n_{Thiol,Pat} = n_{Thiols,excess} = n_{Thiol,Aggregates} \quad (3-12)$$

$n_{Thiols,excess}$ , indicates that more thiols are measured in the solution than would be predicted by the amount of native patatin alone. Therefore, changes in  $n_{Thiols,excess}$  must occur within the protease inhibitor fraction or the aggregate fraction. As shown in our previous work, the reactivity of protease inhibitors in the utilized powder is negligible (Andlinger et al., 2021a). Therefore, it appears appropriate to assume that excess thiols are mainly measured based on the fact that reactive thiols remain unreacted (i.e. not involved in aggregation) within the aggregated fraction ( $n_{Thiol,Aggregates}$ ).

This way, a qualitative description of how the protein denaturation, measured by HPLC, correlates with the loss of free thiol-groups can be obtained. If the loss of free thiols moves in parallel with the denaturation and subsequent aggregation of patatin, the value will not change much. If denaturation and aggregation are much faster than the loss of free thiols, the calculated amount of free thiols in the aggregates will increase.

### 3.3.2.8 Evaluation of Kinetic Parameters

Experiments were repeated in duplicate from two independently prepared solutions. If not described otherwise, the depicted data points describe the average of two independent measurements and error bars the min/max range of the measurements. For the DSC data triplicates were performed.

The formal kinetic data of the loss of native patatin during heating was obtained from the RP-HPLC experiments described above. To derive kinetic parameters from the RP-HPLC data, the loss of native patatin at every point in time ( $C_t$ ) in relation to native patatin in the unheated sample ( $C_0$ ) was fitted by non-linear regression (see Equation (3-13));

$$\frac{C_t}{C_0} = [(n - 1)k_{app} * t + 1]^{\frac{1}{1-n}} \quad \text{for } n \neq 1 \quad (3-13)$$

where  $n$  is the reaction order and  $k_{app}$  is the apparent rate constant.  $K_{app}$  recognizes that initial protein concentration is kept constant throughout the experiments in contrast to the general rate constant  $k$  which is also dependent on initial protein concentration (Loveday, 2016).

### 3.3.3 Results and discussion

#### 3.3.3.1 Relation between the thermal unfolding of patatin and the thermal reaction kinetic parameters of protein aggregation

To investigate the correlation between patatin unfolding and aggregation, two experiments at pH 6 and 7 were conducted. The increase of unfolded protein as a function of temperature was determined by DSC. Furthermore, from the heating of protein solutions under almost isothermal conditions, the apparent rate of denaturation ( $k_{app}$ ) can be obtained. Both values for PPI solutions at pH 6 and pH 7 are depicted in Figure 3-14.

It can be seen that temperature increases led to an increase in the amount of unfolded protein. The peak denaturation temperature ( $T_d$ ) could be determined as the point where 50% of the protein is unfolded. For pH 7, a  $T_d$  of 62.5 °C was determined, which is in accordance with literature data (Schmidt et al., 2019; Creusot et al., 2011; Andlinger et al., 2021a).

For pH 6, a higher  $T_d$  of 65.0 °C was determined. As the IEP of patatin is around 5 the protein molecules at pH 6 exhibit a lower intramolecular electrostatic repulsion. Due to this reduced repulsion, proteins exhibit higher thermal stability against unfolding, which was also shown for whey proteins (Homer et al., 2018).

Regarding  $k_{app}$ , it can be seen that increased temperatures resulted in increased reaction rates. A similar sigmoidal trend to the unfolding data of the protein solution could be observed. However, aggregation occurs at temperatures at which no unfolding could be detected. How the reaction mechanism changes in dependence of the temperature will be assessed in more detail in the next chapter. By plotting the kinetic data according to the Arrhenius presentation changes in the reaction mechanism in dependence of the temperature can be visualized.

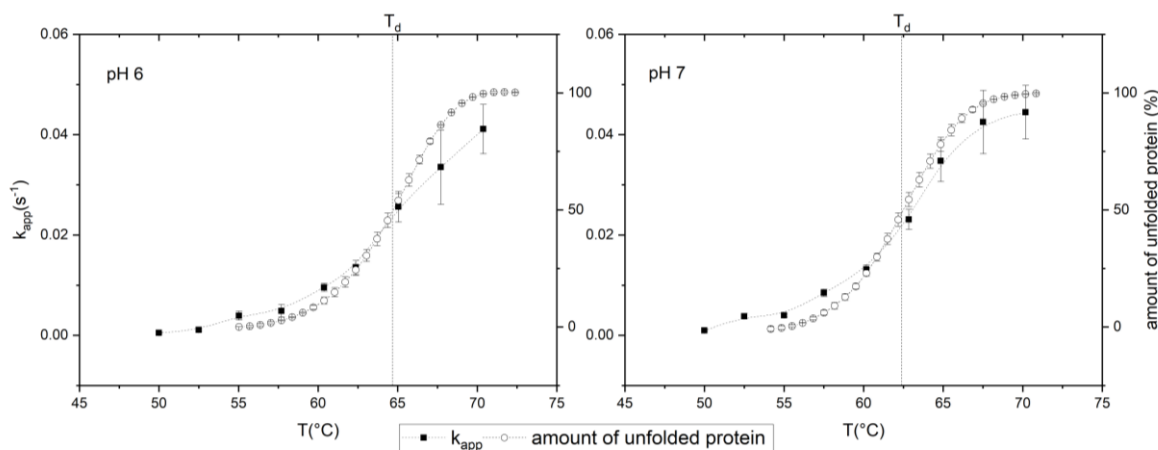


Figure 3-14 Denaturation rate constant  $k_{app}$  for pH 6 (left) and pH 7 (right) dependent on heating temperature. On the second y-axis, the amount of unfolded protein estimated from the integration of the thermogram peak in the DSC is depicted. Error bars of the kinetic data show the difference from a double determination. Error bars of the DSC measurements refer to measurements in triplicate. The  $T_d$  reference line indicates the peak denaturation temperature determined by DSC.

Another parameter obtained by non-linear regression is the reaction order  $n$ , the related data is shown in Table 3-5. It can be seen that increasing the temperature led to lower  $n$  values for both pH values. This trend was previously observed when investigating a similar PPI solution by size exclusion chromatography (Andlinger et al., 2021c).

These results let us conclude that the aggregation of patatin is driven by hydrophobic interactions, which leads to a wide range of reaction orders in dependence of the temperature.

Table 3-5 Aggregation order  $n$  dependent on pH value and heating temperature. Standard errors result from the fit of Equation (3-13)

	50°C	55°C	60°C	65°C	70°C
<b>pH 6</b>	9,1 ±2.0	8,5 ±0.9	3,2 ±0.2	1,2 ±0.2	0,3 ±0.25
<b>pH 7</b>	8,6 ±0.8	3,7 ±0.2	2,2 ±0.1	0,9 ±0.2	$1,3 \cdot 10^{-5}$ ±0.2

In the aforementioned study, it was hypothesized that the high  $n$  value was due to the presence of aggregates in the solution, prior to the heating step. As the kinetics in the here presented study were derived from PPI solutions that were subjected to isoelectric precipitation to remove any aggregates, we can conclude that the high  $n$  values do not stem from the aggregates present prior to heat treatment. How these reaction orders can be interpreted will be explained in the following:

For standard chemical reactions, the reaction order does not change in dependence of the temperature. However, protein unfolding and aggregation are complex reactions, which can be initiated through many different reactive sites of a protein. Fitting  $\beta$ -lg data by non-linear regression revealed changes in the reaction order between 1.5-2.0 (Loveday, 2016). To explain the high reaction order and the wide range of reaction

order described here and for patatin aggregation investigated by SEC (Andlinger et al., 2021c) it is helpful to compare the aggregation of patatin with the aggregation of  $\beta$ -Ig in the presence of NEM. NEM is able to block the free thiol group of  $\beta$ -Ig. This way, the disulfide exchange reaction is interrupted, and aggregation occurs mainly through hydrophobic interactions (Hoffmann & van Mil, 1997). Non-linear regression of  $\beta$ -Ig data in the presence of NEM found reaction orders between 0.57-6.55 depending on protein concentration and pH of the solution (Loveday, 2016). This is a stark indication that hydrophobic interactions lead to a very different reaction mechanism than thiol-/disulfide induced aggregation. Furthermore, when data of patatin aggregation at low concentrations (Pots et al., 1999c) was re-evaluated by our research group through non-linear regression in previous work (Andlinger et al., 2021c) we found a high reaction order of  $8.78 \pm 2.44$  at 50 °C, which decreased to  $2.39 \pm 0.14$  at 65 °C.

The different dependence on temperature may also explain why stark differences between  $\beta$ -Ig and patatin could be found when aggregation at different ionic strengths, pH, and heating conditions was compared (Delahaije et al., 2015). In this study, the amount of denatured protein over the heating time was normalized relative to the time where half of the protein was denatured. For  $\beta$ -Ig, this normalization led to very similar denaturation curves, and all investigated heating conditions produced a similar trend with a reaction order of  $\sim 2.5$ . For patatin, however, this normalization showed marked differences between conditions of fast unfolding and fast aggregation (e.g. heating temperatures at denaturation temperature and above) compared to conditions of slow unfolding and aggregation (e.g. heating temperatures below denaturation temperature). A detailed discussion of the temperature-dependent changes of the reaction mechanism is given in the following.

### **3.3.3.2 Change in reaction behavior of patatin in dependence of the heating temperature**

The logarithmic Arrhenius diagram shows a correlation between reaction rate and reaction temperature. For the aggregation of PPI, the Arrhenius-diagram is shown in Figure 3-15. Unlike other chemical reactions, no linear trend across the whole investigated temperature range could be detected. Instead, depending on the temperature range, different slopes for the reaction in dependence on the temperature could be observed. Different slopes indicate that the reaction mechanisms of protein aggregation change in dependence of the temperature.

This behavior is similar to results reported for  $\beta$ -Ig (Tolkach & Kulozik, 2007). The degree of unfolding was determined as the major influence on the entire denaturation, comprised of unfolding and aggregation.

For patatin, we will describe the changes in aggregation kinetics and explain them by referring back to work by Pots et al. (1998) who looked explicitly at the heat-induced conformational changes of patatin at low protein concentrations with limited chance for aggregation.

The first reaction regime describes the lowest investigated temperatures. From 50 °C to  $T_{\text{onset}}$ , the steepest slope for the reaction was observed. Therefore, protein aggregation already occurs at temperatures below  $T_{\text{onset}}$ , determined by DSC. This can be explained with the structure of patatin. It could be shown that some unfolding of  $\alpha$ -helical structures occurs in the temperature range of 10 °C below  $T_d$  up to  $T_d$ , and some parts of patatin's structure unfold at temperatures as low as 28 °C (Pots et al., 1998). Although these partial unfolding processes are reported in the literature, we did not detect aggregation of patatin when we investigated temperatures below 50 °C. The denaturation of patatin in the investigated time frame was so low that no kinetic parameters could be obtained. It can be concluded that in this temperature range, protein aggregation occurs mainly through the unfolded  $\alpha$ -helical structures as described above

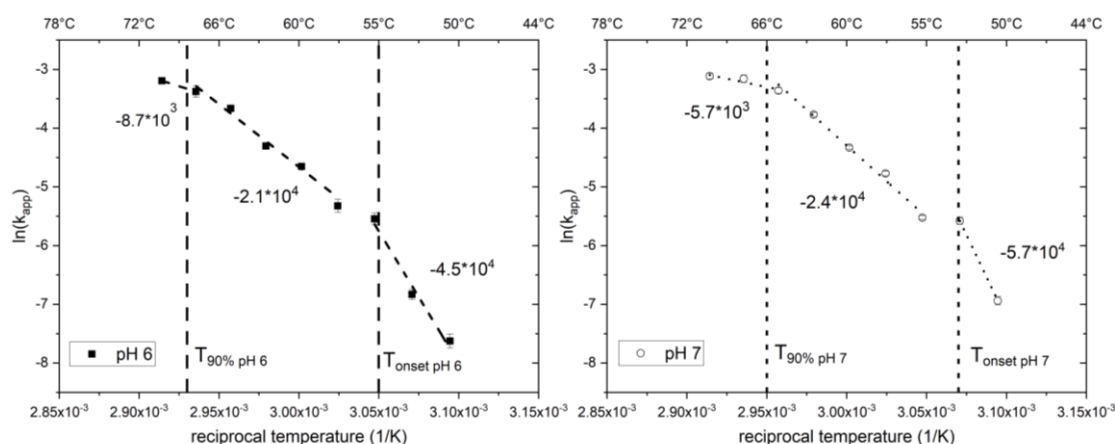


Figure 3-15 Comparison of the Arrhenius diagram of PPI 1 % solution for pH 6 and pH 7. The dashed lines indicate linear fits to the data, with the numbers next to the line representing the obtained slopes.  $T_{\text{onset}}$  reference line marks the beginning of protein unfolding, investigated by DSC at the respective pH value. The  $T_{90\%}$  reference line marks the point at which 90% of the proteins are unfolded. Error bars of the aggregation rate  $k_{\text{app}}$  results from the standard error of the fit of Equation (3-13).

At  $T_{\text{onset}}$ , a change in the temperature dependence of the reaction rate could be observed. It is important to note that this trend occurs for both investigated pH values at their respective  $T_{\text{onset}}$  values.  $T_{\text{onset}}$  marks the temperature at which protein unfolding is so pronounced that an unfolding enthalpy is measured via DSC. The measured enthalpy of unfolding is measured in a temperature range, where losses in secondary structure occur through  $\beta$ -sheets unfolding into random coils (Pots et al., 1998a). Furthermore, exposure of hydrophobic tryptophan aminoacids from the protein core begins. The contact made through hydrophobic aminoacid side chains dominates the aggregation processes in this temperature range, disulfide bonds are only formed in a second step (Andlinger et al., 2021c). However, not each collision of two patatin molecules results in aggregation as long as not all proteins are unfolded. Therefore, this regime can be described as unfolding-limited. The occurrence of an unfolding-limited regime, at temperatures where not each protein is unfolded, was already proposed for  $\beta$ -lg (Tolkach & Kulozik, 2007; Roefs & Kruijff, 1994).



A third change of the reaction rate in dependence of the temperature occurs above temperatures, where 90% of the protein is already unfolded ( $T_{90\%}$ ). Under these conditions, nearly any collision between two particles results in aggregation. Therefore, the temperature dependence of the unfolding reaction is negligible, and the slope flattens accordingly. As the whole process is mainly dependent on the diffusion of the particles towards each other, this regime can be described as diffusion-limited, as it was proposed for  $\beta$ -lg at high temperatures (Tolkach & Kulozik, 2007).

It can be concluded that the reaction mechanism of aggregation changes in dependence on the heating temperature. The reaction starts with a high temperature-dependence. This dependence is reduced when certain temperature thresholds are surpassed. Both temperature thresholds ( $T_{\text{onset}}$  and  $T_{90\%}$ ) are dependent on the unfolding behavior of the molecules, measured by DSC. The unfolding behavior is dependent on the pH with proteins being more resistant to heat at pH values closer to the IEP (Andlinger et al., 2021a; Homer et al., 2018). Therefore, the reaction rate changes, as depicted in the Arrhenius-diagram, occur at higher temperatures for pH 6 compared to pH 7.

Changes in reaction mechanisms can also stem from changes in protein interactions between the protein molecules. For example, in  $\beta$ -lg aggregation, the reaction of thiol-groups forming disulfide bonds dominates the aggregation process (Carrotta et al., 2001). In a recent study, it could be shown that disulfide links also occur in PPI aggregation, and in dependence of the heating temperature, the thiol-groups showed different reactivities (Andlinger et al., 2021c). To verify that the PPI solution used in this study show similar thiol reactivity, despite the lack of aggregates present before heating, the formation of disulfide bonds was investigated in the following.

### **3.3.3.3 Disulfide formation during heat-induced protein aggregation**

From the amount of native patatin and the free thiols in the solution, the amount of free thiols in the aggregates could be estimated. This amount of free thiols in the aggregate fraction can be seen in Figure 3-16.

For both investigated pH values, a similar trend regarding the free thiols in dependence of the heating could be observed. Increasing the temperature led to a higher amount of free thiols in the aggregates, thus to less disulfide bond formation. It can be assumed that the increased unfolding at higher temperatures led to aggregation via hydrophobic side chains from the protein core, rather than disulfide bonds. Therefore, the formation of disulfide bonds plays a smaller role. This trend was more pronounced at pH 6, which resulted in a higher amount of free thiols in the aggregates. This can be explained by the reduced reactivity of the thiol-group at this pH (Hoffmann & van Mil, 1997). Furthermore, the reduced electrostatic repulsion facilitates aggregation through other protein interactions, rather than disulfide bonds (Monahan et al., 1995). The fact that fewer disulfide bonds are formed at higher temperatures is different to the aggregation behavior of  $\beta$ -lg. For  $\beta$ -lg, the free thiol-group, located behind an  $\alpha$ -helix within the protein (Qi et al., 1997), will react more readily at higher temperatures and higher degrees of unfolding (Sava et al., 2005).

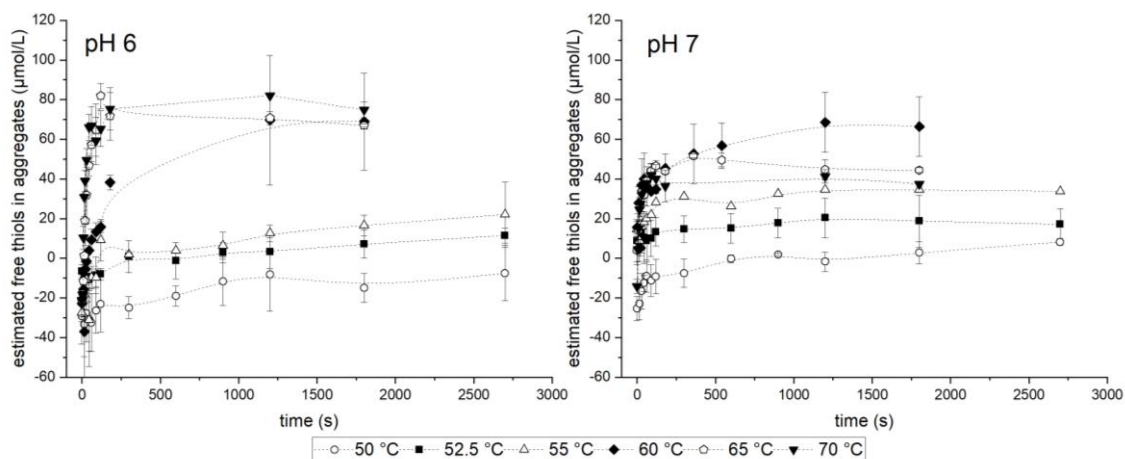


Figure 3-16 Unreacted free thiols within aggregates as calculated by Equation (3-12) of heat-treated PPI samples for pH 6 and pH 7. Data points represent the mean of a double determination and error bars indicate the range of this double measurement.

It could be shown that the protein interactions in PPI aggregation change in dependence of the pH and heating temperature. Changes in the main protein interactions during aggregation can considerably change aggregate shape and size, as shown for ovalbumin from eggs (Ma et al., 2019) and  $\beta$ -lg from whey (Gulzar et al., 2011). Therefore, to characterize the aggregates created under different thermal reaction conditions, the aggregate size was measured by dynamic light scattering, as described in the following.

#### 3.3.3.4 Size of PPI aggregates measured by dynamic light scattering

When investigating the PPI aggregates, a clear difference regarding the aggregate size in dependence of pH and temperature could be observed (Figure 3-17). When interpreting the data, one has to consider that light scattering can not differentiate between bigger or denser aggregates, both will result in increased scattering intensity (Delahaije et al., 2015). However, for simplicity reasons, we will refer to the aggregate size in the following.

For pH 7, the measured size of the aggregates was considerably lower than at pH 6. Therefore, the higher electrostatic repulsion at pH 7, in comparison to pH 6, reduced aggregate growth. It could be seen in Figure 3-17 that by increasing the heating temperature, the measured size increased slightly for pH 7. The increased kinetic energy at elevated temperatures is sufficient to overcome electrostatic barriers between the protein aggregates and unfolded protein molecules, which leads to an increase in aggregate size. Similar observations were reported for  $\beta$ -lg, where higher temperatures at pH 7 led to a larger aggregate size and polydispersity (Vogtt et al., 2011).

Heating the protein solution at pH 6 led to the formation of bigger aggregates for all investigated temperatures. The fact that a reduction in electrostatic repulsion led to an increase in aggregate size was already described for different protein aggregates (Delahaije et al., 2015). Our results also show another interesting effect of the heating temperature on the aggregate size: When patatin was heated at low temperatures and

lower electrostatic repulsion (pH 6), the aggregates are bigger by an order of magnitude compared to the aggregates created at higher temperatures. This observation can be explained as follows: We assume an aggregation scheme were first aggregated proteins form nuclei, which further grow in a secondary step. Such a scheme was proposed by different research groups for  $\beta$ -lg (Roefs & Kruif, 1994; Carrotta et al., 2001). Depending on whether the nucleation or the growth step is facilitated by the reaction conditions, more small and only a few big aggregates form.

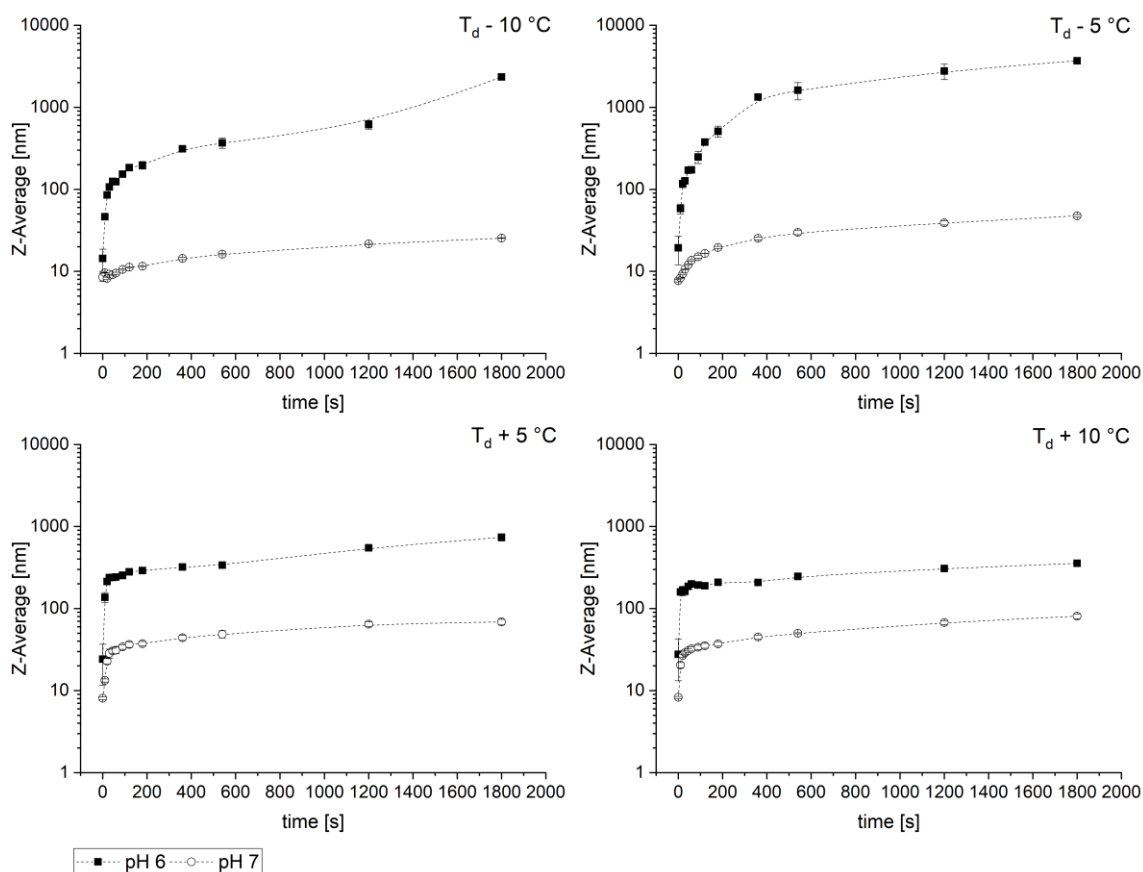


Figure 3-17 Dynamic light scattering measurements of potato protein aggregates in dependence of heating temperature, time, and pH

The low amount of unfolding occurring at lower temperatures in combination with the reduced electrostatic repulsion at pH 6 led to the growth of the aggregates through electrostatic interactions. This is different from what was described for 1%  $\beta$ -lg heated at different temperatures and pH levels. For  $\beta$ -lg at slightly acidic pH (5.7 and 5.9) aggregates had smaller z-average values when heated at low temperatures compared to higher temperatures (Donato et al., 2009). The differences can be explained through the different protein interactions forming the aggregates. For  $\beta$ -lg, aggregate growth is mainly based on the formation of disulfide bonds and less aggregation occurred when thiol groups were blocked (Mulcahy et al., 2017). However, at lower temperatures, the formation of disulfide bonds in  $\beta$ -lg aggregates was reduced. Under these unfolding limited conditions, the formation of nuclei is favored over the growth of existing aggregates. The reduced pH does not help in facilitating aggregate growth as the reactivity of the thiol group is reduced at a pH lower than 7.

Contrary to  $\beta$ -Ig, for patatin, the aggregate growth is facilitated through hydrophobic interactions. Even native patatin has a high exposed hydrophobicity (Creusot et al., 2011), which makes it reasonable to assume that partially unfolded or native patatin can aggregate through hydrophobic, even if unfolding is not complete. Combined with low electrostatic repulsion, hydrophobic patches come into closer proximity and this apparently facilitates the growth of aggregates over the formation of new nuclei. Therefore, patatin also showed reduced importance of disulfide formation in aggregation, similar to other plant proteins like soy (Ruan et al., 2014).

#### **3.3.4 Conclusion**

This study reports on the reaction kinetics of thermally induced unfolding and aggregation of patatin, the main potato protein, as a function of temperature and pH. It could be shown that the RP-HPLC method, adapted from milk protein analysis, was able to investigate aggregation kinetics of patatin in a way comparable to whey proteins. With this method, we were able to show that the critical temperature, where the reaction kinetics change, is pH dependent. At pH 6, the protein is more thermo-resistant and therefore the changes in the reaction kinetics occur at higher temperatures, compared to neutral pH. The change in pH and temperature led to changes in the protein interactions stabilizing the aggregates. Lower pH values and higher temperatures favored the formation of non-covalent bonds over the formation of disulfide bonds. Conditions of slow unfolding and low electrostatic repulsion favored the growth of aggregates, which was different from what is described for  $\beta$ -Ig.

Our findings can help to design process conditions for functionalizing patatin enriched potato protein isolates to utilize patatin in a similar way to whey proteins such as  $\beta$ -Ig. Changing stabilizing bonds and aggregate size can be used to obtain particles for the stabilization of foams and emulsions, or to create gel-based foods with defined characteristics. Furthermore, the results can help to investigate fouling of membranes occurring during filtration processes.

#### **Acknowledgments**

This IGF Project AiF 19712 of the FEI was supported via AiF within the program for promoting the Industrial Collective Research (IGF) of the German Ministry of Economic Affairs and Energy (BMWi), based on a resolution of the German Parliament.

We would like to thank Marc Laus from AVEBE, Veendam, The Netherlands, for providing the potato protein isolate. Furthermore, we would like to thank Lisa Püthoff and Pauline Röscheisen for help with the dynamic light scattering measurements.

### 3.3.5 Supporting Information

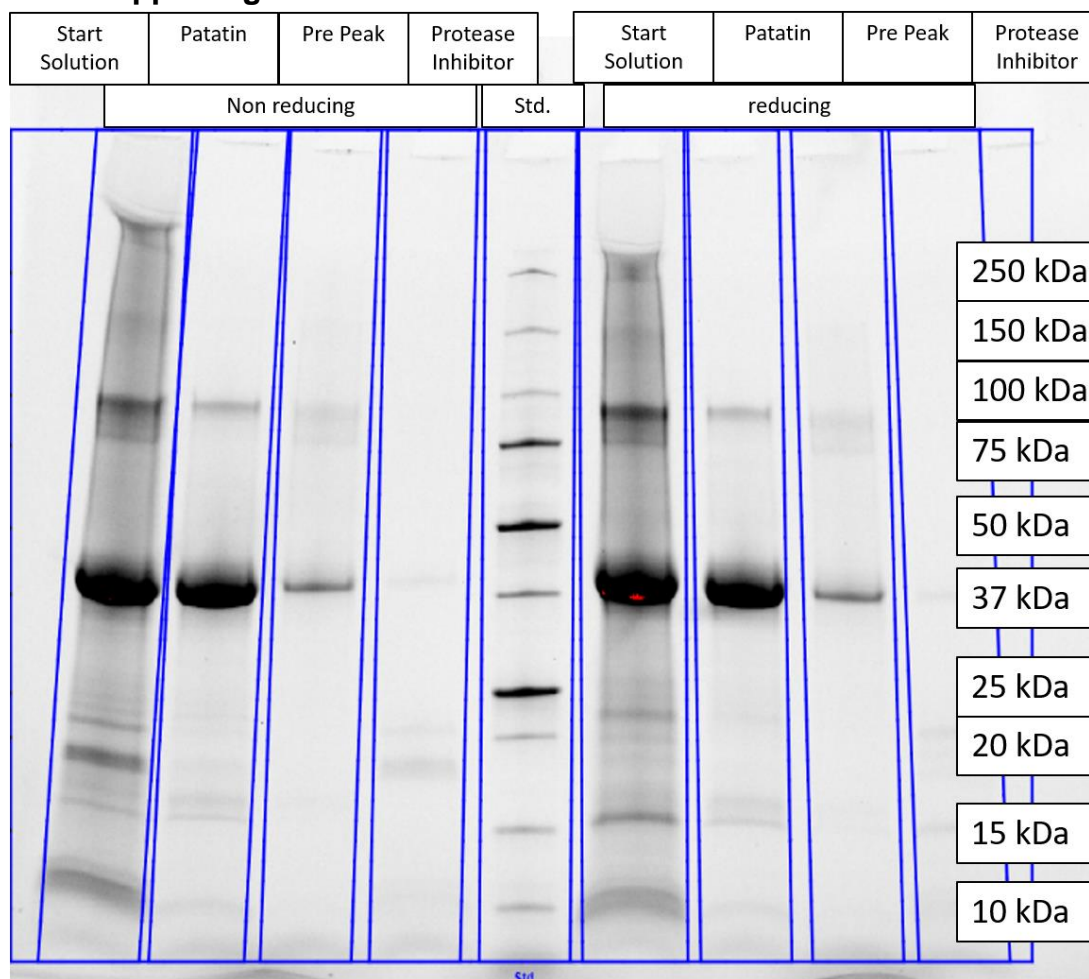


Figure S1 SDS-PAGE of PPI solutions prior to and after fractionation by SEC. The Patatin fraction was used to obtain the calibration standard for the RP-HPLC system.

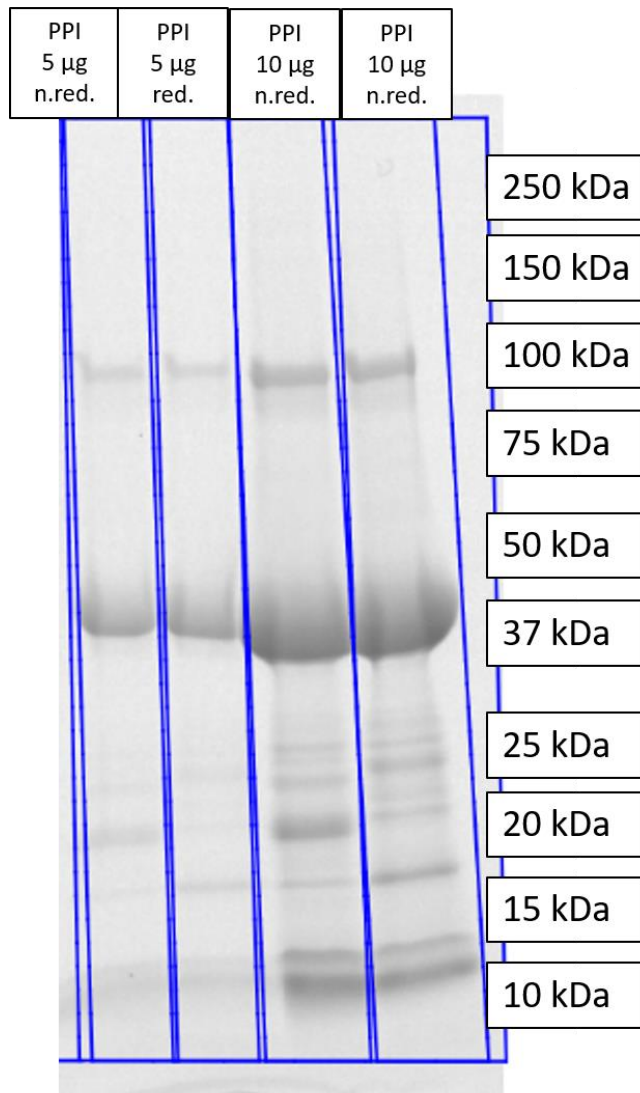


Figure S2 SDS-PAGE of PPI solutions after precipitation at pH 5 and subsequent centrifugation. Amount of protein applied to the SDS PAGE was varied between 10 and 5 µg. Note that compared to the start solution (seen in Figure 1) fewer unspecified protein was found.

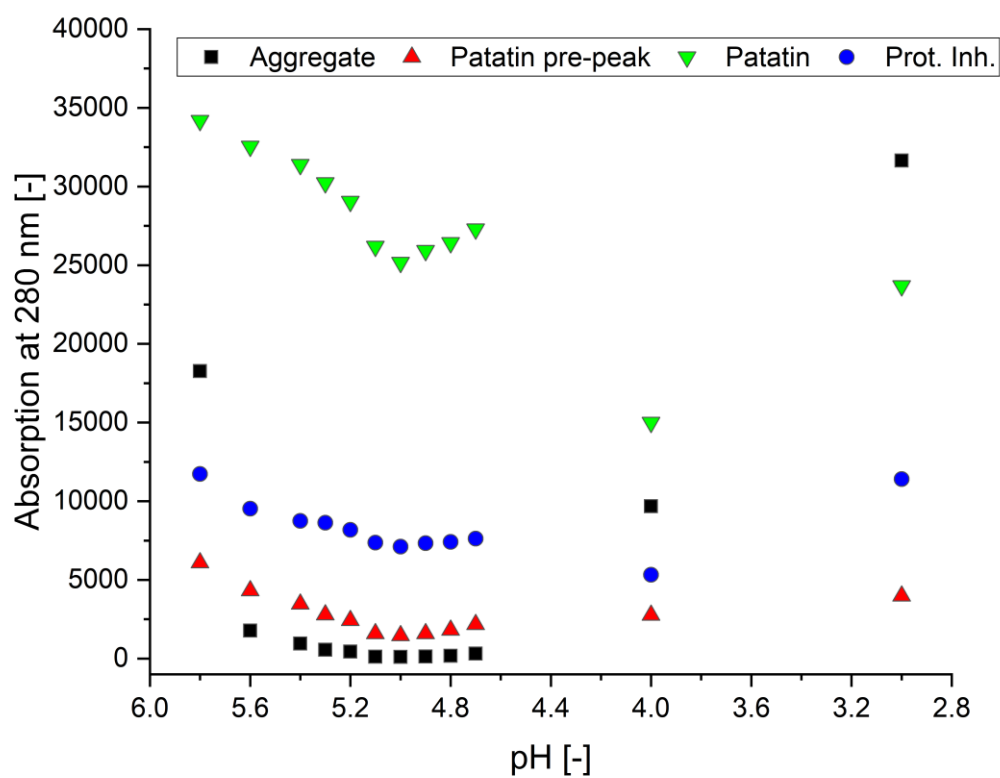


Figure S3 Absorption signals of PPI solutions adjusted to different pH values and filtered through a 0.45  $\mu\text{m}$  syringe filter before SEC measurement. Note that the Aggregate peak nearly disappears when the pH is below 5.8.





### **3.4 Microstructures of potato protein hydrogels and aerogels produced by thermal crosslinking and supercritical drying**

#### Summary and contribution of the doctoral candidate

Protein gels can be transformed into aerogels by supercritical CO<sub>2</sub> extraction. These aerogels are characterized by a high inner surface area and a high porosity, which makes them interesting for many different applications ranging from encapsulation to tissue engineering scaffolds. In the following chapter, potato protein isolate (PPI) was used to create these structures. In previous research on protein aerogels, the formation of disulfide links was always assumed to be a prerequisite for protein aerogel creation. As disulfide links play a subordinated role in PPI aggregation the feasibility to create aerogels from hydrophobic linked proteins was evaluated. The microstructure of the PPI aerogels was also evaluated. The gel properties of PPI were altered through changes in the pH milieu. How these changes influenced the microstructure revealed correlations between rheology and the microstructure of protein gels. The findings were compared to egg white protein (EWP) as a reference protein of animal origin. It could be shown that strong fine-stranded gels, with high porosity, could be formed at neutral and alkaline pH values. Close to the isoelectric point (IEP) weak brittle gels with low porosity could be formed. At very acidic pH the gels had a very high porosity but were weak and brittle. It could be shown that the relation of the storage modulus of the cool gel ( $G'_{cool}$ ) and the storage modulus of the hot gel ( $G'_{hot}$ ) correlated with the inner surface area (BET) of the resulting aerogels. Higher  $G'_{cool}/G'_{hot}$  values were characteristic for lower BET values, and vice versa.

The major contribution of the doctoral candidate was in creating the PPI and EWP hydrogels and the rheological characterization of these gels. The experimental design and the data evaluation were also done by the doctoral candidate. The correlation between rheological properties and microstructure was described by the doctoral candidate through the synthesis of hydro- and aerogel measurements. On the foundation of literature, the doctoral candidate developed a mechanistic description that allowed to describe changes in microstructure through changes in rheological properties of the gels. By creating hydrogels from EWP and using aerogel data from the literature the candidate tested the developed model on a different protein system. Thereby, the general application of the model could be shown. Other contributions included the writing of the original draft as well as responding to reviewer comments.

*Adapted original manuscript<sup>4</sup>*

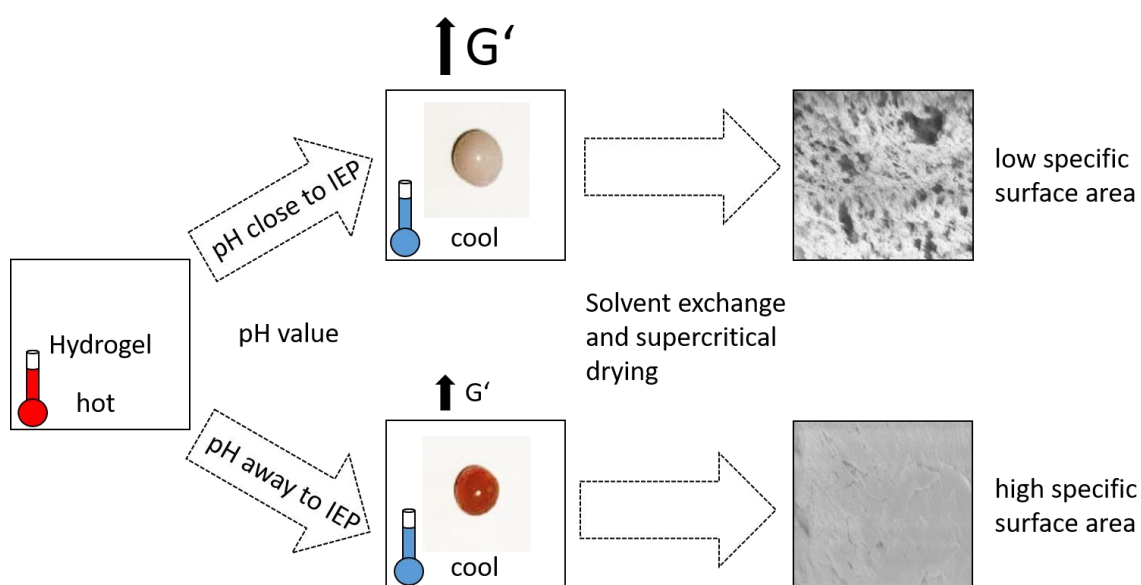
## Microstructures of potato protein hydrogels and aerogels produced by thermal crosslinking and supercritical drying

David J. Andlinger<sup>\*a</sup>, Alina Claire Bornkeßel<sup>b</sup>, Isabella Jung<sup>b</sup>, Baldur Schröter<sup>b</sup>, Irina Smirnova<sup>b</sup>, Ulrich Kulozik<sup>a</sup>

<sup>a</sup>Technical University of Munich, Chair of Food and Bioprocess Engineering, Weißenstephaner Berg 1, 85354, Freising, Germany

<sup>b</sup>Hamburg University of Technology, Institute of Thermal Separation Processes, Eißendorfer Straße 38, 21073, Hamburg, Germany

### Graphical Abstract



<sup>4</sup> (Adaptions refer to formatting issues: e.g., numbering of sections, figures, tables and equations, abbreviations, axis labeling, figure captions and style of citation). Reference lists of all publication based chapters were merged at the end of this thesis to avoid duplications.

Original publication: Andlinger, D. J., Bornkeßel, A. C., Jung, I., Schröter, B., Smirnova, I., & Kulozik, U. (2021). Microstructures of potato protein hydrogels and aerogels produced by thermal crosslinking and supercritical drying. *Food Hydrocolloids*, 112, 106305. <https://doi.org/10.1016/j.foodhyd.2020.106305>  
Permission for the reuse of the article is granted by Elsevier Limited.

## Abstract

Aerogels are highly porous structures created from hydrogels by solvent exchange and supercritical CO<sub>2</sub> drying. They can be produced from proteins and used for encapsulation of active ingredients. In this work, the structural relationship between various protein based hydrogels and aerogels was investigated. We compare egg white protein (EWP) and patatin rich potato protein isolates (PPI) in terms of gel and aerogel production thereof. Thereby, aerogels were produced for the first time from patatin-rich potato protein isolates. Both protein sources can form strong hydrogels, but they differ in their molecular properties, especially regarding the presence of reactive groups available for covalent crosslinking. Therefore, we studied the rheological profiles of hydrogels of both protein groups and applied the ratio of elastic modulus at gel formation temperature ( $G'_{hot}$ ) and after cooling to ambient temperature ( $G'_{cool}$ ) as criterion for comparing gel formation capacities produced from structurally different proteins. The ratio  $G'_{cool}/G'_{hot}$  was also identified as an indicator of the relation of non-covalent bonds to covalent and/or hydrophobic interactions and for characterizing aerogel structural properties. PPI hydrogels were found to be dominated by hydrophobic interactions, while covalent disulfide bonds determine EWP hydrogel stabilization. Nevertheless, PPI and EWP hydrogel and aerogels showed similar stabilities. More than the protein source, the pH during hydrogel formation was found to decisively influence the protein interaction potential and gel/aerogel characteristics. Irrespective of the protein source low pH led to brittle aerogels with high specific surface areas and low  $G'_{cool}/G'_{hot}$  ratios. At a pH close to the isoelectric point (IEP) brittle gels with low specific surface areas and high  $G'_{cool}/G'_{hot}$  ratios were measured. At alkaline pH gels were most stable, the specific surface area and  $G'_{cool}/G'_{hot}$  ratios were intermediate. Overall, the results help to control the structural properties of gels and aerogels towards potential applications in food systems.

### 3.4.1 Introduction

Aerogels represent a novel group of structured materials characterized by low density, high porosity and high specific surface area. Their structures can be generated by a three step process: Production of a hydrogel using inorganic or biopolymers with physical, chemical or ionic crosslinking of biopolymers leading to gelation; solvent exchange of water by alcohol (or any other organic solvent) to obtain an alcogel; finally, the alcogel is subjected to supercritical CO<sub>2</sub> (scCO<sub>2</sub>) extraction to obtain the aerogel. The aerogel, is a porous, dry material structured by the hydrogel network.

For life and food science applications, aerogels made of organic materials are desired as they are biocompatible and biodegradable (Stergar & Maver, 2016). For example, polysaccharide aerogels from starch and alginate were successfully used as drug carriers (Mehling et al., 2009) and composite materials where shown to act as tissue engineering scaffolds and wound dressing (Lu et al., 2014). In the field of food engineering, aerogels made from protein hydrogels show some promising applications. Microscopic egg white protein (EWP) aerogel particles were shown to be suitable as an encapsulation system for fish oil, rich in essential unsaturated fatty acids (Selmer et al., 2019). The controlled release of fish oil in simulated intestinal fluids was shown for

heat set whey protein gels (WPI) and transglutaminase-crosslinked sodium caseinate aerogels as well (Kleemann et al., 2020a; Plazzotta et al., 2020). WPI aerogels were also successfully used create oleogels with certain rheological properties (Plazzotta et al., 2020).

Although aerogels were already formed based on these different biopolymers, it would be of great interest to establish a quantitative relationship between aerogel properties and the chemical composition of the biopolymer in order to be able to create aerogel structures in a targeted, predictable manner (Smirnova & Gurikov, 2018). For protein based aerogels, a recent study showed that the specific surface area of aerogels could be manipulated by adjusting the pH of the solution from which the hydrogel is formed (Kleemann et al., 2018). For egg white and whey protein hydrogels, formed at alkaline pH, high specific surface areas in the aerogel could be created. The high specific surface area was explained by the ordered structure and elastic properties of hydrogels at alkaline pH.

Whereas for animal derived proteins hydrogel formation mechanism are already quite established for many novel protein sources there is little research done.

Plant proteins are one of these novel class of biopolymers used in food manufacturing. Potato protein isolate (PPI), for instance, is a novel non-allergenic protein source with comparable gelation properties as whey and egg proteins (Creusot et al., 2011). After the removal of starch, the potato protein is obtained from potato fruit juice by filtration and chromatography (Løkra & Strætkvern, 2009). One important gel forming protein in the potato tuber is patatin, a 40 kDa sized glycoprotein with no internal disulfide bridges and one free thiol group (Racusen & Weller, 1984). Depending on the purification methods other lower molecular weight proteins from the heterogenous class of protease inhibitors can be also present (Pouvreau et al., 2001). Patatin forms gels at lower temperatures and concentrations when compared to whey or egg white proteins. However, the gels made from patatin also exhibited a lower fracture point (Creusot et al., 2011). The lower fracture point was explained by the lack of a continuous disulfide mediated polymer network. Although some disulfide linked trimeric structures were found in heat induced patatin aggregates the exact influence of disulfide bonds on the aggregation mechanism remains elusive (Pots et al., 1999a). Another study investigated the gelation properties of different potato protein isolates in dependence of pH (neutral to acidic range) and ionic strength (Schmidt et al., 2019). The influence of alkaline conditions on gelation were not investigated. Beside this, gelation and microstructural properties of this novel protein source were not documented in detail.

It is therefore of high interest to understand the gelation mechanisms of emerging plant protein sources and to compare them with those of well established proteins used as functional ingredients, e.g.  $\beta$ -lactoglobulin ( $\beta$ -Lg).  $\beta$ -Lg based gels are primarily structured by the formation of disulfide bonds resulting from a thiol/disulfide exchange reactions, thus creating a covalent network throughout the gel (Langton & Hermansson, 1992). For many plant proteins, however, network spanning disulfide links are not expected for the reasons given above, and non-covalent bonds should play a more decisive role (Martin et al., 2014). However, the contribution of each of the various non-

covalent interactions is often not further assessed, and the differentiation between hydrophobic and van der Waals interactions, for example, is often limited. Patatin can be used as a model protein for studying the gelation mechanism, which involve hydrophobic rather than disulfide interactions. It should only create one disulfide bond with another patatin monomer, which is then blocked, and therefore should not form a disulfide network like the whey protein  $\beta$ -lg. EWP is another animal derived protein which exhibits high technofunctionality (Brand et al., 2014). The egg white proteins ovalbumin and ovotransferrin also participate in thiol-disulfide exchanges (Weijers et al., 2006). By the creation of aerogels from patatin-rich PPI hydrogels we can thus investigate the applicability of PPI for aerogel creation and determine microstructural properties like the specific surface area, skeletal density and others.

In this context, we will assess the increase in elastic modulus ( $G'$ ) of a hot protein gel upon cooling to ambient temperature by the ratio ( $G'_{cool}/G'_{hot}$ ) as a potential indicator of the relative roles of hydrogen and van der Waals interactions in relation to hydrophobic and covalent bonds. This was first proposed for heat induced WPI gels in the presence of chaotropic and kosmotropic salts (Bowland et al., 1995). These authors found that this ratio was indicative of certain microstructures in the WPI gels. Thus, the ( $G'_{cool}/G'_{hot}$ ) ratio will be used as a rheological characteristic of protein hydrogels correlated with structural properties of the corresponding aerogels. By measuring the specific surface area of the aerogels a quantifiable indicator of the microstructure is obtained, which can be related to the rheological properties of the hydrogel. By comparing PPI to EWP, both in dependence of the pH, the influence of different protein interactions in hydrogels will be assessed. The aim is to clearly differentiate between hydrophobic interactions and other non-covalent bonds. Thus, we aim to establish a relationship between covalent and non-covalent protein interactions and structural properties for different protein systems.

### **3.4.2 Materials and methods**

#### **3.4.2.1 Materials**

Commercial PPI powder (Solanic 200) with a high content of patatin, was kindly provided by AVEBE (Veendam, The Netherlands). The protein powder had a protein content of 88.6% (w/w). Patatin content was determined as 60 % of total protein by SDS-PAGE (data not shown). The total protein content was determined using the method of Dumas with an accuracy of  $\pm 0.1\%$  (w/w) (Vario MAX CUBE, Elementar Analysensysteme GmbH, Hanau, Germany). The powder was solubilized in deionized water and stirred overnight. On the next day, the solution was centrifuged at 6000g for 15 min to eliminate insoluble components. The protein concentration of the final solution was determined by using the method of Dumas, similar to the protein powder. To investigate the influence of protein concentration solutions were adjusted to 5, 7.5, 10, 12.5 and 15% (w/w) using deionized water. To investigate the influence of pH, the solutions were adjusted with 1 M HCl and 1 M NaOH to pH 3.0, 6.0, 7.0, 8.0 and 9.0. A stock solution was used and the solutions were afterwards adjusted to a protein con-

centration of 10% (w/w). The PPI solution at pH 3 would gel instantly, without the application of heat. Therefore, these was adjusted to a protein concentration of 7.5% (w/w) to avoid too early gelation.

From each protein solution two types of hydrogels were prepared: For rheological characterization of the hydrogel structure, hydrogels were prepared in a rheometer as described below. For aerogel production and characterization, hydrogel spheres were prepared as described below.

Liquid pasteurized egg white protein with a protein content of around 11 % (w/w) was obtained from OVOBEST Eiprodukte GmbH & Co. KG (Neuenkirchen-Vörden, Germany). The pH of the samples was adjusted with 1 M HCl and 1 M NaOH to pH 2, 3.5, 4.6, 7, 9, and 11.5 as described elsewhere (Selmer, Kleemann, Kulozik, Heinrich, & Smirnova, 2015)

#### **3.4.2.2 Modulated differential scanning calorimetry (mDSC)**

The denaturation temperatures of 1% (w/w) PPI solutions at pH 6, 7, 8, 9 were measured by using  $T_{\text{zero}}$ -calibrated modulated differential scanning calorimetry (mDSC Q1000, TA Instruments, New Castle, United Kingdom). For the measurement of each solution with an individual pH, 20  $\mu\text{L}$  of the solution was filled into a hermetically sealed aluminum pan. As a reference, an empty aluminum pan was used. The temperature was gradually heated from 25 to 90  $^{\circ}\text{C}$  with a heating rate of 2 K/min. The experiment was conducted in duplicate and both, onset temperature and denaturation temperature, were determined.

#### **3.4.2.3 Rheological characterization of the hydrogels**

Viscoelastic properties of protein solutions were monitored by using small-amplitude oscillatory measurements on a Paar Physica MCR 302 (Anton Paar, Graz, Austria) stress-controlled rheometer, using a concentric cylinder geometry (inner and outer cylinder diameter 26.65 mm and 28.90 mm, respectively). 19.1 mL of the sample was filled into the rheometer cup. A lid prevented evaporation during measurement. The samples were heated and cooled using a Peltier element. After a 10 min equilibration phase, the sample was heated rapidly to the desired temperature. Then the temperature was held for 30 min.

This was analogous to the heating procedure occurring during capsule formation (see below). After the heating step the gelled sample was cooled down to 20  $^{\circ}\text{C}$  and kept at this temperature for 30 min. After this time a strain sweep was applied increasing the strain from 0.1% to 100% within 30 min.  $G'$  and  $G''$  during all steps were recorded. The limit of linear viscoelasticity defined as the point where a significant decline of  $G'$  was detected by the rheometer software. For the EWP hydrogels the heating was done for 10 min at 85  $^{\circ}\text{C}$  to make the hydrogels comparable with already published data (Selmer et al., 2015).

#### **3.4.2.4 Hydrogel capsule preparation**

PPI hydrogel capsule were prepared as a base for aerogel particle generation as described for other protein hydrogels (Kleemann et al., 2018). 65.5  $\mu\text{L}$  of protein solution

was pipetted into each cavity of an oil covered form made of Polytetrafluoroethylene (PTFE). The cavity was a semi-sphere with a diameter of 5 mm. Due to the surface tension, a spherical droplet formed spontaneously from the protein solution. In total, 48 cavities could be filled in parallel with protein solution. The PTFE-form was then immersed into a double-walled beaker filled with commercial sunflower oil. The temperature of the oil bath was set 10 °C above the denaturation temperature, determined by mDSC. The solution at pH 3, for which the denaturation temperature could not be determined, was heated at 70 °C in order to ensure complete unfolding. After heating for 30 min under stirring, the PTFE-form with the now formed hydrogel beads was put into sunflower oil at room temperature to allow the gels to cool. Afterwards, the gels were carefully removed from the form. The gel beads were kept immersed in oil until further measurements to prevent dehydration.

#### **3.4.2.5 Solvent exchange and alcogel characterization**

To induce the solvent exchange from water to ethanol within the gel network the gel beads were first rinsed in ethanol to eliminate excess oil. Afterwards, around 40 beads were transferred into a falcon tube filled with 50 mL of 99.8% denatured ethanol. The tubes were shaken in an overhead tumbler overnight. From 5 of the obtained alcogels beads the breakage force was measured in a texture analyzer and the remaining beads were dried as described below. Before the compression test, the samples were equilibrated at room temperature and surface ethanol was gently removed.

One alcogel bead at a time was compressed in a texture analyzer (TA.XT plus, Stable Micro Systems, Godalming, UK) to 60% of their initial height with an acrylic glass piston ( $d = 12$  mm). The piston speed was set to 0.1 mm/s. The point at which the sample fractured was taken from the compression curve and recorded as the breakage force.

#### **3.4.2.6 Supercritical drying**

The supercritical drying was done as was presented elsewhere (Selmer et al., 2015). The most important steps are as follows. The supercritical drying was conducted at 11-12 MPa and 40-60 °C in a 250 mL high pressure autoclave for three hours using a continuous supercritical CO<sub>2</sub> flow. First, the autoclave was preheated by a thin electrical band heater. The alcogels were packed in filter paper, placed into the autoclave and soaked in ethanol to prevent shrinkage due to evaporation of ethanol from the alcogel before exposure to supercritical CO<sub>2</sub>. The system was pressurized to 11.0–12.0 MPa with CO<sub>2</sub> by a Maximator pump (Model G35D). The outlet valve was adjusted to a flow of CO<sub>2</sub> of 2–4 L/min, the continuous CO<sub>2</sub> flow was provided for 3 h. The drying time of 3 h was used to ensure complete drying of the macroscopic capsules.

Finally, the pressure was released with a pressure release rate of 1 bar/min at constant temperature (40-60 °C). It took 40–60 min until atmospheric pressure was reached.

#### **3.4.2.7 Aerogel characterization**

Scanning electron micrographs of the samples were done at 5 kV using a detector for secondary electrons (Leo Gemini Zeiss 1530, Oberkochen, Germany). To analyze the internal structure of the aerogel spheres, the samples were crushed into smaller pieces

which were then investigated. To avoid charging of the samples, they were sputtered with gold (7 nm thickness).

Low temperature N<sub>2</sub> adsorption–desorption analysis was used to investigate the physical properties of the aerogels (Nova 3000e Surface Area Analyzer, Quantachrome Instruments, Boynton Beach, USA). The specific surface area was determined using the BET (Brunauer–Emmet–Teller) method. The pore volume and mean pore diameter were estimated by the BJH (Barrett–Joyner–Halendia) method. All samples were degassed under vacuum at 40 °C for 20 h prior to analysis.

Breaking and compression tests were done to analyze the mechanical stability (Texture Analyzer TA.XT plus, Stable Micro Systems, Godalming, UK). The spherical samples were compressed uniaxial to 8% strain or rather to the first fracture of the structure (0.01 mm/s test speed). In order to analyze the dry aerogel structure, the samples were dried for another 10 h under vacuum at 50 °C and then stored in an exsiccator with silica gel particles prior to analysis. The mechanical tests were done inside a tempered room (T = 20 °C). Each sample was measured directly after it was taken out of the exsiccator. The skeletal density of the aerogel network was measured according to the Archimedes principle through helium pycnometry with a multivolume pycnometer 1305 (Micrometrics, Norcross, USA).

The size of the alco- and aerogels was measured with a Camsizer XT system. By comparing the sizes of the capsules, the shrinkage resulting from drying could be determined.

#### **3.4.2.8 Statistical methods**

All experiments were done in duplicate if not stated otherwise. Experiments were performed from two individually prepared protein solutions. The depicted data points describe the average between two measurements and error bars describe the upper and lower data points. For the textural characterization of the alcogel and aerogels at least 5 gels spheres were used per solution. For BET-surface area and BJH-pore size analysis, one N<sub>2</sub> adsorption-desorption analysis with a sufficient amount of aerogel was performed. Error analysis for the BET system showed that the relative error of the measurement was 10%.

### **3.4.3 Results and discussion**

#### **3.4.3.1 Influence of protein concentration on potato protein gelation and stability after solvent exchange**

Patatin was shown to form hydrogels at lower protein concentrations, when compared to other food proteins (Creusot et al., 2011). Furthermore, the good solubility of PPI allows to investigate a wide range of protein concentrations and the impact the protein content has on stability and density of the hydro- and alcogel network. In order to improve the understanding of the structural relation between hydrogels, alcogels and aerogels, we investigate, which influence the protein concentration has on the shrinking behavior of the alcogel during drying and on the resulting specific surface area of the



aerogel. For hydrogels, the storage modulus and breakage force were taken as a measurement for gel strength.

Figure 3-18 shows that increasing the protein concentration leads to a higher storage modulus in case of protein hydrogels. Higher protein contents in the solution lead to denser structure and more intermolecular links between the molecules forming the gels. Further, increasing protein concentration usually leads to increased aggregation due to more intermolecular collisions (Delahaije et al., 2016). The solvent exchange from water to ethanol leads to an increased hardness of the gel spheres. The force necessary to break these gels after complete solvent exchange, is also given in Figure 3-18.

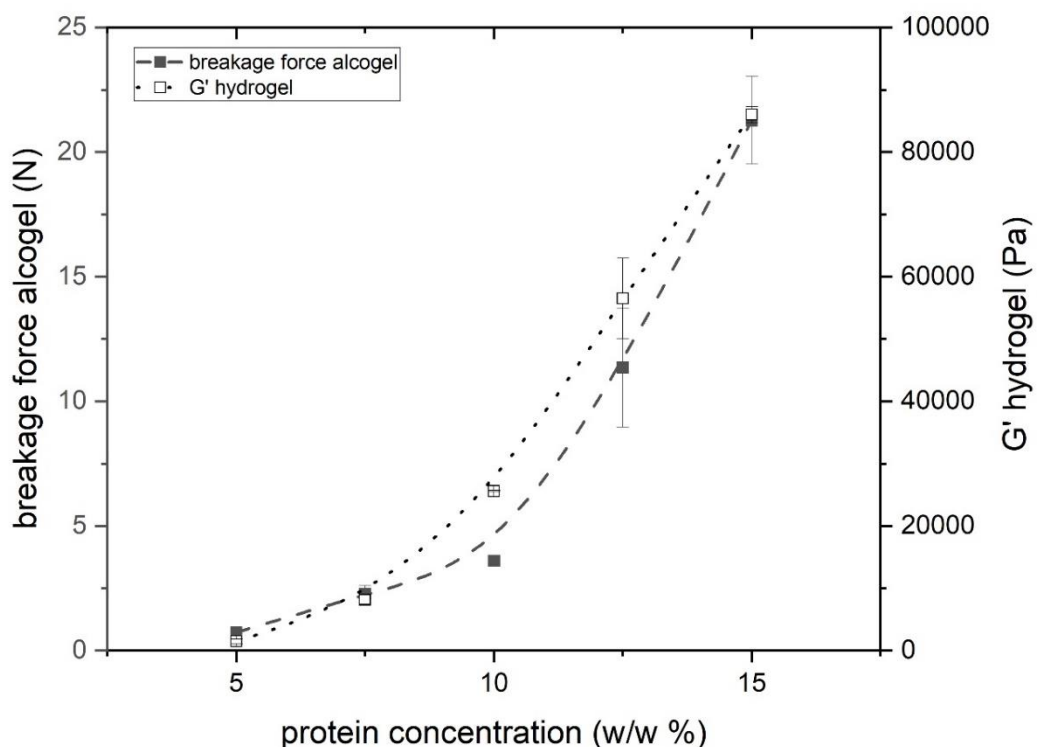


Figure 3-18 Alco- and hydrogel strength in dependence of the protein concentration of the precursor protein solution, measured by breakage force and storage modulus, respectively.

To explain this behavior, two effects of solvent exchange on the gel network, namely shrinkage and specific electrostatic interactions due to the change of solvent's permittivity, should be considered. The change of the medium from water to ethanol results in a reduced affinity between the protein network and the solvent (Gurikov et al., 2019). Preferred interaction affinity between polymer chains instead of the polymer-solvent interactions was already correlated with increased shrinkage for alginate systems (Subrahmanyam et al., 2015). This study showed that the kinetic of the solvent exchange is similar to the process of swelling. For WPI hydrogels it could be shown that the mesh size of WPI gels was the lowest when the swelling was done at a state of low electrostatic repulsion of the gels (Betz et al., 2012). The change of the medium from

water to ethanol decreases electrostatic repulsion of the protein side chains by lowering the dielectric constant of the medium (Zirbel & Kinsella, 1988). Therefore, the protein network mesh is supposed to be denser when ethanol is present in the gel network, explaining the shrinkage and hardening. All hydrogels shrank uniformly, and no instability of the gel network was observed. In patatin gelation, disulfide bonds are expected to play only a minor role (Creusot et al., 2011; Schmidt et al., 2019). Therefore, patatin provides the first example of protein alcogels which are not covalently crosslinked, in contrast to disulfide linked EWP (Selmer et al., 2015) and WPI gels or covalently cross-linked sodium caseinate (Kleemann et al., 2018). Thereby, the non-covalent protein interactions formed at the investigated protein concentrations are strong enough to withstand the changes induced through the solvent exchange. It can be assumed that these forces are mostly based on hydrophobic interactions between the hydrophobic amino acid residues usually buried in the core region of the protein.

After supercritical drying the skeletal density of the aerogel network and the breakage force of the aerogels were measured, as seen in Figure 3-19.

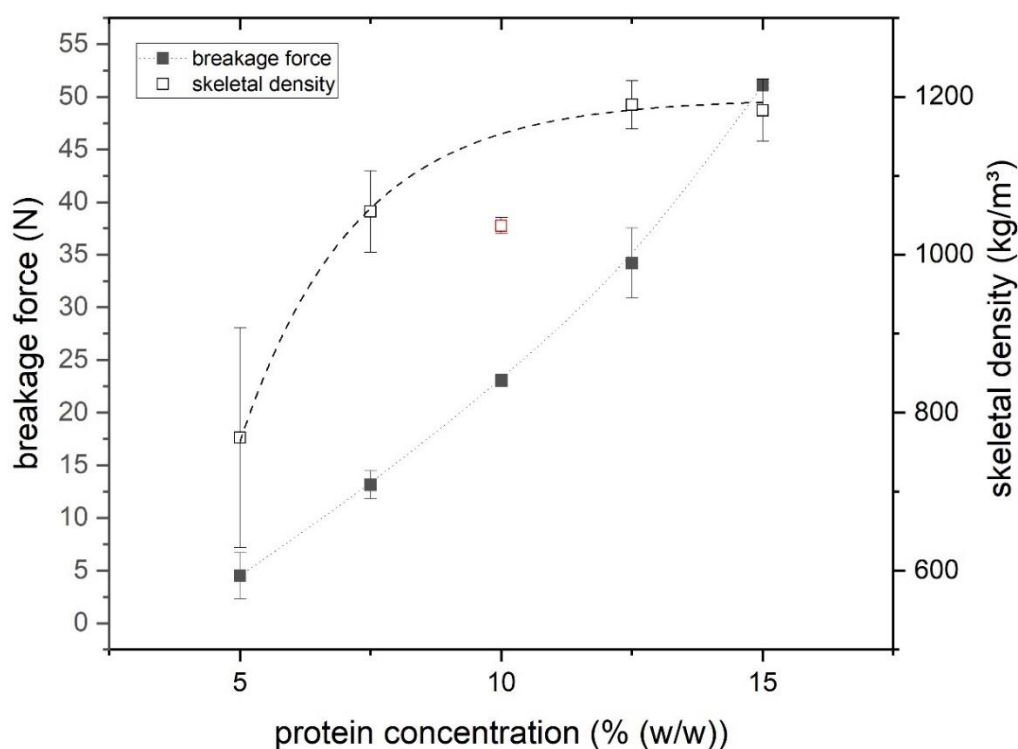


Figure 3-19 Breakage force and skeletal density of the PPI aerogels in dependence of protein content in the precursor protein solution. The asymptotic progression of the skeletal density is meant as a guide for the eye.

The breakage force increased with increasing protein concentration thus indicating stronger aerogel networks similar to the findings for the hydro- and alcogels Figure 3-18. The measurement of the skeletal density of the supercritical dried aerogels reveals that the density of the gel matrix backbone increases steeply and then plateaus-

off with increasing protein concentration. From the change in skeletal density we can deduce how the gel structure changes during heat-set PPI gelation. The heat-set protein gelation starts with the formation of aggregates from unfolded protein monomers. These primary aggregates then associate to build macroscopic gel structures.

For  $\beta$ -lactoglobulin (Gimel et al., 1994) and patatin (Delahaije et al., 2015), primary aggregates were shown to be independent of the protein concentration, albeit for a low protein concentration range. Therefore, it can be assumed, that not the structure of these primary aggregates, but the interaction between these aggregates changes in dependence of the protein concentration. Increasing particle attraction was shown to be one of the most important factors for the transition of a fluid to a gel (Richard et al., 2018) in simple colloidal polymer models. These particle attractions were also shown to be responsible for the development of density fluctuations during gelation. In line with these findings, increasing the volume fraction of protein particles will lead to denser regions as can be seen from the development of the skeletal density.

How the protein concentration could influence the particle interactions is explained in the following: In general, when the aggregation is fast and interactions between the primary aggregates are strong, e.g. when electrostatic repulsion between the primary aggregates is reduced, a higher degree of phase separation with denser structures can be observed (Clark et al., 2001). Small angle X-ray scattering revealed that protein systems exhibited micro-phase separation upon aggregation (Nicolai & Durand, 2007). This is different to what was found for polysaccharides like chitosan, where phase separation only occurred upon scCO<sub>2</sub> drying (Takeshita et al., 2019). Aggregation rates of patatin have been reported to be way faster than those of  $\beta$ -lactoglobulin (Delahaije et al., 2015). Furthermore, the low protein concentration necessary for gelation of patatin was explained by the high exposed hydrophobicity of patatin in comparison to other food proteins (Creusot et al., 2011). The hydrophobic surface of the protein tries to avoid contact with the polar water phase. By increased attraction of the patatin molecules through the hydrophobic surface other short-ranged interactions between the monomers, like hydrogen and electrostatic interactions, can occur as well. This results in patatin molecules forming clusters. Fast aggregation in combination with a high exposed hydrophobicity can explain why denser clusters form during PPI gelation and more phase separation occurs.

At low protein concentrations, the skeletal backbone of the protein gel is build up more loosely than at high protein concentrations. This loose structure can also help to explain other phenomena occurring during drying. Alkogels, when subjected to supercritical CO<sub>2</sub> drying, also shrink to some extent, similar to what was described for the hydrogels when subjected to solvent exchange. As the gel backbone is denser for more concentrated gels, there is less room for shrinkage during the drying step as can be seen in Figure 3-20.

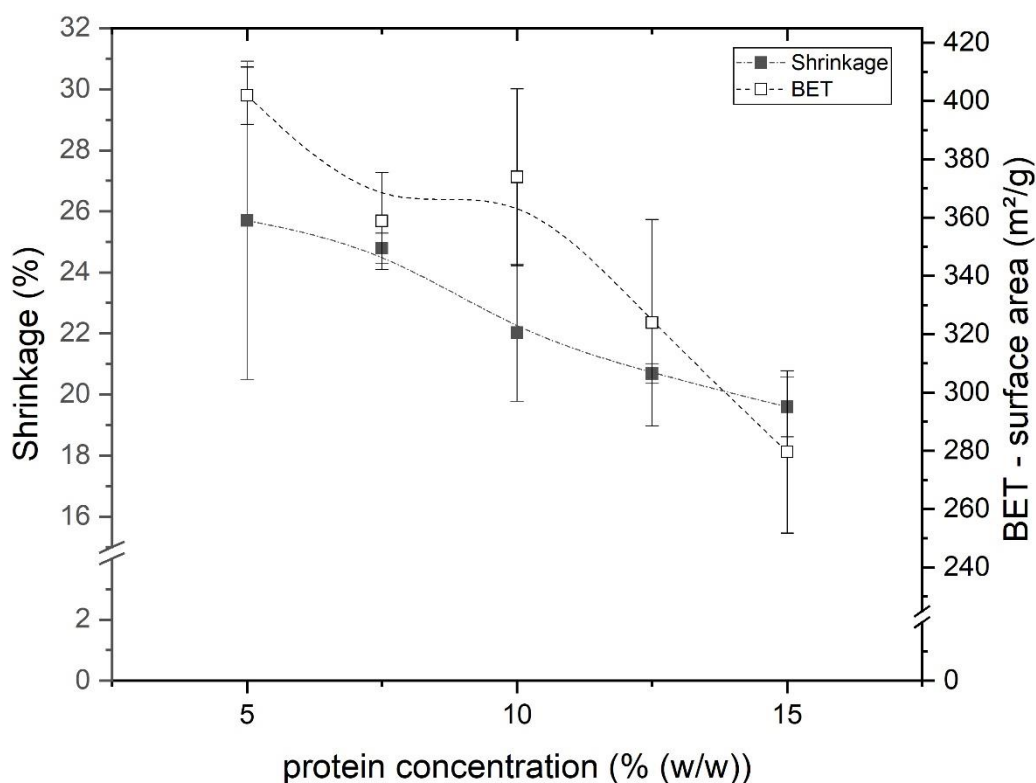


Figure 3-20 Shrinkage during supercritical drying and BET surface area of the PPI aerogels in dependence of the protein concentration. Note the breaks on both axis.

With increasing protein concentration, the measured BET surface area decreased as well. For other protein systems a decrease in BET surface area was observed when the amount of short range protein interactions was increased, e.g. with pH values close to the IEP or at NaCl concentrations of up to 400 mM (Kleemann et al., 2018; Selmer et al., 2015). This supports our assumption that increasing protein concentration leads to an increase in short range protein interactions that result in structures with lower specific surface areas.

#### **3.4.3.2 Impact of pH on hydrogel, alcogel and aerogel structure**

The temperature dependent unfolding of the PPI solutions was investigated by modulated differential scanning calorimetry, the results can be seen in Figure 3-21. For pH 7, a peak denaturation temperature of  $60.8 \pm 0.4$  °C and a denaturation onset temperature of  $50.7 \pm 0.9$  °C was measured. These denaturation and onset temperatures are in very good agreement with values published for patatin rich potato protein isolates at pH 7 (Creusot et al., 2011; Schmidt et al., 2019). Here, we extend the effect of pH into the alkaline region, which was shown by Kleemann et al. (2018) to be of high impact on the aerogel structure.

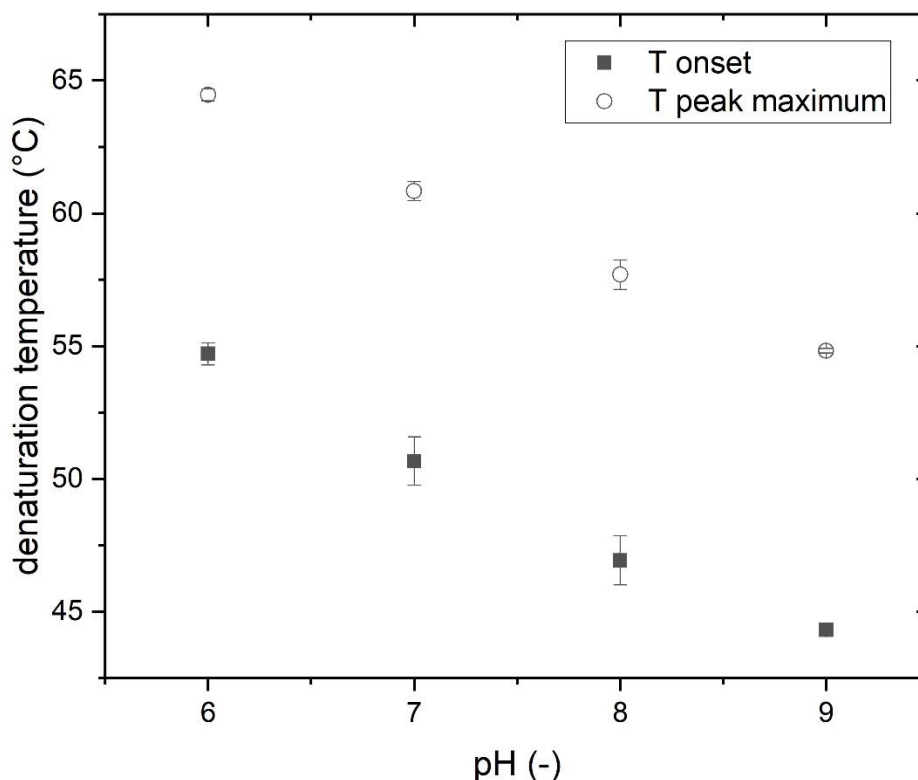


Figure 3-21 Onset and peak denaturation temperatures of PPI solutions determined by mDSC.

Increasing the pH leads to increased intramolecular repulsion of the protein side chains and subsequently to decreased unfolding temperatures as was already shown for whey proteins (Paulsson et al., 1985). As the rate of unfolding in a protein influences the aggregation and subsequently the gelation, all pH experiments were conducted at 10 °C above the measured denaturation temperature to ensure total unfolding of the proteins with comparable rates (Delahaije et al., 2015). For pH 3 no peak in the thermal flux signal could be detected. This can be explained by the pH induced denaturation of the protein solution at this pH. From fluorescence spectroscopy measurements it is known that patatin in acidic solutions unfolds and exposes its hydrophobic amino acids to the solvent (Pots et al., 1998a). It can therefore be assumed that at this pH that aggregation in a concentrated system is fast, because the hydrophobic amino acids will aggregate to reduce their contact to the aqueous solvent. This leads to a denatured and aggregated solution before the measurement of the thermal unfolding takes place.

When investigating the structural stability of PPI hydro- versus alcogels, a clear deviation between the alco- and hydrogel state can be seen in dependence of the pH, as depicted in Figure 3-22.

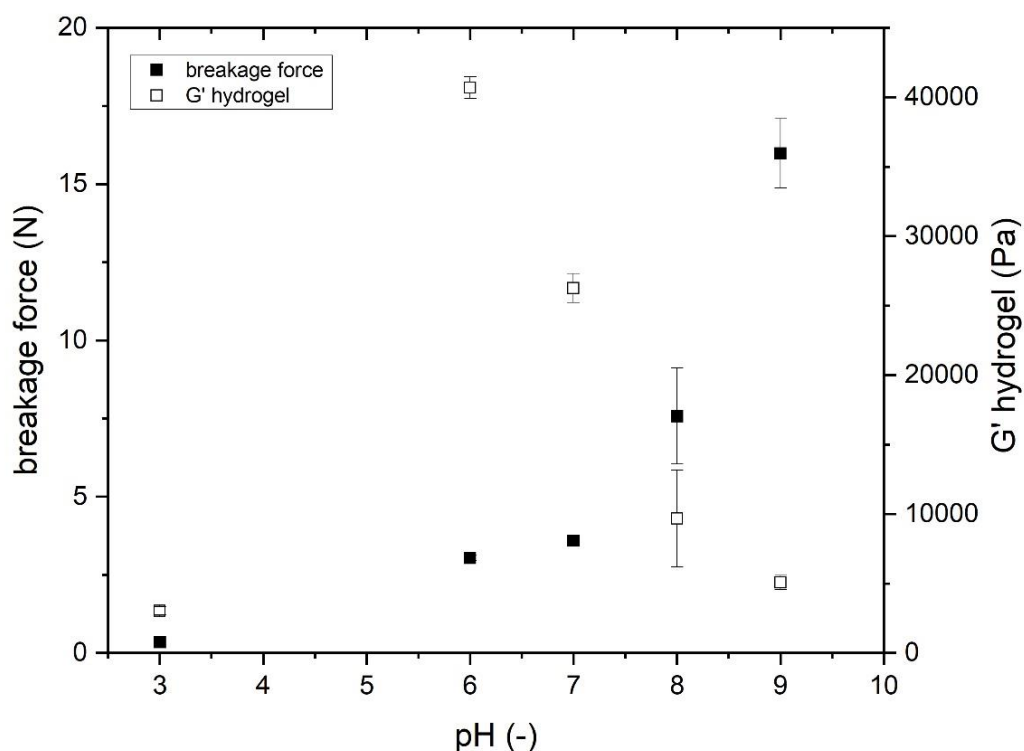


Figure 3-22 Alco- and hydrogel strength in dependence of the pH of the precursor protein solution, measured by breakage force and storage modulus, respectively.

The hardest alcogels were created from alkaline PPI solutions whereas the strongest hydrogels, indicated by a high  $G'$ -value, were created at pH 6. The IEP of patatin is around pH 5 (Racusen & Foote, 1980). Therefore, at pH 6, the net charge on the protein is already low. Only the gels in the acidic region had low  $G'$ -values and low breakage forces due to their brittle structure, which is in accordance to the results for WPI gels (Kleemann et al., 2018) and EWP gels (Selmer et al., 2015). The high stability of the hydrogels in the pH range close to the IEP can be explained by increased hydrophobic and non-covalent bond formation during gelation. These types of bonds increase the  $G'$  of hydrogels upon cooling (Homer et al., 2018; Martin et al., 2014).

Similar to our findings, an increase in  $G'$  for protein solutions gelled close to the IEP was reported for  $\beta$ -lg (Stading & Hermansson, 1990). Contrary to our findings for a patatin rich PPI gel, a decrease in pH from neutral pH to the IEP an decrease in  $G'$  was reported (Schmidt et al., 2019). However, these authors used a different purification method for producing PPI from potato fruit juice, heated the PPI solution at higher temperatures and had no adjustment of the heating temperature in dependence of the unfolding temperature resulting in different kinetics of unfolding and subsequently in different gelation. Furthermore, gels were not directly generated at the pH of the IEP as these brittle gels were not suitable to withstand the process of ethanol exchange and supercritical drying.

In the study by Stading & Hermansson (1990) it was also found that an increase in ionic strength from 15 to 200 mM resulted in an increase in  $G'$  for patatin rich potato protein gels. Contrary to that Creusot et al. (2011) found that an addition of 100 mM NaCl decreased  $G'$  of patatin gels. For spray and freeze dried potato protein powders, which were not enriched or purified for higher patatin levels, the resulting gels decreased in  $G'$  with increased ionic strength (Schmidt et al., 2019). This indicates the importance of patatin and protease inhibitor composition in determining gelation properties of PPI solutions. This shows that for PPI gels the composition plays an important role, determining how the gel responds to different electrostatic interactions. Furthermore, the response to increased ionic strength and reduced pH may differ. Still, more research has to be done to understand the contribution of different protein and non-protein components in potato protein isolates.

At higher pH values, proteins carry more charges and short-range interactions are less likely. The gels are expected to be highly ordered as the building blocks of the gel network are finely stranded aggregates, as opposed to the particulate dense aggregate networks close to the IEP (Nicolai et al., 2011).

For WPI and EWP hydrogels, the hardening effect of ethanol was explained by increased electrostatic interactions within the gel network as well as the shrinkage during solvent exchange (Kleemann et al., 2018). After supercritical drying, the hardest WPI/EWP gels were created from hydrogels produced at alkaline pH. It was shown that for WPI and EWP gels the decisive factor for aerogel stability was stability against deformation of the respective hydrogel. Hydrogel samples at alkaline conditions could withstand a high deformation before the loss of linear viscoelastic behavior indicated an irreversible destruction of the gel microstructure.

The high resistance against deformation of alkaline WPI/EWP gels can be explained with an increased accessibility of the sulfhydryl groups to form disulfide bonds at alkaline conditions (Monahan et al., 1995) and the resulting polymerization of the gel network due to disulfide mediated exchange reactions (Leeb et al., 2018; Roefs & Kruif, 1994).

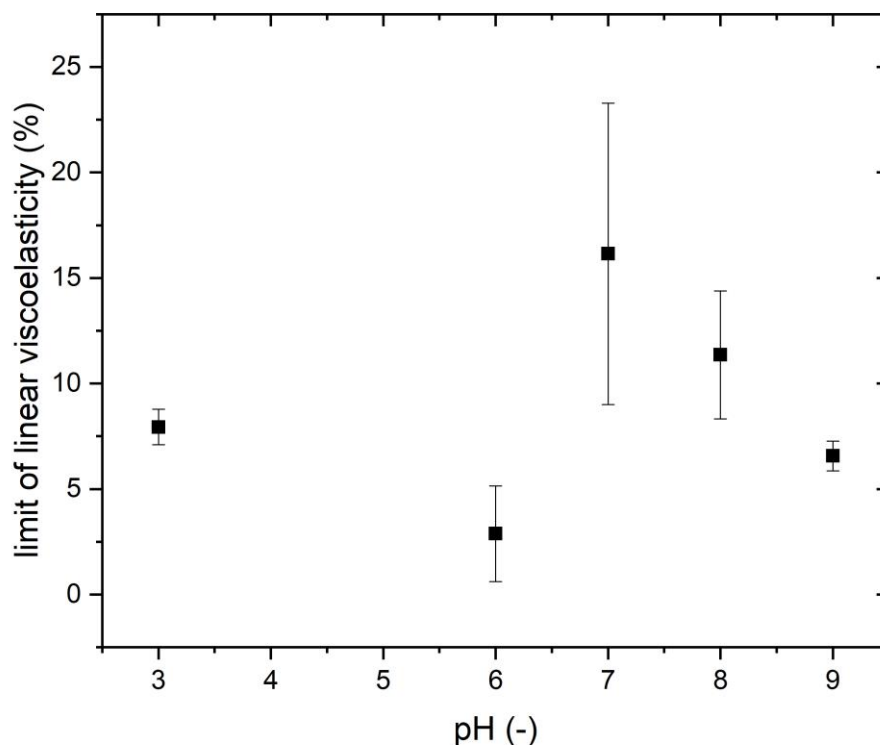


Figure 3-23 Limit of linear viscoelasticity of PPI hydrogels, determined by an amplitude sweep in a rheometer.

Therefore, the limit of linear viscoelasticity (LVE) of the PPI hydrogels was investigated in dependence of the pH, see Figure 3-23. The values at neutral and acidic conditions are comparable for the values reported for gels from PPI solutions rich in patatin (Schmidt et al., 2019). Close to their IEP, the gels are very brittle and exhibit low resistance against deformation. This is probably due to the formation of big, spherical aggregates when the electrostatic repulsion is reduced (Delahaije et al., 2015). For alkaline conditions, a decrease in LVE with increasing pH was found for PPI, contrary to what was observed for EWP and WPI. According to a study on globular protein gelation the interactions of primary aggregates are very important for the overall heat-set gelation (Clark et al., 2001) and this step is mostly influenced by short-lived non-covalent bonds.

Therefore, reducing the strength of these bonds might be sufficient to reduce the overall gel stability, measured by the limit of linear viscoelastic behavior. Patatin gels were already shown to break at smaller strains when compared to other food protein gels (Creusot et al., 2011). For cold set WPI gels, blocking of thiol groups resulted in reduced stability against deformation (Alting et al., 2000), indicating the importance of covalent crosslinks for the gel stability. When electric repulsion between protein aggregates is increased due to a high pH, covalent cross links can be weakened as the protein molecules are repulsed from each other. For very alkaline conditions, the influ-



ence of electrostatic repulsion alone was sufficient to dissolve  $\beta$ -lactoglobulin aggregates, because under these conditions the aggregates were not strongly cross-linked by covalent disulfide bonds (Mercadé-Prieto et al., 2007). All this gives us indication that patatin gels are mainly crosslinked by non-covalent bonds which are weakened by increased electrostatic repulsion. For the application of PPI aerogels, e.g. as an encapsulation system, a certain stability of the aerogel matrix is required. Therefore, the stability of PPI aerogels against deformation was investigated and compared to other protein aerogels from literature.

The breakage force of the PPI aerogels follows a similar trend as determined for the alcogels as shown in Figure 3-24. Higher pH values led to stronger aerogels which is comparable to the trend seen for egg white aerogels (Selmer et al., 2015). As the PPI gels do not exhibit a comparably high deformability, which was previous thought to be the main determining factor for the production of stable aerogels (Kleemann et al., 2018), we can now state that a low deformability of the pre-cursor protein hydrogels is not necessarily an indication for instable aerogels.

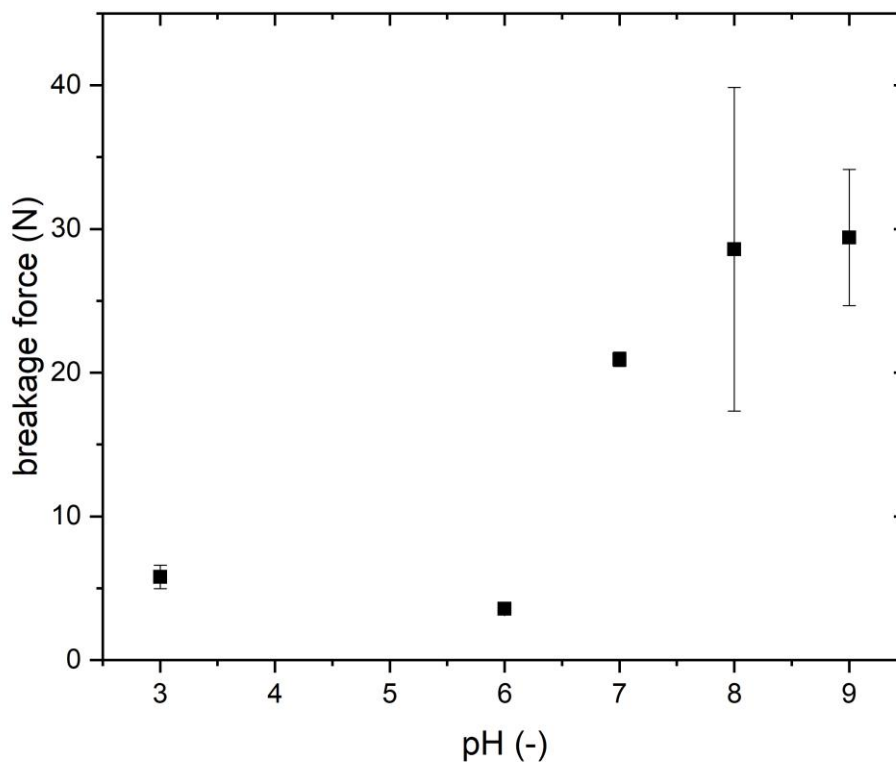


Figure 3-24 Load of PPI aerogel particles until breakage occurs, determined by compression test, in dependence of the pH value of the precursor solution.

A breakage force of 25 N for a 10 % (w/w) PPI solution gel capsule is remarkably similar to the breakage force reported for EWP capsules (10 % w/w) in alkaline conditions (Selmer et al., 2015). In alkaline conditions, thiol groups in proteins are more reactive and lead to polymerization during heat induced gelation (Monahan et al., 1995). This thiol-mediated polymerization was the main explanation for the increased stability of

the EWP aerogels. With the supercritical drying of PPI, we could show that potato protein is similarly able to form strong aerogels without the need for thiol mediated polymerization.

Another important factor in determining the applicability of PPI for encapsulation and other life science application is the microstructure of the dried aerogel network. For instance, high specific surface areas were necessary for high fish oil loading capacities in EWP and WPI aerogels (Selmer et al., 2019).

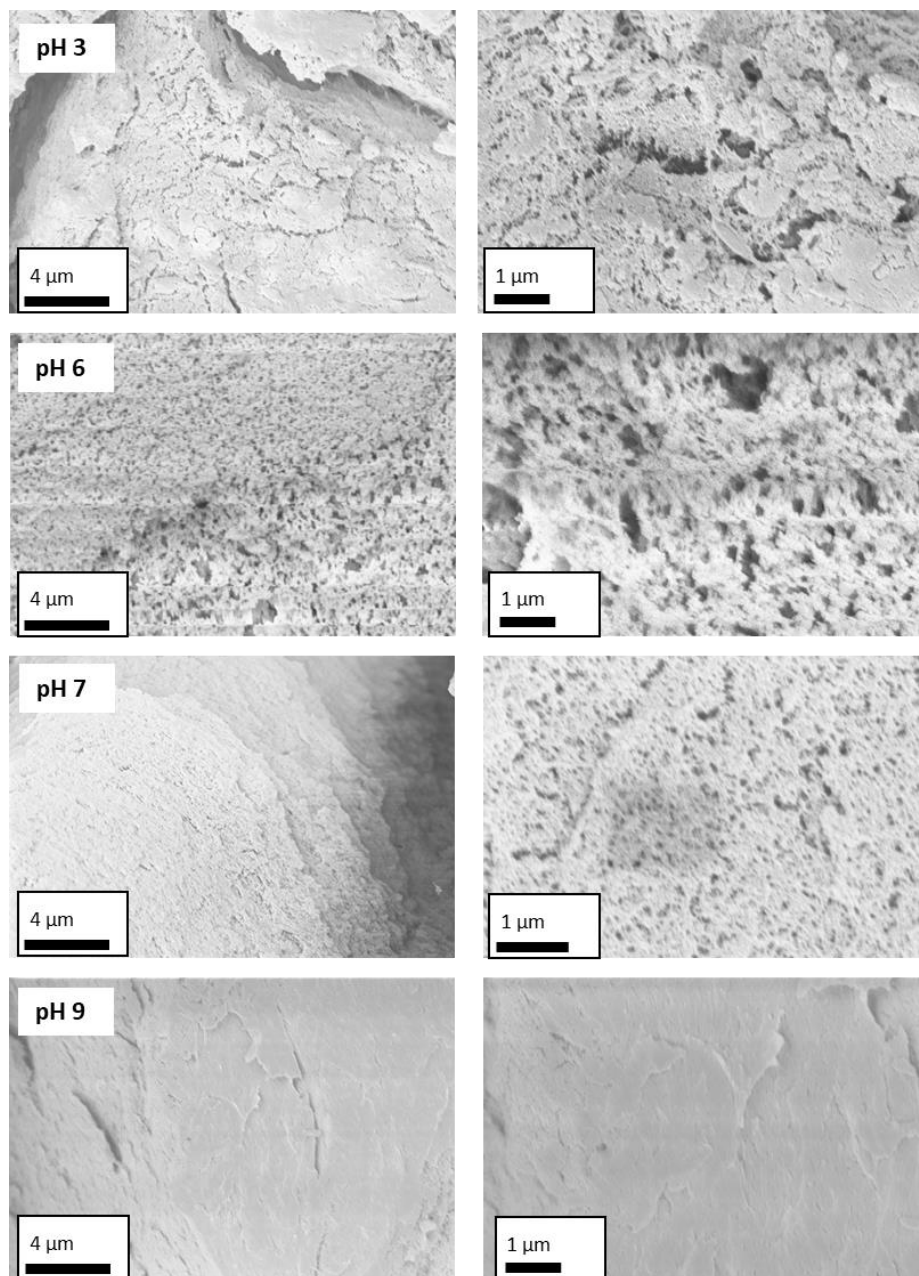


Figure 3-25 SEM pictures of PPI aerogels in two different magnifications indicated by the scale bars at the bottom. The pH of the precursor solution is given in the top left corner.

The change of PPI gel microstructure in dependence of the pH was investigated by SEM, see Figure 3-25. For PPI aerogels at pH 3 a fine porous surface can be seen, similar to what was observed for acidic EWP aerogels (Selmer et al., 2015).

However, the otherwise homogenous network has many cracks which might result from the brittleness of the gel structure, resulting in the low breakage force of the alcohol aerogels as well as in the low LVE of the hydrogel. The IEP of patatin is around 5 (Racusen & Foote, 1980). Therefore, at pH 6, the already considerably reduced electrostatic repulsion leads to a coarser structure with large macropores. Similar structures were already described for WPI gels (Langton & Hermansson, 1992) and EWP gels (Handa et al., 1998) close to their respective IEPs. Reduced electrostatic repulsion does not only induce the formation of denser/bigger aggregates due to increased protein interactions (Delahaije et al., 2015), but also favors phase separation (Clark et al., 2001) resulting in large pores, devoid of any protein. Increasing the electrostatic repulsion by increase of the pH to 7 the network appears to be more homogeneous and no large pores are visible. A further increase to pH 9 attenuates this trend and the surface of the protein appears to be smooth. Skeletal densities were very similar for all pH values (the lowest value for pH 7 was  $1048.6 \pm 117.3 \text{ kg/m}^3$ , and highest for pH 9 was  $1185.8 \pm 75.3 \text{ kg/m}^3$ ). Our findings on the influence of protein concentration on aerogel structures indicates that the overall density of the gel backbone is mostly influenced by protein concentration, while the meso- and micro-pores appear to be mostly influenced by the pH.

The pore size distribution obtained by nitrogen adsorption measurement yields further insights into the microstructure of the PPI aerogels. The pore size distributions of the PPI aerogels made from hydrogels of different pH values are given in Figure 3-26. Nitrogen adsorption can only measure micro- and meso-pores below 100 nm in size. This explains why for pH 6 low pore volumes are measured as most of the measured pore volume is assumed to be within large pores, as seen in the SEM pictures of Figure 3-25. For high electrostatic repulsion at acidic and alkaline conditions, more pore volume is present within micro-pores of smaller pore diameters. As these pores are only few nanometers in diameter, one can assume that these pores are within the primary aggregates making up the gel network. This supports the assumption made for the microstructure, based on the SEM pictures: An increase in electrostatic repulsion leads to an increase in smaller pores and a reduction in larger pores. This further clarifies that between the visible cracks at pH 3 there are indeed finely structured areas which consist of micro-pores. In addition, the homogenization of the pore network can be seen, as the width of the distribution is reduced by increased electrostatic repulsion.

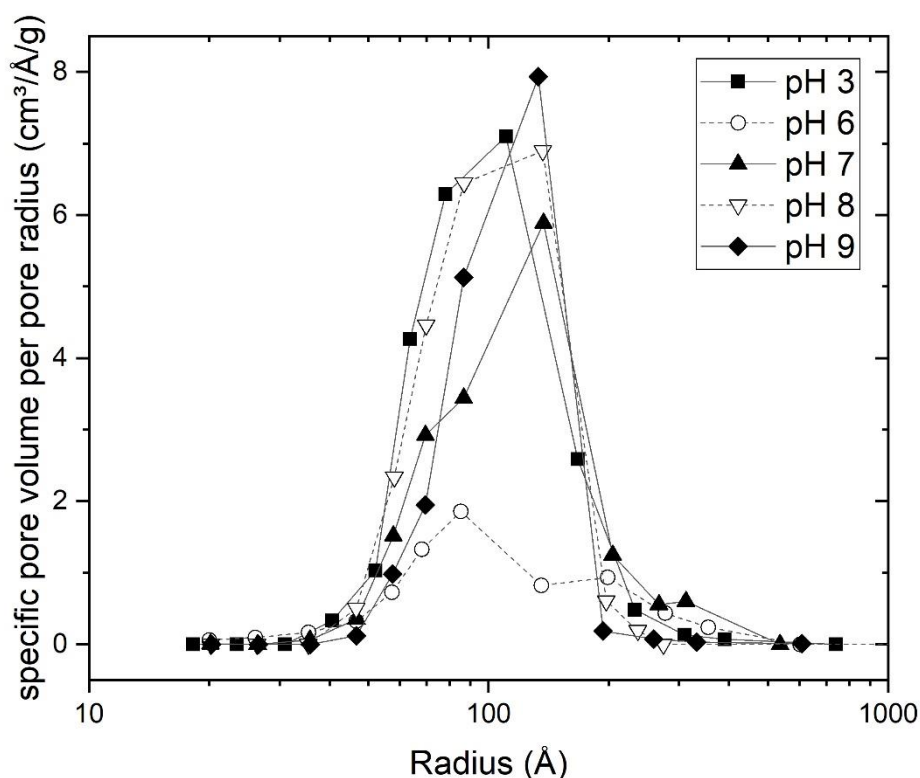


Figure 3-26 Pore size distribution of PPI aerogels made from protein solutions of different pH values, measured by nitrogen adsorption. The standard deviation of the double measurement was omitted for clarity.

### 3.4.3.3 Relationship between hydrogel rheology and aerogel microstructure

Aerogel structures are dependent on the structure of their respective precursor hydrogels, which was already shown for some food proteins (Kleemann et al., 2018). However, some assumptions made for covalently crosslinked WPI and EWP gels are not applicable for non-covalently linked PPI gels. This can be seen in the relation between limit of linear viscoelasticity and stability of PPI aerogels (Figure 3-23 and Figure 3-24). As the pH influences the gelation mechanism and the gelation mechanism influence the rheological properties of the gel network, obviously a rheological factor should help in explaining the interplay between structure and gelation mechanism.

The value  $G'$  of the cooled gel in relation to  $G'$  of the hot gel was recently used to identify the formation of apparent covalent and non-covalent bonds in heat-set protein gels (Martin et al., 2014). Higher  $G'_{cool}/G'_{hot}$  ratios were associated with more apparent non-covalent bonds. Cross-linked gels from WPI and EWP had ratios around 2, whereas pea and soy protein gels had higher values between 3 and 4. Even higher  $G'_{cool}/G'_{hot}$  ratios were found for Rubisco protein from spinach, the brittle structure of which was explained by the lack of covalent bonds. Another study compared patatin,  $\beta$ -lactoglobulin and ovalbumin. Patatin had higher  $G'_{cool}/G'_{hot}$  ratios than the other gels, indicating formation of more non-covalent bonds (Creusot et al., 2011).

In Figure 3-27, the  $G'_{cool}/G'_{hot}$  ratios of PPI hydrogels at different pH values are shown. Furthermore, the insets show the visual appearance of the hydrogels at the respective pH values.

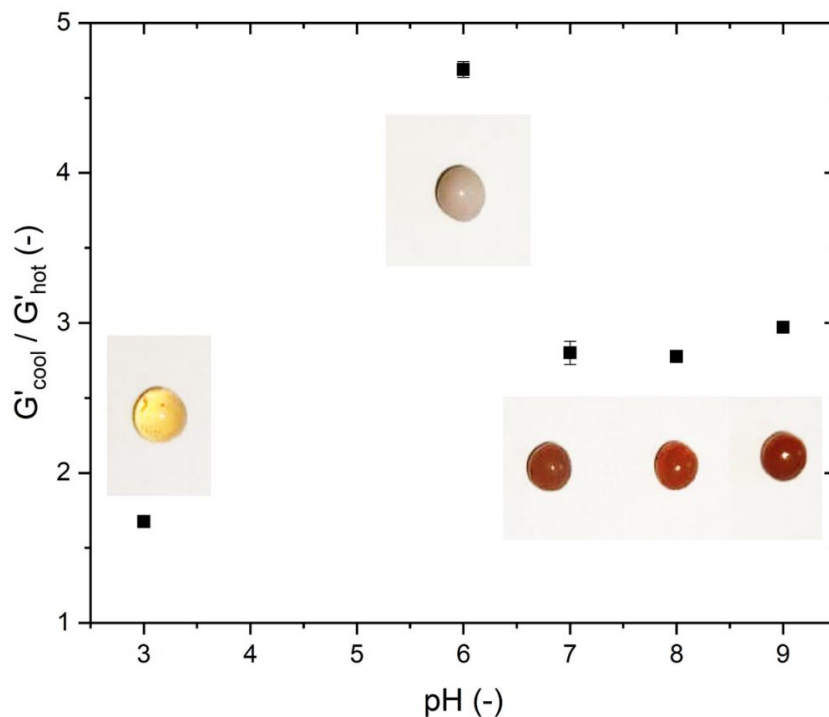


Figure 3-27 The ratio of  $G'$  of the hydrogel after cooling to  $G'$  of the hydrogel in the heated state in dependence of the pH of the precursor solution. The insets show the visual appearance of the corresponding hydrogel capsules.

The  $G'_{cool}/G'_{hot}$  ratios for pH values close to the IEP, at neutral and alkaline conditions compare well with the values reported in literature for patatin rich potato protein gels (Schmidt et al., 2019). An increase of the pH did not lead to a decrease of the  $G'_{cool}/G'_{hot}$  ratio, which would indicate the formation of more apparent covalent bonds. This supports our findings when investigating the LVE range, i.e. that an increase in pH did not induce the formation of more covalent bonds. Close to the IEP the  $G'_{cool}/G'_{hot}$  ratio increases, indicating more apparent non-covalent bonds. This can be explained by the increased electrostatic and other short-ranged interactions that can form upon reduction of electrostatic repulsion.

When inspecting the visual appearance of the hydrogel capsules three groups could be differentiated. For pH 3 a transparent yellowish gel was obtained, close to the IEP the gel became opaque and at pH 7 and more alkaline conditions the gel became transparent again with a brownish color. The pH dependent color change is probably due to oxidation of polyphenols found in potato products (Akyol et al., 2016). The transition from transparent to opaque gels with decreased electrostatic repulsion is due to increased hydrogen and electrostatic bonds in the network and the formation of bigger

and denser aggregates, which scatter incoming light resulting in the opaque appearance (Mehalebi et al., 2008).

The ratio  $G'_{cool}/G'_{hot}$  was shown to measure interactions within the gel network. It can be used to explain the pH dependent change in microstructure for PPI aerogels. One important factor for probing the microstructure of an aerogel is the specific surface area, accessible by nitrogen adsorption. For EWP and WPI aerogels, it was found that dense, particulate protein aerogels exhibit low specific surface areas, whereas fine stranded aerogels exhibit high specific surface areas (Kleemann et al., 2018; Selmer et al., 2015).

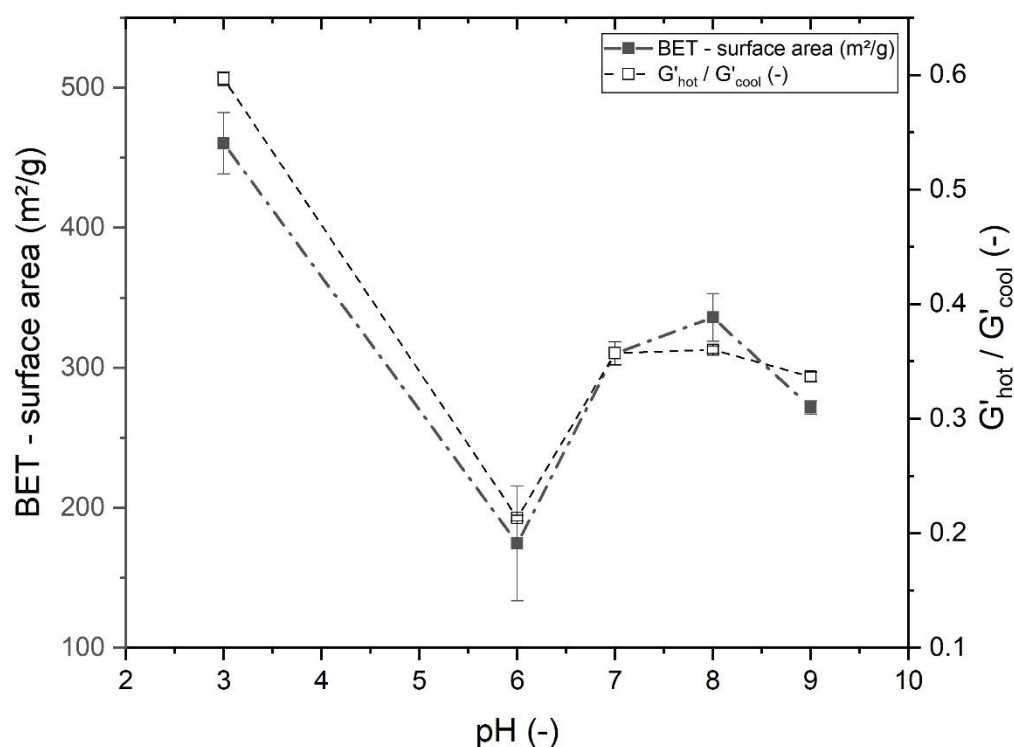


Figure 3-28 The dependence of the specific surface area of the PPI aerogels, measured through BET on pH of the precursor solution. And the dependence of the  $G'$  of the PPI hydrogel in the hot state in relation to  $G'$  in the cooled state measured by small angle oscillatory rheometry.

For the transparent, fine stranded gels the acidic gels exhibited higher specific surface areas than the alkaline gels. This trend could be also seen for PPI aerogels, see Figure 3-28. Close to the IEP the gels were particulate with a low specific surface area. At neutral and alkaline conditions, the gels had higher specific surface areas, and the highest values were found for acidic PPI capsules. Increased charge on the proteins leads to fine stranded gel microstructure as discussed earlier. However, the nominal charge difference between the pH and the IEP could not explain the difference in BET surface area for alkaline and acidic gels, as the alkaline gels should carry more charge than the acidic gels for the investigated pH values. The formed microstructures there-

fore are different between acidic and alkaline hydrogels. The microstructure of the aerogel should be directly determined by the microstructure of the hydrogel, as no adverse affect on the microstructure by the aerogel process is expected. For thermally induced WPI gels a correlation between the microstructure and the factor  $G'_{hot}/G'_{cool}$  the inverse of the  $G'_{cool}/G'_{hot}$ , was found (Bowland et al., 1995). To see whether this factor also helps in explaining pH induced changes of the microstructure in PPI  $G'_{hot}/G'_{cool}$  instead of  $G'_{cool}/G'_{hot}$  was plotted against the specific surface area, as can be seen in Figure 3-28. By using  $G'_{hot}/G'_{cool}$  we avoid a crossover of the curves, and the correlated change of both the rheological value and the specific surface area in dependence of the pH value becomes apparent. A decrease in the  $G'_{hot}/G'_{cool}$  factor correlates well with a decrease in specific surface area as a function of pH.

Changes in the relation between  $G'_{cool}$  and  $G'_{hot}$  indicate changes in protein interactions and a change in BET surface area indicates changes in the gel microstructure. As changes in protein interactions are known to influence the microstructure of gels a correlation between the protein interactions, measured by  $G'_{cool}/G'_{hot}$ , and the microstructure, measured by BET-surface area, seems reasonable. In the following we will try to explain this correlation.

To assess whether the correlation between  $G'_{cool}/G'_{hot}$  and the specific surface area also holds for other protein systems, hydrogels made from egg white were analyzed for their  $G'$  increase upon cooling.  $G'_{cool}/G'_{hot}$  ratios were plotted against the BET values published for EWP aerogel capsules (Selmer et al., 2015). Increasing  $G'_{cool}/G'_{hot}$  values led to lower specific surface areas, see Figure 3-29. The lowest BET values were obtained for gels produced close to the IEP of the main proteins and these values exhibited the highest values of  $G'_{cool}/G'_{hot}$ . Close to the IEP the electrostatic repulsion between protein molecules is greatly reduced and non-covalent interactions like electrostatic, hydrogen and van der Waals interactions play a more pronounced role. The highest BET values were found for the acid gels for both protein systems and these also exhibited the lowest  $G'_{cool}/G'_{hot}$  values.

Heat set gelation of acidic protein gels can occur very fast for concentrated protein systems as was already shown for  $\beta$ -Lactoglobulin (Gosal et al., 2004b). The aggregates formed at higher concentrations in acidic conditions are characterized as worm like short fibrils (van den Akker et al., 2011), not too different from the worm-like fibrils seen at neutral conditions and low ionic strength (Durand et al., 2002).

This is seen as a strong indication that the  $G'_{cool}/G'_{hot}$  ratio is indicative for the microstructure in a protein gel, as was proposed for the gelation of WPI in dependence of different kosmotropic and chaotropic salts in the aqueous phase (Foegeding et al., 1995). The most abundant proteins in EWP are ovalbumin and ovotransferrin constituting 54 and 12 % of total protein, respectively (Hacohen et al., 2018). Both proteins possess thiol groups either free or in disulfide bonds. Therefore, EWP gels are covalently linked through thiol-disulfide exchange (Arntfield et al., 1991), even to a degree that disruption of other non-covalent bonds will not disrupt the overall hydrogel structure (Martin et al., 2014). These strong covalent disulfide bonds can only be expected for alkaline conditions, where the thiol group is deprotonated and reactive. For low pH

values no thiol-disulfide exchange is expected, as was shown for WPI solutions (Shimada & Cheftel, 1989).

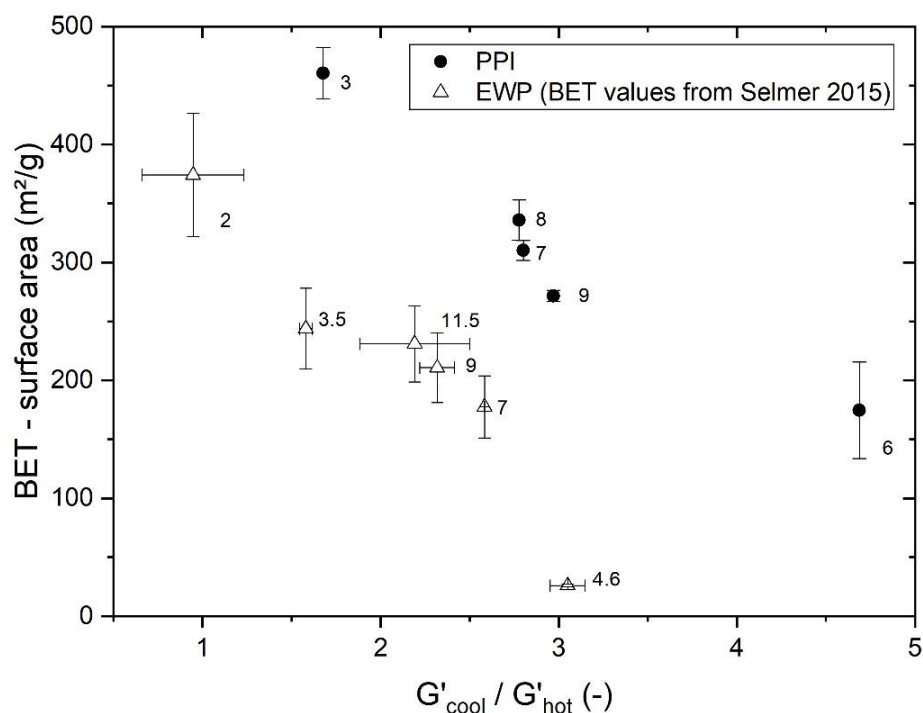


Figure 3-29 Relation between the specific surface area of the aerogel and the  $G'_{cool} / G'_{hot}$  ratio of the hydrogel precursor. The BET values from EWP were taken from (Selmer et al., 2015). Numbers next to the data points indicate pH of the respective protein solution.

Therefore, hydrophobic interactions are expected to play a major role in the aggregation process of EWP as they also determine the shape of fibril or amorphous aggregates in proteins (Shivu et al., 2013). For patatin different unfolding mechanisms in dependence of the pH were shown as well (Pots et al., 1998b). At acidic conditions, the protein unfolds and hydrophobic amino acid side chains increased the solvent exposure, making hydrophobic interactions of these chains during gelation very likely. It should be noted that patatin lacks internal disulfide bridges and therefore should unfold to a higher degree than disulfide linked proteins like  $\beta$ -lactoglobulin. Acid induced gelation of EWP results in low strain/stress gels which have no free thiol groups for gel spanning disulfide mediated polymerization (Weijers et al., 2006). Blocking of non-covalent interactions by SDS at pH 7 leads to a similar, finely stranded, EWP gel microstructure as pH 11. This indicates the randomness of such non-covalent interactions and their coarsening effect on the microstructure (Handa et al., 1998).

To further understand the meaning of  $G'_{cool} / G'_{hot}$  ratios we discuss the dependence on ionic strength and salt types, as these influence gelation considerably. An increase in  $G'_{cool} / G'_{hot}$  ratio upon salt addition was seen for various food proteins (Creusot et al., 2011). This increase in  $G'_{cool} / G'_{hot}$  ratio can be explained by a change in microstructure. The salt dependent change of WPI gels in the presence of different salts was studied extensively (Bowland et al., 1995). Increasing the molarity of the ions resulted in a



transition of the microstructure from fine stranded to mixed to particulate. Less ions were needed when the salt had a higher structure stabilizing effect, according to the Hofmeister range. A notable difference was found for the chaotropic salt NaSCN as high molarities reduced the  $G'_{cool}/G'_{hot}$  ratio despite exhibiting mixed microstructures (microscopy pictures of the microstructure are given elsewhere (Bowland & Foegeding, 1995)). These anions induce unfolding in proteins by destabilizing their tertiary structure and promote hydrophobic interactions. As hydrophobic interactions are stronger at elevated temperatures (Nakai, 1988) a decrease of  $G'$  upon cooling can be interpreted as more hydrophobic interactions in relation to hydrogen bonds. These findings show that it is important to separate hydrophobic interactions from other non-covalent interactions when talking about gelation mechanism.

Our findings regarding the  $G'_{cool}/G'_{hot}$  ratio can be summarized as follows: When comparing similar microstructures, the relation  $G'_{cool}/G'_{hot}$  can allow to make assumptions about covalent bonds present within the gel network as evidenced by EWP, which BET surface area being constantly below that of PPI gels. However, within one protein type, low  $G'_{cool}/G'_{hot}$  ratios are indicative of hydrophobic interactions that result in a fine stranded gel with a high specific surface area. Gelation in an environment of reduced electrostatic repulsion and in alkaline conditions still resulted in fine stranded gels but the  $G'_{cool}/G'_{hot}$  ratios are increased and the specific surface area reduced when compared to the very acidic conditions. This increase in  $G'_{cool}/G'_{hot}$  indicates relatively more hydrogen bonds and/or electrostatic and van der Waals interactions in relation to hydrophobic/covalent interactions. For conditions close to the IEP, the protein structure is well stabilized, unfolding is limited and hydrophobic and covalent bonds are expected to play minor roles. The predominance of hydrogen and other non-covalent bonds lead to random aggregation resulting in low BET values and high  $G'_{cool}/G'_{hot}$  values

#### 3.4.4 Conclusion

In this work it was shown for the first time that patatin rich potato protein isolate (PPI) can form stable hydrogels, which can be transformed into aerogels. The density of the skeletal backbone of the protein network increased with increasing concentration and plateaued when a protein concentration of 10 % was passed. The storage modulus increased linearly with increasing protein concentration. This indicates that the density of the backbone plays a minor role in explaining the hydrogel and aerogel strength and most likely interactions between the proteins are more important.

PPI hydrogels hardened during solvent exchange to ethanol. The hardest alcogels and aerogels were found for hydrogels gelled at high pH values, similar to what was shown in the literature for EWP and WPI. However, not many covalent crosslinks are expected in PPI gels, as was also indicated by the lower range of LVE with increasing pH. This shows that PPI gels can withstand the shrinkage during solvent exchange and supercritical drying and yield stable aerogels with a comparable hardness to EWP. This high stability of the aerogels could be achieved without the generation of disulfide linked bonds and the characteristic high deformability accompanying these type of bonds.

Further, we showed that for two protein systems, EWP and PPI, the change in the ratio of  $G'$  of the cooled hydrogel and  $G'$  of the hot hydrogel ( $G'_{cool}/G'_{hot}$ ) can be used as a parameter to estimate the change in the specific surface area of the dried aerogel. A high value indicates large pores and a coarse microstructure with a low specific surface area, as seen in the corresponding SEM picture. Vice versa, a low  $G'_{cool}/G'_{hot}$  ratio indicates a fine stranded network with a high specific surface area. Further investigations of the  $G'_{cool}/G'_{hot}$  ratio show that for protein gelation it is important to separate hydrophobic interactions from other non-covalent bonds like van der Waals and hydrogen bonds. Furthermore, as PPI can form similar microstructures as EWP without covalent bonds at the same extent, the formation of microstructure for these protein hydrogels should be mainly driven by hydrophobic interactions.

Overall, successful formation of patatin-based aerogels was shown along with the possibility to tailor their properties by the gelation process. We expect that patatin aerogels are interesting candidates for the applications in food industry, such as carrier matrix, thickening agent etc. and will explore those in the future.

### **Acknowledgements**

This IGF Project AiF 19712 of the FEI was supported via AiF within the program for promoting the Industrial Collective Research (IGF) of the German Ministry of Economic Affairs and Energy (BMWi), based on a resolution of the German Parliament.

We would like to thank Marc Laus from AVEBE, Veendam, The Netherlands, for providing the potato protein isolate, Klaus Mielke from OVOBEST Eiprodukte GmbH & Co. KG, Neuenkirchen-Vörden, Germany, for providing the pasteurized egg white protein.

### **3.5 Viscoelasticity and protein interactions of hybrid gels produced from potato and whey protein isolates**

#### Summary and contribution of the doctoral candidate

In previous chapters, we could show that PPI has a very different aggregation and gelation mechanism than WPI and different protein interactions dominate these gels. In this chapter both protein systems were investigated on their own as well as in mixtures. Thus we were able to create gels with different structures and gelation mechanisms. It could be shown that WPI gels were dominated by disulfide links and PPI by hydrophobic interactions. Up to 50:50 mixtures, the PPI properties dominated and gels were rather brittle and weak. A higher WPI content led to stronger and more elastic gels. The formation of disulfide bonds could be enhanced when pH was shifted towards alkaline levels. At a pH value of 5, both protein systems yielded very weak and brittle gels. Therefore, it could be concluded that at this pH the differences between the protein systems were very small. Nevertheless, it could be found that at pH 5 WPI gels were mainly stabilized through electrostatic and PPI through hydrophobic interactions. The presence of salt did influence WPI gels more than PPI gels. Although disulfide links still dominated in WPI gels the primary aggregates were particulate rather than fine stranded which influenced the network stability negatively. It could be shown that changes in the storage modulus of the protein in dependence of the temperature could be explained by changes in the protein interactions that dominate in the protein gel.

The major contribution of the doctoral candidate was developing the utilized methods. The experimental design and the data evaluation were also done by the doctoral candidate. The correlation between  $G'_{cool}/G'_{hot}$  and the protein interactions needed explanations from the literature, which were provided by the doctoral candidate. The different behavior of WPI and PPI towards milieu changes could be explained by the molecular structure of their main proteins. The resulting mechanism for gel formation was developed by the doctoral candidate. Other contributions included the writing of the original draft as well as responding to reviewer comments.

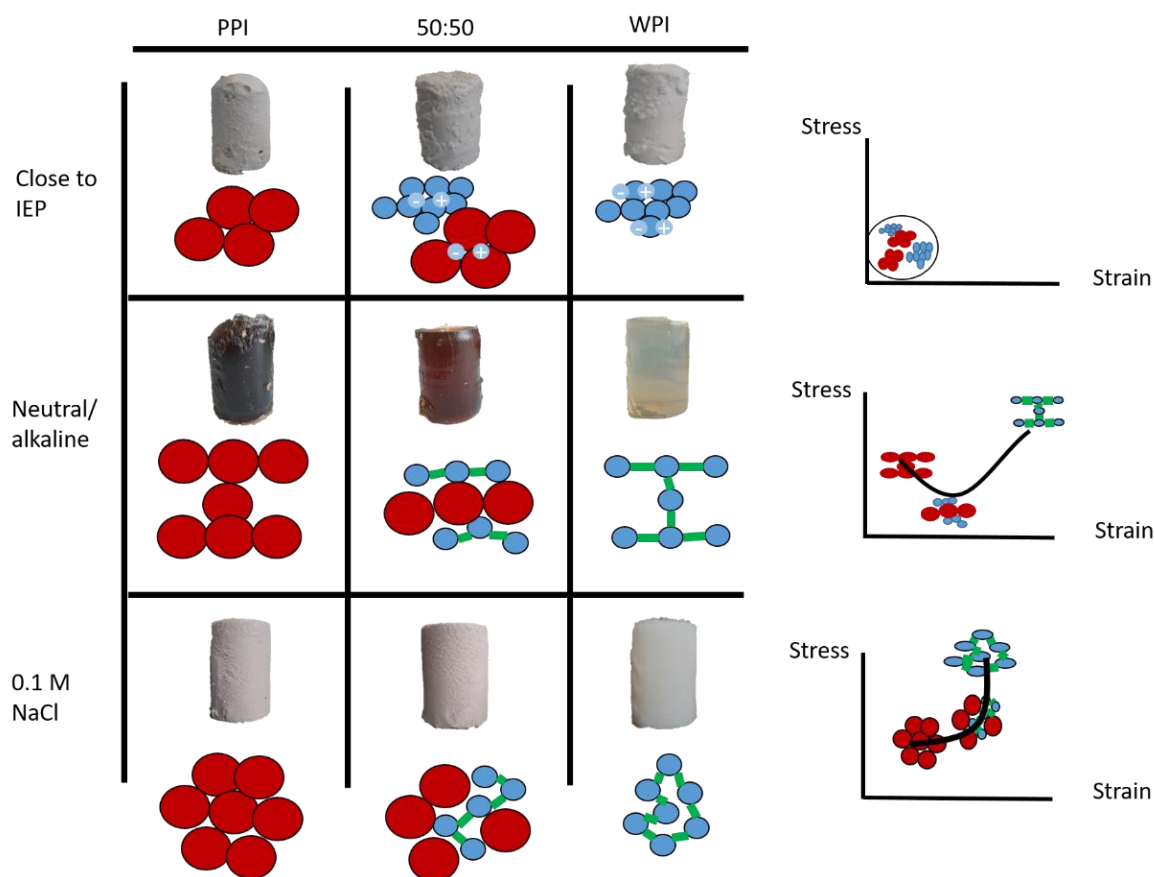
*Adapted original manuscript*<sup>5</sup>

## Viscoelasticity and protein interactions of hybrid gels produced from potato and whey protein isolates

David J. Andlinger\*, Lena Rampp, Caren Tanger, Ulrich Kulozik

Chair of Food and Bioprocess Engineering, TUM School of Life Science, Technical University of Munich, Weihenstephaner Berg 1, 85354, Freising, Germany

### Graphical Abstract



<sup>5</sup> (Adaptions refer to formatting issues: e.g., numbering of sections, figures, tables and equations, abbreviations, axis labeling, figure captions and style of citation). Reference lists of all publication based chapters were merged at the end of this thesis to avoid duplications.

Original publication: Andlinger, D. J., Rampp, L., Tanger, C., & Kulozik, U. (2021). Viscoelasticity and Protein Interactions of Hybrid Gels Produced from Potato and Whey Protein Isolates. *ACS Food Science & Technology*, 1(7), 1304–1315. <https://doi.org/10.1021/acsfoodscitech.1c00163>

Reprinted (adapted) with permission from Viscoelasticity and Protein Interactions of Hybrid Gels Produced from Potato and Whey Protein Isolates. Copyright 2021 American Chemical Society.

## Abstract

Controlling the textural properties of protein gels is of high importance for designing food and other protein products. The combination of animal-derived proteins and plant-based proteins offer the possibility to create nutritional, sustainable, and also textural advantageous products. However, interactions between proteins from different sources and with different molecular features are not well understood yet. By analyzing the interactions between whey (WPI) and potato proteins (PPI), we can determine how gel structures in protein gels form. Through different mixing ratios, pH levels and ionic strength, we show how the formation of disulfide and hydrophobic bonds influence the textural properties of protein gels. It could be shown that up to a 50:50 mixing ratio, the properties of PPI dominate WPI. Gels with a high elasticity could be formed only through the development of a continuous disulfide network.

### 3.5.1 Introduction

The gelation of proteins plays an important role in the development of texture in food. One of the most widely applied methods to denature proteins and induce gelation is through the application of heat (Clark et al., 2001). In this process, proteins unfold and interact through exposed hydrophobic residues (Shivu et al., 2013). This initial aggregation is then often accompanied by crosslinking of the aggregates through newly created disulfide bonds through the thiol-disulfide exchange (Bauer et al., 2000).

A protein with a strong tendency to form gels stabilized by disulphide bonds upon thiol-disulfide exchange is  $\beta$ -lactoglobulin ( $\beta$ -lg), the major protein in whey protein isolates (WPI) (Leeb et al., 2018). Through the formation of many covalent disulfide links, the gels from WPI are very elastic compared to other protein sources (Martin et al., 2014). Important for a high reactivity of the thiol group is a pH of 7 or above (Monahan et al., 1995). Furthermore, at this pH, the proteins tend to form finely structured gels (Kleemann et al., 2018). At pH closer to the isoelectric point (IEP), particulate gels are formed with different optical and textural properties.

The gelation mechanism of WPI and other animal-derived proteins are well understood, and therefore applications as foaming agents (Dombrowski et al., 2017), emulsifier (Delahaije et al., 2013), or fat replacement (Wolz & Kulozik, 2017) are well established. However, there is an increased interest in substituting animal-derived protein with alternative proteins, for example to obtain healthier products (Borderías et al., 2020)

Therefore, the gelation mechanisms of other protein sources are investigated as well. Thereby, significant differences between the protein sources in regards to aggregation (Delahaije et al., 2015) and gelation (Creusot et al., 2011) behavior are observed. It is clear that not every protein can be easily substituted with another as molecular features of the different sources are too different.

Another strategy to increase the use of plant proteins is the partial replacement of animal-derived proteins by plant proteins. For example, hybrid aggregates from pea globulins and  $\beta$ -lg were created through thermal denaturation (Chihi et al., 2016). Thereby, it could be shown that  $\beta$ -lg was incorporated into the pea globulin aggregates, leading

to denser aggregates. This was possible through the development of additional disulfide bonds within the aggregates clearly showing synergistic interactions between the proteins. However, for soy protein and WPI mixtures increasing soy protein content led to phase separation of the protein systems (Comfort & Howell, 2002) and also reduced resistance against fracture (Jose et al., 2016). Therefore, the hybridization of protein systems not always successful and can lead to undesired side effects. It can be concluded that most research on hybrid protein systems was done on whey and legume proteins, as a recent review showed (Alves & Tavares, 2019).

However, legume proteins are considerably larger than whey and egg proteins, and their tertiary and quaternary structure is different as well, leading to different gelation mechanism (Arntfield et al., 1991). Furthermore, legume proteins often need a certain amount of salt to solubilise (Tanger et al., 2020) and form gels. This is why studies investigating the properties of Soy-WPI (Jose et al., 2016) or rapeseed-WPI (Ainis et al., 2018) hybrid gels were all performed at an elevated ionic strength of 0.1-0.3 M NaCl. However, the addition of salt alters the gelation mechanism of WPI towards coarser structures with different textural properties than fine-stranded WPI gels (Urbonaite et al., 2016).

Another protein showing promising gelation (Schmidt et al., 2019), emulsification, and foaming properties (Schmidt et al., 2018) is the potato protein patatin. Contrary to legume proteins it is very soluble even at low ionic strength. This protein has a molecular weight of around 40 kDa, which is comparable to ovalbumin from egg, and an IEP of around pH 5 (Racusen & Weller, 1984). Patatin does not contain internal disulfide bond and has only one free thiol group. Therefore, it does not form covalently crosslinked elastic gels (Creusot et al., 2011). The main aggregation and gelation mechanisms are found to be dominated by hydrophobic interactions (Andlinger et al., 2021c). Hydrophobic interactions are less specific than covalent bonds and led to different gel structures. For example, blocking of hydrophobic interactions led to a finer microstructure in egg white protein (Handa et al., 1998). Nevertheless, patatin rich potato protein isolate (PPI) was shown to form finely stranded hydrogels with a similar microstructure as egg white protein at neutral and alkaline conditions and without the need to add salt (Andlinger et al., 2021a).

In this work, heat-set hydrogels from whey and potato proteins at different mixing ratios were created. Both proteins were expected to interact through different protein interactions. This will allow investigating the influence of these interactions on the textural properties of protein gels. The protein interactions were further altered through changes in the pH value and ionic strength. The resulting protein interactions within the gels were quantified by a protein interaction assay. This was accompanied by gel characterizations via non-destructive oscillatory rheometry as well as destructive compression tests. This way, we investigated the relation between protein interactions and structural properties of the hydrogels from globular proteins. The obtained relationship between molecular features, protein interactions and structural properties will help to design protein gels with targeted properties for food and life science applications.

### **3.5.2 Materials and methods**

#### **3.5.2.1 Materials**

Commercial PPI powder (Solanic 200™) with a high content of patatin was obtained from AVEBE (Veendam, The Netherlands). The protein powder had a protein content of 88.6% (w/w). Commercial WPI (BiPRO™) powder was obtained from Agropur Dairy Cooperative (Saint-Hubert, Longueuil, Canada). The protein powder had a protein content of 90.9% (w/w). The protein content was determined using the method of Dumas with an accuracy of  $\pm 0.1\%$  (w/w) (Vario MAX CUBE, Elementar Analysensysteme GmbH, Hanau, Germany). The powder was solubilized in deionized water and stirred overnight. Afterwards, the solution was centrifuged at 6000 g for 15 min to eliminate insoluble components (around 5% of protein content in PPI, below 1% in WPI). WPI and PPI Solutions with protein concentrations of 15% (w/w) were created. These 15% solutions then were mixed in different proportions to create hybrid protein solutions. The protein solutions were adjusted to a pH of 5,7 and 9 by using NaOH and HCl with a molarity of 0.1 or 1 M.

#### **3.5.2.2 Rheological characterization of the hydrogels**

Viscoelastic properties of PPI/WPI solutions were investigated by oscillatory measurements, as described elsewhere (Tanger et al., 2021b). For this a Paar Physica MCR 302 (Anton Paar GmbH, Graz, Austria) stress-controlled rheometer with a concentric cylinder geometry CC10 (bob diameter 9.995 mm, cup diameter 10.842 mm). The temperature of the rheometer was controlled with a Peltier element cooled by an accompanying recirculating cooler model Haake DC1 (Thermo Haake GmbH, Karlsruhe, Germany). For the gelation experiments, 1.02 mL of the protein solution was filled in the rheometer geometry. The sample was covered with silicone oil (Polydimethylsiloxane 20 cSt) to prevent evaporation.

After a 10 min equilibration phase at 25 °C, a deformation of 0.02 % and a frequency of 10 rad/s, the sample was heated to 85 °C with a heating ramp of 2 °C/min and kept at 85 °C for 15 min. 85 °C is well above the determined peak denaturation temperature of 73 °C determined for this WPI (Tanger et al., 2021c) and complete unfolding of the protein should be ensured.

Afterward, the sample was cooled down with a cooling ramp of 2 °C/min to 25 °C the deformation and frequency were kept at 0.02 % and 10 rad/s throughout the whole experiment, respectively. After 5 min of equilibration, a frequency sweep from 0.1 to 100 rad/s was conducted. The deformation was kept at 0.02 %.

#### **3.5.2.3 Texture profile analysis**

For texture analysis, the prepared 15% protein solutions were gelled by heating them in metal cylinders in a water bath at 85 °C for 15 minutes. Immediately after heating, the samples were cooled down in iced water for about two minutes. Then cylinders with a diameter of 16 mm were cut out, which were then cut into cylindrical pieces with a height of 20 mm. The cylinders were compressed to 90% of their initial height at a compression speed of 1 mm/s using a Texture Analyzer with a flat plate probe with a diameter of 60 mm, similar what was used by other researchers for a wide variety of

food proteins (Martin et al., 2014; Schmidt et al., 2019). The gels created from solutions at pH 7 and pH 9 were investigated by a measuring cell with an allowed maximum load of 50 kg, the gels at pH 5 by a measurement cell with an allowed maximum load of 500 g. The force and distance at fracture were derived from the obtained fracture-strain curves. True fracture stress  $\sigma_T$  and true fracture strain  $\varepsilon_T$  were calculated according to Equation (3-14) and (3-15). With  $F$  being the measured force (N),  $A$  is the contact surface of the gel cylinder ( $m^2$ ),  $H_0$  is the initial height of the gel cylinder, and  $\Delta H$  is the measured distance the cylinder is compressed until fracture.

$$\sigma_T = \frac{F}{A} * \frac{H_0 - \Delta H}{H_0} \quad (3-14)$$

$$\varepsilon_T = -\ln\left(\frac{H_0 - \Delta H}{H_0}\right) \quad (3-15)$$

#### 3.5.2.4 Protein interaction assay

Protein hydrogels were dissolved in different buffer systems B1 – B3 to investigate the dominant protein interaction forces stabilizing the gels. A detailed description of method development and validation is given elsewhere (Tanger et al., 2021a). Each hydrogel was gently separated into smaller fragments by pressing the gel through a garlic press. The nitrogen content was assessed by the method by Dumas. For each hydrogel, three times 0.5 g of this hydrogel were weighed into a falcon tube, and 20 g of a buffer was added to each gel. The buffers used are given in Table 3-6. The buffer cleaves either electrostatic and hydrogen bonds (ES), hydrophobic interactions (Hy), or disulfide bonds (SS). The tubes were shaken at room temperature overnight prior to analysis.

Afterwards, the solutions were centrifuged at 10,000 g for 20 min. The supernatant was analyzed for total nitrogen content by the method of Dumas. To calculate the relative contribution of each protein-protein interaction, the amount of protein bonds cleaved by the different buffer systems ( $C_{n,bond,Bx}$ ) was calculated. This is shown in Equation (3-16):

$$C_{n,bond,Bx} = \frac{(m_s + m_{gel})}{m_{gel}} * C_{n,sup,Bx} \quad (3-16)$$

From knowing which buffer dissolves which protein interaction (see Table 3-6), we can derive the following equations to calculate the amount of protein bound by the different types of protein interaction ( $P(X)$ ).

$$P(ES) = \frac{C_{n,bond,B1}}{C_{n,gel}} \quad (3-17)$$

$$P(Hy) = \frac{C_{n,bond,B2}}{C_{n,gel}} - \frac{C_{n,bond,B1}}{C_{n,gel}} \quad (3-18)$$

$$P(SS) = \frac{C_{n,bond,B3}}{C_{n,gel}} - \frac{C_{n,bond,B2}}{C_{n,gel}} \quad (3-19)$$



Table 3-6 Composition of the buffers used in the protein interaction assay

Buffer	NaH <sub>2</sub> PO <sub>4</sub> / Na <sub>2</sub> HPO <sub>4</sub> [mol/L]	SDS [g/L]	DTT [g/L]	pH	Type of protein interaction
B1	0.05	-	-	7.5	ES
B2	0.05	2	-	7.5	ES, Hy
B3	0.05	2	15	7.5	ES, Hy, SS

With  $m_s$  being the initial mass of the buffer (20 g),  $m_{gel}$  being the mass of the gel (0.5 g) and  $C_{n,sup,Bx}$  being nitrogen in the supernatant in % dissolved by buffer Bx.

### 3.5.2.5 SDS polyacrylamide gel electrophoreses

An SDS polyacrylamide gel electrophoresis (PAGE) was performed to detect covalently linked aggregates formed in the heat gelation process that could not be cleaved by buffer B2 but were still soluble in this buffer. These oligomers were so large that they remained in the pocket of the SDS PAGE gel. The supernatants of buffer B2 samples were used for this electrophoresis. 40  $\mu$ L of the samples were filled into two 2 mL screw-top reaction tubes each. Then 60  $\mu$ L of reducing and non-reducing SDS PAGE sample buffer were added to one tube each. After short centrifugation at 7000 g, the samples were heated in a shaking heat block for 5 min at 100 °C in order to guarantee SDS-induced protein denaturation. Samples were centrifuged at 7000 g again and 10  $\mu$ L of each sample were loaded onto a prepacked 4-20% stain free TGX gradient polyacrylamide gel. 7  $\mu$ L of a Precision Plus Protein™ Unstained Standard were loaded as a size marker with proteins of molecular weight from 10 to 250 kDa. The electrophoresis was run for approximately 45 min at 300 V, 35 W, and 40 mA/gel in the presence of an SDS-PAGE running buffer. The gels were then analyzed by using a ChemiDoc™ XRS+ Molecular Imager system that scanned protein bands at 300 nm. These bands were quantified by using the Software Image Lab 6.0.

### 3.5.2.6 Determination of exposed hydrophobicity

For the determination of the exposed surface hydrophobicity ( $S_0$ ) 1% protein solutions were heated. The lower protein concentration ensured that no gelation occurred and solutions were transparent enough to obtain reliable fluorescence intensity values. As a pH level of 5 resulted in turbid solutions, the gel with thus pH could not be investigated.

A 1.41 mM N,N-dimethyl-6-propionyl-2-naphthylamine solution (PRODAN) was prepared by dissolving PRODAN in pure methanol to ensure complete dissolution of the fluorescence probe. The solution was kept at – 40 °C under the exclusion of light. For each measurement, small aliquots of the sample were taken from the freezer. Aluminum foil ensured the exclusion of light from the solution, and it was kept over ice for the whole time. Protein solutions were diluted to 1 mg/mL. 1 mL of the diluted solution

was transferred into a deep well plate. The PRODAN solution was added in amounts of 0, 5, 10, 15, 20, 25, 30, 40, and 50  $\mu\text{L}$ . Afterwards, the solution was thoroughly mixed with a pipette. 100  $\mu\text{L}$  of the mixed solutions were transferred to a black 96-well plate (Greiner chimney flat back 96 well), and the mixture was incubated for 30 min at room temperature in the dark. All solutions were transferred in triplicate onto the plate. After incubation, the solutions were excited at 365 nm in a Tecan Spark microplate reader (Tecan Group Ltd., Männedorf, Switzerland). The emission spectra between 400 and 650 nm were recorded. A maximum was detected at 440 nm, and the absorption value at this wavelength was plotted against the amount of PRODAN added. For most solutions, 30  $\mu\text{L}$  marked the beginning of a plateau in the fluorescence intensity indicating saturation of all hydrophobic binding sites. The fluorescence intensity over the amount of PRODAN in the linear region before the plateau was fitted by linear regression, and the slope of regression was taken as a measure of  $S_0$ .

#### **3.5.2.7 Experimental design**

All experiments were performed in triplicate from three independently prepared solutions. If not described otherwise, the depicted data points represent the average of three measurements and error bars the standard deviation from these triplicates. For the texture analyzer measurements, two hydrogel cylinders were measured per gelled solution.

### **3.5.3 Results and discussion**

#### **3.5.3.1 Visual appearance of PPI/WPI hybrid gels**

The gelled protein solutions differed considerably in their optical appearance. Pictures of the gelled cylinders before they were cut for compression tests are shown in Figure 3-30.

It can be seen that pH and mixing ratio, as well as the addition of salt, changed the optical appearance of the gels. At pH 5, gels were opaque, and the surface appeared rough. Both being indications of a particulate gel.  $\beta$ -lg and patatin have an isoelectric point (IEP) close to pH 5 (Creusot et al., 2011). Therefore, the reduced electrostatic repulsion at this pH favors the formation of aggregates, large enough to scatter incoming light (Nicolai & Durand, 2013).



Figure 3-30 Optical appearance of protein solutions gelled for 15 min at 85 °C in dependence of pH and salt content as well as mixing ratio of WPI and PPI.

There was no difference between the different mixing ratios indicating the formation of similar structures, independent of the protein type. At neutral pH levels, gels differed considerably. Gels containing PPI had a brown color which probably derived from residual oxidized polyphenols in the protein isolate, such as chlorogenic acid (Løkra et al., 2009). Gels with a WPI content of 75-100% were transparent, indicating the formation of a finely stranded gel network (Nicolai & Durand, 2013). PPI-dominated gels were more opaque, probably due to the tendency of patatin to form larger or denser aggregates than  $\beta$ -lg (Delahaije et al., 2015). The surface of the PPI and WPI gels at pH 7 appeared smooth as expected for fine-stranded gels. Increasing the pH to alkaline levels resulted in even more transparent gels. This can be explained by the increased electrostatic repulsion between the proteins, which favored the formation of smaller and more linear aggregates, which have a lower tendency to scatter light (Nicolai et al., 2011). The addition of salt reduces the electrostatic repulsion, which led to opaque gels. However, the texture appeared smoother than at pH 5.

All these different optical appearances are created by different protein interactions. How these protein interactions differ between whey and potato proteins and how they can be influenced by changes in the pH are explained in the following section. The effect of salt addition will be explained in a separate section at the end of the manuscript.

### 3.5.3.2 Protein interactions of heat-induced PPI/WPI hybrid gels

The protein gels were dissolved in different buffers to determine the protein interactions that stabilize the gels. The determined proportions of these protein interactions can be seen in Figure 3-31. At neutral and alkaline pH levels, similar dependences on the mixing ratio could be observed. Increasing WPI content led to increased stabilization

by disulfide bonds. This can be explained by looking at the main proteins of WPI and PPI.

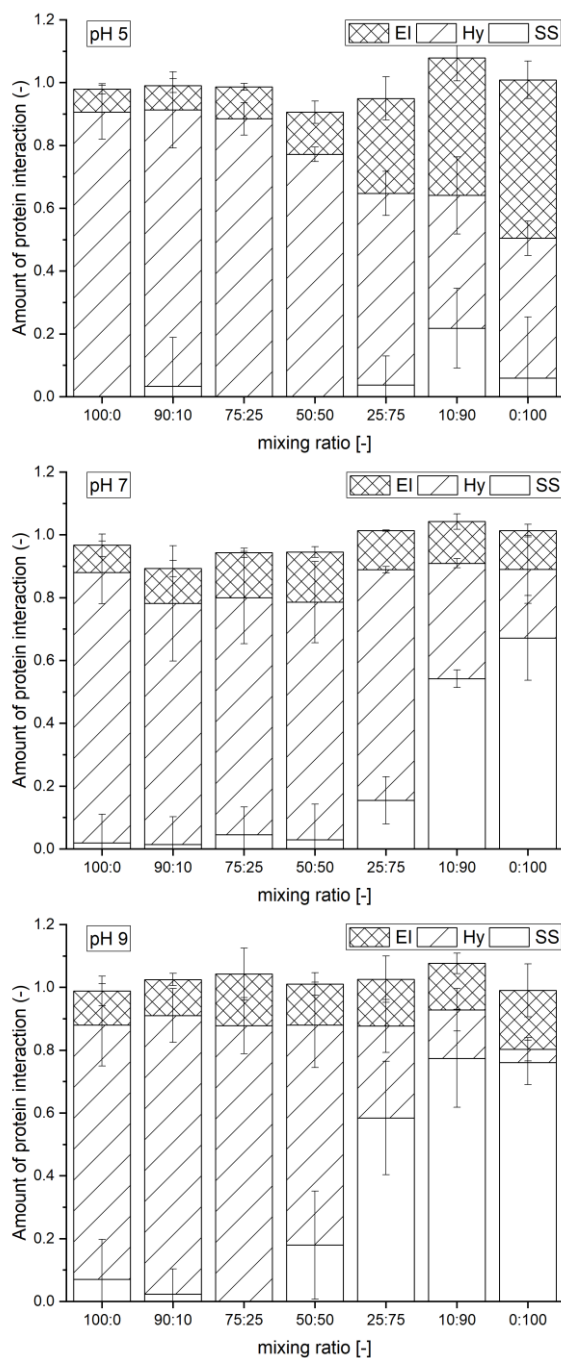


Figure 3-31 Amount of protein interactions stabilizing the protein gels in dependence on the mixing ratio (PPI/WPI) at pH 5, 7 and 9

The whey protein  $\beta$ -lg is known to form continuous disulfide-linked gels at neutral and alkaline pH through the thiol-disulfide exchange (Nicolai et al., 2011). Increasing the pH increased the formation of disulfide bonds due to the higher reactivity of the thiol group (Monahan et al., 1995). With increasing PPI content, the amount of disulfide-linked protein is reduced. At a mixing ratio of 50:50, the amount of disulfide-linked proteins is very low, especially at pH 7. This indicates that no continuous disulfide network could be formed when a high amount of patatin was present. Therefore, it can be concluded that patatin blocks the thiol-mediated polymerization of the gel network. Patatin only contains one free thiol group and no internal disulfide bonds (Delahaije et al., 2015; Creusot et al., 2011), which explains why the interaction of a  $\beta$ -lg with patatin leads to a termination of the reaction. Although patatin is not expected to exhibit mainly disulfide stabilized networks at higher pH values, some small amount of disulfide-linked protein was detected. The fact that PPI forms disulfide-linked aggregates to a certain degree was described recently (Andlinger et al., 2021c). The most important protein interactions in PPI gels are hydrophobic interactions. As patatin possesses no internal disulfide bonds,

the hydrophobic amino acids from the protein core can readily unfold upon heating. These amino acids aggregate as exposure to the polar water phase are energetically unfavored (Kronberg, 2016).

At pH 5 the amount of disulfide bonds within the gel is severely reduced for all mixing ratios. This can be explained by the reduced reactivity of thiol groups at this pH value (Monahan et al., 1995).

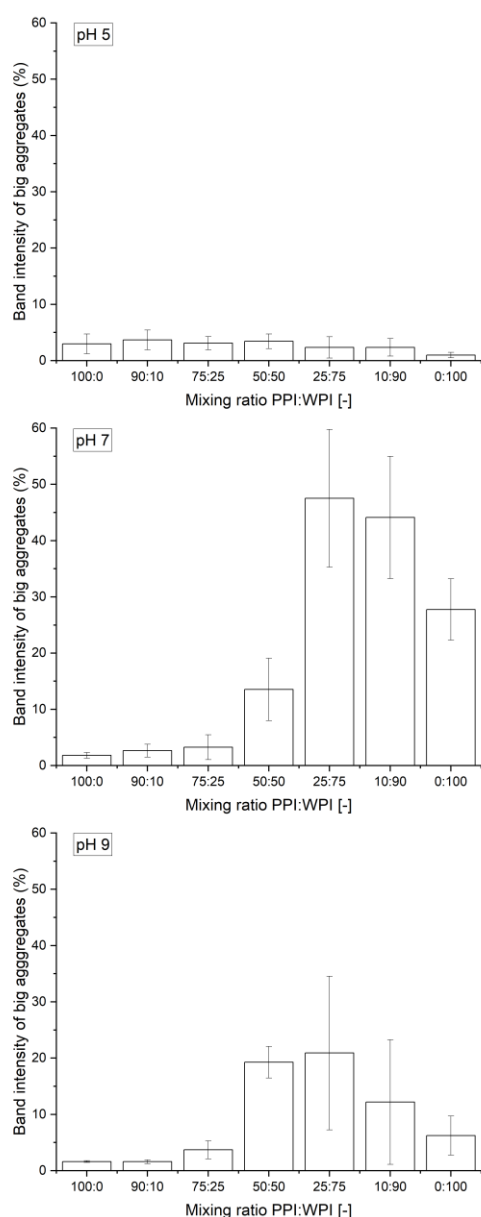


Figure 3-32 relative band intensity of the big aggregates protein extracted by buffer B2 from PPI/WPI hybrid gels in dependence of pH and mixing ratio.

As expected, the amount of disulfide-linked aggregates was very low at pH 5. This confirms that disulfide linkage is indeed severely reduced at this pH. This is in contrast

However, there were still differences between the protein mixtures. For the PPI/WPI ratios of 25:75 up to 0:100, the main interactions were of electrostatic nature. This can be explained by the different unfolding behavior of  $\beta$ -lg and patatin.  $\beta$ -lg peak denaturation temperature ( $T_d$ ) is reported to be at 75-85 °C (Tolkach & Kulozik, 2007; Creusot et al., 2011; Delahaije et al., 2015). This is considerably higher than patatin's  $T_d$  of around 60 °C (Schmidt et al., 2019; Creusot et al., 2011; Delahaije et al., 2015). The high-temperature stability of  $\beta$ -lg is due to the higher amount of internal disulfide bonds. This increased molecular stability will lead to a lower degree of hydrophobic amino acids from the core being exposed, limiting the interactions through these hydrophobic interactions. Furthermore, the repulsion between the proteins is reduced at pH levels close to the isoelectric point (IEP) of  $\beta$ -lg (Homer et al., 2018) and patatin (Andlinger et al., 2021a). Therefore, interactions via electrostatic interactions are more likely to occur.

The utilized protein interaction assay is limited in its detection of disulfide bonds, which will be addressed in the following. The SDS in buffer B2 should dissolve protein linked through hydrophobic interactions. However, some of the solubilized proteins might be aggregates that do not sediment during sample preparation. These aggregates are therefore detected as hydrophobic linked proteins, although they can be linked by disulfide bonds. In order to quantify the amount of disulfide-linked aggregates,

an SDS-PAGE analysis under non-reduced conditions was performed. The protein amount was estimated by comparing the band intensity of the protein bands. The amount of big protein aggregates that were too large to enter the PAGE gel can be seen in Figure 3-32.

to the findings at neutral and alkaline pH. At these pH levels, a considerable amount of disulfide-linked protein aggregates could be detected. Although the protein interaction assay (Figure 3-31) showed a higher amount of disulfide bonds at pH 9, a lower amount of disulfide-linked aggregates could be detected in buffer B2 at pH 7. This can be interpreted as follows: At pH 7, disulfide bonds do not form a continuous network throughout the gel. Rather, smaller disulfide-linked aggregates are bound to other aggregates through hydrophobic interactions. When these hydrophobic linked aggregates are dissolved by buffer B2 the disulfide-linked aggregates remain in solution and can be detected in the SDS-PAGE. At pH 9 the increased reactivity of the thiol group results in disulfide links throughout the gel. Therefore, the amount of detected protein in buffer B2 is low, as it does not dissolve the disulfide network. Subjecting these aggregates to a reducing buffer showed an increase in the whey proteins  $\alpha$ -lactalbumin ( $\alpha$ -la) and  $\beta$ -lg (see Supporting Information). Therefore, it can be concluded that these disulfide-linked aggregates mainly consist of whey proteins, and no hybridization could be observed. This is contrary to what was reported for soy protein, where for 70:30 soy protein/WPI mixtures, considerable formation of disulfide-linked hybrid-aggregates was reported (Roesch & Corredig, 2005).

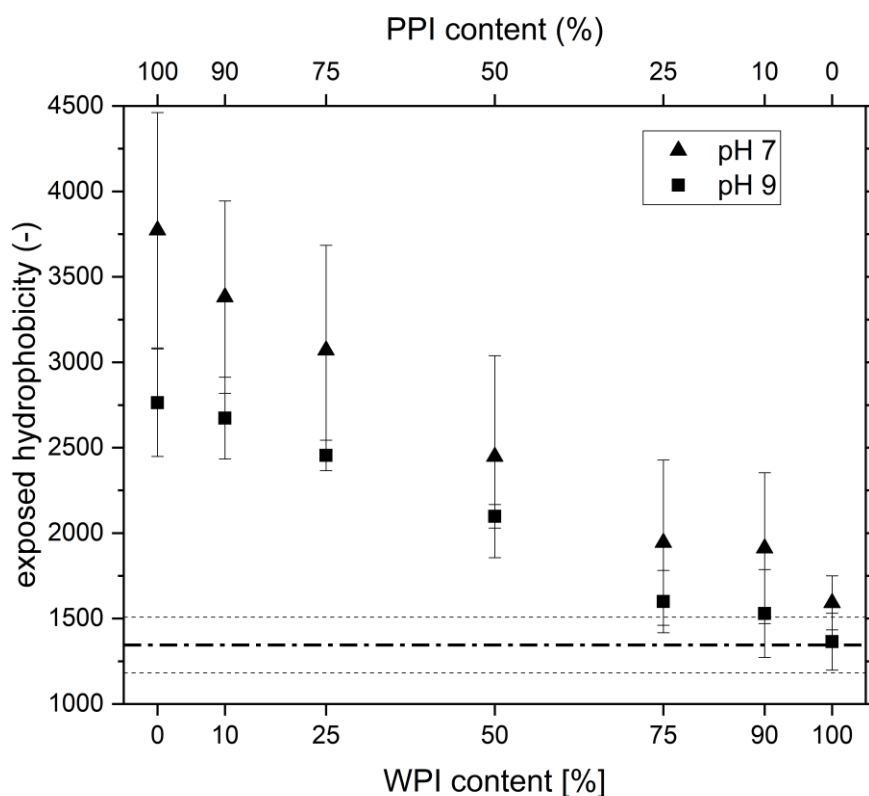


Figure 3-33 Exposed hydrophobicity of 1% PPI/WPI solutions at pH 7 and 9. Solutions at pH 5 were too turbid for measurements. Errors bars on the data points indicate the standard deviation. The mean of all unheated solutions are shown as the reference line, with the upper and lower limit being the standard deviation of all unheated solutions.

Another important factor in determining protein interactions within gels is the change in exposed hydrophobicity ( $S_0$ ) of a protein solution upon heating. Results for 1% heated and native protein solutions are depicted in Figure 3-33.

It can be seen that heating PPI solutions lead to a strong increase in  $S_0$ , which is due to the high degree of unfolding of hydrophobic amino acid side chains (Andlinger et al., 2021c). Furthermore, it can be seen that increasing the WPI content led to a notable reduction in exposed hydrophobicity. For a WPI content above 75% the differences between the heat unfolded proteins were negligible. As explained before, the unfolding of hydrophobic amino acids from the protein core is hindered by internal disulfide bonds in whey proteins.

Increasing the pH led to a reduction in  $S_0$  for all investigated solutions. This can be explained as follows. Upon unfolding, hydrophobic amino acids rearrange to form new hydrophobic clusters. These hydrophobic clusters are then stabilized via disulfide bonds, especially at alkaline pH (Betz et al., 2012). The hydrophobic patches are not accessible to the fluorescent probe and therefore exhibit lower  $S_0$  values. Although disulfide bonds play a smaller role in PPI gelation, this effect was also demonstrated recently in PPI aggregates (Andlinger et al., 2021c).

It could be shown that the formed protein interactions differed widely between protein solutions in dependence of the protein composition and pH value. How these protein interactions influence the rheological characteristics of the protein gels are detailed in the following section.

### **3.5.3.3 Rheological characteristics of heat-induced PPI/ WPI hybrid gels**

One important rheological characterization is the cold setting behavior of a protein gel. For this  $G'$  of the gel at room temperature ( $G'_{cool}$ ) is related to  $G'$  of the gel at gelation temperature ( $G'_{hot}$ ). This ratio can be used to assess the relation of different protein interactions within a gel (Creusot et al., 2011; Martin et al., 2014; Schmidt et al., 2019). In general, high values indicate the dominance of hydrogen and electrostatic interactions over hydrophobic and covalent bonds (Bowland et al., 1995). Similarly, low values indicated the dominance of hydrophobic and covalent bonds over hydrogen and electrostatic interactions.

The ratio of  $G'_{cool}/G'_{hot}$  was recently shown to indirectly characterize the microstructural changes in egg white and potato protein gels, in dependence of the pH (Andlinger et al., 2021a). It was shown that close to the isoelectric point of these proteins the  $G'_{cool}/G'_{hot}$  ratio increased. The same trend was found for the PPI/WPI hybrid gels (Figure 3-34). Gels at pH 5 had consistently higher values than gels at neutral pH. For WPI content of 75% and above, the  $G'_{25\text{ }^\circ\text{C}}/G'_{85\text{ }^\circ\text{C}}$  ratio was even higher, which is probably due to the formation of more electrostatic interactions.



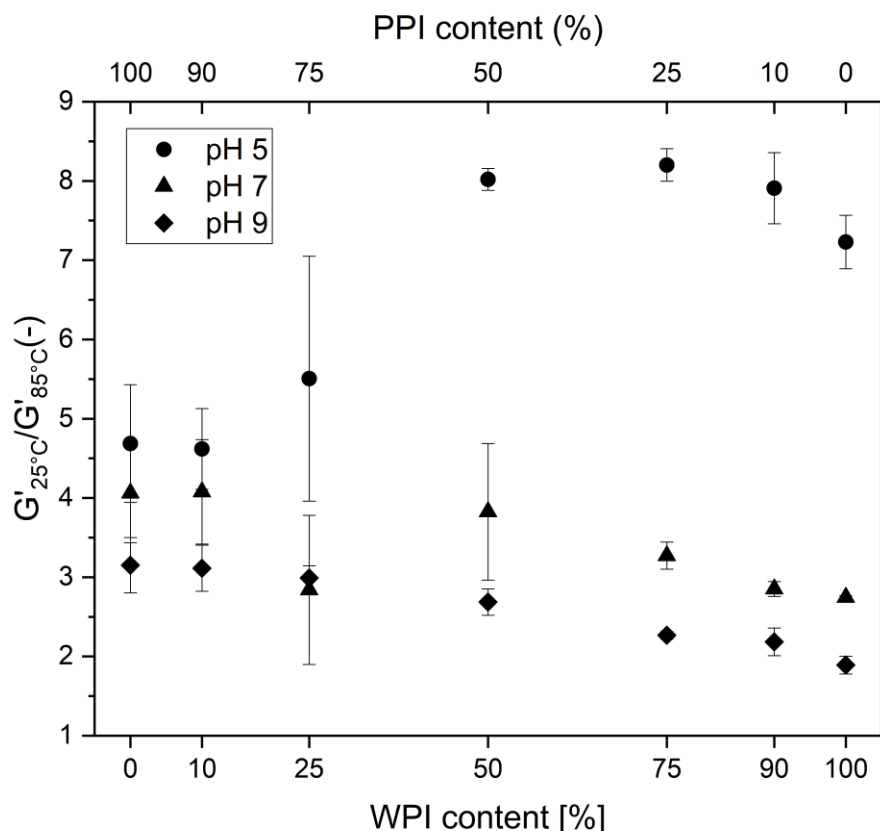


Figure 3-34  $G'$  of heat-set PPI-WPI gels at 25 °C in relation to  $G'$  at 85 °C.

At alkaline pH levels, the  $G'_{25^\circ\text{C}}/G'_{85^\circ\text{C}}$  ratio was lower throughout the mixing ratios. This is probably due to the formation of more disulfide bonds, especially for WPI dominated gels.

Two data points cannot be fully explained by this reasoning. The 50:50 mixture at pH 5 exhibited high  $G'_{25^\circ\text{C}}/G'_{85^\circ\text{C}}$  ratio, although no increase in electrostatic interactions within the gel could be detected (Figure 3-31). The second data point differing from the described trends is the 75:25 ratio of PPI/WPI at pH 7. The  $G'_{25^\circ\text{C}}/G'_{85^\circ\text{C}}$  ratio with  $\sim 3$  was lower than  $\sim 4$  found for 100:0, 10:90, and 50:50. This could be explained by different microstructures. High  $G'_{\text{cool}}/G'_{\text{hot}}$  ratios are found for particulate gels, such as WPI gels at high salt (Bowland & Foegeding, 1995) or pea protein gels. Different microstructures between particulate and fine-stranded are described for heat-set WPI gels in dependence of the salt content (Bowland et al., 1995). Although particulate gels had high  $G'_{\text{cool}}/G'_{\text{hot}}$  ratios than fine-stranded gels, the gels with a mixed microstructure had even higher ratios. Therefore, it could be possible that a mixed microstructure between fine-stranded and particulate was formed for these gels.

In order to evaluate the stability of the heat-set gels  $G'$  of the gel at ambient temperature can be used as an indication of stiffness (Figure 3-35). Increasing the pH to alkaline levels reduced  $G'$  for all mixing ratios. This was already observed for WPI (Kleemann et al., 2018) and PPI (Andlinger et al., 2021a) gels. The increased electrostatic repulsion and the development of more linear strands might be responsible for this.



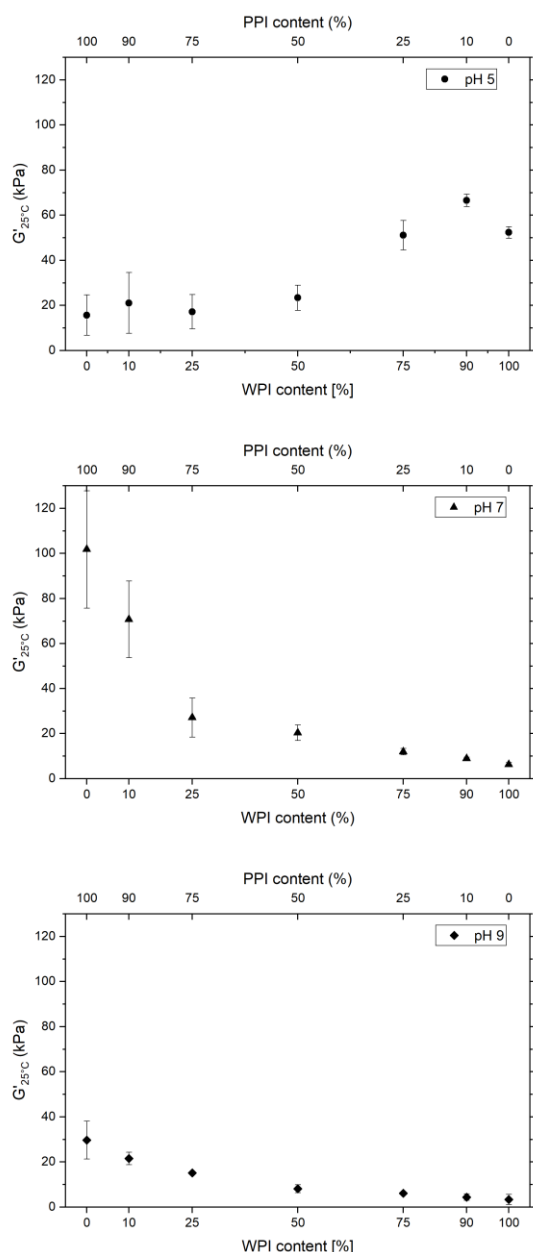


Figure 3-35  $G'$  of heat-set PPI-WPI gels after cooling down to 25 °C

to the  $G'$  of 50:50 mixtures to be nearly unaffected by the pH change, as  $G'_{25^\circ\text{C}}$  was around 20 kPa for both pH values.

We can conclude that smaller, disulfide-linked aggregates at pH 7 and 9 led to lower  $G'$  value. At pH 5 a denser and more aggregated network results in higher  $G'$  values in WPI gels. PPI deviates from this trend, with lower  $G'$  close to IEP compared to pH 7. Although this trend was also observed by others for different PPI formulations (Schmidt et al., 2019) it can not be fully explained. Patatin is known to form aggregates bigger by order of magnitude compared to whey proteins (Delahaije et al., 2015), and patatin gels are less crosslinked, compared to whey or soy proteins (Creusot et al., 2011), especially at pH 5 (Schmidt et al., 2019). The combination of very large aggregates

For WPI dominated gels, adjusting the pH to 5 led to an increase in  $G'$ . This can be explained by the low amount of disulfide bonds at this pH. At first, this is unexpected, as a lower amount of covalent bonds should lead to a less crosslinked network, which should not be able to absorb a lot of deformation energy, hence leading to a lower  $G'$ . Nevertheless, increasing  $G'$  for WPI gels close to the IEP are well documented (Homer et al., 2018; Mehalebi et al., 2008). Furthermore, one study explicitly showed that  $G'$  in WPI increased with decreasing disulfide linkage within the gel (Havea et al., 2009). One has to consider that the protein network at pH 5 is denser than at pH 7 and 9, and aggregate might have a bigger size. Both phenomena of densification and increasing aggregate size were shown to increase the storage modulus in different hydrogels, such as EtOH pretreated WPI gels (Nikolaidis & Moschakis, 2018) and soy protein gels (Wu et al., 2017). An increase in pH severely reduced  $G'_{25^\circ\text{C}}$ , which is probably due to the formation of more disulfide bonds (Kleemann et al., 2018).

Contrary to this, for PPI a higher  $G'$  was found for pH 7 compared to pH 5. The contrary behavior of WPI and PPI towards the pH changes from 7 to 5 led

with a low amount of crosslinking might explain the low amount of energy that can be stored in patatin networks at pH 5, resulting in a low  $G'$ . For example, it is possible that the gel is formed by precipitated protein aggregates which are not well interconnected.

Rheometer measurements allow investigating the gelation in situ. As the protein solutions were heated with a constant temperature ramp, we can compare the temperature and time dependent change in  $G'$  for these solutions. Gelation curves of different solutions are presented in the following (see Figure 3-36).

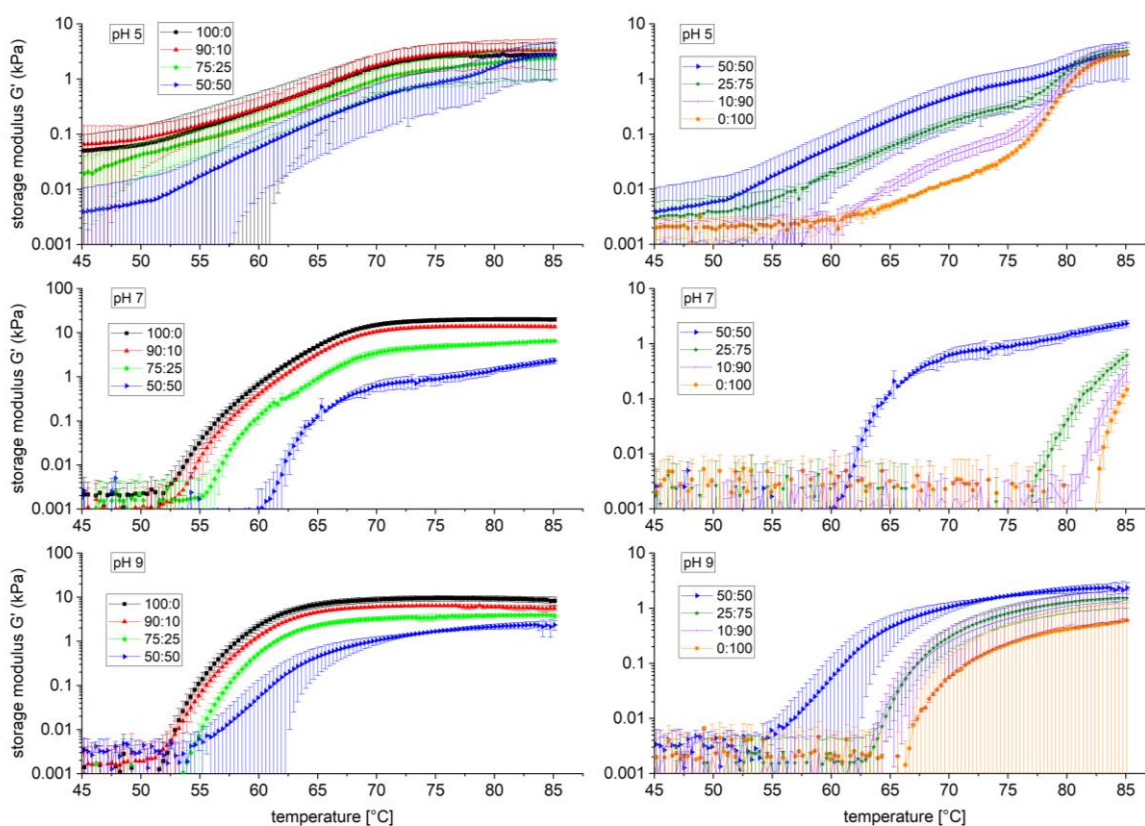


Figure 3-36 Storage modulus ( $G'$ ) of PPI/WPI hybrid gels in dependence of the heating temperature, during the temperature sweep for different pH values. PPI/WPI 50:50 mixtures are depicted in for PPI and WPI dominated mixtures for comparison

It is already known that patatin forms gels at much lower temperatures than  $\beta$ -lg (Creusot et al., 2011), which can be seen in Figure 3-36. It can be seen that the 50:50 solution had a gelation behavior similar to PPI-dominated mixtures with onsets of gelation lower than WPI-dominated mixtures. This was true for all investigated pH values.

However, there were still some notable differences for different mixing ratios. Solutions with high PPI content exhibited an exponential increase in  $G'$ , around the temperature of unfolding. After this,  $G'$  plateaued indicating a slow down in network formation speed. Solutions from 50:50 mixtures, on the other hand, showed an almost linear relationship between temperature and  $G'$ . It can be assumed that the patatin network forms first, followed by the formation of the  $\beta$ -lg network. This is especially apparent for pH 7 (right side of Figure 3-36), where  $G'$  increases again at around 80 °C. This temperature is around the denaturation temperature of  $\beta$ -lg. For the WPI dominated solutions, the gel formation starts to occur around this temperature. The same trends

could be found when investigating the loss factor, and the change in  $G''$  of these gels (see Fig 3 and 4 in Supporting information). The change in loss factor from above 1 to below 1 indicates the formation of gels, with loss factor = 1 being the point of the gelation where  $G'=G''$ , often referred as point of gelation (Estévez et al., 2016). For pH 5 the loss factor was often already below 1 even before heating which explains the very viscous behaviour of the solutions and which was already observed by others (Schmidt et al., 2019).

Interestingly, both acidification and alkalization reduced the onset of gelation for the protein solutions. This can be explained as follows: Increasing the pH leads to lower temperatures of denaturation for  $\beta$ -lg (Boye & Alli, 2000) and patatin (Andlinger et al., 2021a). As unfolding is facilitated, the gelation is occurring at lower temperatures as well. At pH values close to the IEP, proteins get more heat stable, and unfolding is reduced. However, the reduced electrostatic repulsion between proteins at this pH enables aggregation, even without extended unfolding (Homer et al., 2018).

As a final characterization of the rheological properties of the gels, the loss factor and the slope of the frequency dependence of the heat-set PPI/WPI gels shall be evaluated. The results for both values can be seen in Figure 3-37. The loss factor ( $\tan \delta$ ) describes the ratio of the loss modulus  $G''$  to the storage modulus  $G'$ . A higher value indicates a more viscous rather than elastic behavior of the sample. The slope of the frequency dependence ( $n$ ) is derived from the frequency sweep and is used to differentiate between physical-linked gels with a high frequency dependence, and cross-linked gels with a low frequency dependence (Creusot et al., 2011).

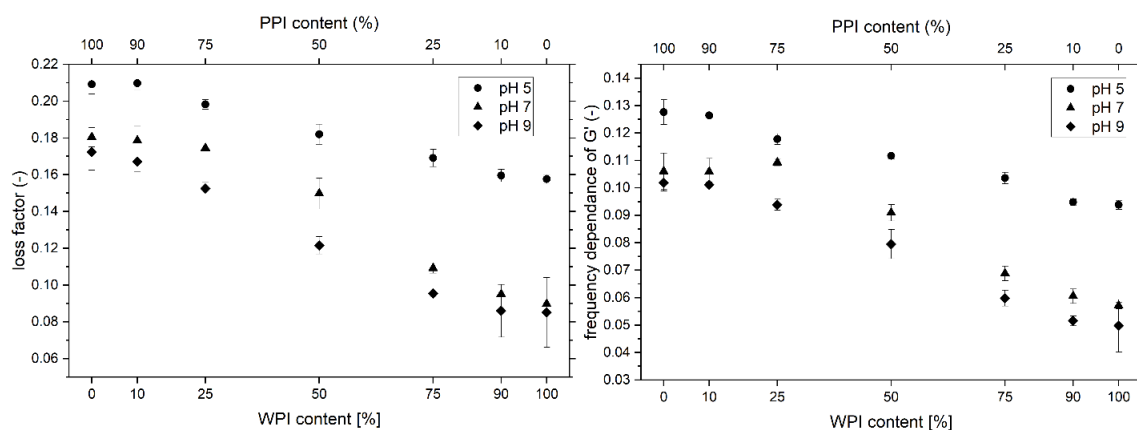


Figure 3-37 Loss factor ( $\tan \delta$ ) and frequency dependence ( $n$ ) of PPI/WPI hybrid gels after cool down to ambient temperature

$\tan \delta$  and  $n$  exhibited very similar trends and are therefore discussed together in the following. The gels created at pH 5 exhibited the highest values for  $n$  and  $\tan \delta$ . Therefore, these gels can be characterized as the least elastic and least crosslinked. Increasing the pH led to a higher amount of crosslinking, and therefore to more elastic gels for all mixing ratios. This is corresponding well with the change from particulate to fine-stranded gels, as described above.

Changes in protein composition showed that PPI gels had higher  $\tan \delta$  and  $n$  values than WPI gels. The reason why WPI exhibited lower  $\tan \delta$  and  $n$  values is probably due to the high amount of covalent crosslinks, typical for WPI gelation.

To summarize, the change in rheological properties in dependence of the mixing ratio and pH value could be well explained by changes in protein interactions. To fully characterize the gel properties of PPI/WPI hybrid gels were also evaluated at breakage after large deformation.

### 3.5.3.4 Textural properties of heat-induced PPI/WPI hybrid gels

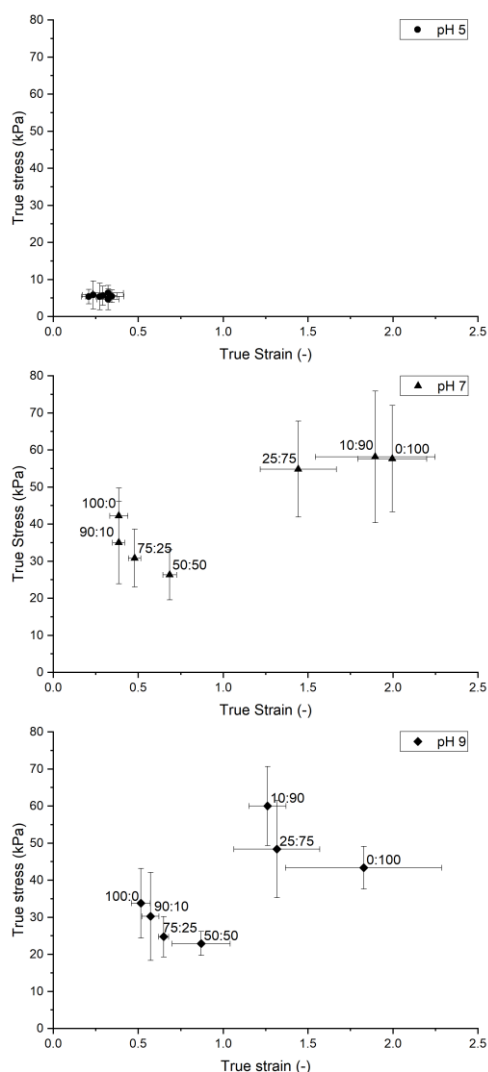


Figure 3-38 True stress and true strain of PPI/WPI hybrid gels for different pH levels. The numbers indicate the PPI/WPI mixing ratio. For pH 5 the samples were all very brittle and no differences between the samples could be observed.

Although rheological data characterizes gel structures very accurately and kinetic gelation behavior can be evaluated, there is often little correlation between rheological data and sensorial properties of food.

Therefore, heat-set hybrid gels were also evaluated with a texture analyser to complete the rheological data at small deformation with compressions test until fracture of the sample.

True stress and true strain of the heat-set gels can be seen in Figure 3-38. A strong influence of pH on the textural properties was identified. At pH 5, gels were very brittle and had low stress and strain values at breakage. Furthermore, the differences between the samples were low. This indicates that the similar optical appearance of the gel cylinders (Figure 3-30) correlated with similar textural properties. The formation of large aggregates at these pH values led to brittle structures in the gels. This correlates well with the results from loss factor and the frequency dependence (Figure 3-37). The high values for  $\tan \delta$  and  $n$  at pH 5 indicated large aggregates with lower time stability ( $n$ ) as well as weaker network bonds (loss factor) (Borderías et al., 2020). Contrary to this, at neutral and alkaline pH levels, differences between the different PPI/WPI gels were clearly distinguishable.

Gels with a high PPI content had lower stress and strain values at breakage compared to gels with a high WPI content. Increasing the WPI content increased the elasticity of the gels. However, the change did not occur in a gradual way. Up to 50:50 PPI/WPI

mixing ratio, the gels could be described as PPI dominated with similar properties, although the elasticity could be improved by increased WPI content, as measured through a higher strain value at breakage. Increasing the WPI content from 50% to 75% and higher led to a more extreme change in textural properties, with strain and stress values at breakage increasing considerably. Thus, two distinctive groups of textural properties could be observed in hydrogels in dependence of the protein interactions. All three gels with the highest strain and stress values at breakage were WPI dominated gels that exhibited a high amount of disulfide links, as shown by the protein interaction assay. Increasing the pH from 7 to 9 led, for most of the gels, to higher elasticity and lower stress values. The increase in pH leads to the formation of more disulfide bonds, which explains the increase in strain. The reduced stress values may be explained by a higher electrostatic repulsion between the amino acid side chains and the creation of more linear aggregates. Besides changes in pH, the change ionic strength of the solution is one of the most important milieu conditions influencing the structure formation of protein gels in food. The most important findings of the influence of ionic strength will be shown in the following section.

### 3.5.3.5 Influence of salt on heat-induced PPI/WPI hybrid gels

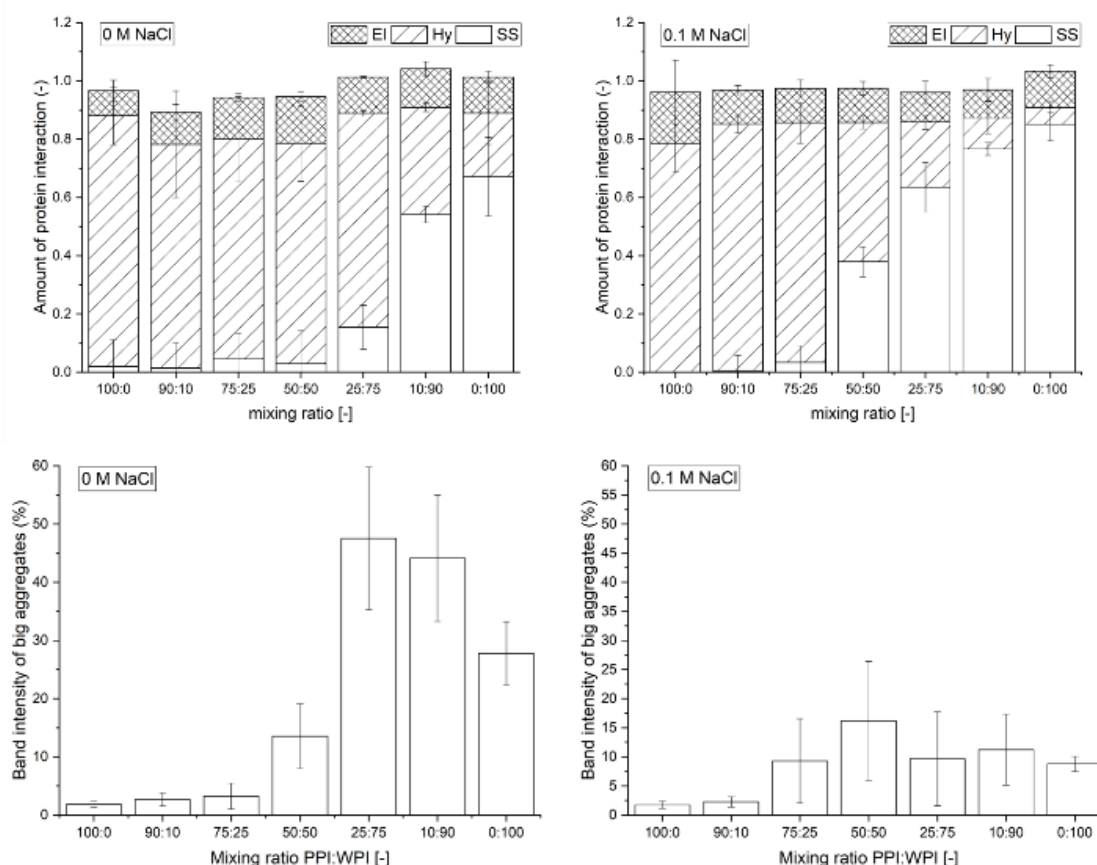


Figure 3-39 Protein interaction assay (top) and SDS-PAGE (bottom) of PPI/WPI gels with and without the addition of salt.

The influence of a higher ionic strength on the formation of protein interactions, investigated by protein interaction assay and SDS-PAGE, can be seen in Figure 3-39. The



addition of salt led to more protein being detected as disulfide-linked, and simultaneously fewer disulfide-linked aggregates were found in the B2 buffer, observed by SDS-PAGE. This indicates that the disulfide bonds stabilized larger aggregates. Increased ionic strength was shown to increase aggregate size in different food proteins, through the screening of electric charges (Delahaije et al., 2015). The ions of the salts interact with charged sites of proteins leading to an overall lower net charge and/or charge density on the protein particle. This leads to lower electrostatic repulsion between the proteins and thus allows aggregates to grow in size, similar to what is observed for protein aggregation close to the IEP (Nicolai et al., 2011). This leads to the formation of large aggregates, explaining the opaque appearance of the gels (see Figure 3-30). Such gels can be characterized as particulate gels.

It can be seen in Figure 3-40, how this restructuring of disulfide bonds within the aggregates influences the rheological properties. It is evident that the influence of salt addition has a more pronounced effect on the WPI-dominated gels compared to the PPI-dominated gels. The addition of salt led to  $G'$  values for the WPI gels that were very similar to the PPI gels. Regarding the loss factor, an increase could be measured for all gels upon salt addition. This indicates the formation larger aggregates with weaker network bonds, as described before.

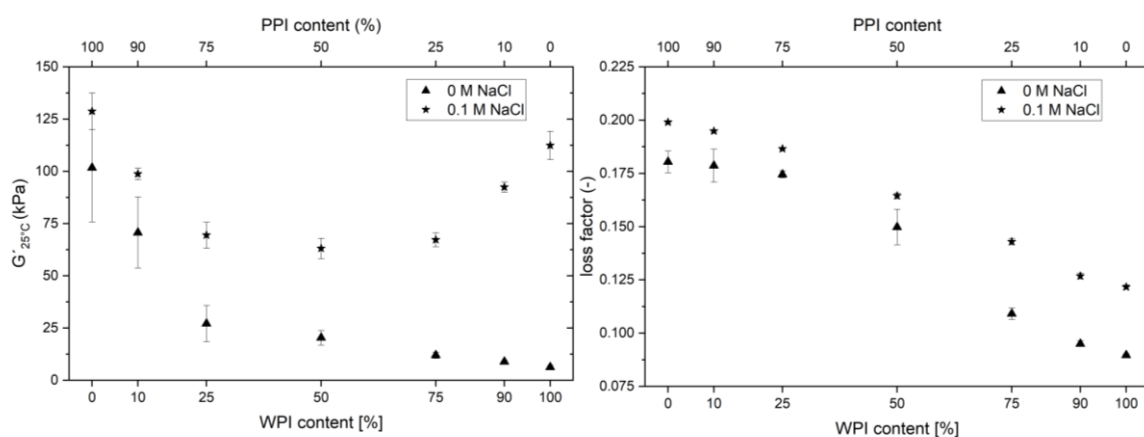


Figure 3-40 Influence of salt addition on  $G'$  of the heat-set gels at ambient temperature.

The higher  $G'$  value indicates the formation of stiffer gels, especially as the trend of the loss factor did not change upon salt addition. The formation of stiffer gels with higher  $G'$  is typical for particulate gels (Homer et al., 2018). Patatin forms bigger/denser aggregates compared to  $\beta$ -lg, even without the addition of salt (Delahaije et al., 2015). As the protein interaction assay indicated, there was no noticeable change in protein interactions between and within the aggregates.

This change in structure is even more apparent when investigating the textural properties at large deformation, as seen in Figure 3-41. The addition of salt has nearly no effect on the textural properties at breakage of pure PPI gels. However, increasing WPI content led to a more pronounced shift to gels with lower strains but higher stress at breakage. This change in stress and strain was already described for WPI gels that changed from fine-stranded to particulate (Homer et al., 2018).

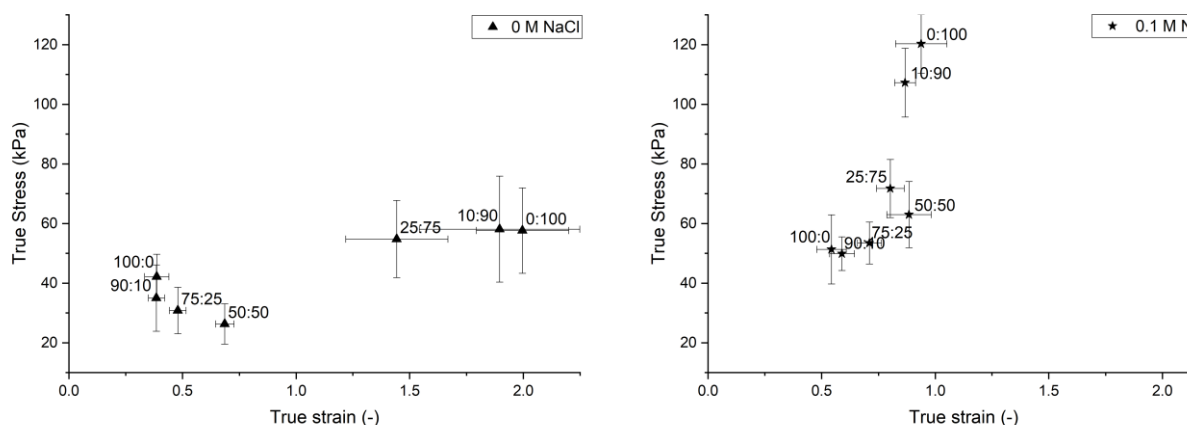


Figure 3-41 Influence of the addition of salt on the textural properties of PPI/WPI hybrid gels at pH 7.

Therefore, the rearrangement of the proteins within the aggregates had a major influence on macroscopic properties. The decreased strain values indicate that disulfide bonds were not involved in connecting large parts of the gels.

### 3.5.4 Conclusion: Relationship between gelation mechanism and textural properties in PPI/WPI hybrid gels

We investigated how protein interactions, rheological properties at low deformation without breakage, and textural properties at breakage of PPI/WPI hybrid gels can be influenced by changes in pH and salt milieu. Possible gelation mechanisms and common correlations between molecular protein features and textural/rheological gel properties shall be proposed in the following.

PPI/WPI hybrid gels from 15% (w/w) protein solutions exhibited a split in two distinct groups for most of the measured attributes. PPI-dominated gels were less disulfide-linked and more brittle than WPI dominated gels. At mixtures of 50:50 PPI properties dominated the different properties. This is probably due to the fact that at ~ 7.5% (w/w) the commercial isolates used in this study had different minimal gelling concentration under the investigated conditions. The PPI was able to form gels, whereas the WPI was not (Andlinger et al., 2021a). This is probably due to patatin being able to form gels at lower concentrations than  $\beta$ -lg (Creusot et al., 2011). Therefore, it can be assumed that the main backbone of the gel is formed by patatin. Nevertheless, the WPI "filling" of this gel leads to improvements in deformability. This is different from what was reported for rapeseed protein which only modified WPI gels under conditions where it also formed gels on its own (Ainis et al., 2018).

The influence of pH can be summarized as follows: pH close to the IEP leads to big aggregates with nearly no disulfide linkage. This resulted in brittle, weak, and opaque gels with nearly no difference between the protein types, indicating the formation of big particulate aggregates. At neutral and alkaline pH, strong, elastic, and transparent gels could be obtained, indicating the formation of finely stranded aggregates. Nevertheless, there were clear differences between PPI and WPI dominated gels.

WPI dominated gels exhibited considerably higher stress and strain values due to a high amount of disulfide bonds. Important to note that PPI gels at neutral and alkaline

pH levels exhibited higher stress and strain values compared to IEP, although the dominating protein interaction is hydrophobic at all pH values. As these gels were quite transparent, the formation of fine-stranded aggregates can be assumed.

The influence of primary aggregate structure is further evident when considering the influence of salt. Here, we could show that the addition of salt led to opaque gels with less elasticity. Nevertheless, it was shown that for WPI, disulfide bonds are formed in high amounts. However, these bonds are formed within big primary aggregates and do not span across the whole gel. This led to harder but less elastic gels.

Understanding these mechanisms will help to design protein gels with tailor-made properties for food and life science applications.

### **Author Contributions**

David J. Andlinger: Investigation, Conceptualization, Writing - Original Draft; Project Administration, validation, methodology, data curation

Lena Rampp: Investigation, validation, formal analysis

Caren Tanger: Writing - Review & Editing, methodology; validation, conceptualization

Ulrich Kulozik: Writing - Review & Editing; Funding acquisition; Supervision

### **Funding Sources**

This IGF Project AiF 19712 of the FEI was supported via AiF within the program for promoting the Industrial Collective Research (IGF) of the German Ministry of Economic Affairs and Energy (BMWi), based on a resolution of the German Parliament.

### **ACKNOWLEDGEMENT**

We would like to thank Marc Laus from AVEBE, Veendam, The Netherlands, for providing the potato protein isolate.



### **3.6 Hydro- and aerogels from ethanolic potato and whey protein solutions: Influence of temperature and ethanol concentration on viscoelastic properties, protein interactions, and microstructure**

#### Summary and contribution of the doctoral candidate

In the previous chapters, it could be shown that WPI and PPI do react differently towards milieu changes. Furthermore, we demonstrated that aerogel creation allows investigating the microstructure of gels. In order to produce aerogels hydrogels first have to be washed with ethanol (EtOH) to induce a solvent exchange from water to EtOH, within the gel pores. This chapter investigated how the utilization of EtOH before the solvent exchange might be beneficial for the aerogel process. Therefore, the gelation properties of WPI and PPI solutions in the presence of EtOH were investigated. This way it was investigated if gelation of protein solutions could be enhanced to make the gelation process more efficient. Furthermore, the applicability of EtOH as a structuring agent to induce novel structures in food proteins was assessed.

In general, the addition of EtOH facilitated the gelation of proteins by heat, mainly by lowering the temperature necessary for unfolding. Investigations into protein interactions showed that higher EtOH concentration changed the protein interactions for WPI from disulfide-linked to electrostatic interactions, similar to what was shown for the hybrid gels in the previous chapter under pH conditions close to the isoelectric point. PPI gels remained dominated by hydrophobic interactions. However, the rheological characterization of the cold setting behavior ( $G'_{cool}/G'_{hot}$ ) indicated that the hydrophobic interactions were enhanced with increasing EtOH content. The obtained aerogels had high inner surface areas and thus could be used for different applications in the future.

The doctoral candidate was responsible for the development of the methods used for this study. Furthermore, the influence of EtOH had to be tested by a wide array of preliminary tests before the final experimental setup, used in this study, could be developed. The findings on protein interactions, rheology as well as aerogel microstructure were interpreted by the candidate after broad literature research. Other contributions included conceptualization of the experiments, writing of the original draft, responding to reviewer comments as well as data curation and statistical analysis.

Adapted original manuscript<sup>6</sup>

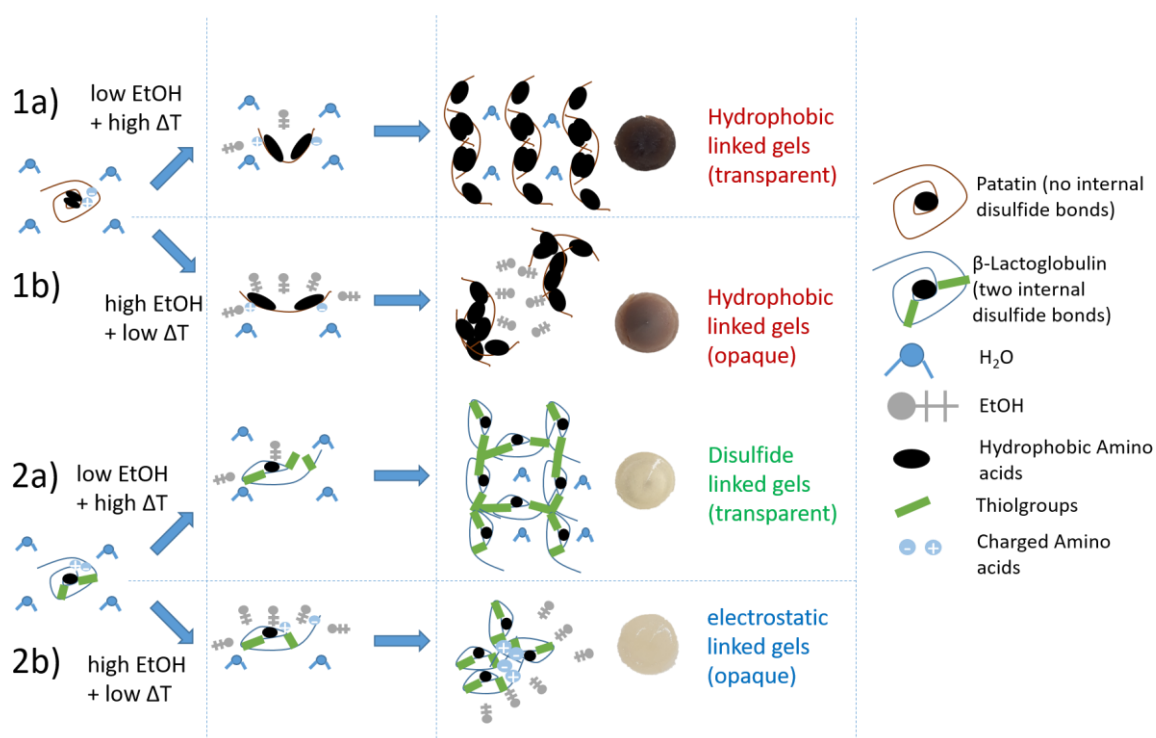
## Hydro- and aerogels from ethanolic potato and whey protein solutions: Influence of temperature and ethanol concentration on viscoelastic properties, protein interactions and microstructure

David J. Andlinger<sup>\*a</sup>, Lisa Schlemmer<sup>a</sup>, Isabella Jung<sup>b</sup>, Baldur Schröter<sup>b</sup>, Irina Smirnova<sup>b</sup>, Ulrich Kulozik<sup>a</sup>,

<sup>a</sup> Chair of Food and Bioprocess Engineering, TUM School of Life Sciences, Technical University of Munich, Weihenstephaner Berg 1, 85354, Freising, Germany

<sup>b</sup> Institute of Thermal Separation Processes, Hamburg University of Technology, Eißendorfer Straße 38, 21073, Hamburg, Germany

### Graphical Abstract



<sup>6</sup> (Adaptions refer to formatting issues: e.g., numbering of sections, figures, tables and equations, abbreviations, axis labeling, figure captions and style of citation). Reference lists of all publication based chapters were merged at the end of this thesis to avoid duplications.

Original publication: Andlinger, D. J., Schlemmer, L., Jung, I., Schröter, B., Smirnova, I., & Kulozik, U. (2021). Hydro- and aerogels from ethanolic potato and whey protein solutions: Influence of temperature and ethanol concentration on viscoelastic properties, protein interactions, and microstructure. *Food Hydrocolloids*, 125, 107424. <https://doi.org/10.1016/j.foodhyd.2021.107424>

Permission for the reuse of the article is granted by Elsevier Limited.

## Abstract

Denaturation, aggregation, and gelation of protein solutions can be induced through increased temperatures and the presence of organic solvents. Depending on the molecular features of the involved proteins, the denaturation conditions lead to very different gel properties. However, it is poorly understood how organic solvents in combination with heat treatments can be used to modify the textural properties of protein gels. In this study the combined effects of heat and ethanol (EtOH) treatment on hydrogel formation by whey (WPI) and potato protein isolates (PPI) were investigated. The different protein hydrogels were subjected to a complete solvent exchange with EtOH and dried with supercritical CO<sub>2</sub> to obtain aerogels with a high inner surface area. Increasing EtOH concentration during thermally induced hydrogel formation reduced the temperature of unfolding up to a point where denaturation occurred at room temperature. WPI and PPI formed very different gels in the presence of EtOH. WPI gels with an EtOH content below 10% (w/w) were elastic and mainly linked through disulfide bonds. Higher EtOH content led to weak gels, mainly linked through electrostatic and hydrogen bonds. For PPI gels, increasing EtOH content did not influence the protein interactions within the gels, and textural properties were very similar. The textural properties of the resulting aerogels were dependent on the type of protein interactions created in the hydrogels. This work provides insights into the way food proteins form gel networks and how these interactions can be manipulated to produce gels with tailor-made properties.

### 3.6.1 Introduction

Aqueous protein solutions can form stable hydrogels when environmental conditions induce denaturation of the proteins. Denaturation occurs when the native protein structure unfolds,

and amino acids from the hydrophobic core are exposed to the solvent phase (Tanford, 1968). These unfolded proteins then tend to aggregate. Depending on the protein system, crosslinking of the aggregates through thiol-disulfide exchanges can also occur (Roefs & Kruif, 1994). During this process, a free thiol group, usually from a cysteine side chain in protein 1, breaks a disulfide bond in another protein molecule (protein 2). One thiol group from the disulfide bond in protein 2 can then react with the thiol group from protein 1 linking the proteins together. The second free thiol group from protein 2 then can perform another thiol-disulfide exchange and continue the polymerization reaction. Alternatively, it can react with another free thiol group, without breaking disulfide bonds, thus terminating the polymerization. This sort of reaction is well documented for whey proteins (Schokker et al., 2000; Monahan et al., 1995). Conditions leading to denaturation include elevated temperatures and organic solvents, among others (Nikolaidis et al., 2017). Although gelation can occur in nearly all protein systems, the conditions of gelation can differ greatly, depending on the molecular structure of the protein and milieu conditions.

Understanding how gelation can be influenced is a prerequisite for a wide variety of fields in the life sciences. The application of hydrogels ranges from the construction of

tissue engineering scaffolds (Venkatesan et al., 2015) to the creation of fat replacers for food applications (Wolz & Kulozik, 2017). Especially for the food industry, protein gels are one of the most important textural agents.

The influence of elevated temperatures on the gelation behavior of different food proteins has already been broadly investigated (Martin et al., 2014; Clark et al., 2001). However, gelation of proteins can also occur through the addition of organic solvents. For example, addition of ethanol (EtOH) was shown to induce gelation in  $\beta$ -lactoglobulin ( $\beta$ -lg) (Renard et al., 1999). The denaturing effect of EtOH on whey protein isolate (WPI) was shown to be stronger than heating under certain conditions (Nikolaidis et al., 2017). Furthermore, acid induced gels could be obtained without heating through the additional use of EtOH on WPI (Wagner et al., 2020a).

EtOH has numerous effects on proteins that are often only described for diluted protein systems. EtOH influences the secondary structure of proteins by refolding of  $\beta$ -strands into  $\alpha$ -helices. This leads to the exposure of hydrophobic side chains and subsequently to aggregation of the proteins (Yoshida et al., 2010). Furthermore, the dielectric properties of the solutions are changed in dependence of the EtOH content which will also influence electrostatic repulsion between the protein molecules (Uversky et al., 1997).

These aggregates are then linked forming gels, usually accompanied by the formation of  $\beta$ -sheets. However, solvent and protein concentrations have a strong influence on the gel structure and interactions (Yoshida et al., 2014). How EtOH can be used as a textural agent for concentrated protein systems with its effect on rheology and microstructure has not been investigated so far, to the best of our knowledge.

Furthermore, investigations of the effect of EtOH on food proteins are mostly performed with WPI as the model substances. However, molecular properties and structures of other proteins and the impact on aggregation and gelation behavior can differ greatly between the sources (Delahaije et al., 2015; Creusot et al., 2011). Therefore, with the advent of many new proteins, especially from plant sources, established state of knowledge regarding mechanisms and kinetics of gelation of animal-derived proteins from egg or milk is required to be revisited and extended. This will help to use plant based proteins as viable replacements for animal derived proteins. Furthermore, these protein sources can be used in its own right with novel functionalities. Therby, extending the tool box for food products structural design. This way a more sustainable diet with a higher variety of protein sources can possibly achieved in the future.

Patatin from the potato tuber is one such protein that is able to form gels comparable to  $\beta$ -lactoglobulin ( $\beta$ -lg), the major whey protein, and ovalbumin, an important egg protein (Creusot et al., 2011). The gelation of patatin through heat (Schmidt et al., 2019) and high pressure (Katzav et al., 2020) were recently investigated in detail. It could be shown that patatin forms gels at lower temperatures and protein concentrations compared to  $\beta$ -lg. Furthermore, these gels were less elastic indicating a lack of covalent bonds within the gel. This gelation behavior was explained by patatin's molecular features: Unfolding is facilitated by the lack of internal disulfide bonds, leading to unfolding at lower temperatures and the dominance of hydrophobic interactions of amino acid

from the protein core. However, no gelation mechanism in the presence of EtOH is described. As the gelation mechanism of patatin is driven by hydrophobic interactions instead of disulfide bond formation as in WPI, the influence of EtOH on the gel properties should be different for both protein systems.

One interesting, novel application of food protein gels is the creation of aerogels. For the creation of these structures, hydrogels are subjected to a solvent exchange with EtOH, followed by a drying step with supercritical carbon dioxide (scCO<sub>2</sub>). As EtOH is miscible with scCO<sub>2</sub>, no phase boundaries occur and the solvent is extracted without any collapse of the gel structure. Through this method, highly porous aerogels were created from egg, whey and casein proteins (Kleemann et al., 2018) as well as potato proteins gels (Andlinger et al., 2021a). Protein aerogels were already successfully used as an encapsulation and controlled release system for fish oil (Selmer et al., 2019; Kleemann et al., 2020a) Furthermore, WPI aerogels were shown to induce oleogelation when dispersed in sunflower oil (Plazzotta et al., 2020).

Aim of this work is to increase the understanding of effects of EtOH addition on gelation and microstructure of food protein gels. For this, two protein isolates from whey (WPI) and potato protein (PPI) were selected. Concentrated protein solutions were mixed with EtOH/water mixtures with different content of EtOH. The influence of EtOH on protein gelation was then investigated by DSC, rheometry, and protein-protein interaction assay. Hydrogels were created in the form of macro-capsules, which were subjected to solvent exchange by EtOH. The textural properties of these hydro- and alcogel capsules before and after the solvent exchange were assessed. Aerogels produced from the alcogels were obtained after scCO<sub>2</sub> extraction of ethanol. These were characterized by skeletal density and specific surface area to describe the microstructure of the gel network. The new knowledge gained will help to create novel protein structures in hydro-, alco- and aerogel form in different sectors of food and biotechnology.

### 3.6.2 Materials and Methods

#### 3.6.2.1 Preparation of protein mixtures with variable EtOH content

Commercial PPI powder (Solanic 200™) with a high content of patatin was obtained from AVEBE (Veendam, The Netherlands). The protein powder had a protein content of 88.6% (w/w). Commercial WPI (BiPRO™) powder was obtained from Agropur Dairy Cooperative (Saint-Hubert, Longueuil, Canada). The protein powder had a protein content of 90.9 % (w/w). The protein content was determined using the method of Dumas with an accuracy of ± 0.1% (w/w) (Vario MAX CUBE, Elementar Analysensysteme GmbH, Hanau, Germany). The powder was solubilized in deionized water and stirred overnight at 4° C.

To achieve final protein concentrations of 5, 7.5 and 10% for PPI and 15 and 17.5% for WPI following procedure was performed.

First, a protein concentration with double the concentration of the final value were created (between 10 and 35%). Afterwards, the solution was centrifuged at 6000g for 15 min to eliminate insoluble components (around 5% of protein content in PPI, below 1%

in WPI). These protein solutions were adjusted to a pH of 7 by using NaOH and HCl with a molarity of 0.1 or 1 M.

In a second step, water-EtOH solutions were prepared containing 0-50% (w/w) EtOH. The protein solutions were then mixed with EtOH-water mixtures in proportion of 1:1. The EtOH-water solution was added slowly to the protein solution under constant stirring. Depending on the EtOH content, protein-EtOH-water mixtures with final concentration of EtOH between 0 and 25% (w/w) could be produced. Afterwards, the EtOH-water-protein mixture was used for subsequent gelation experiments.

All protein and EtOH concentrations given in this study are referring to the final concentration of protein and EtOH in the EtOH-water-protein mixture.

In supporting Fig.1, all investigated protein-EtOH combinations are depicted and it can be seen, which combinations led to controlled gelation, spontaneous gelation or no gelation at all.

### **3.6.2.2 Modulated differential scanning calorimetry (mDSC)**

The denaturation temperatures of the EtOH-water-protein mixture were measured by using  $T_{\text{zero}}$ -calibrated modulated differential scanning calorimetry (mDSC Q1000, TA Instruments, New Castle, United Kingdom). From each mixture, 20  $\mu\text{L}$  was filled into a hermetically sealed aluminum pan. As a reference, an empty aluminum pan was used. The temperature was gradually heated from 25 to 90 °C with a heating rate of 2 K/min. Peak denaturation temperature ( $T_d$ ), as well as enthalpy of unfolding ( $\Delta H$ ), was determined.

### **3.6.2.3 Rheological characterization of the hydrogels**

Viscoelastic properties of protein mixtures were monitored by using small-amplitude oscillatory measurements on a Paar Physica MCR 302 (Anton Paar, Graz, Austria) stress-controlled rheometer, using a concentric cylinder geometry (inner and outer cylinder diameter 26.65 mm and 28.90 mm, respectively). The rheometer cup was filled with 19.1 mL of the sample. The mixture was covered with silicone oil (Polydimethylsiloxane, 20 cSt) to prevent evaporation during measurement. The samples were heated and cooled using a Peltier element. The frequency was set at 10 rad/s, and deformation was at 0.05% during the oscillatory experiments.  $G'$  and  $G''$  were recorded throughout the experiment

After a 10 min equilibration phase, the sample was heated rapidly to 10 °C above  $T_d$ , determined by mDSC. By heating 10 °C above  $T_d$ , similar kinetics of unfolding, aggregation and gelation are expected for the samples. This allows for a better comparability between the protein systems, as already proposed by other research groups (Creusot et al., 2011; Delahaije et al., 2015). Furthermore, by applying this heating regime instead of a fixed temperature, one can prevent EtOH evaporation, which would occur at temperatures at 70°C and above.

Then the temperature was held for 30 min. The  $G'$  value after 30 min holding time at this elevated temperature is defined as  $G'_{\text{hot}}$ . After the heating step, the gelled sample

was cooled down to 20 °C and kept at this temperature for 30 min. The  $G'$  value after 30 min holding time at this ambient temperature is defined as  $G'_{cool}$ .

### 3.6.2.4 Hydrogel capsule preparation

The hydrogel capsules were prepared as a precursor for aerogel particle generation, as described for other protein hydrogels (Andlinger et al., 2021a). From the protein mixture 65.5  $\mu$ L was pipetted into each cavity of an oil-covered form made of PTFE. The cavity was a semi-sphere with a diameter of 5 mm. Due to the surface tension, a spherical droplet formed spontaneously from the protein mixture. In total, 48 cavities could be filled in parallel with the protein mixture. The PTFE-form was then immersed into a double-walled beaker filled with commercial sunflower oil. The temperature of the oil bath was set 10 °C above  $T_d$ , determined by mDSC. After heating for 30 min under stirring, the PTFE-form with the formed hydrogel beads was put into sunflower oil at room temperature to allow the gels to cool. Afterwards, the gels were carefully removed from the form. The gel beads were kept immersed in oil until further measurements to prevent dehydration.

### 3.6.2.5 Protein interaction assay

Protein hydrogels were dissolved in different buffer systems to investigate the dominant protein interaction forces stabilizing the gels. A detailed description of method development and validation is given elsewhere (Tanger et al., 2021a). Each hydrogel was gently homogenized by pressing the gel through a garlic press, and the nitrogen content was assessed by the method by Dumas. For each hydrogel 3 times, 0.5 g of this hydrogel was weighed into a falcon tube, and 20 g of a buffer was added to each gel. The buffers used are given in Table 3-7. The buffer cleaves either electrostatic and hydrogen bonds (ES), hydrophobic interactions (Hy), or disulfide bonds (SS). The tubes were shaken at room temperature overnight.

Table 3-7 Composition of the three different buffers used for the protein interaction assay

Buffer system	NaH <sub>2</sub> PO <sub>4</sub> / Na <sub>2</sub> HPO <sub>4</sub> [mol/L]	SDS [g/L]	DTT [g/L]	pH	Dissolved protein interaction
B1	0.05	-	-	7.5	ES
B2	0.05	2	-	7.5	ES,Hy
B3	0.05	2	15	7.5	ES,Hy,SS

Afterwards, the solutions were centrifuged at 10,000 g for 20 min. The supernatant was analyzed for total nitrogen content by the method of Dumas. To calculate the relative contribution of each protein-protein interaction, the concentration of protein bonds that are cleaved by the different buffer systems ( $C_{n,bond,Bx}$ ) has to be calculated by Eq. (3-20):

$$C_{n,bond,Bx} = \frac{(m_s + m_{gel})}{m_{gel}} * C_{n,sup,Bx} \quad (3-20)$$

With  $m_s$  being the initial mass of the buffer (20 g),  $m_{gel}$  being the mass of the gel (0.5 g) and  $C_{n,sup,Bx}$  being nitrogen in the supernatant in % dissolved by buffer Bx.

From knowing which buffer dissolves which protein interaction (see Table 3-7), we can deduce the following equations to calculate the amount of protein bound by the different protein interactions (P(X)).

$$P(ES) = \frac{C_{n,bond,B1}}{C_{n,gel}} \quad (3-21)$$

$$P(Hy) = \frac{C_{n,bond,B2}}{C_{n,gel}} - \frac{C_{n,bond,B1}}{C_{n,gel}} \quad (3-22)$$

$$P(SS) = \frac{C_{n,bond,B3}}{C_{n,gel}} - \frac{C_{n,bond,B2}}{C_{n,gel}} \quad (3-23)$$

### 3.6.2.6 Solvent exchange to obtain alcogels

To induce the solvent exchange from water to EtOH within the gel network, the gel beads were first rinsed in ethanol to eliminate excess oil. Afterwards, around 40 beads were transferred into a falcon tube filled with 50 mL of 99.8% denatured ethanol. The tubes were shaken in an overhead tumbler overnight. From five of the obtained alcogels as well as of five hydrogel beads, the breakage force was measured in a texture analyzer. The remaining beads were dried as described below.

### 3.6.2.7 Textural characterization of alcogels

Before the compression test, the samples were equilibrated at room temperature, surface ethanol was gently removed. One bead at a time was compressed in a texture analyzer (TA.XT plus, Stable Micro Systems, Godalming, UK) to 60% of their initial height with an acrylic glass piston (d = 12 mm). The piston speed was set to 0.1 mm/s. The point at which the sample fractured was taken from the compression curve and recorded as the breakage force. For the hydrogels, a measurement cell with a maximum load of 500 g, and for the alcogels, a cell with a maximum load of 50 kg was used.

### 3.6.2.8 Supercritical drying

The supercritical drying was done as described elsewhere (Selmer et al., 2015). The most important steps are as follows. The supercritical drying was conducted at 11 - 12 MPa and 40 - 60 °C in a 250 mL high-pressure autoclave for three hours using a continuous supercritical CO<sub>2</sub> flow. First, the autoclave was preheated by a thin electrical band heater. The alcogels were packed in filter paper, placed into the autoclave, and soaked in ethanol to prevent shrinkage due to evaporation of ethanol from the alcogel before exposure to supercritical CO<sub>2</sub>. The system was pressurized to 11.0 – 12.0 MPa with CO<sub>2</sub> by a Maximator pump (Model G35D). The outlet valve was adjusted to a flow of CO<sub>2</sub> of 2 – 4 L/min, and the continuous CO<sub>2</sub> flow was provided for 3 h. Finally, the pressure was released slowly within 40–60 min at constant temperature (40 - 60 °C) until atmospheric pressure was reached.



### **3.6.2.9 Aerogel characterization**

Low-temperature N<sub>2</sub> adsorption-desorption analysis was used to investigate the physical properties of the aerogels (Nova 3000e Surface Area Analyzer, Quantachrome Instruments, Boynton Beach, USA). The specific surface area was determined using the BET (Brunauer–Emmet–Teller) method. The pore volume and mean pore diameter were estimated by the BJH (Barrett–Joyner–Halendia) method. All samples were degassed under vacuum at 40 °C for 20 h prior to analysis.

Breaking and compression tests were done to analyze the mechanical stability (Texture Analyzer TA.XT plus, Stable Micro Systems, Godalming, UK). The spherical samples were compressed uniaxially to 8% strain or rather to the first fracture of the structure (0.01 mm/s test speed). In order to analyze the dry aerogel structure, the samples were dried for another 10 h under vacuum at 50 °C and then stored in an desiccator with silica gel particles prior to analysis. The mechanical tests were done inside a tempered room (T = 20 °C). Each sample was measured after it was taken out of the desiccator.

The skeletal density of the aerogel network was measured according to the Archimedes principle through helium pycnometry with a multivolume pycnometer 1305 (Micro-metrics, Norcross, USA).

### **3.6.2.10 Gel nomenclature**

Following descriptions are used for the different gel states throughout the manuscript.

Hydrogels: All gels created from water-EtOH-protein mixture, also including the ones with 0% EtOH

Alcogels: All gels obtained after complete solvent exchange of hydrogels to EtOH

Aerogels: All gels obtained after supercritical drying of alcogels

### **3.6.2.11 Statistical methods**

All experiments were done in duplicate from two independently prepared solutions. If not described otherwise, the depicted data points describe the average between two measurements and error bars the upper and lower measurements. For the texture analyzer measurements characterization of the alcogel and hydrogels, at least five gels spheres were used per mixture.

## **3.6.3 Results and discussion**

### **3.6.3.1 Thermal properties of ethanolic protein mixtures measured by DSC**

Differences in thermal stability of WPI and PPI, measured by the peak denaturation temperature ( $T_d$ ), can be seen in Figure 3-42 A. Without the addition of EtOH, WPI exhibited a  $T_d$  of around 70 °C, which is higher than the  $T_d$  of PPI of around 60 °C. This can be explained by comparing the  $T_d$  of  $\beta$ -lg and patatin, their respective main proteins. For pure  $\beta$ -lg,  $T_d$  between 75 and 80 °C are reported (Tolkach & Kulozik, 2007; Creusot et al., 2011; Delahaije et al., 2015). However, the investigated WPI does contain not only  $\beta$ -lg but also  $\alpha$ -lactalbumin ( $\alpha$ -la) for which a  $T_d$  of around 60 °C was reported (Relkin et al., 1992). As both peaks could not be resolved, the combined peak

area of  $\beta$ -lg and  $\alpha$ -la was measured at around 70 °C. For patatin,  $T_d$  values of around 60 °C were reported (Creusot et al., 2011; Delahaije et al., 2015; Schmidt et al., 2019).

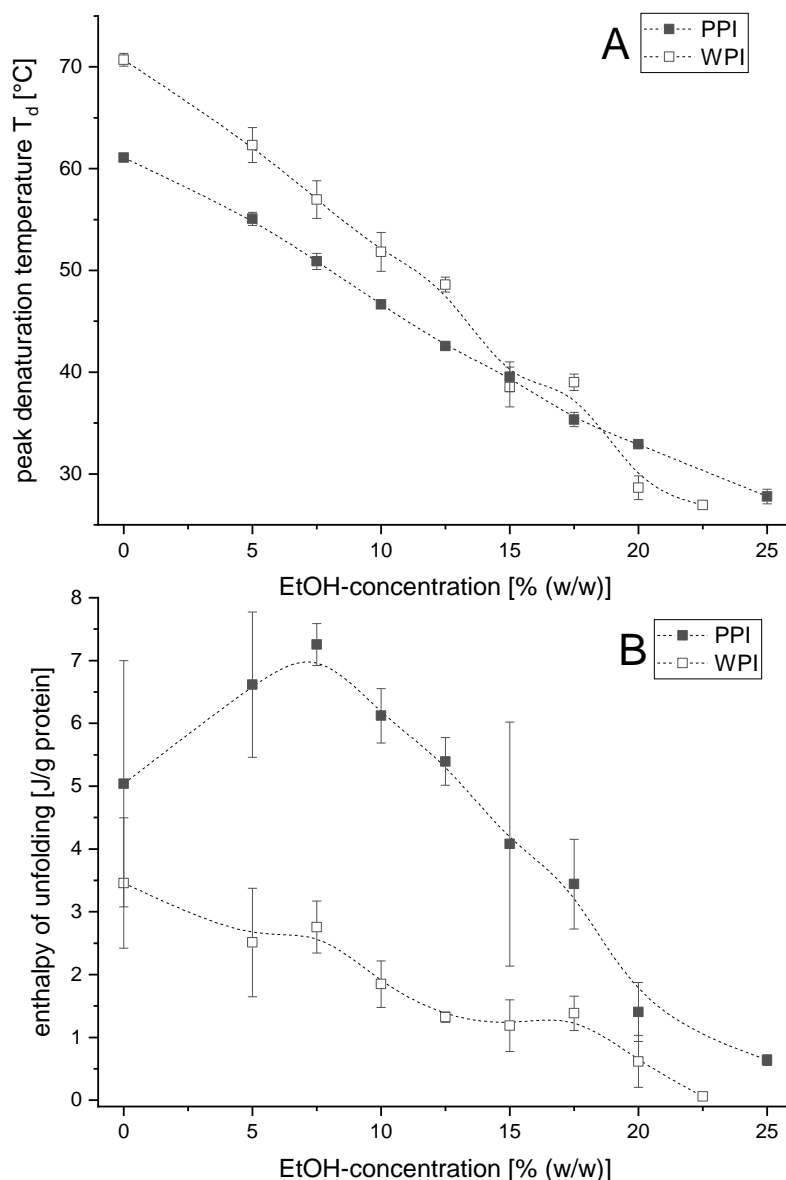


Figure 3-42 (A) Denaturation temperatures of WPI and PPI in dependence of the EtOH-concentration. (B) Enthalpy of unfolding of ethanolic WPI and PPI solutions, in dependence of the EtOH-concentration. The  $T_d$  and enthalpy values are the average of two protein concentrations per protein type (7.5 and 10% PPI and 15 and 17.5% WPI). Each concentration was measured in duplicate.

Both protein systems exhibited a decrease in  $T_d$  with increasing EtOH concentration, indicating lower stability against heat-induced unfolding. Furthermore, for an EtOH concentration over 20% (w/w), the measured  $T_d$  for both protein systems was already close to room temperature. This corresponds well to other works reporting that a concentration of 20% EtOH is able to induce a considerable degree of denaturation in globular proteins (Nikolaidis et al., 2017).

The addition of ethanol was already shown to reduce the thermal stability of a WPI solution (Nikolaidis & Moschakis, 2018). However, in the aforementioned study, WPI was only dissolved in 50% EtOH, and the detected peak area was very low. With the

data presented here, we obtained a linear correlation between EtOH content and the heat stability of different protein systems. The observed destabilization of the proteins can be explained as follows. Ethanol, like other alcohols, has a lower dielectric constant than water. This leads to the intramolecular destabilization of proteins. For example,  $\beta$ -Ig was shown to lose its retinol-binding properties in EtOH, a clear indication for loss of tertiary structure (Dufour et al., 1993). Furthermore, an increased alcohol concentration leads to increased exposure of hydrophobic amino acids from the protein core, which was measured by the use of a hydrophobic fluorescence dye (Uversky et al., 1997). Besides the destabilization of intramolecular hydrogen bonds, alcohols provide hydrophobic residues, which allow partial solvation of hydrophobic amino acids that would reside within the protein core under polar conditions of a pure water phase (Buck, 1998).

In addition to  $T_d$ , the enthalpy of unfolding ( $\Delta H$ ) was measured as well, and the results for WPI and PPI are shown in Figure 3-42 B. It can be seen that both protein systems exhibited different trends as a function of the EtOH content. For WPI, a clear decrease in  $\Delta H$  with increasing EtOH concentration can be seen. This indicates that less energy is needed to unfold the proteins in solution. This can be explained by the destabilizing effect of EtOH, as was already discussed for the change in  $T_d$ . It is possible that also some degree of denaturation occurs just by alcohol addition. This will lead to less protein unfolding during the DSC heating experiment, leading to a lower measured  $\Delta H$ .

For PPI, a local maximum for  $\Delta H$  at around 7.5% EtOH could be detected. The higher  $\Delta H$  indicates that more energy is required to unfold the protein structure. This difference between PPI and WPI can be explained by comparing the protein structure of  $\beta$ -Ig and patatin. Alcohols were shown to stabilize  $\alpha$ -helical structures and even lead to the formation of  $\alpha$ -helices from  $\beta$ -strands (Dufour & Haertlé, 1990). As patatin was found to have a high amount of  $\alpha$ -helices (Pots et al., 1998a), this stabilizing effect on the tertiary structure can explain the increase in  $\Delta H$ . However, when the EtOH concentration was increased further, the denaturing effects of EtOH dominate, leading to a decrease in  $\Delta H$ . For patatin, it can be concluded that although the  $\alpha$ -helices are stabilized by EtOH, the overall structure of the protein is more susceptible to heat-induced denaturation. This can be due to a change in the aggregation mechanism from a few to more intermediates, as was shown for heat-induced  $\beta$ -Ig denaturation in dependence of alcohol concentration (Yoshida et al., 2014).

### **3.6.3.2 Rheological properties of hydrogels gelled in the presence of ethanol**

Hydrogels from ethanolic-water protein mixtures were created by heating the mixtures at temperatures 10 °C above the determined  $T_d$  for 30 min to ensure complete unfolding. After cooling the mixture down to ambient temperature, the storage modulus ( $G'_{cool}$ ) of the gel was used to evaluate the stiffness of the gel. The values for PPI and WPI can be seen in Figure 3-43 A and B, respectively.

In both protein systems, a higher  $G'$  was measured for higher protein concentrations. Hydrogels from PPI could be created from concentrations as low as 5% (w/w) protein. Such low protein concentrations led to very soft gels with a low  $G'$  value. Comparison

of the absolute  $G'$  values between the protein sources was not possible as different protein concentrations had to be used in preparation of the gels due to their individual functional gel formation characteristics.

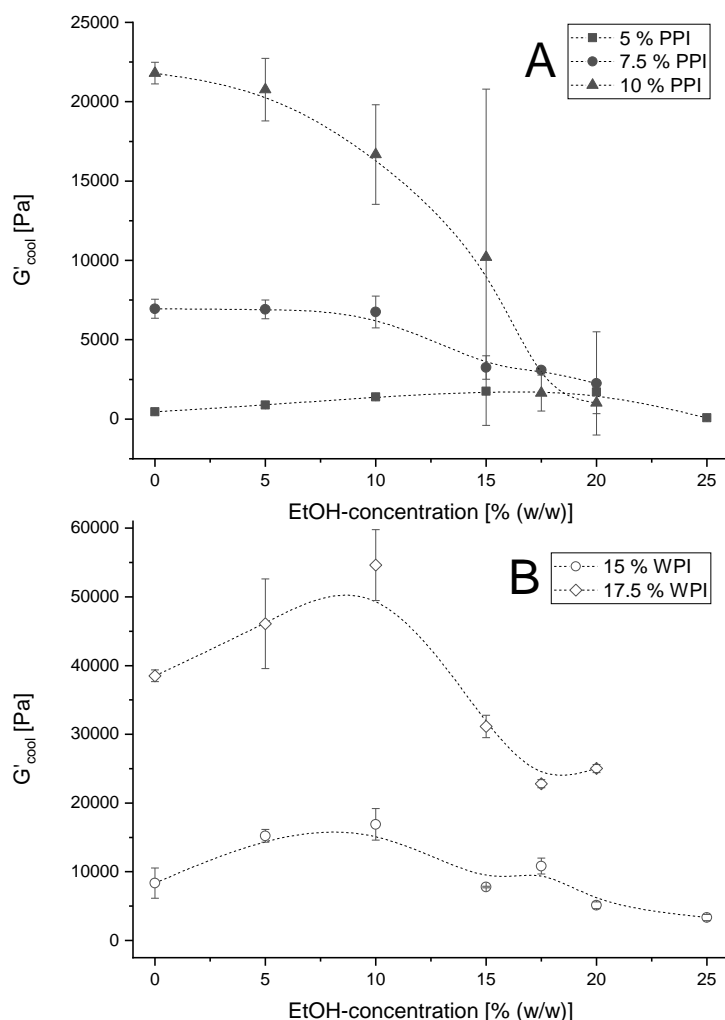


Figure 3-43 Elastic modulus of PPI (A) and WPI (B) hydrogels, at room temperature, in dependence of the ethanol concentration during gelation.

For both protein systems, the gels produced at a high EtOH content had a cream-like texture and the lowest  $G'$  value. These gels were shown to be the most opaque, which indicates the formation of aggregates large enough to scatter incoming light (see supporting information for pictures of the gels). The spontaneous gelation occurring at high EtOH content is apparently detrimental to the development of an elastic gel network with high  $G'$ . At lower EtOH concentrations, stronger gels could be produced. However, some differences between WPI and PPI could be observed. When investigating an EtOH range between 0 - 10%, an increase in  $G'$  was observed for WPI. For WPI mixtures containing 10% EtOH, an increase in gel strength, measured by compressions tests, was already described in the literature (Zirbel & Kinsella, 1988).

This increase can be explained as follows: EtOH has a lower permittivity than water. Therefore, EtOH-water mixtures increase electrostatic interactions between charged

amino acid side chains (Kleemann et al., 2020b). These interactions stabilize the gel structure and increase the hardness of a gel. Furthermore, a recent study on the gelation properties of acid-induced ethanolic WPI solutions found no significant changes in the microstructure of WPI gels up to an EtOH concentration of 10% (w/w) (Wagner et al., 2020a). Therefore, as long as the EtOH treatment does not affect the microstructure negatively, EtOH is capable of increasing  $G'$  of a heat-induced WPI gel.

For PPI, the effect of EtOH content on  $G'$  differed in dependence of the protein concentration. For low protein concentrations,  $G'$  increased in dependence of the EtOH concentration. Similar to WPI, the explanation could be a decreased repulsion between the protein strings which increase the network strength. Contrary to WPI,  $G'$  does not decrease above 10% EtOH. This might be explained by the different gel structures of 15% and 17.5% WPI and 5% PPI. Whereas WPI formed very stable elastic gels at low EtOH concentrations and paste-like soft gels at higher EtOH concentrations, the PPI gels at 5% were very soft throughout the investigated EtOH concentration range. The aggregates formed in presence of EtOH seem to be better suitable to form an elastic gel network. These gels were also rather transparent up to 20% EtOH (see supporting information for pictures of the gels) indicating that no big aggregates were formed in the process.

At the highest protein concentration, the structure was negatively influenced by increasing EtOH content. This is probably due to changes in the microstructure of patatin gels induced by changes in the aggregation rate. The heat-induced aggregation rate of patatin was already shown to be higher than  $\beta$ -lg (Delahaije et al., 2015). Furthermore, patatin was shown to have a high exposed hydrophobicity (Creusot et al., 2011) which explains why gelation of patatin at low electrostatic repulsion was facilitated in comparison to  $\beta$ -lg. The tendency to form big aggregates in a short time, which is detrimental for an elastic gel with high  $G'$ , might override any positive effects due to increased electrostatic repulsion.

In order to understand the different viscoelastic behavior of gels, the types of protein-interactions within the gel are very important. Therefore, the effect of ethanol on these interactions is investigated in more detail in the following.

### **3.6.3.3 Protein interactions in protein hydrogels gelled in the presence of ethanol**

When assessing gel structures, the formation of different interactions between the protein side chains plays an important role. One parameter used by many researchers for the characterization of heat-induced gels is the relation between  $G'$  of the cooled gel to  $G'$  of the hot gel (Schmidt et al., 2019; Martin et al., 2014; Creusot et al., 2011). As hydrogen and electrostatic interactions increase upon cooling, high  $G'_{\text{cool}}/G'_{\text{hot}}$  ratios are associated with a dominance in the formation of electrostatic and hydrogen bonds. Low  $G'_{\text{cool}}/G'_{\text{hot}}$  ratios are associated with the dominance of hydrophobic and covalent bonds as these increase in strength upon heating (Bowland et al., 1995).

In a recent study it was found that the relation  $G'_{cool}/G'_{hot}$  can be used to describe the pH-dependent changes in protein interactions and microstructure in egg white and potato protein gels (Andlinger et al., 2021a). Higher  $G'_{cool}/G'_{hot}$  ratios were found for gels created close to the IEP, indicating the formation of more electrostatic or hydrogen bonds in relation to hydrophobic and covalent bonds. This was explained by the more compact structure of proteins close to their IEP, limiting the reactivity of hydrophobic or thiol groups. Furthermore, at this pH, the electrostatic repulsion between proteins is low, resulting in closer contact between monomers and allowing for more electrostatic interactions through amino acid sidechains.

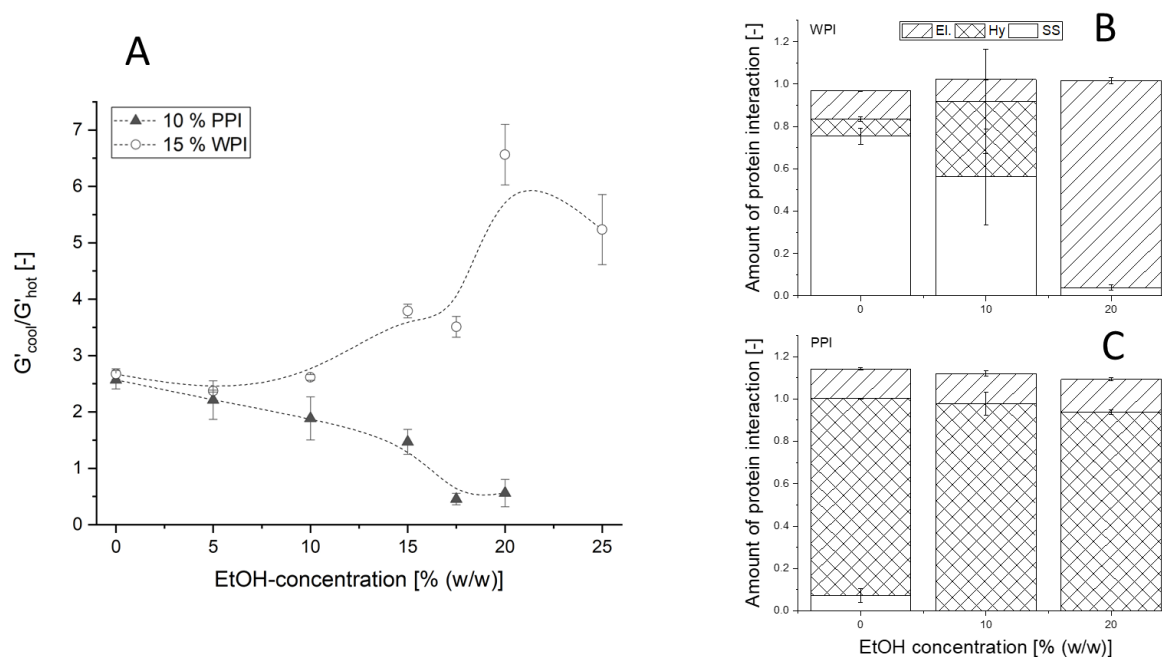


Figure 3-44 Comparison of the ratio of  $G'$  of 10 % (w/w) PPI and 15 % (w/w) WPI hydrogels after cooling to  $G'$  of these hydrogels in the heated state, in dependence of ethanol (A). Amount of protein linked through specific interactions within PPI hydrogels, in dependence of the EtOH content, for WPI (B) and PPI (C)

For WPI gels, increases in the EtOH concentrations, led to an increase in  $G'_{cool}/G'_{hot}$  (see Figure 3-44 A). Therefore, the interactions within the gel can be stated to be dominated by electrostatic and hydrogen bonds. This can be explained by the decreased permittivity of the ethanolic solution compared to the pure water solution. The reduced permittivity facilitates the aggregation through electrostatic interactions. The change from a disulfide-linked gel to a gel stabilized through electrostatic interactions can also be seen in the protein interaction assay (Figure 3-44 B). Without the addition of EtOH, the WPI gels are mainly stabilized through disulfide bonds. When the EtOH content during gelation is increased to 10%, hydrophobic interactions play a more prominent role, and disulfide bonds are decreased. At 20% EtOH, the gels are mainly linked through electrostatic interactions indicating.

The reaction mechanism of WPI in the presence of EtOH can be explained as follows. In the absence of EtOH,  $\beta$ -lg can form disulfide-linked aggregates upon heating (Roefs & Kruif, 1994). During heat-induced aggregation, the free cysteine group at position

121 was shown to be involved in the formation of disulfide bonds (Croguennec, O'Kennedy, & Mehra, 2004). However, this cysteine group can only participate in aggregation if the  $\alpha$ -helix shielding the reactive 121-cysteine residue unfolds (Qi et al., 1997). However, EtOH stabilizes  $\alpha$ -helices in protein structures (Yoshida et al., 2010). Therefore, in the presence of EtOH, the 121-cysteine residue should not be accessible for thiol-disulfide exchanges between the protein monomers. Furthermore, the hydrophobic core of  $\beta$ -Ig resides within a  $\beta$ -barrel structure which is partially stabilized through disulfide bonds (Qin et al., 1998). Therefore, unfolding of hydrophobic groups to the same degree as for patatin does not seem likely. The interactions most likely occurring are electrostatic interactions. The reduced permittivity allows for more interactions of charged amino acid side groups. As the investigated protein system is highly concentrated, interactions between protein monomers can readily occur. Furthermore, it has to be mentioned that the heating temperatures set in this study are always relative to the unfolding temperature measured by DSC. Therefore, at high EtOH concentrations, the heating is done at lower temperatures, which might be insufficient to unfold the  $\alpha$ -helix shielding the 121-cysteine residue.

For PPI, a different trend in dependence of the EtOH concentration was observed. All PPI gels were mainly stabilized through hydrophobic interactions (Figure 3-44 C). The low amount of internal disulfide bonds and the high degree of unfolding in PPI led to a dominance of hydrophobic interactions. At 0% EtOH even a small amount of disulfide bonds was detected. That PPI is able to form disulfide bonds linked aggregates, was shown in a recent study (Andlinger et al., 2021c).

Increasing the EtOH content led to a reduction in the  $G'_{cool}/G'_{hot}$  factor, even below 1, indicating a strong dominance of hydrophobic interactions over electrostatic and hydrogen bonds (Figure 3-44 A). How EtOH is able to facilitate the interaction of hydrophobic groups is explained in the following.

EtOH has chaotropic properties and is able to unfold proteins. The alkyl group of EtOH forms apolar regions, facilitating the unfolding of hydrophobic amino acid groups into these regions (Yoshida et al., 2014). Hydrophobic interactions weaken at lower temperatures (Kronberg, 2016), thus explaining decreasing the  $G'_{cool}/G'_{hot}$  factors. A  $G'_{cool}/G'_{hot}$  factor below 1 was reported for WPI solutions heated in the presence of 500 mmol/L Natriumthiocyanat (NaSCN) (Bowland et al., 1995). NaSCN is a chaotropic salt inducing high degrees of unfolding of proteins. Furthermore, due to its molecular structure, it changes the orientation of water molecules and increases the solubility of hydrophobic components in water (Nakai, 1988; Kronberg, 2016). Therefore, when heating and milieu conditions favor hydrophobic interactions, the gels show  $G'_{cool} < G'_{hot}$ .

It can be concluded that EtOH has different influences on the type of protein interactions stabilizing the gels, depending on the molecular features of the various proteins. In the following, the impact of different protein interactions on the textural properties of hydrogels, alcogels and aerogel will be assessed.

### 3.6.3.4 Textural properties of gel beads before and after complete solvent exchange with EtOH

The force necessary to break PPI and WPI gel beads was investigated by a compression test (see Figure 3-45). WPI beads at EtOH concentrations of up to 10% (w/w) were harder than the PPI gels, probably due to the occurrence of strong disulfide links within the gel network. The higher protein concentration for WPI might also play a role. However, a recent study directly comparing the textural properties of WPI and PPI gels at the same protein concentration, showed that higher forces are necessary to break WPI gels, in comparison to PPI gels (Andlinger et al., 2021b).

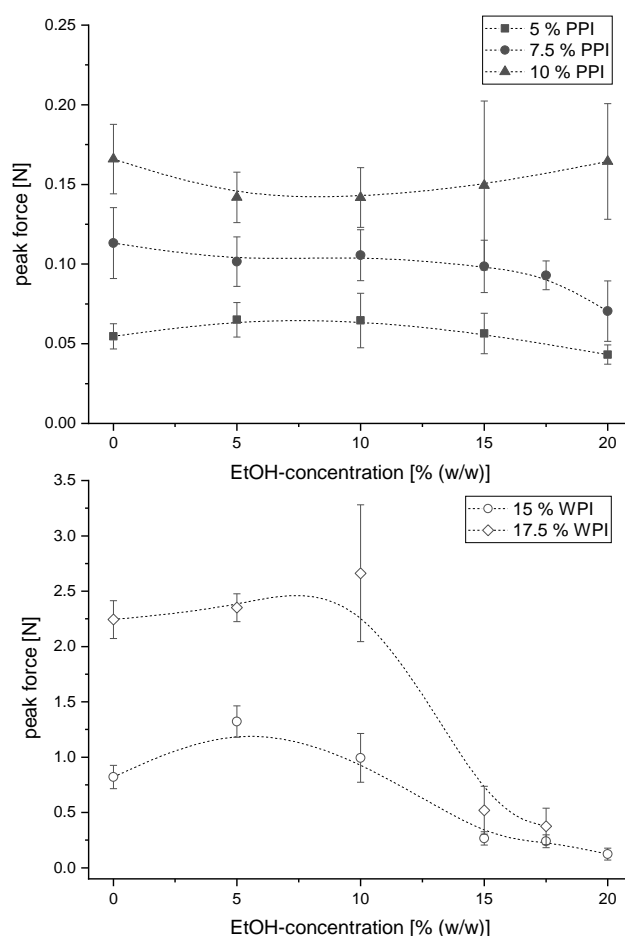


Figure 3-45 Hardness of PPI (top) and WPI (bottom) hydrogel capsules in dependence of the ethanol concentration, measured by the maximum force necessary to break the gel beads.

This trend is supported by the results from the rheological quantifications (Figure 3-43): WPI showed some increase in strength at low addition of EtOH, indicated by an increase in the force necessary to break the capsules (Figure 3-45). As already discussed for the rheological measurements, this can be explained by an increase in electrostatic interactions between the amino acid side chains. A change in gel structure occurred when EtOH concentration exceeded 10% (w/w). At high EtOH concentrations, the peak force necessary to fracture the beads decreased rapidly, indicating the formation of a much weaker gel network. This is in accordance with results described



for the rheological measurements (Figure 3-43). Contrary to that, textural properties of PPI were not effected by the addition of EtOH, which is in agreement with the results of the rheological characterizations of the according hydrogels. Therefore, it can be concluded that macroscopic deformation in PPI is not influenced by the addition of EtOH in the investigated concentration range. Furthermore, the impact of EtOH on macroscopic compressional deformation was similar as observed by the microscopic deformation measured by the rheometer.

The hydrogel beads were subjected to a complete solvent exchange from water to EtOH. Afterwards, the force necessary to break PPI and WPI gel beads was investigated by a compression test (Figure 3-46). For all alcogels, higher forces were necessary to induce breakage in the gels compared to the hydrogel beads.

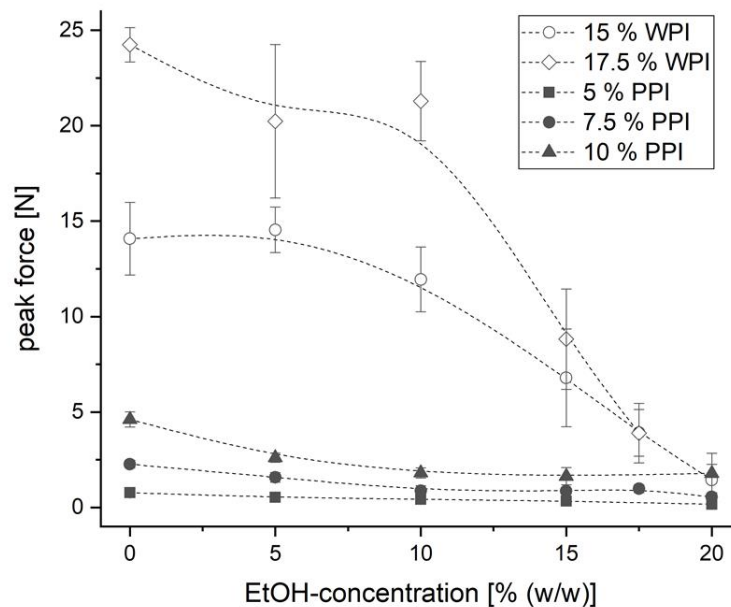


Figure 3-46 Hardness of PPI and WPI alcogels in dependence of the ethanol concentration in the hydrogel

The change from water to EtOH was already shown to substantially harden the gel network of WPI and egg white protein (EWP) gels (Kleemann et al., 2020b). The hardening was mainly explained by the lower permittivity of EtOH, which increased interactions between the amino acid side chains. The fact that electrostatic interactions and hydrogen bonds indeed play a role in the interactions promoted by EtOH can be seen when comparing WPI hydro- and alcogels.

For WPI hydrogels (Figure 3-45), an increase in hardness was obtained with the addition of EtOH, up to 10% (w/w). This hardening effect is not apparent in the WPI alcogels (Figure 3-46), where hardness of the gel beads was similar in the range 0-10% (w/w) EtOH. In this EtOH range, the protein network should be formed by fine protein strands with a significant amount of covalent crosslinking. These protein strands increase in hardness due to the presence of 5 - 10% (w/w) EtOH in the hydrogel (Figure 3-45).

However, the additional hardening effect is nullified when most water is exchanged with EtOH in the final alcogel (Figure 3-46). As the network structure of 0 and 10% EtOH gels is not considerably different both gel structures led to similar alcogel strength.

Although all PPI hydrogels exhibited similar breakage forces, the corresponding PPI alcogels' hardness decreased when a higher amount of EtOH was present during gelation. This can be explained by a change in microstructure induced by the different EtOH contents. With increasing EtOH content, the hydrogels were more opaque, indicating the formation of bigger aggregates and areas devoid of protein (Nicolai, 2019). The change from fine-stranded and transparent gels towards particulate and opaque gels influences the hardening behavior of protein gels. From research on the hardening of WPI and EWP alcogels, it is known that finer stranded and less particulated gels lead to a more pronounced hardening upon solvent exchange (Kleemann et al., 2020b). Through scCO<sub>2</sub> drying, the alcogels can be processed into porous aerogels. How EtOH can be used to influence the texture and microstructure of the aerogels will be evaluated in the following.

#### **3.6.3.5 Aerogel characterization**

Drying by scCO<sub>2</sub> was already used to create highly porous aerogels from WPI (Kleemann et al., 2018) and PPI alcogels (Andlinger et al., 2021a). From these studies, it is known that the microstructure of the hydrogel is highly correlated with the microstructure of the resulting aerogel. In the following section, the microstructure and textural properties of the corresponding aerogels will be assessed in relation to the properties of the foregoing hydrogels.

From Figure 3-47, it can be seen that PPI and WPI had similar skeletal densities without the addition of EtOH and that increasing EtOH concentration in the hydrogel leads to lower skeletal densities in the resulting aerogels. Both observations shall be explained in the following:

From previous research it is known that the skeletal density of PPI aerogels increased considerably when the protein concentration was increased from 5 to 10% (Andlinger et al., 2021a). The fact that PPI has the same density as WPI although the protein concentration is lower leads to the conclusion that PPI forms denser networks. This corresponds well with research on protein aggregates that showed that patatin indeed has the tendency to form bigger and denser aggregate structures compared to the whey protein  $\beta$ -lg (Delahaije et al., 2015).

The second effect relate to the different dependencies of the protein sources on EtOH concentration. A lower skeletal density can be interpreted as a looser overall gel network structure. Therefore, changing the properties of the protein mixture through the addition of EtOH changed the way the protein strands interacted. A decrease in skeletal density was also found in PPI aerogels when the protein concentration was decreased (Andlinger et al., 2021a). This decrease was explained by decreased interactions between the PPI molecules. Particle-particle interactions are the main driving

force behind sol-gel transitions, shown in model systems with colloidal polymers (Richard et al., 2018). More attractive forces lead to a higher degree of micro-phase separation between proteins and solvent (Nicolai & Durand, 2007), and this correlates with the development of denser structures (Clark et al., 2001). Therefore, structures with lower densities are indicative of reduced attraction between the protein aggregates. The reduced interaction between the aggregates can be induced by increased interactions between the protein aggregates and the solvent.

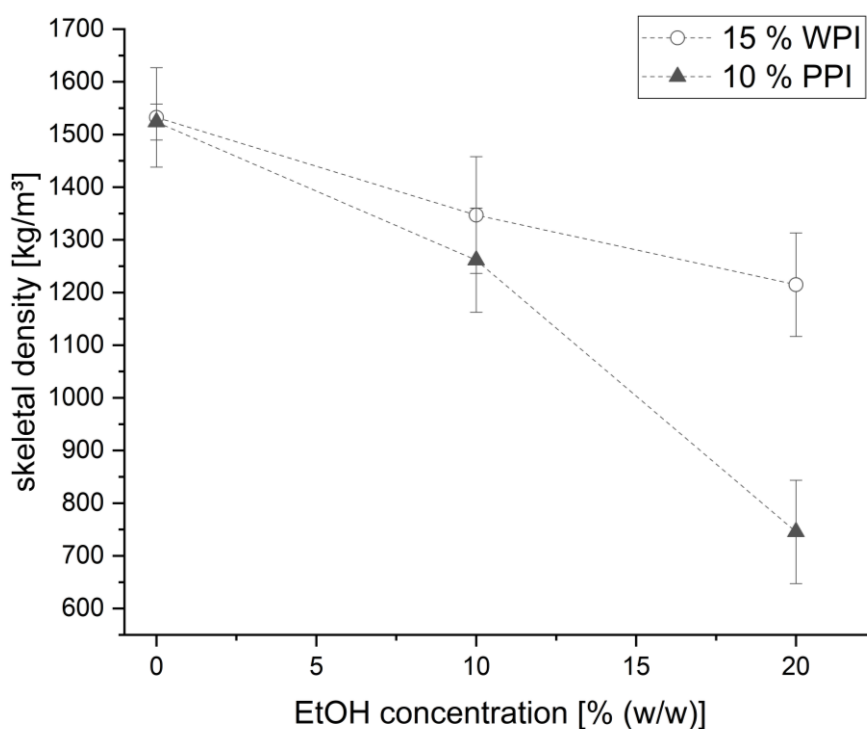


Figure 3-47 Skeletal density of WPI and PPI Aerogels in dependence of the EtOH content in the precursor protein mixture.

Interactions between biopolymers, such as proteins, and solvents are not yet fully understood and dependent on the solvent and the respective polymer. Nevertheless, the following general trend can be observed: increased interactions between solvent and the biopolymer led to swelling and looser structures, whereas increased biopolymer interactions lead to shrinkage and denser structures (Gurikov et al., 2019). However, the effect of different solvents is difficult to predict, as hydrophobic parts of the solvent should increase the solubility of unfolded protein side chains, whereas the reduced permittivity should promote more intense interactions. It can be concluded that up to 20% (w/w) EtOH, the increase in EtOH allows for better solubility of the heat-unfolded proteins in the solution, and thus gels with a lower skeletal density are produced. As PPI aggregates are expected to be more hydrophobic than WPI (Creusot et al., 2011), this effect might be even more pronounced for PPI as seen in the lower skeletal density for PPI at higher EtOH concentration.

Another important parameter to describe the microstructure of aerogels is the specific surface area measured by nitrogen absorption (BET). The addition of EtOH only had a minor influence on the specific surface area measured (BET). The aerogels all had

BET values of around 300 m<sup>2</sup>/g with only the 20% EtOH PPI gel below this value with around 250 m<sup>2</sup>/g (see Table 3-8).

Table 3-8 Specific surface area (BET) of PPI (10%) and WPI (15%) aerogels in dependence of the EtOH during gelation

BET [m <sup>2</sup> /g]	0% (w/w) EtOH	10% (w/w) EtOH	20% (w/w) EtOH
WPI	307 ± 17	332 ± 19	306 ± 7
PPI	301 ± 46	307 ± 7	245 ± 2

High BET values > 300 m<sup>2</sup>/g for protein aerogels were found for gels that are finely stranded and either stabilized by covalent or hydrophobic interactions (Kleemann et al., 2018; Selmer et al., 2015; Andlinger et al., 2021a). In these studies, lower BET values for protein aerogels were found when protein solutions were gelled at pH levels close to their respective IEPs. Increasing the EtOH content up to 20% (w/w) had no strong effect on the measured BET surface. Therefore, the change from disulfide-linked to electrostatic linked hydrogels, shown in Figure 3-44, did not significantly influence the BET value. This is contrary to what was shown for the influence of pH on the microstructure, where the development of more electrostatic/hydrogen bonds close to the IEP led to a reduction in BET (Andlinger et al., 2021a; Selmer et al., 2015). Although increases in EtOH content should induce more compact structures through increased aggregation and reduced permittivity, high BET values indicate the development of small pores with considerable surface areas. Therefore, the presence of hydrophobic residues from EtOH apparently has a positive effect on the development of porous structures.

The strength of the capsules was assessed through compression tests, similar to the hydro- and alcogels. The results are summarized in Table 3-9. It can be seen that depending on the protein type, the addition of EtOH to the pre cursor mixture influenced the aerogel strength differently. PPI aerogels were easier to break compared WPI gels. The lower protein concentration, as well as the lack of disulfide bonds within the protein network, might explain the reduced strength. A similar explanation was reported before to explain the lower force necessary to break EWP aerogels in relation to WPI aerogels (Kleemann et al., 2018). Interesting to note is that for 20% (w/w) EtOH, the WPI aerogels were brittle, and no useful results could be determined. Apparently, the change from disulfide-linked to electrostatic linked gels severely reduced the strength of the gel network.

Table 3-9 Force necessary to induce breakage in PPI (10%) and WPI (15%) aerogels in dependence of the EtOH during gelation

Breakage Force [N]	0% (w/w) EtOH	10% (w/w) EtOH	20% (w/w) EtOH
WPI	77.4 ± 5.7	50.1 ± 1.3	n.d.
PPI	19.1 ± 0.4	9.8 ± 0.3	14.7 ± 8.0

### 3.6.3.6 Scheme of the proposed gelation mechanism influenced by EtOH in concentrated protein systems.

The impact of EtOH on the complex reaction mechanism in concentrated systems of proteins with different molecular features is summarized in the following. Fig. 7 schematically depicts the proposed reaction mechanism. For both protein systems, EtOH decreases the electrostatic repulsion between amino acid side chains due to a decreased permittivity and reduces the energy required for heat-induced protein denaturation. The reduced permittivity allows the formation of bigger aggregates resulting in increased opaqueness.

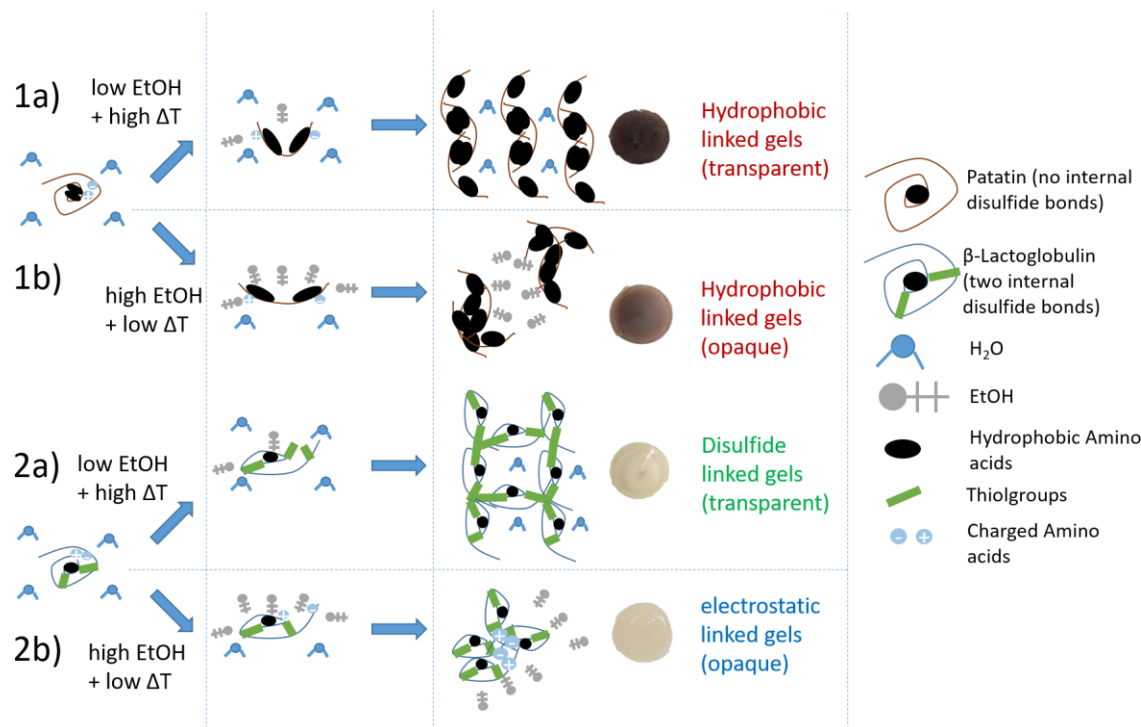


Figure 3-48 Proposed gelation mechanism of EtOH influence on the heat-induced gel formation of PPI (1 a and b) and WPI (2 a and b). When EtOH content was low, a high temperature increase (high ΔT) was necessary to induce gelation. Similar, when EtOH content was high, a low temperature increase (low ΔT) was necessary to induce gelation.

At EtOH concentrations of around 20% (w/w), the denaturing effect of EtOH leads to unfolding at nearly room temperatures (Figure 3-48- 1b and 2b). Depending on molecular features, the aggregation mechanism of PPI and WPI are influenced differently. Patatin's hydrophobic core is not stabilized by any internal disulfide bonds and readily unfolds (Figure 3-48– 1b). This allows hydrophobic amino acid groups to be exposed to the EtOH phase. Therefore, the aggregation mechanism remains dominated by hydrophobic interactions.

For β-Ig the reaction mechanism changes in dependence on the EtOH concentration. At low EtOH concentration, the applied temperature leads to unfolding in the region of the free thiol group, leading to the formation of disulfide bridges (Figure 3-48– 2a). At high EtOH concentrations, the region of the free thiol group is stabilized. Furthermore, the disulfide bonds in β-Ig stabilize the protein core. This limits hydrophobic interactions and leads to gels being stabilized by electrostatic interactions (Figure 3-48– 2b).

Additionally, the presence of EtOH during gelation leads to a looser microstructure, which shows that change in solvent properties can influence the gelation process.

#### **3.6.4 Conclusion**

The impact of EtOH as a structuring agent on protein mixtures forming gels was evaluated. Through the combined application of heat and EtOH, different viscoelastic properties of the resulting gels could be induced. The effect of EtOH differed between the protein sources, and depending on their molecular features, different gelation mechanisms could be proposed.

The results can be used in different ways. Through the addition of EtOH, protein aerogels can be produced at lower temperatures compared to pure water solutions. The microstructure can be modulated for encapsulation purposes. The time-consuming step of solvent exchange can be shortened by already introducing ethanol in the hydrogel matrix. Furthermore, the results can help to create hydrogels with specific properties regarding gel strength, cold setting behavior, and rheology. For example the hydrophobic nature of EtOH induced PPI gels might be advantageous for stabilization of oil/water and air/water interfaces. Future research should evaluate the applicability of these hydrogels in foodstuff as emulsifiers or structuring and foaming agents.

#### **Acknowledgements**

This IGF Project AiF 19712 of the FEI was supported via AiF within the program for promoting the Industrial Collective Research (IGF) of the German Ministry of Economic Affairs and Energy (BMWi), based on a resolution of the German Parliament.

We would like to thank Marc Laus from AVEBE, Veendam, The Netherlands, for providing the potato protein isolate.

### 3.6.5 Supporting Information

Table S1: PPI gels after rheological measurements in dependence on ethanol and protein concentration

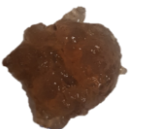



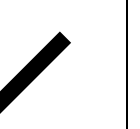
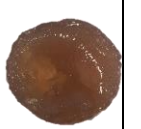







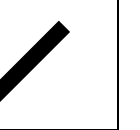






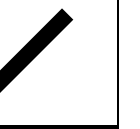




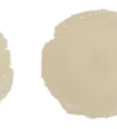
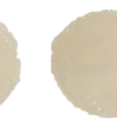








Ethanol concentration [% (w/w)]		0	5	10	15	17.5	20	25
5 % PPI								
7.5 % PPI								
10 % PPI								

Table S2 WPI gels after rheological measurements in dependence on ethanol and protein concentration

Ethanol concentration [% (w/w)]		0	5	10	15	17.5	20	25
15 % WPI								
17.5 % WPI								

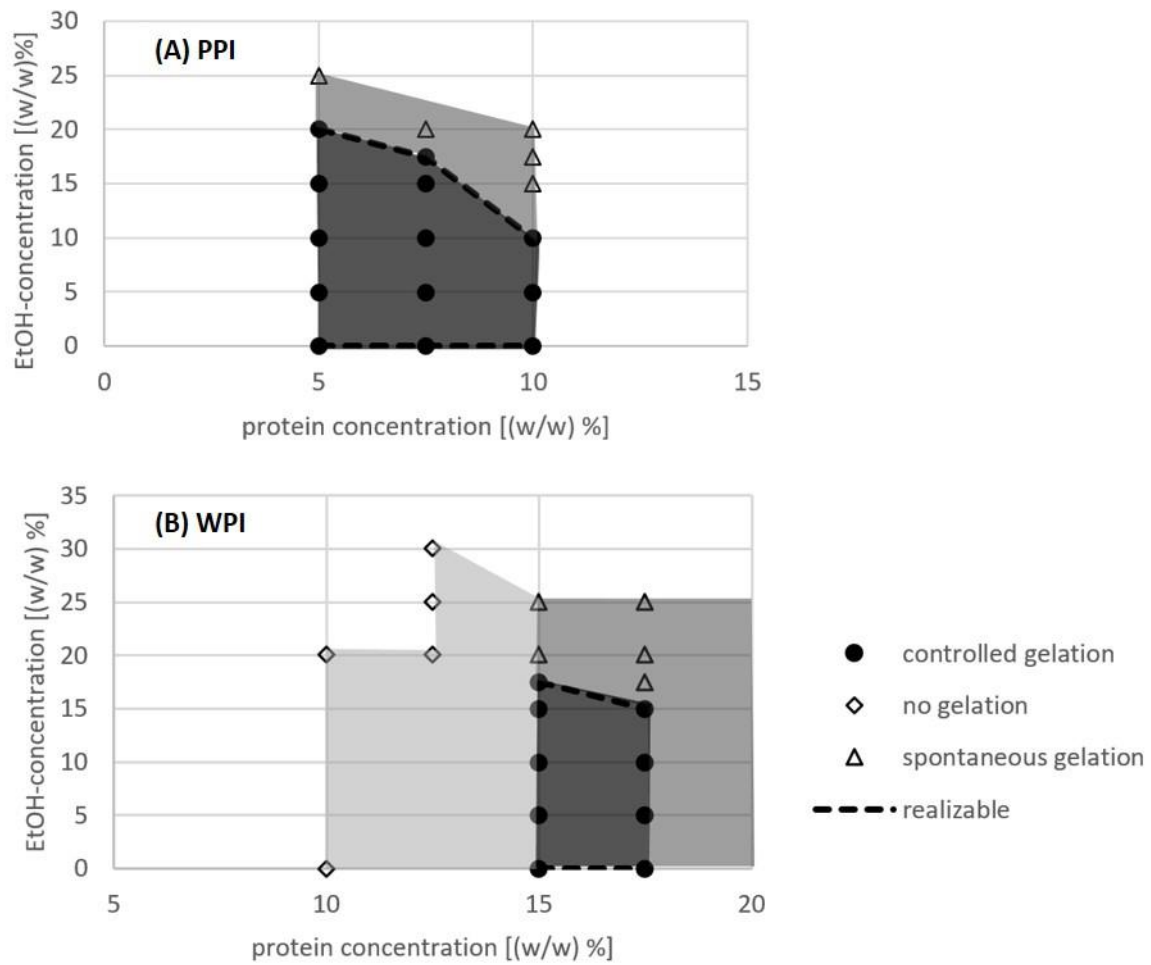


Figure S1 Overview on tested protein-EtOH combinations. The symbols indicate if gelation occurred upon solvent-protein contact (spontaneous), during the rheometer trials (controlled gelation) or never at all.



## 4 Overall discussion and main findings

Aerogels from proteins are a novel class of biopolymer-based structures with possible applications in a wide variety of fields. Previous work showed that aerogels created from WPI and EWP hydrogels showed very promising results regarding the application as encapsulation matrices (Kleemann et al., 2020a). How these globular protein hydrogels can principally be influenced and what impact a change in milieu conditions has on alco- and aerogels is qualitatively depicted in Figure 4-1.

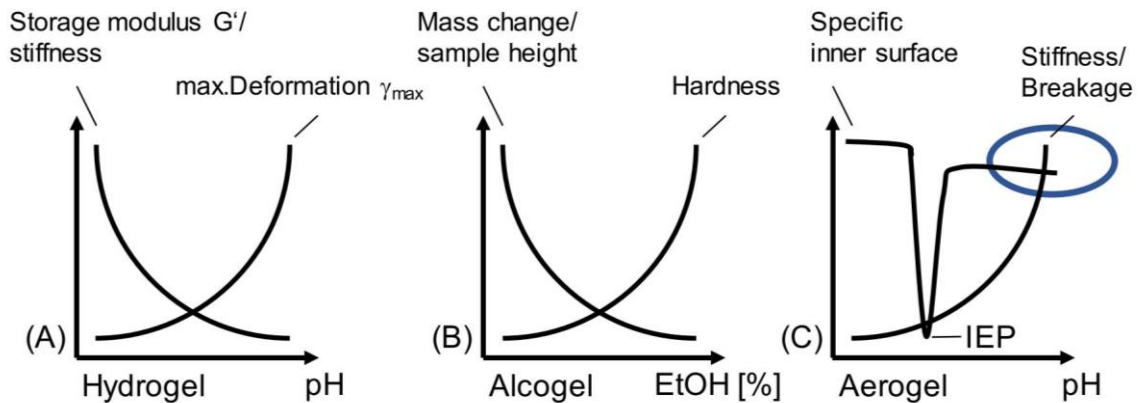


Figure 4-1 Schematic depiction of correlations between structural properties of hydro-, alco- and aerogels from globular egg and whey proteins and pH as well as EtOH content, adapted from Kleemann, (2021). The blue circle highlights the properties of high mechanical stability and high surface area which is desired for aerogel applications such as encapsulation.

It could be shown that at a high pH hydrogels showed high deformability. These alkaline gels were also the hardest after complete solvent exchange into an alcolgel. Furthermore, these alcolgels could be transformed into hard aerogels with high specific inner surface areas (BET). Close to the IEP, however, brittle gels with low BET values were obtained. Based on their results Kleemann et al., (2018) hypothesized the mixture of high electrostatic repulsion and the formation of disulfide bonds is necessary to create stable aerogels with high inner surface areas.

To extend the knowledge on the mechanism of aerogel creation from the animal-derived egg and dairy protein systems to plant-based proteins, patatin was chosen as a model system. This potato protein is water-soluble and therefore suitable for comparison with water-soluble animal-derived proteins such as WPI and EWP. As the aerogel drying process keeps the pore structure of the gel intact valuable insight into PPI gelation could be obtained.

When PPI aerogels were first created (see chapter 3.4) it came as a surprise that PPI could form stable aerogels with high inner BET surface areas, as PPI lacks the chance for stabilization through disulfide bonds (Creusot et al., 2011).

Therefore, in this thesis, the aggregation mechanism was investigated in detail to investigate how structures can be formed from PPI solutions (see section 4.1). This helped to understand how PPI reacts to different milieu conditions such as salt, pH, and ethanol content. Furthermore, differences in the gelation behavior of plant- and

animal-based proteins could be explained by differences in the molecular structure of the main proteins (see section 4.2). Throughout the study, correlations between rheological gel properties and changes in protein interactions were identified. These will be discussed in conjunction further below (see section 4.3).

It is expected that the approach taken in this work can be used as a guideline to assess technological functionalities of more new protein sources and it presents a set of tools to compare them with well-established proteins from the dairy and egg industry.

#### **4.1 Aggregation behavior of potato proteins**

The comparison between patatin gelation and other globular food proteins showed some differences (Creusot et al., 2011). Based on the molecular structure of the proteins and their measured exposed hydrophobicity it was concluded that hydrophobic interactions, rather than covalent disulfide bonds played a major role in patatin gelation. Although PPI aggregates were mainly linked through hydrophobic interactions, the occurrence of trimeric structures that only dissolved in the presence of reducing buffers was shown (Pots et al., 1999a). From this, the formation of covalent bonds was concluded, while the details of how they were formed remained elusive. The aggregation mechanism was described as a two-step process, similar to  $\beta$ -Lg, where a reversible unfolding step led to an irreversible formation of bigger aggregates (Pots et al., 1999c). PPI's aggregation behavior was described to show similar overall trends as egg and whey proteins, albeit faster aggregation into bigger aggregates was noted (Delahaije et al., 2015).

However, clear differences in the aggregation curves of patatin and  $\beta$ -Lg could be found in the data presented by Delahaije et al (2015). For  $\beta$ -Lg, different conditions could be fitted onto one master curve with respect to time, for patatin, however, differences were visible between conditions of fast and slow aggregation. These differences can be explained with the clear changes in the reaction order as described in chapters 3.2 and 3.3. The temperature dependence of the reaction rate showed that patatin already exhibited aggregation at a low temperature range at which no unfolding could be detected in DSC measurements. This was not found for  $\beta$ -Lg as discussed in chapter 3.3. At high temperatures, patatin aggregated very fast. Under these conditions, the unfolded structures tend to form aggregates first through hydrophobic interactions, then followed by linkage through covalent bonds. It could be shown that patatin is indeed able to form larger covalently linked aggregates, a fact which was unknown so far.

Furthermore, it could be shown how the aggregation could be influenced to modify different functional or structural properties of the aggregates. For example, the exposed hydrophobicity ( $S_0$ ) of PPI aggregates could be influenced by the pH during aggregation. During aggregation, the protein unfolds and hydrophobic amino acid side chains from the core are exposed. Some of these side chains will be oriented outwards, thus increasing  $S_0$ . Some of these side chains, however, will cluster together, driven by the hydrophobic effect (Kronberg, 2016), linking protein monomers in the process. These newly formed hydrophobic patches can then be stabilized by the formation of disulfide bonds. The result that newly formed hydrophobic patches can be stabilized

by disulfide links was already shown for WPI (Betz et al., 2012). With the results of this thesis, it could be shown that a similar mechanism is at work for PPI although the disulfide linkage is occurring to a lower degree compared to WPI. The results indicated that the formation of disulfide links is a secondary step in the aggregation behavior (see chapter 3.2). It could be shown that a higher pH led to aggregates with lower  $S_0$ . It appeared reasonable to assume that the higher reactivity of thiol groups at higher pH led to a higher degree of disulfide formation around the newly formed hydrophobic patches, thus limiting the amount of exposed hydrophobic groups, lowering the measured  $S_0$ . A higher degree of disulfide linkage, in combination with higher resistance against unfolding, could also explain why WPI aggregates showed considerably lower  $S_0$  values compared to PPI aggregates (see chapter 3.5.3.2).

It thus became clear that the aggregation mechanism of patatin differs in many ways from  $\beta$ -lg. This explains why the attempt by Delahaije et al., (2015) to find one protein property such as charge, exposed hydrophobicity, or amount of free thiol groups was unsuccessful in predicting reaction rates of ovalbumin, patatin, and  $\beta$ -lg. The different reaction mechanisms between protein sources were especially apparent when investigating the aggregation mechanism at low electrostatic interactions (pH close to IEP) and low unfolding (lower T). Whereas  $\beta$ -lg had a smaller aggregate size compared to neutral conditions (Donato et al., 2009) patatin aggregates grew by an order of magnitude (see chapter 3.3). The main explanation for this can be found when comparing the major protein interactions that are responsible for aggregate formation. For  $\beta$ -lg, the formation of disulfide bonds is essential for aggregate growth, and the reactivity of the thiol group is limited at low pH values. Therefore,  $\beta$ -lg aggregates do not grow a lot at these pH values especially under conditions of low unfolding. Contrary to this, patatin is mainly stabilized through hydrophobic interactions, and these interactions are not negatively impacted by lower pH values. Furthermore, patatin has a higher  $S_0$  than  $\beta$ -lg even in its native state. Thus interactions between unfolded proteins and natively folded proteins can easily occur. This combination allows patatin aggregates to grow in size through the formation of non-covalent bonds.

From the results of this thesis, a specific aggregation mechanism of patatin could be derived. The mechanism is depicted in Figure 4-2 and explained in the following.

Elevated temperatures lead patatin to reversible unfold. The unfolding leads to the exposure of hydrophobic groups from the core. Unfolded monomers can then connect through hydrophobic interactions. Depending on the speed of unfolding and the electrostatic repulsion between the monomers different aggregates can form. If electrostatic repulsion between the monomers is low, the growth of aggregate is preferred over the formation of new aggregates. This is especially evident under conditions of slow unfolding (e.g. heating temperatures below the peak denaturation temperature). Under these conditions not every collision of two protein monomers results in aggregation (this reaction regime is called unfolding limited and is explained in more detail in chapter 3.3). Under these conditions, an unfolded protein will rather react with the aggregate as the aggregated structure already provides exposed hydrophobic side

chains. In a second step, covalent links stabilize the aggregates, albeit to a lesser extent than at higher pH values (see chapter 3.2.3.3 for details on the protein interactions forming the aggregates). Due to the large aggregate size, the solution turns turbid.

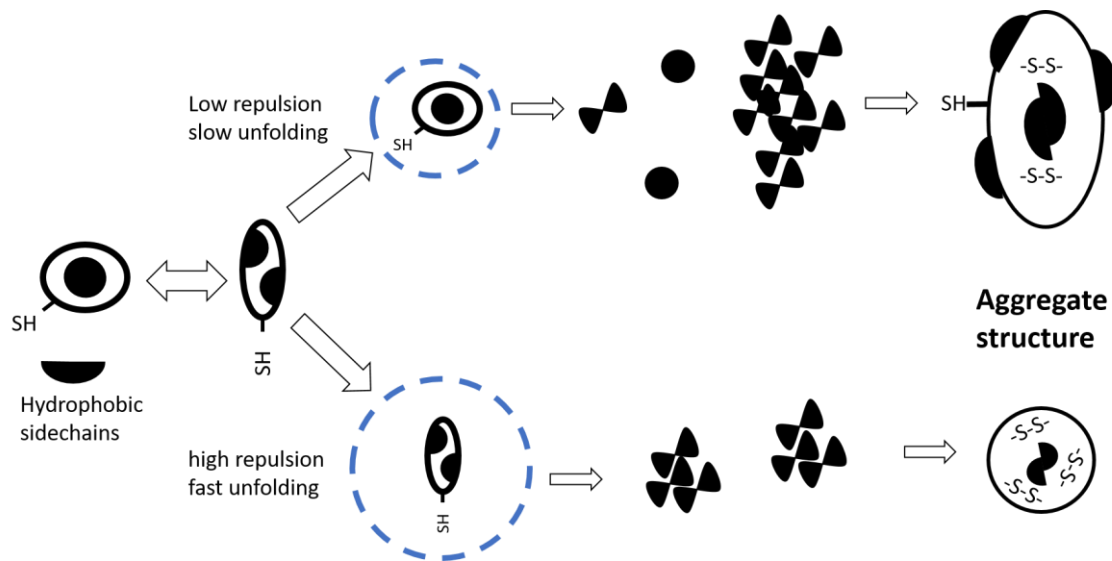


Figure 4-2 Schematic representation of the heat-induced aggregation mechanism of patatin, based on the results from chapters 3.2 and 3.3. Under conditions of low repulsion/slow unfolding, the growth of aggregates is preferred over the formation of new aggregates resulting in fewer but bigger aggregates. Contrary, under conditions of high repulsion/fast unfolding the formation of new aggregates, is preferred, resulting in more but smaller aggregates. Depending on the reaction pathway smaller or bigger aggregates with less or more exposed reactive side chains will be obtained.

Under conditions of high repulsion and high unfolding, most patatin monomers are unfolded and interaction between hydrophobic side chains from the protein core can easily occur (this reaction regime is called diffusion-limited and is explained in more detail in chapter 3.3). As nearly all molecules are unfolded they tend to react with each other readily and more aggregates are produced rather than growth of existing aggregates. The secondary formation of disulfide bonds stabilizes the proteins resulting insoluble aggregates and a clear solution. Although stabilization through disulfide bonds plays a secondary role its importance in determining aggregate functionality was especially evident when disulfide formation was completely blocked. Under these conditions, the PPI solution gelled, even at 1% protein far below the usual 5-6% necessary for gelation (see chapter 3.2.2.6).

Although the general mechanism in patatin aggregation was similar to  $\beta$ -Ig, with hydrophobic interactions taking place before the formation of disulfide bonds, the dominance of hydrophobic interactions over covalent bonds led to different aggregate growth behavior and aggregation kinetics as explained above. The here proposed aggregation mechanism can be used as a template for other proteins that aggregate mainly through hydrophobic interactions. However, one has to consider that patatin is a water-soluble protein. Therefore, considerable differences from other proteins such as salt soluble protein fractions from pea soy and other legumes are expected.

One still open question is how exactly patatin can form bigger covalently linked aggregates although only one thiol group is present per patatin molecule. As any considerable interactions between patatin and protease inhibitors could be ruled out in chapter 3.2, interactions between patatin molecules seem the most likely. In this thesis, covalently linked aggregates were found with a molecular weight of over 250 kDa, which is even bigger than the trimeric structures (108 kDa) described in the literature (Pots et al., 1999a). As these aggregates did not dissolve in a non-reducing buffer some sort of covalent bonds needs to stabilize their structure. It is possible to assume that the mostly hydrophobically linked aggregates are “patched” together by covalent bonds at a few spots, thus preventing the dissolution in a non-reducing buffer. Another possibility is that crosslinking of patatin could further be enhanced by the occurrence of patatin variants with more than one free thiol group. Although patatin is described in the literature with only one free thiol group there are patatin variants that do possess two cysteine groups (UniProt entry P07745 and P15477) which might occur to some amount in commercial PPI. The occurrence of these variants might affect the gelation mechanism of PPI and would be an interesting topic for future investigations.

As could be shown above, the focus of this thesis was to investigate the influence of the “classic” protein interactions on PPI aggregation. However, to conclude this section, two other mechanisms that might influence the aggregation behavior of potato proteins shall be presented and discussed in the following. One newly discovered protein interaction that was just recently found to stabilize the protein structure of transaldolase is the so-called lysine-oxygen-cysteine-bridge (NOS bridge) (Wensien et al., 2021). It could be shown that lysin and cysteine residues can form a covalent bridge by incorporating a reactive oxygen species. Although this protein interaction was just recently discovered, the authors of this study found NOS bridges across all domains of life, by comparing simulation results with protein data bank entries. If these bridges also can occur upon heat-induced aggregation remains to be seen. However, patatin could be an interesting protein to study this effect as it is very rich in lysine and contains cysteine groups.

Another crosslinking mechanism that may be of interest in plant protein aggregation is the cross-linking of proteins through polyphenols. A recent study could show that the presence of polyphenols weakened the network of pea protein gels (Chen et al., 2021). It could be shown that larger aggregates were formed in the presence of the polyphenols and that hydrophobic bonds, as well as hydrogen bonds, were weakened throughout the gel. As potato-derived products can also contain significant amounts of polyphenols (Akyol et al., 2016) similar effects might occur in potato protein aggregation and gelation as well. Both mechanisms should be considered for future research on potato proteins. This way the ability to fine-tune techno-functional properties of plant protein isolates will be further refined.

#### **4.2 Influence of milieu conditions on potato- and animal-derived protein gels**

In chapters 3.2 and 3.3, the aggregation of PPI was investigated to understand the mechanism behind this reaction. Based on these results gelation of WPI and PPI can be compared on a mechanistic level. Therefore the comparative results of PPI and

WPI gelation in chapters 3.5 and 3.6 shall be interpreted on a higher level in the following. For simplicity, the focus will lay on the two proteins that determine the gelation behavior of the isolates the most,  $\beta$ -lg for WPI and patatin for PPI.

It could be shown that WPI and PPI behaved differently in response to different milieu conditions. For WPI changes in the protein interactions that stabilize the gel network from disulfide-linked to electrostatically linked could be observed. For PPI the main stabilizing force was hydrophobic interactions, more or less independently of the milieu conditions. How the different milieu conditions influence the gelation behavior shall be explained in the following and is schematically depicted in Figure 4-3.

$\beta$ -lg formed disulfide-linked, short worm-like aggregates under conditions of high electrostatic repulsion and unfolding ( $\beta$ -lg green arrow). This reaction involves the unfolding of the  $\alpha$ -helix shielding the 121-Cysteine group in  $\beta$ -lg (Qi et al., 1997). As long as the  $\alpha$ -helix can fully unfold, the thiol group can initiate thiol-disulfide exchanges and disulfide links are the main protein interaction that stabilizes the WPI gels (Sava et al., 2005). If milieu conditions stabilize the  $\alpha$ -helix structure and reduce repulsion between the protein monomers the protein interactions are changed. Stabilization, especially of the  $\alpha$ -helix, prevents the thiol group from being exposed and thus prevents the formation of disulfide bonds. To change the protein interactions from disulfide-links to electrostatic links the unfolding and aggregation mechanism of whey proteins, especially  $\beta$ -lg, has to be altered.

In this thesis, the change in gelation mechanism was induced through pH values close to the IEP (see chapter 3.5) as well as the presence of EtOH (see chapter 3.6). As schematically depicted,  $\beta$ -lg formed electrostatic-linked gels under conditions where certain secondary protein structures are stabilized and the electrostatic repulsion between monomers is reduced ( $\beta$ -lg blue arrow). The simultaneous reduction of electrostatic repulsion allows the protein monomers to come in closer contact. This allows side chains with weak, short-ranged interaction to build weak bridges between the monomers. Electrostatic interactions are some of these short-ranged interactions and were determined as the main stabilizing protein interactions for these conditions. The gels were described as brittle and opaque indicating the formation of particulate rather than fine-stranded structures, as depicted in Figure 4-3.

The main protein interactions stabilizing PPI gels, however, could not be altered by the change in pH or EtOH content. This can be explained by the different molecule structures and the resulting different unfolding and aggregation mechanisms of patatin in comparison to  $\beta$ -lg. Whereas the thiol-disulfide exchange in WPI is initiated by one specific thiol group (the 121-Cys group), the hydrophobic links between patatin monomers can occur through very different side chains. One mode of aggregation is through unfolded hydrophobic amino acids from the protein core (see chapter 3.2). Furthermore, patatin is very hydrophobic overall, even in its native state (Creusot et al., 2011), which explains the aggregation of patatin even at a very low degree of unfolding (see chapter 3.3). So, although the protein sites involved in the patatin aggregation and gelation might change in dependence on the milieu, the aggregation through hydrophobic interactions is always dominant. However, very different structures could be

observed. In dependence on the pH particulate to fine-stranded gels could be created (see chapter 3.4). For gels created in the presence of EtOH the dense PPI network could be loosened with increasing EtOH content (see PPI gels at high EtOH content in chapter 3.6).

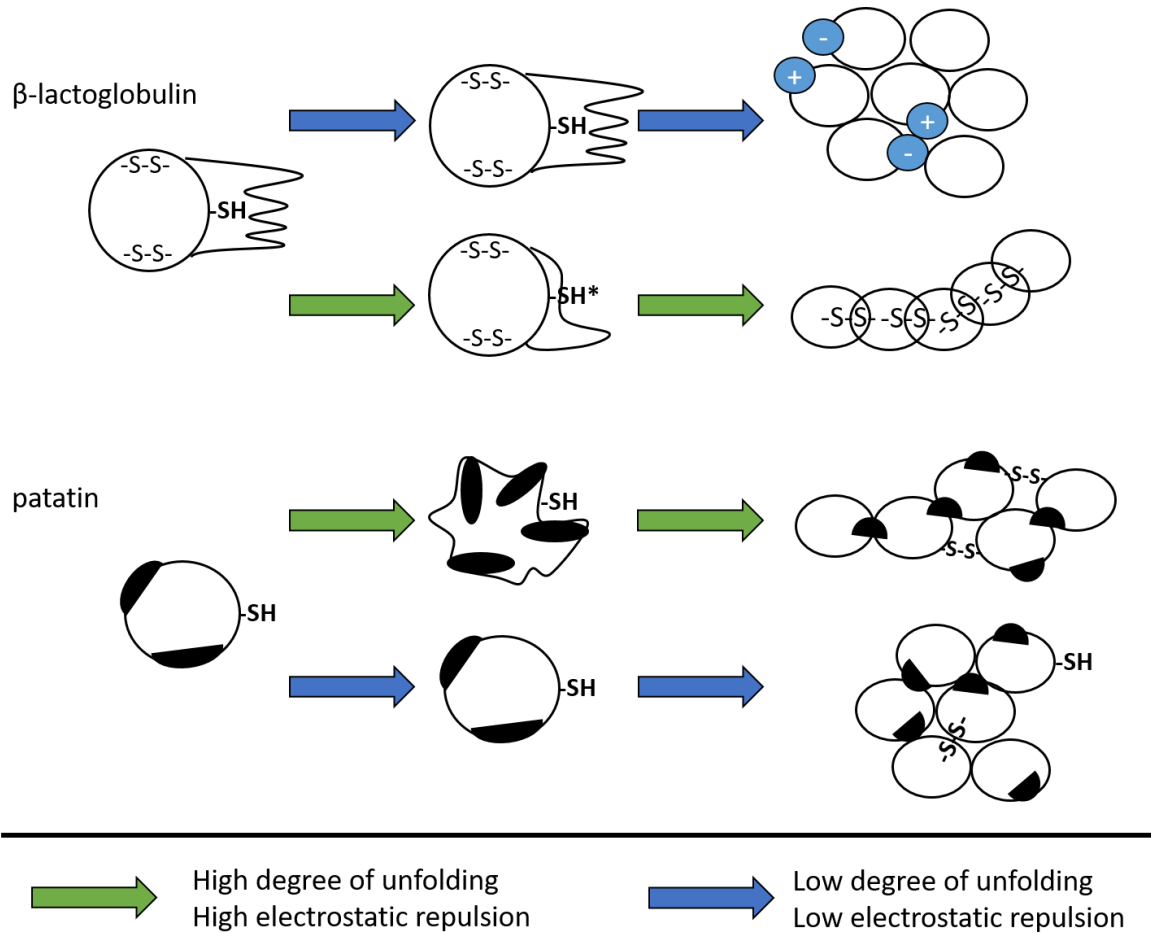


Figure 4-3 Schematic representation of the gelation mechanism of  $\beta$ -lg and patatin in dependence of the milieu conditions. Blue arrows describe reaction pathways under conditions of high protein stability and low electrostatic repulsion (e.g. high EtOH content or pH values close to the IEP). Green arrows describe reaction pathways and conditions of low protein stability and higher electrostatic repulsion (e.g. neutral to alkaline pH and low ionic strength). For  $\beta$ -lg, the  $\alpha$ -helix is schematically drawn. Black spots represent hydrophobic patches

From these findings, different methods for designing protein-based matrices for the food- and bio-industry can be deduced. Depending on the milieu conditions WPI and PPI can produce very similar or completely different textures and microstructures. Therefore when designing a new protein matrix, or trying to substitute one protein with another protein the different gelation mechanisms in dependence on the milieu have to be understood. For example, at pH 7 there were clear differences with WPI gels being strong and elastic and PPI weaker and more brittle (see chapter 3.5). The differences could be explained by differences in protein interaction that stabilize the gels, with strong covalent disulfide bonds in WPI and weaker, non-covalent hydrophobic interactions in PPI.

However, WPI and PPI gels were both very weak and brittle, when created at pH values close to the IEP. For WPI the change from covalent disulfide bonds at pH 7 to non-

covalent electrostatic bonds explained the change in gel properties. However, not only the protein interactions but also the structure of the protein gels played a role in textural properties. At pH 5 PPI gels were weaker and more brittle compared to pH 7, although PPI was stabilized through hydrophobic interactions at both pH values. The formation of bigger aggregates, visible by the change from transparent to opaque gels, could explain the weaker, brittle structure. Close to the IEP the aggregation is very fast and mainly driven by the low electrostatic repulsion between the protein monomers. Although WPI gels were mainly stabilized through electrostatic interactions and PPI gels through hydrophobic interactions the textural properties were very similar at pH 5 with weak and brittle gels for both systems.

For aqueous systems, partially comprised of organic solvents (see chapter 3.6), the textural properties of PPI were nearly unaffected by EtOH and the gels, whereas WPI gels became weak and brittle with higher EtOH content. Again, changes in the main protein interactions could explain these differences. The PPI gels were mainly stabilized through hydrophobic interaction. For WPI the higher EtOH content led to a change from disulfide to electrostatic interactions and the gel properties changed from strong and elastic to weak and brittle. As described above, the different gelation mechanisms occurring in dependence of the milieu could be explained by different unfolding and aggregation mechanisms of the main proteins, patatin and  $\beta$ -lg.

It can be concluded that a detailed investigation into the molecular structure of proteins, including primary, secondary and tertiary structure, is generally required to understand and predict the aggregation and gelation behavior of proteins.

### **4.3 Correlation between rheological properties and the type of protein-protein interactions in protein gels**

Throughout this thesis, it could be shown that  $G'$  of the gel at ambient temperatures in relation to  $G'$  of a gel at elevated temperatures ( $G'_{cool}/G'_{hot}$ ) was indicative of the interactions within the protein gel (see chapters 3.4, 3.5, and 3.6). In the following, the findings of these chapters shall be summarized and a mechanistic explanation of the correlation of  $G'_{cool}/G'_{hot}$  and the protein interactions in a protein gel shall be given. Based on these findings a dynamic temperature sweep will be proposed to obtain more details on the influence of protein interactions on hydrogel stability.

Proteins are linked through very different protein interactions (see chapter 1.1.1), which do not behave uniformly upon heating. The first protein interactions that shall be examined in more detail are electrostatic interactions, also including hydrogen bonds and van der Waals forces. These interactions are based on the attraction of opposite charges. When the temperature has increased the movement of the molecules increases and the attraction between the opposite charges is reduced. This behavior is most similar to a metallic spring. Within the spring, a lattice of electrically charged atoms is responsible for the strength of the metal network. This lattice elongates when it is heated, especially under load. Examples of this behavior can be found in the literature for pea protein gels that were found to be mainly stabilized by electrostatic inter-



actions (Sun & Arntfield, 2012). These gel exhibited higher  $G'$  values at ambient temperature compared to the high temperatures of gelation. Similarly, the addition of kosmotropic ions favored the formation of electrostatic interactions in WPI gels and thus increased  $G'$  upon cooling (Bowland et al., 1995).

Hydrophobic bonds, on the other hand, have a very different temperature dependence. Hydrophobic interactions increase in strength at higher temperatures (Kronberg, 2016). Therefore, if gels are mainly stabilized by hydrophobic interactions the strength of the network should increase when the temperature increases. That increased hydrophobic interactions changed the temperature-dependent rheological properties of hydrogels was described by Bowland et al., (1995), for WPI gels. The protein interactions stabilizing the gel were altered through the addition of different salts. WPI, gelled in the presence of the chaotropic ion  $\text{SCN}^-$ , exhibited an increase in  $G'$  upon heating. Chaotropic ions unfold proteins in a way that favors the exposure of hydrophobic groups from the protein core (see chapter 1.3.3 for more on chaotropic salts). Therefore a WPI gel in the presence of chaotropic ions should be mainly linked through hydrophobic interactions rather than disulfide or electrostatic links.

The third and final protein interactions that shall be examined regarding their temperature dependence are covalent bonds. Covalent bonds lead to a network similar to a rubber band. The temperature dependence of rubber is a classic example to explain thermodynamics in general and entropy in particular (Feynman et al., 1965), which shall be explained in the following for an ideal rubber:

Without the application of external forces, a rubber band can be approximated, on a molecular level, as a bundle of “spaghetti”. The crosslinks between these “spaghettis” force the bundle to be intertwined and twisted rather than elongated. In their coiled and twisted state, the degrees of freedom are higher than in the elongated state, the disorder is increased and therefore the entropy is increased as well. If the rubber band is elongated, for example when an external force is applied, the previously coiled form of the rubber is stretched and the “spaghettis” have fewer possibilities to orient themselves. Therefore, a higher state of order with a lower degree of freedom is reached and the entropy of the system is lowered. If the temperature of this system is increased, the movement of the molecules will lead the system to increase the entropy of the system. This is achieved by preferring the coiled state over the elongated state.

Therefore, a rubber band contracts upon temperature increase, exercising a force on any object attached to the rubber band. In the measurement system of this thesis, the elongation of the sample does not happen with a weight attached but rather in a rheometer. The sample is sheared and depending on the connections within the sample the resistance against this deformation is higher or lower, resulting in higher or lower  $G'$  measurements, respectively. Thus, In a highly covalently linked gel, temperature increase should lead to increased contraction and therefore raise  $G'$ .

However, real rubber-like elastomers seldom behave like the aforementioned ideal rubbers (Mark, 1981). The deviation of WPI gels from an ideal rubber was already noticed by Bowland et al., (1995), where no increase in  $G'$  upon heating could be found.

However, in this study fine stranded gels, which are more covalently linked, exhibited lower  $G'$  increases upon cooling in comparison to other gels. This is also the reason why lower  $G'_{cool}/G'_{hot}$  values were found for gels dominated by disulfide bonds in comparison to non-covalent bonds (Martin et al., 2014). These results responded well to results from this thesis where lower  $G'_{cool}/G'_{hot}$  values were found for covalently cross-linked WPI in comparison to PPI (see chapter 3.5) and lower  $G'_{cool}/G'_{hot}$  values for covalently cross-linked EWP gels in comparison to PPI (see chapter 3.4).

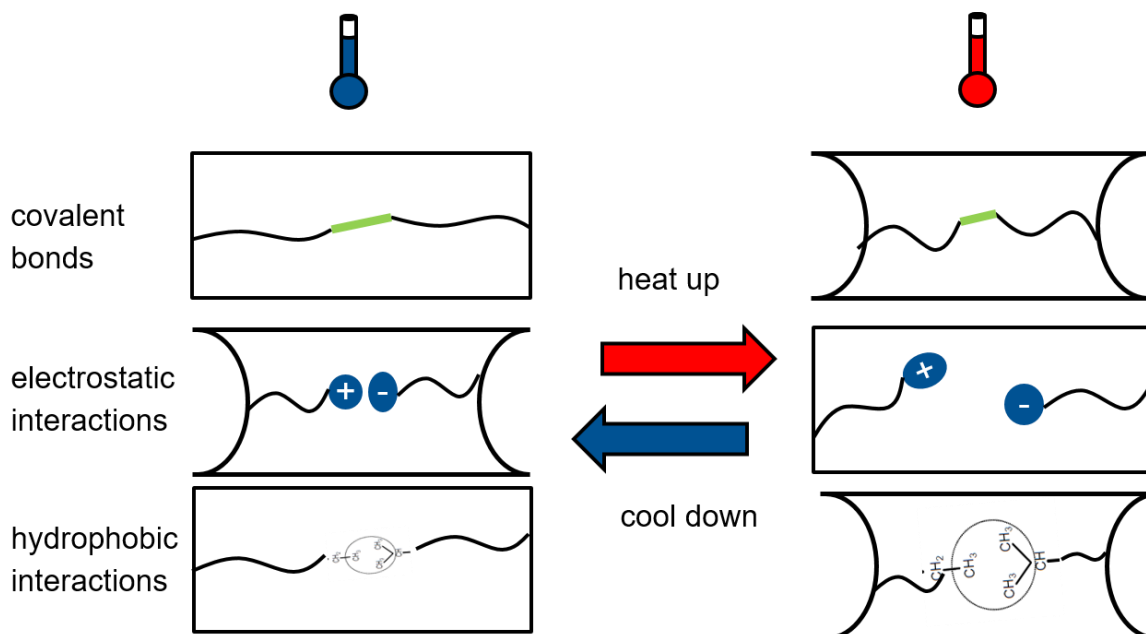


Figure 4-4 Schematic representation of the protein interactions in a gel at low and high temperature levels.

The findings of this thesis and the results presented in the literature can be schematically summarized, as depicted in Figure 4-4. Covalent and hydrophobic interactions increase their influence on the gel network with increasing temperatures, whereas electrostatic interactions are weakened. The influence is thermoreversible. The strength of the protein interactions directly influences the strength of the overall gel. The strength of the gel network can be measured by  $G'$ , through rheological measurements. Therefore changes in  $G'$  in dependence of the temperature can be correlated with changes in protein interactions.

The forces in Figure 4-4, that increase upon heating and the forces that increase upon cooling can be correlated according to the following relation (see Equation (4-1)). If  $G'$  increases upon cooling the influence of electrostatic interactions dominate over hydrophobic interactions. Likewise, lower  $G'_{cool}/G'_{hot}$  values can be indicative of hydrophobic and/or covalent bonds.

$$\frac{G'_{cool}}{G'_{hot}} \xrightleftharpoons{\text{dependence}} \frac{\text{electrostatic interactions and hydrogen bonds}}{\text{hydrophobic interactions and disulfide bonds}} \quad (4-1)$$

As it could be shown,  $G'$  changes in dependence of the temperature, and the results of this thesis (chapter 3.4 to 3.6) showed that these changes can be well explained by

changes in protein interactions. Why different protein interactions behave differently towards temperature changes was explained above.

Although these findings are by themselves helpful in assessing protein interactions in protein gels, there are still some limitations one has to be aware of. Heating conditions throughout the studies were different for different protein gels. This led to the measurement of  $G'_{\text{hot}}$  at different temperatures and thus a higher or lower temperature difference had to be overcome to cool the gels to ambient temperature. Furthermore, the unfolding, aggregation, and gelation might still be ongoing at elevated temperatures. Likewise, some cross-linked protein strands might rearrange during cooling. This would make the measurements of  $G'_{\text{hot}}$  and  $G'_{\text{cool}}$  a measurement of a system still forming interactions and microstructure. Therefore, to exclude these unwanted effects and to fully utilize the correlation between  $G'_{\text{cool}}/G'_{\text{hot}}$  values and protein interactions, a new, temperature-dependent, rheological test was used for hydrogel characterization.

For this, some of the gel systems of this thesis were reanalyzed and were supplemented with protein systems from the literature. The gels were created, either by enzymatic crosslinking or heat-induced gelation. Instead of comparing  $G'$  during the gelation at elevated temperatures, gels were first created and then cooled to room temperature (20 °C). Only after the gels reached room temperature and changes in the viscoelastic properties were completed, the gels were subjected to a temperature sweep. Thereby, the temperature was gradually increased from 20 °C to 50°C with a 1 °C/min heating ramp. The storage modulus ( $G'$ ) and loss factor ( $\tan \delta$ ) were recorded throughout the experiment. By subjecting all gels to the same temperature difference differences in gelation temperature of the different gel systems did not have too much of an influence. Furthermore, by constantly measuring  $G'$  over the defined temperature range  $G'_{\text{cool}}/G'_{\text{hot}}$  becomes a dynamic measurement that allows to investigate of the change in  $G'$  as a true function of temperature, described as  $G'(T)$  in the following.

First, the influence of covalent bonds on  $G'(T)$  should be investigated. For this, a protein system from the literature shall be introduced. Sodium caseinate (NaCas) is a protein mixture of milk-derived proteins with low molecular weight. As NaCas is rich in lysine and glutamine these proteins can be crosslinked through the application of the enzyme transglutaminase (Tgase). Tgase is able to form an isopeptide bond between lysine and glutamine residues thus forming a covalent bond. This way strong, covalently cross-linked hydrogels can be produced, as detailed by Kleemann et al., (2018). Provided that time and temperature of the enzyme treatment are kept constant, the degree of crosslinking is directly correlated with the amount of enzyme interacting with the proteins. To investigate the influence of the degree of crosslinking on  $G'(T)$  four levels of crosslinking were induced in a 10% NaCas solution by adjusting the Tgase activity from 0.5 U/g to 5 U/g. The results can be seen in Figure 4-5. To compare just the temperature dependence of gels with different strength all  $G'(T)$  values were normalized against  $G'$  at room temperature ( $G'(20\text{ °C})$ ).

It can be seen that an increasing concentration of Tgase led to a lower temperature dependence of  $G'$ . Higher enzyme concentrations should lead to a higher degree of

crosslinking in the gel. A higher degree of crosslinking makes the hydrogel more rubber-like. Therefore, increasing the temperature should lead to increases in  $G'$  in an ideal rubber. However, as was discussed above, a complex protein gel is not an ideal rubber and therefore an increase in  $G'(T)$  was not expected. Rather a lower amount of  $G'(T)$  decrease was expected from the data on WPI by Bowland et al., (1995) and Martin et al., (2014) as well as the data PPI/WPI and EWP from chapter 3.5 and 3.4. Nevertheless a lower temperature dependence of  $G'$  could be observed with an increasing degree of crosslinking. To complete the impact of temperature on the viscoelastic properties the loss modulus ( $\tan \delta$ ) was investigated as well. Lower  $\tan \delta$  is thereby indicative for more elastic gels, as was also shown for WPI/PPI hybridgels in chapter 3.5.

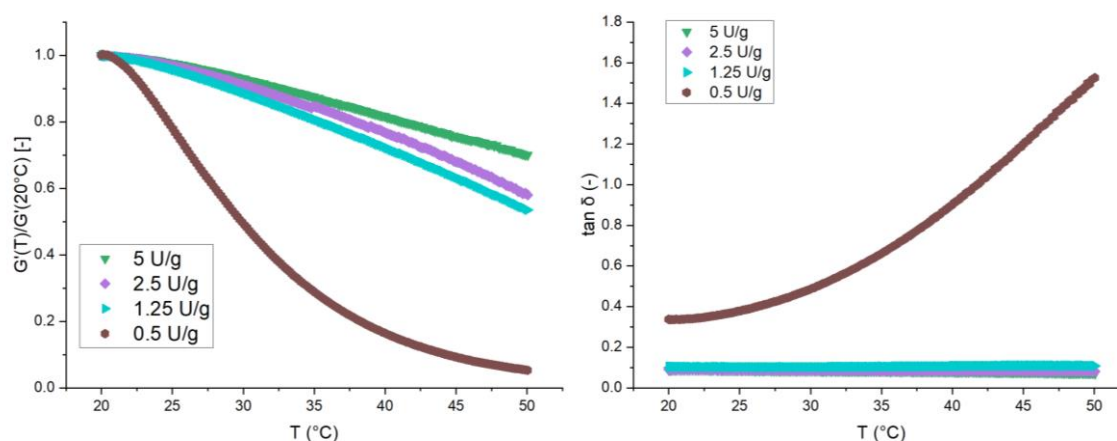


Figure 4-5 change in  $G'$  and  $\tan \delta$  of enzymatically crosslinked NaCas gels in dependence of the temperature at different enzyme concentrations. For better comparability  $G'$  at each temperature point is normalized to  $G'$  at  $20^\circ\text{C}$ .

The  $\tan \delta$  of the NaCas gels, seen in Figure 4-5, exhibited a low temperature dependence, at least for the three highest degrees of crosslinking. Therefore, the relation between  $G'$  and  $G''$  and thus the dominance of elastic over viscous properties within the gels, remained steady throughout the temperature range. For the lowest crosslinking degree a different trend could be observed. The lowest amount of transglutaminase was not able to form a continuous cross-linked gel. This is apparent when looking at  $\tan \delta$  which showed higher values than the completely cross-linked gels, indicating a higher proportion of viscous properties. Furthermore, the transition from a solid gel to a liquid sol ( $\tan \delta > 1$ ) at temperatures  $> 40^\circ\text{C}$  could be observed. In a similar way, heat-set gels from WPI and PPI were investigated by the aforementioned temperature sweep. The results will be viewed in light of the temperature dependence of covalent bonds described above for NaCas. Furthermore, electrostatic and hydrophobic will also play a more important role in these gels. Protein solutions of WPI (15% protein; 7.5 % for pH 3) and PPI (10% protein) were heated for 30 min at different pH and temperature levels (see Figure 4-6). After the heating period, the gels were cooled down to room temperature ( $20^\circ\text{C}$ ). This was followed by a temperature sweep from  $20^\circ\text{C}$  to  $50^\circ\text{C}$ , as described above.

The protein samples exhibited different temperature dependences of  $G'$  as well as the measured  $\tan \delta$ . The different gel structures that were produced in dependence of the pH and the implications these structures have on the temperature of  $G'$  and  $\tan \delta$  shall be explained in the following.

First of all the WPI gel at pH 10 showed a low temperature-dependence of  $G'$  and a stable and low  $\tan \delta$ . At pH 10 the thiol groups in WPI are highly reactive and the high electrostatic repulsion between the protein monomers leads to a very finely-stranded gel. This explains why aerogels from WPI at pH 10 were shown to have a high inner surface area (Kleemann et al., 2018). Therefore a high degree of crosslinking can be assumed in WPI gelled at pH 10. This high degree of crosslinking through disulfide bonds explains why WPI at pH 10 behaved similarly to the NaCas gels cross-linked by isopeptide bonds. Although the crosslinking mechanisms are different, both types of bonds, disulfide bonds and transglutaminase induced peptide bonds, are covalent chemical bonds that make the protein gel more “rubber-like”.

PPI gels at pH 7 and WPI gels at pH 3 showed a different temperature dependence. Both systems decreased in  $\tan \delta$  in dependence of the temperature, which can be interpreted as a sort of solidification as the elastic contribution in the gel increases (a higher proportion of  $G'$  in relation to  $G''$ ).  $G'$  decreased in dependence of the temperature, although for WPI at pH 3 the  $G'$  increased above 40 °C. WPI at this pH is expected to be mainly linked through hydrophobic interactions (Monahan et al., 1995). As hydrophobic interactions increase upon heating, some increase in  $G'$  is reasonable to assume. The high charge around the monomers at pH 3 should further prevent the occurrence of other short-ranged interactions. Furthermore, the high charge of the protein should lead to a higher degree of unfolding with complete exposure of hydrophobic groups from the protein core. As PPI at pH 7 is lacking such high charges the influence of electrostatic and other short-ranged interactions cannot be neglected.

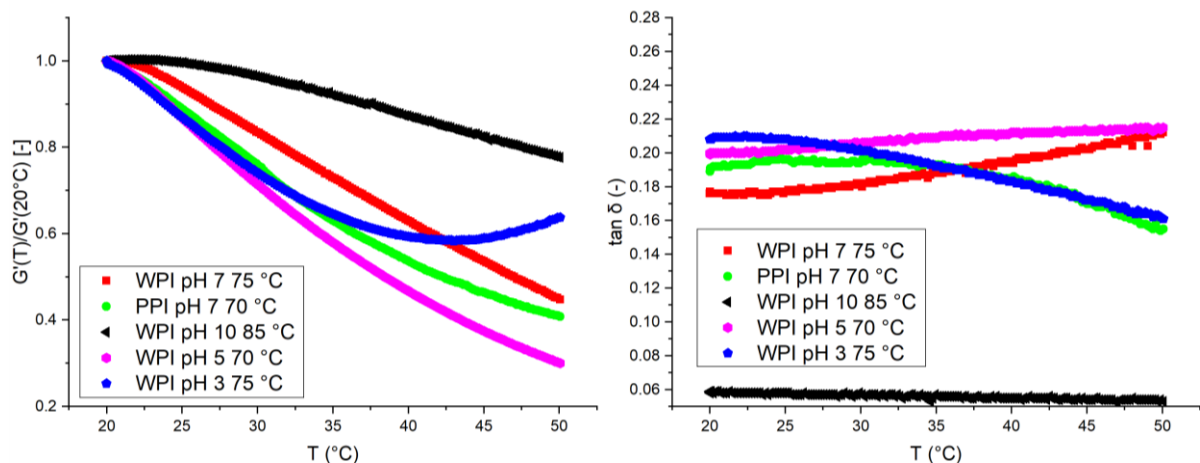


Figure 4-6 change in  $G'$  and  $\tan \delta$  of heat-induced WPI and PPI gels in dependence of the temperature. For better comparability  $G'$  at each temperature point is normalized to  $G'$  at 20°C.

WPI at pH 7 exhibited a higher temperature dependence than WPI at pH 10 but a lower than PPI at pH 7. Regarding  $\tan \delta$ , an increase in dependence of the temperature could be observed, indicating a more viscous behavior. The higher temperature dependence

and increase in viscosity indicate a lower amount of crosslinking in WPI at pH 7 compared to 10, which is reasonable to assume. That  $\tan \delta$  increased rather than decreased could hint at the low amount of hydrophobic interactions in WPI at pH 7 compared to PPI and WPI at pH 3. Instead, electrostatic interactions should play a role in WPI gelation, as was shown before (see chapters 3.5 and 3.6). These bonds decrease in strength with increasing temperature and could well explain the decrease in  $G'$  as well as the increase in  $\tan \delta$  in dependence of the temperature. The temperature-dependent behavior of electrostatic interaction is also evident for WPI at pH 5 which was already shown to be mainly stabilized by electrostatic interactions (see chapter 3.1). WPI at pH 5 exhibited the highest loss of  $G'$  in dependence on the temperature. This was also accompanied by a small increase in  $\tan \delta$ . The loss in  $G'$  can be easily explained by the predominant electrostatic interactions that stabilize this protein gel. As explained in the introduction to this chapter, electrostatic interactions are very susceptible to increases in thermal movement.

To complete the types of proteins investigated in this thesis, protein gels from PPI and WPI at high EtOH concentrations were evaluated by the same temperature sweep, as well (see Figure 4-7).

It can be seen that PPI and WPI gels behaved differently in dependence on the temperature. PPI gels with 20% EtOH exhibited an increase in  $G'$  above 40 °C and a decrease in  $\tan \delta$ , which is very similar to what was described for the hydrophobic linked WPI pH 3 gels. Similar to WPI at pH 3, PPI gels at 20% EtOH were shown to be mainly hydrophobically linked (see chapter 3.6).

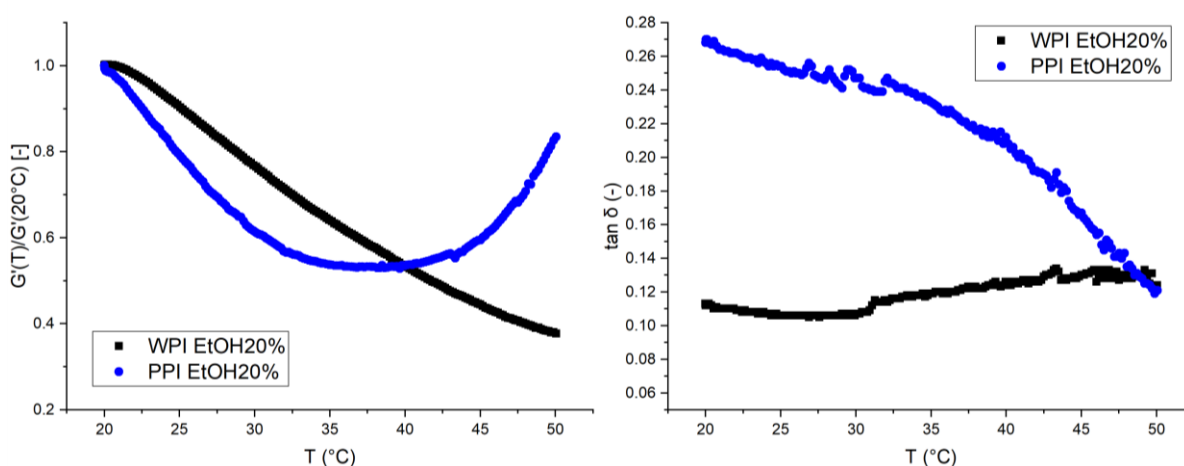


Figure 4-7 change in  $G'$  and  $\tan \delta$  of heat-induced WPI and PPI gels with 20% EtOH in dependence of the temperature. For better comparability  $G'$  at each temperature point is normalized to  $G'$  at 20°C.

Furthermore, it was proposed that patatin may unfold to a higher degree in ethanolic solutions another similarity between this protein system and WPI at pH 3. This might explain why PPI gels at 20% EtOH (Figure 4-7) behaved more as one would expect from hydrophobic linked WPI gels than PPI without any EtOH addition (Figure 4-6). WPI in the presence of 20% EtOH on the other hand exhibited a stark decrease in  $G'$  accompanied by a slight increase in  $\tan \delta$ . This behavior was very similar to WPI at

pH 5. Both gels are mainly stabilized through electrostatic links (see chapters 3.1 and 3.6) which should explain the temperature dependence of their viscoelastic properties.

From these rheological characterizations of different protein gels following trends can be concluded: Although very different protein gels were investigated, their viscoelastic properties in dependence of the temperature, mainly  $G'$  and  $\tan \delta$ , could be explained by the occurrence and strength of different protein interactions. Depending on the protein interactions the strength of the interactions either decreased or increased in dependence on the temperature, according to the relationship described in Equation (4-1).

The results could be well explained by the protein interactions that were described across the chapters of this thesis as well as literature data. Some general trends regarding in the change of viscoelastic properties in hydrogels in dependence on temperature could be found. For covalent links, a low temperature dependence of  $G'$  and  $\tan \delta$  could be found. Low  $\tan \delta$  further indicated very elastic gels. The strong chemical bonds, therefore, resisted breakage induced through temperature changes. For electrostatic interactions, the big decreases in  $G'$  and small increases in  $\tan \delta$  could be found. This showed that interactions became considerably weaker with increasing temperatures. Hydrophobic interactions showed first a small decrease followed by an increase in  $G'$ . Furthermore,  $\tan \delta$  decreased with higher temperatures indicating the formation of more elastic and less viscous gels. All these changes in viscoelastic properties of hydrogel linked by different protein interactions are schematically summarized in Figure 4-8.

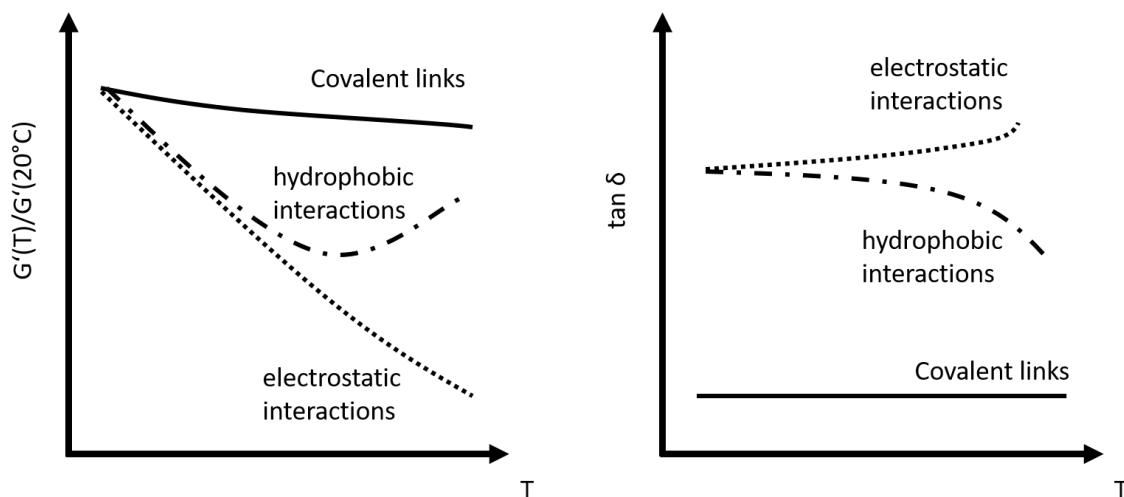


Figure 4-8 Schematic representation of the changes in viscoelastic properties in dependence of the temperature for different protein gels. These general relationships between protein interactions within protein gels, rheological properties ( $G'$  and  $\tan \delta$ ), and the temperature ( $T$ ) were derived from the protein gels analyzed in Figure 4-5 to Figure 4-7.

Therefore, the here presented temperature sweep performed on a fully formed hydrogel allows investigating protein interactions in an easy to conduct way by a swift rheological measurement. In the future, this measurement could be used on very different gel types, not just protein gels, and will be a useful addition to rheological characterizations such as frequency and amplitude sweeps.





## 5 Summary & Zusammenfassung

### 5.1 Summary

Proteins are one of the basic components of food. These bio-molecules can unfold and aggregate under conditions of stress, such as increased temperatures or in the presence of organic solvents. These aggregated proteins then can even form higher-order structures such as hydrogels. Hydrogels are porous, water-filled structures and are one of the most important structural agents in food formulations. Understanding the relationship between protein folding and unfolding behavior and the resulting aggregation and gelation events is very important for the creation of foodstuff in a predictable and targeted manner.

The structure-function relationship between molecule structure and gelation properties is especially important concerning the new wave of proteins entering the market. Novel protein sources, especially from plants, are of interest to the food industry as they present a new and more sustainable alternative to animal-derived proteins. However, a simple substitution of animal proteins is not always possible as plant proteins often exhibit very different techno-functional properties. Furthermore, plant proteins offer the possibility, not only to substitute animal proteins but also to create completely novel textures.

One such protein is patatin which is obtained from the potato tuber. Although it is also a water-soluble protein, similar to whey proteins, it exhibits very different gelation properties. Instead of strong covalent disulfide links, patatin utilizes hydrophobic interactions to form gels. However, details of its aggregation and gelation properties were not widely known before this thesis.

A very interesting, novel application of proteins is the creation of aerogels. These structures are obtained from hydrogels in a two-step process. First, the hydrogels are washed in ethanol (EtOH) to exchange the water within the gel network pores with EtOH. These alcogels then can be dried through an extraction step with supercritical CO<sub>2</sub> (scCO<sub>2</sub>). After the extraction of EtOH a dry, porous protein network is obtained. This gel structure is called aerogel. These aerogels can be used to encapsulate hydrophobic nutra- and pharmaceuticals with a controlled release mechanism. Also, applications in biomedicine, packaging, or as oil structuring agents for food application were explored recently. Besides these interesting fields of application, the creation of aerogels has underutilized scientific implications. The gentle drying through scCO<sub>2</sub> preserves the pore structure and therefore the analysis of the aerogels can give valuable information about the microstructure of protein gels.

All this led to the following objectives of this thesis:

- To investigate the aggregation mechanism of the novel protein source potato protein in form of a potato protein isolate (PPI)
- To assess the feasibility to produce stable, porous aerogels from non-covalently linked potato proteins
- To describe protein interactions and microstructure of potato protein gels

- To explore the possibility to use EtOH as a way to influence the gelation of potato and whey proteins
- To compare potato and whey protein gelation and understand the link between molecular differences of the protein structure and different responses towards changes in milieu and heating conditions

To achieve these objectives, the following investigations were conducted. A new method was developed to quantify the protein interactions that stabilize a protein hydrogel, namely electrostatic, hydrophobic, and disulfide bonds. It could be shown that these major three protein interactions could be reliably and reproducibly detected and the method can track changes in the gelation behavior of a protein source under different conditions.

Furthermore, the unfolding and aggregation mechanism of PPI was investigated in detail. For this, different analytical chromatographic methods were established. It could be shown that PPI can form covalently linked aggregates. However, the main interactions were still hydrophobic. The size and exposed hydrophobicity of PPI aggregates could be influenced by the pH conditions. Lower pH values led to bigger aggregates with higher exposed hydrophobicity and vice versa. The size could be further influenced by the temperature during aggregation. At pH closer to the isoelectric point (IEP) lower temperatures led to bigger aggregates compared to higher temperatures. Furthermore, it could be shown that the aggregation mechanism of PPI changes in dependence on the temperature. The research into the aggregation mechanism revealed that PPI aggregates through a very different mechanism, compared to WPI. How these different mechanisms then led to novel gel structures was further investigated.

Aerogels from PPI hydrogels were successfully created. This way the feasibility to create highly porous, mechanically stable aerogels from a primarily hydrophobically linked protein gel could be shown. PPI aerogels with similar inner surface areas (BET) as WPI aerogels could be produced. Furthermore, a direct correlation between the pH-dependent microstructure and a rheological parameter could be found. The rheological characterization evaluated the storage modulus of the gel at ambient temperature ( $G'_{cool}$ ) in relation to the storage modulus of the gel at gelation temperature ( $G'_{hot}$ ). Higher BET values were measured for gels with low  $G'_{cool}/G'_{hot}$  values and vice versa. The  $G'_{cool}/G'_{hot}$  values changed independently of the pH, with high  $G'_{cool}/G'_{hot}$  values for pH values at very acidic conditions, low values close to the IEP, and intermediate values for neutral and alkaline pH values. A similar correlation between  $G'_{cool}/G'_{hot}$  values and BET was also found for egg white protein aerogels, indicating a general correlation between  $G'_{cool}/G'_{hot}$  and microstructure for protein gels.

In order to better understand how protein interactions influence gel microstructures PPI and WPI hybrid gels with different ratios of PPI and WPI were created. This way gels with a wide range of textures and viscoelastic properties could be created. Up to a ratio of 50:50, PPI was the protein with the dominating properties resulting in brittle gels with low elasticity. It could be clearly shown that up to 50:50 mixtures no continuous disulfide networks could be built up which explains the weakness and low elasticity of these

gels. With increasing WPI content the gels were stronger and more elastic. Interestingly at pH 5 close to the IEP of WPI and PPI, the textural properties were very similar independent of the mixing ratio. This is especially interesting as, at pH 5, WPI was stabilized through electrostatic and PPI through hydrophobic interactions. The opacity for these gels indicated the formation of big aggregates. Therefore, it is important to understand that not only protein interactions determine macroscopic textural properties but also the size and structure of the aggregates that build up the gels. Changes in protein interactions correlated with changes in  $G'_{cool}/G'_{hot}$  values which indicated the strong correlation between these parameters.

In the last part of the study ethanol (EtOH) was used to induce novel structures in PPI and WPI gels. These ethanolic hydrogels were then successfully processed into aerogels. At higher EtOH concentrations the gelation mechanism von WPI changed from disulfide-linked to electrostatic linked gels, contrary to PPI which remained hydrophobically linked. Nevertheless, both gel systems opaque at higher EtOH concentrations, similar to gelation at pH close to their IEPs. The microstructural analysis of the aerogels showed that high BET values could be created for both protein systems with and without the addition of EtOH. Nevertheless, BET and skeletal density could be changed through the addition of EtOH, emphasizing the possibility to tailor aerogel properties according to the need of possible applications. Furthermore, by reducing the denaturation temperature the addition of EtOH allowed the creation of gels at lower temperatures compared to protein systems without EtOH.

This thesis highlights the differences that occur in the gelation of different protein systems for example PPI and WPI. WPI was mainly dependent on the reactivity of its free thiol group. When the reactivity was reduced through milieu conditions (high EtOH or pH close to IEP) the protein interactions occurring changed from disulfide-linked to electrostatic linked. Contrary to this PPI is mainly dependent on hydrophobic interactions. These interactions can occur on many different reactive sites on the proteins. Especially the developed protein interactions assay, as well as the rheological characterization of  $G'_{cool}/G'_{hot}$  were shown to be a useful tool to understand how protein structures are formed.

## 5.2 Zusammenfassung

Proteine sind einer der Hauptbestandteile von Lebensmitteln. Diese Biomoleküle können sich unter bestimmten Bedingungen, wie erhöhten Temperaturen oder in Gegenwart organischer Lösungsmittel, entfalten und aggregieren. Diese aggregierten Proteine können dann Strukturen höherer Ordnung wie Hydrogele bilden. Hydrogele sind poröse, wassergefüllte Strukturen und gehören zu den wichtigsten Strukturgebern in Lebensmitteln. Das Verständnis der Beziehung zwischen dem Faltungs- und Entfaltungsverhalten von Proteinen und den daraus resultierenden Aggregations- und Gelierungsvorgängen ist für die vorhersehbare und gezielte Herstellung von Lebensmitteln unabdingbar.

Die Struktur-Funktions-Beziehung zwischen Molekülstruktur und Geliereigenschaften ist besonders wichtig für neue Proteine, die auf den Markt kommen. Neuartige Proteinquellen, insbesondere aus Pflanzen, sind für die Lebensmittelindustrie von Interesse, da sie eine neue und nachhaltigere Alternative zu Proteinen tierischen Ursprungs darstellen. Eine einfache Substitution von tierischen Proteinen ist jedoch nicht immer möglich, da Pflanzenproteine oft sehr unterschiedliche techno-funktionelle Eigenschaften aufweisen. Darüber hinaus bieten pflanzliche Proteine die Möglichkeit, nicht nur tierische Proteine zu ersetzen, sondern auch völlig neue Texturen zu schaffen.

Ein solches Protein ist Patatin, das aus der Kartoffelknolle gewonnen wird. Obwohl es ebenfalls ein wasserlösliches Protein ist, ähnlich wie Molkenproteine, weist es ganz andere Geliereigenschaften auf. Anstelle von starken kovalenten Disulfidbindungen nutzt Patatin hydrophobe Wechselwirkungen, um Gele zu bilden. Die Details seiner Aggregations- und Gelierungseigenschaften waren jedoch vor dieser Arbeit noch nicht allgemein bekannt.

Eine sehr interessante, neuartige Anwendung von Proteinen ist die Herstellung von Aerogelen. Diese Strukturen werden in einem zweistufigen Verfahren aus Hydrogelen gewonnen. Zunächst werden die Hydrogele in Ethanol (EtOH) gewaschen, um das Wasser in den Poren des Gel-Netzwerks mit EtOH auszutauschen. Diese Alkogegele können dann durch einen Extraktionsschritt mit überkritischem CO<sub>2</sub> (scCO<sub>2</sub>) getrocknet werden. Nach der Extraktion von EtOH erhält man ein trockenes, poröses Proteinnetzwerk. Diese Gelstruktur wird als Aerogel bezeichnet. Diese Aerogele können zur Verkapselung von hydrophoben Nährstoffen und Arzneimitteln mit einem kontrollierten Freisetzungsmechanismus verwendet werden. Kürzlich wurden auch Anwendungen in der Biomedizin, in der Verpackungstechnologie oder als Ölstrukturierungsmittel (Oleogelator) für Lebensmittel erforscht. Neben diesen interessanten Anwendungsgebieten hat die Herstellung von Aerogelen noch ungenutzte wissenschaftliche Implikationen. Durch die schonende Trocknung mit scCO<sub>2</sub> bleibt die Porenstruktur erhalten, so dass die Analyse der Aerogele wertvolle Informationen über die Mikrostruktur von Proteingelen liefern kann.

All dies führte zu den folgenden Zielen dieser Arbeit:

- Untersuchung des Aggregationsmechanismus der neuen Proteinquelle Kartoffelprotein in Form eines Kartoffelproteinisolats (PPI)
- Bewertung der Machbarkeit der Herstellung stabiler, poröser Aerogele aus nicht kovalent gebundenen Kartoffelproteinen
- Beschreibung der Proteininteraktionen und der Mikrostruktur von Kartoffelproteingelen
- Untersuchung der Möglichkeit, die Gelierung von Kartoffel- und Molkenproteinen mit EtOH zu beeinflussen
- Vergleich der Gelierung von Kartoffel- und Molkenproteinen und Verständnis des Zusammenhangs zwischen den molekularen Unterschieden in der Proteinstruktur und den unterschiedlichen Reaktionen auf Veränderungen des Milieus und der Erhitzungsbedingungen

Um diese Ziele zu erreichen, wurden folgende Untersuchungen durchgeführt. Es wurde eine neue Methode zur Quantifizierung der Proteinwechselwirkungen entwickelt, die ein Proteinhydrogel stabilisieren, vor allem elektrostatische, hydrophobe und Disulfidbindungen. Es konnte gezeigt werden, dass diese drei wichtigsten Proteinwechselwirkungen zuverlässig und reproduzierbar nachgewiesen werden können und die Methode Veränderungen im Gelierverhalten einer Proteinquelle unter verschiedenen Bedingungen verfolgen kann.

Darüber hinaus wurde der Entfaltungs- und Aggregationsmechanismus von PPI im Detail untersucht. Dazu wurden unterschiedliche chromatographische Analyseverfahren angewendet. Es konnte gezeigt werden, dass PPI kovalent verknüpfte Aggregate bilden können. Die wichtigsten Wechselwirkungen waren jedoch weiterhin hydrophober Natur. Die Größe und die Hydrophobizität der PPI-Aggregate konnten durch die pH-Bedingungen beeinflusst werden. Niedrigere pH-Werte führten zu größeren Aggregaten mit höherer Hydrophobizität und umgekehrt. Die Größe konnte auch durch die Temperatur während der Aggregation beeinflusst werden. Bei einem pH-Wert, der näher am isoelektrischen Punkt (IEP) liegt, führten niedrigere Temperaturen zu größeren Aggregaten im Vergleich zu höheren Temperaturen. Außerdem konnte gezeigt werden, dass sich der Aggregationsmechanismus von PPI in Abhängigkeit von der Temperatur ändert. Die Untersuchung des Aggregationsmechanismus ergab, dass PPI im Vergleich zu WPI über einen ganz anderen Mechanismus aggregiert. Wie diese unterschiedlichen Mechanismen dann zu neuartigen Gelstrukturen führen, wurde weiter untersucht.

Es wurden erfolgreich Aerogele aus PPI-Hydrogelen hergestellt. Auf diese Weise konnte gezeigt werden, dass es möglich ist, hochporöse, mechanisch stabile Aerogele aus einem primär hydrophob verknüpften Proteingel herzustellen. Es konnten PPI-Aerogele mit ähnlichen inneren Oberflächen (BET) wie WPI-Aerogele hergestellt werden. Weiterhin konnte eine direkte Korrelation zwischen der pH-abhängigen Mikrostruktur und einem rheologischen Parameter gefunden werden. Bei der rheologischen Charakterisierung wurde der Speichermodul des Gels bei Raumtemperatur ( $G'_{cool}$ ) im Verhältnis zum Speichermodul des Gels bei Geliertemperatur ( $G'_{hot}$ ) bewertet. Höhere BET-Werte wurden für Gele mit niedrigen  $G'_{cool}/G'_{hot}$ -Werten gemessen und umgekehrt. Die

$G'_{cool}/G'_{hot}$ -Werte änderten sich unabhängig vom pH-Wert, mit hohen  $G'_{cool}/G'_{hot}$ -Werten für pH-Werte bei sehr sauren Bedingungen, niedrigen Werten in der Nähe des IEP und mittleren Werten für neutrale und alkalische pH-Werte. Eine ähnliche Korrelation zwischen  $G'_{cool}/G'_{hot}$ -Werten und BET wurde auch für Eiklar-Aerogele festgestellt, was auf eine allgemeine Korrelation zwischen  $G'_{cool}/G'_{hot}$  und der Mikrostruktur von Proteingelen hinweist.

Um besser zu verstehen, wie Proteininteraktionen die Gelmikrostrukturen beeinflussen, wurden PPI- und WPI-Hybridgele mit unterschiedlichen Verhältnissen von PPI und WPI hergestellt. Auf diese Weise konnten Gele mit einer breiten Palette von Texturen und viskoelastischen Eigenschaften hergestellt werden. Bis zu einem Verhältnis von 50:50 war PPI das Protein mit den dominierenden Eigenschaften, was zu spröden Gelen mit geringer Elastizität führte. Es konnte deutlich gezeigt werden, dass bis zu 50:50-Mischungen keine kontinuierlichen Disulfidnetzwerke aufgebaut werden konnten, was die Schwäche und geringe Elastizität dieser Gele erklärt. Mit zunehmendem WPI-Gehalt wurden die Gele stärker und elastischer. Interessanterweise waren bei einem pH-Wert von 5, der in der Nähe des IEP von WPI und PPI lag, die textuellen Eigenschaften unabhängig vom Mischungsverhältnis sehr ähnlich. Dies ist besonders interessant, da bei pH 5 die WPI durch elektrostatische und die PPI durch hydrophobe Wechselwirkungen stabilisiert wurden. Die Undurchsichtigkeit dieser Gele deutet auf die Bildung großer Aggregate hin. Daher ist es wichtig zu verstehen, dass nicht nur Proteinwechselwirkungen die makroskopischen Textureigenschaften bestimmen, sondern auch die Größe und Struktur der Aggregate, die die Gele bilden. Änderungen der Proteinwechselwirkungen korrelierten mit Änderungen der  $G'_{cool}/G'_{hot}$ -Werte, was auf eine starke Korrelation zwischen diesen Parametern hinweist.

Im letzten Teil der Studie wurde Ethanol (EtOH) verwendet, um neue Strukturen in PPI- und WPI-Gelen zu erzeugen. Diese ethanolischen Hydrogele wurden dann erfolgreich zu Aerogelen verarbeitet. Bei höheren EtOH-Konzentrationen änderte sich der Gelierungsmechanismus in WPI von disulfidisch verknüpften zu elektrostatisch verknüpften Gelen, im Gegensatz zu PPI, das hydrophobisch verknüpft blieb. Dennoch waren beide Gelsysteme bei höheren EtOH-Konzentrationen undurchsichtig, ähnlich wie bei der Gelierung bei einem pH-Wert in der Nähe ihrer IEPs. Die mikrostrukturelle Analyse der Aerogele zeigte, dass für beide Proteinsysteme mit und ohne Zusatz von EtOH hohe BET-Werte erzielt werden konnten. Die BET-Werte und die Skelettdichte konnten jedoch durch die Zugabe von EtOH verändert werden, was die Möglichkeit unterstreicht, die Eigenschaften der Aerogele je nach den Anforderungen möglicher Anwendungen anzupassen. Durch die Verringerung der Denaturierungstemperatur ermöglichte die Zugabe von EtOH außerdem die Herstellung von Gelen bei niedrigeren Temperaturen im Vergleich zu Proteinsystemen ohne EtOH.

Diese Arbeit zeigt die Unterschiede bei der Gelierung verschiedener Proteinsysteme am Beispiel von PPI und WPI auf. WPI war hauptsächlich von der Reaktivität seiner freien Thiolgruppe abhängig. Wurde die Reaktivität durch Milieubedingungen (hoher EtOH-Gehalt oder pH-Wert nahe IEP) reduziert, änderten sich die auftretenden Proteininteraktionen von kovalent gebunden zu elektrostatisch gebunden. Im Gegensatz

dazu ist PPI hauptsächlich auf hydrophobe Wechselwirkungen angewiesen. Diese Wechselwirkungen können an vielen verschiedenen reaktiven Stellen auf den Proteinen auftreten. Insbesondere der entwickelte Assay für Proteininteraktionen sowie die rheologische Charakterisierung von  $G'_{cool}/G'_{hot}$  haben sich als nützliches Werkzeug erwiesen, um zu verstehen, wie Proteinstrukturen gebildet werden.





## 6 References

- Ainis, W.N.; Ersch, C.; Ipsen, R. (2018): Partial replacement of whey proteins by rapeseed proteins in heat-induced gelled systems: Effect of pH. *Food Hydrocolloids*. 77: 397–406 DOI: 10.1016/j.foodhyd.2017.10.016.
- Akyol, H.; Riciputi, Y.; Capanoglu, E.; Caboni, M.F.; Verardo, V. (2016): Phenolic Compounds in the Potato and Its Byproducts: An Overview. *International journal of molecular sciences*. 17 (6): 835 DOI: 10.3390/ijms17060835.
- Alting, A.C.; Hamer, R.J.; Kruif, C.G. de; Visschers, R.W. (2000): Formation of Disulfide Bonds in Acid-Induced Gels of Preheated Whey Protein Isolate. *Journal of Agricultural and Food Chemistry*. 48 (10): 5001–5007 DOI: 10.1021/jf000474h.
- Alves, A.C.; Tavares, G.M. (2019): Mixing animal and plant proteins: Is this a way to improve protein techno-functionalities? *Food Hydrocolloids*. 97: 105171 DOI: 10.1016/j.foodhyd.2019.06.016.
- Andlinger, D.J.; Bornkeßel, A.C.; Jung, I.; Schröter, B.; Smirnova, I.; Kulozik, U. (2021a): Microstructures of potato protein hydrogels and aerogels produced by thermal crosslinking and supercritical drying. *Food Hydrocolloids*. 112: 106305 DOI: 10.1016/j.foodhyd.2020.106305.
- Andlinger, D.J.; Rampp, L.; Tanger, C.; Kulozik, U. (2021b): Viscoelasticity and Protein Interactions of Hybrid Gels Produced from Potato and Whey Protein Isolates. *ACS Food Science & Technology*. 1 (7): 1304–1315 DOI: 10.1021/acsfoodscitech.1c00163.
- Andlinger, D.J.; Röscheisen, P.; Hengst, C.; Kulozik, U. (2021c): Influence of pH, Temperature and Protease Inhibitors on Kinetics and Mechanism of Thermally Induced Aggregation of Potato Proteins. *Foods*. 10 (4): 796 DOI: 10.3390/foods10040796.
- Andrews, D.L.; Beames, B.; Summers, M.D.; Park, W.D. (1988): Characterization of the lipid acyl hydrolase activity of the major potato (*Solanum tuberosum*) tuber protein, patatin, by cloning and abundant expression in a baculovirus vector. *Biochemical Journal*. 252 (1): 199–206 DOI: 10.1042/bj2520199.
- Anema, S.G.; Lee, S.K.; Klostermeyer, H. (2006): Effect of protein, nonprotein-soluble components, and lactose concentrations on the irreversible thermal denaturation of beta-lactoglobulin and alpha-lactalbumin in skim milk. *Journal of Agricultural and Food Chemistry*. 54 (19): 7339–7348 DOI: 10.1021/jf061508.
- Arntfield, S.D.; Murray, E.D.; Ismond, M.A.H. (1991): Role of disulfide bonds in determining the rheological and microstructural properties of heat-induced protein networks from ovalbumin and vicilin. *Journal of Agricultural and Food Chemistry*. 39 (8): 1378–1385 DOI: 10.1021/jf00008a005.

- Badkar, A.; Yohannes, P.; Banga, A. (2006): Application of TZERO calibrated modulated temperature differential scanning calorimetry to characterize model protein formulations. *International journal of pharmaceutics*. 309 (1-2): 146–156 DOI: 10.1016/j.ijpharm.2005.11.026.
- Baetens, R.; Jelle, B.P.; Gustavsen, A. (2011): Aerogel insulation for building applications: A state-of-the-art review. *Energy and Buildings*. 43 (4): 761–769 DOI: 10.1016/j.enbuild.2010.12.012.
- Baldwin, A.J. (2010): Insolubility of milk powder products - - A minireview. *Dairy Science & Technology*. 90 (2): 169 – 179 DOI: 10.1051/dst/2009056.
- Bártová, V.; Bárta, J. (2009): Chemical composition and nutritional value of protein concentrates isolated from potato (*Solanum tuberosum* L.) fruit juice by precipitation with ethanol or ferric chloride. *Journal of Agricultural and Food Chemistry*. 57 (19): 9028–9034 DOI: 10.1021/jf900897b.
- Bauer, R.; Carrotta, R.; Rischel, C.; Øgandal, L. (2000): Characterization and Isolation of Intermediates in  $\beta$ -Lactoglobulin Heat Aggregation at High pH. *Biophysical Journal*. 79 (2): 1030–1038 DOI: 10.1016/S0006-3495(00)76357-0.
- Betz, M.; Hörmansperger, J.; Fuchs, T.; Kulozik, U. (2012): Swelling behaviour, charge and mesh size of thermal protein hydrogels as influenced by pH during gelation. *Soft Matter*. 8 (8): 2477–2485 DOI: 10.1039/C2SM06976H.
- Borderías, A.J.; Tovar, C.A.; Domínguez-Timón, F.; Díaz, M.T.; Pedrosa, M.M.; Moreno, H.M. (2020): Characterization of healthier mixed surimi gels obtained through partial substitution of myofibrillar proteins by pea protein isolates. *Food Hydrocolloids*. 107: 105976 DOI: 10.1016/j.foodhyd.2020.105976.
- Bourne, M.C. (2002): *Food texture and viscosity*. 2nd ed. San Diego: Academic Press ISBN: 9780121190620.
- Bowland, E.L.; Foegeding, A.E. (1995): Effects of anions on thermally induced whey protein isolate gels. *Food Hydrocolloids*. 9 (1): 47–56 DOI: 10.1016/S0268-005X(09)80193-8.
- Bowland, E.L.; Foegeding, A.E.; Hamann, D.D. (1995): Rheological analysis of anion-induced matrix transformations in thermally induced whey protein isolate gels. *Food Hydrocolloids*. 9 (1): 57–64 DOI: 10.1016/S0268-005X(09)80194-X.
- Boye, J.I.; Alli, I. (2000): Thermal denaturation of mixtures of  $\alpha$ -lactalbumin and  $\beta$ -lactoglobulin: a differential scanning calorimetric study. *Food Research International*. 33 (8): 673–682 DOI: 10.1016/S0963-9969(00)00112-5.
- Boye, J.I.; Ma, C.-Y.; Ismail, A.; Harwalkar, V.R.; Kalab, M. (1997): Molecular and Microstructural Studies of Thermal Denaturation and Gelation of  $\beta$ -Lactoglobulins A

- and B. *Journal of Agricultural and Food Chemistry*. 45 (5): 1608–1618 DOI: 10.1021/jf960622x.
- Brand, J.; Pichler, M.; Kulozik, U. (2014): Enabling egg white protein fractionation processes by pre-treatment with high-pressure homogenization. *Journal of Food Engineering*. 132: 48–54 DOI: 10.1016/j.jfoodeng.2014.02.012.
- Branden, C.I.; Tooze, J. (2012): *Introduction to Protein Structure*: CRC Press ISBN: 9781136969898.
- Broersen, K.; Van Teeffelen, Annemarie M. M.; Vries, A.; Voragen, A.G.J.; Hamer, R.J.; De Jongh, Harmen H. J. (2006): Do Sulfhydryl Groups Affect Aggregation and Gelation Properties of Ovalbumin? *Journal of Agricultural and Food Chemistry*. 54 (14): 5166–5174 DOI: 10.1021/jf0601923.
- Buck, M. (1998): Trifluoroethanol and colleagues. *Quarterly Reviews of Biophysics*. 31 (3): 297–355.
- Bushell, G.C.; Yan, Y.D.; Woodfield, D.; Raper, J.; Amal, R. (2002): On techniques for the measurement of the mass fractal dimension of aggregates. *Advances in Colloid and Interface Science*. 95 (1): 1–50 DOI: 10.1016/S0001-8686(00)00078-6.
- Cairolì, S.; Iametti, S.; Bonomi, F. (1994): Reversible and irreversible modifications of  $\beta$ -lactoglobulin upon exposure to heat. *Journal of Protein Chemistry*. 13 (3): 347–354 DOI: 10.1007/BF01901568.
- Carrotta, R.; Bauer, R.; Waninge, R.; Rischel, C. (2001): Conformational characterization of oligomeric intermediates and aggregates in beta-lactoglobulin heat aggregation. *Protein Science*. 10 (7): 1312–1318 DOI: 10.1110/ps.42501.
- Chen, D.; Zhu, X.; Ilavsky, J.; Whitmer, T.; Hatzakis, E.; Jones, O.G.; Campanella, O.H. (2021): Polyphenols Weaken Pea Protein Gel by Formation of Large Aggregates with Diminished Noncovalent Interactions. *Biomacromolecules*. 22 (2): 1001–1014 DOI: 10.1021/acs.biomac.0c01753.
- Chihi, M.-L.; Mession, J.-L.; Sok, N.; Saurel, R. (2016): Heat-Induced Soluble Protein Aggregates from Mixed Pea Globulins and  $\beta$ -Lactoglobulin. *Journal of Agricultural and Food Chemistry*. 64 (13): 2780–2791 DOI: 10.1021/acs.jafc.6b00087.
- Clark, A.H.; Kavanagh, G.M.; Ross-Murphy, S.B. (2001): Globular protein gelation—theory and experiment. *Food Hydrocolloids*. 15 (4-6): 383–400 DOI: 10.1016/S0268-005X(01)00042-X.
- Cleland, W.W. (1964): Dithiothreitol, a New Protective Reagent for SH Groups. *Biochemistry*. 3: 480–482 DOI: 10.1021/bi00892a002.

- Cochereau, R.; Nicolai, T.; Chassenieux, C.; Silva, J.V. (2019): Mechanism of the spontaneous formation of plant protein microcapsules in aqueous solution. *Colloids and Surfaces A: Physicochemical and Engineering Aspects*. 562: 213–219 DOI: 10.1016/j.colsurfa.2018.11.019.
- Comfort, S.; Howell, N.K. (2002): Gelation properties of soya and whey protein isolate mixtures. *Food Hydrocolloids*. 16 (6): 661–672 DOI: 10.1016/S0268-005X(02)00033-4.
- Creusot, N.; Wierenga, P.A.; Laus, M.C.; Giuseppin, M.L.F.; Gruppen, H. (2011): Rheological properties of patatin gels compared with  $\beta$  - lactoglobulin, ovalbumin, and glycinin. *Journal of the Science of Food and Agriculture*. 91 (2): 253 – 261 DOI: 10.1002/jsfa.4178.
- Croguennec, T.; O’Kennedy, B.T.; Mehra, R. (2004): Heat-induced denaturation/aggregation of  $\beta$ -lactoglobulin A and B: kinetics of the first intermediates formed. *International Dairy Journal*. 14 (5): 399–409 DOI: 10.1016/j.idairyj.2003.09.005.
- Dachmann, E.; Nobis, V.; Kulozik, U.; Dombrowski, J. (2020): Surface and foaming properties of potato proteins: Impact of protein concentration, pH value and ionic strength. *Food Hydrocolloids*. 107: 105981 DOI: 10.1016/j.foodhyd.2020.105981.
- Delahaije, R.J.B.M.; Gruppen, H.; van Eijk Boxtel, E.L.; Cornacchia, L.; Wierenga, P.A. (2016): Controlling the Ratio between Native-Like, Non-Native-Like, and Aggregated  $\beta$ -Lactoglobulin after Heat Treatment. *Journal of Agricultural and Food Chemistry*. 64 (21): 4362–4370 DOI: 10.1021/acs.jafc.6b00816.
- Delahaije, R.J.B.M.; Wierenga, P.A.; Giuseppin, M.L.F.; Gruppen, H. (2014): Improved emulsion stability by succinylation of patatin is caused by partial unfolding rather than charge effects. *Journal of colloid and interface science*. 430: 69–77 DOI: 10.1016/j.jcis.2014.05.019.
- Delahaije, R.J.B.M.; Wierenga, P.A.; Giuseppin, M.L.F.; Gruppen, H. (2015): Comparison of heat-induced aggregation of globular proteins. *Journal of Agricultural and Food Chemistry*. 63 (21): 5257–5265 DOI: 10.1021/acs.jafc.5b00927.
- Delahaije, R.J.B.M.; Wierenga, P.A.; van Nieuwenhuijzen, N.H.; Giuseppin, M.L.F.; Gruppen, H. (2013): Protein concentration and protein-exposed hydrophobicity as dominant parameters determining the flocculation of protein-stabilized oil-in-water emulsions. *Langmuir : the ACS journal of surfaces and colloids*. 29 (37): 11567–11574 DOI: 10.1021/la401314a.
- Dill, K.A. (1999): Polymer principles and protein folding. *Protein science : a publication of the Protein Society*. 8 (6): 1166–1180 DOI: 10.1110/ps.8.6.1166.

- Dissanayake, M.; Ramchandran, L.; Piyadasa, C.; Vasiljevic, T. (2013): Influence of heat and pH on structure and conformation of whey proteins. *International Dairy Journal*. 28 (2): 56–61 DOI: 10.1016/j.idairyj.2012.08.014.
- Dombrowski, J.; Gschwendtner, M.; Kulozik, U. (2017): Evaluation of structural characteristics determining surface and foaming properties of  $\beta$ -lactoglobulin aggregates. *Colloids and Surfaces A: Physicochemical and Engineering Aspects*. 516: 286–295 DOI: 10.1016/j.colsurfa.2016.12.045.
- Donato, L.; Kolodziejczyk, E.; Rouvet, M. (2011): Mixtures of whey protein microgels and soluble aggregates as building blocks to control rheology and structure of acid induced cold-set gels. *Food Hydrocolloids*. 25 (4): 734–742 DOI: 10.1016/j.foodhyd.2010.08.020.
- Donato, L.; Schmitt, C.; Bovetto, L.; Rouvet, M. (2009): Mechanism of formation of stable heat-induced  $\beta$ -lactoglobulin microgels. *International Dairy Journal*. 19 (5): 295–306 DOI: 10.1016/j.idairyj.2008.11.005.
- Dufour, E.; Bertrand-Harb, C.; Haertlé, T. (1993): Reversible effects of medium dielectric constant on structural transformation of beta-lactoglobulin and its retinol binding. *Biopolymers*. 33 (4): 589–598 DOI: 10.1002/bip.360330408.
- Dufour, E.; Haertlé, T. (1990): Alcohol-induced changes of beta-lactoglobulin-retinol-binding stoichiometry. *Protein engineering*. 4 (2): 185–190 DOI: 10.1093/protein/4.2.185.
- Durand, D.; Christophe Gimel, J.; Nicolai, T. (2002): Aggregation, gelation and phase separation of heat denatured globular proteins. *Physica A: Statistical Mechanics and its Applications*. 304 (1-2): 253–265 DOI: 10.1016/S0378-4371(01)00514-3.
- Dyson, J.H.; Wright, P.E.; Scheraga, H.A. (2006): The role of hydrophobic interactions in initiation and propagation of protein folding. *Proceedings of the National Academy of Sciences*. 103 (35): 13057–13061 DOI: 10.1073/pnas.0605504103.
- Egelanddal, B.; Fretheim, K.; Harbitz, O. (1986): Dynamic rheological measurements on heat-induced myosin gels: An evaluation of the method's suitability for the filamentous gels. *Journal of the Science of Food and Agriculture*. 37 (9): 944–954 DOI: 10.1002/jsfa.2740370916.
- Elgar, D.F.; Norris, C.S.; Ayers, J.S.; Pritchard, M.; Otter, D.E.; Palmano, K.P. (2000): Simultaneous separation and quantitation of the major bovine whey proteins including proteose peptone and caseinomacropeptide by reversed-phase high-performance liquid chromatography on polystyrene–divinylbenzene. *Journal of Chromatography A*. 878 (2): 183–196 DOI: 10.1016/S0021-9673(00)00288-0.

- Estévez, N.; Fuciños, P.; Bargiela, V.; Pastrana, L.; Tovar, C.A.; Luisa Rúa, M. (2016): Structural and thermo-rheological analysis of solutions and gels of a  $\beta$ -lactoglobulin fraction isolated from bovine whey. *Food chemistry*. 198: 45–53 DOI: 10.1016/j.foodchem.2015.11.090.
- Euston, S.R. (2013): Molecular dynamics simulation of the effect of heat on the conformation of bovine  $\beta$ -lactoglobulin A. *Food Hydrocolloids*. 30 (2): 519–530 DOI: 10.1016/j.foodhyd.2012.07.016.
- Fayaz, G.; Calligaris, S.; Nicoli, M.C. (2020): Comparative Study on the Ability of Different Oleogelators to Structure Sunflower Oil. *Food Biophysics*. 15 (1): 42–49 DOI: 10.1007/s11483-019-09597-9.
- Felix, M.; Perez-Puyana, V.; Romero, A.; Guerrero, A. (2017): Development of thermally processed bioactive pea protein gels: Evaluation of mechanical and antioxidant properties. *Food and Bioproducts Processing*. 101: 74–83 DOI: 10.1016/j.fbp.2016.10.013.
- Feynman, R.P.; Leighton, R.B.; Sands, M. (1965): The Feynman Lectures on Physics; Vol. I. *American Journal of Physics*. 33 (9): 750–752 DOI: 10.1119/1.1972241.
- Foegeding, A.E.; Bowland, E.L.; Hardin, C.C. (1995): Factors that determine the fracture properties and microstructure of globular protein gels. *Food Hydrocolloids*. 9 (4): 237–249 DOI: 10.1016/S0268-005X(09)80254-3.
- Foegeding, E.A. (2006): Food Biophysics of Protein Gels: A Challenge of Nano and Macroscopic Proportions. *Food Biophysics*. 1 (1): 41–50 DOI: 10.1007/s11483-005-9003-y.
- Gimel, J.C.; Durand, D.; Nicolai, T. (1994): Structure and distribution of aggregates formed after heat-induced denaturation of globular proteins. *Macromolecules*. 27 (2): 583–589 DOI: 10.1021/ma00080a037.
- Gómez-Guillén, M.C.; Borderías, A.J.; Montero, P. (1997): Chemical Interactions of Nonmuscle Proteins in the Network of Sardine (*Sardina pilchardus*) Muscle Gels. *LWT - Food Science and Technology*. 30 (6): 602–608 DOI: 10.1006/fstl.1997.0239.
- Gosal, W.S.; Clark, A.H.; Ross-Murphy, S.B. (2004a): Fibrillar beta-lactoglobulin gels Part 1. Fibril formation and structure. *Biomacromolecules*. 5 (6): 2408–2419 DOI: 10.1021/bm049659d.
- Gosal, W.S.; Clark, A.H.; Ross-Murphy, S.B. (2004b): Fibrillar beta-lactoglobulin gels Part 2. Dynamic mechanical characterization of heat-set systems. *Biomacromolecules*. 5 (6): 2420–2429 DOI: 10.1021/bm049660c.

- Gulzar, M.; Bouhallab, S.; Jeantet, R.; Schuck, P.; Croguennec, T. (2011): Influence of pH on the dry heat-induced denaturation/aggregation of whey proteins. *Food chemistry*. 129 (1): 110–116 DOI: 10.1016/j.foodchem.2011.04.037.
- Gurikov, P.; Subrahmanyam, R.; Griffin, J.S.; Steiner, S.A.; Smirnova, I. (2019): 110th Anniversary: Solvent Exchange in the Processing of Biopolymer Aerogels: Current Status and Open Questions. *Industrial & Engineering Chemistry Research*. 58 (40): 18590–18600 DOI: 10.1021/acs.iecr.9b02967.
- Hacohen, N.; Ip, C.J.X.; Gordon, R. (2018): Analysis of Egg White Protein Composition with Double Nanohole Optical Tweezers. *ACS Omega*. 3 (5): 5266–5272 DOI: 10.1021/acsomega.8b00651.
- Handa, A.; Takashi, K.; Kuroda, N.; Froning, G.W. (1998): Heat-induced Egg White Gels as Affected by pH. *Journal of Food Science*. 63 (3): 403–407 DOI: 10.1111/j.1365-2621.1998.tb15752.x.
- Haug, I.J.; Skar, H.M.; Vegarud, G.E.; Langsrud, T.; Draget, K.I. (2009): Electrostatic effects on  $\beta$ -lactoglobulin transitions during heat denaturation as studied by differential scanning calorimetry. *Food Hydrocolloids*. 23 (8): 2287–2293 DOI: 10.1016/j.foodhyd.2009.06.006.
- Havea, P.; Watkinson, P.; Kuhn-Sherlock, B. (2009): Heat-induced whey protein gels: protein-protein interactions and functional properties. *Journal of Agricultural and Food Chemistry*. 57 (4): 1506–1512 DOI: 10.1021/jf802559z.
- Hines, M.E.; Foegeding, A.E. (1993): Interactions of alpha-lactalbumin and bovine serum albumin with beta-lactoglobulin in thermally induced gelation. *Journal of Agricultural and Food Chemistry*. 41 (3): 341–346.
- Hoffmann, M.A.M.; van Mil, P.J.J.M. (1997): Heat-Induced Aggregation of  $\beta$ -Lactoglobulin: Role of the Free Thiol Group and Disulfide Bonds. *Journal of Agricultural and Food Chemistry*. 45 (8): 2942–2948 DOI: 10.1021/jf960789q.
- Homer, S.; Lundin, L.; Dunstan, D.E. (2018): A detailed investigation of whey protein isolate solutions and gels reveals a number of novel characteristics. *Food Hydrocolloids*. 77: 566–576 DOI: 10.1016/j.foodhyd.2017.10.035.
- Hua, Y.; Cui, S.W.; Wang, Q.; Mine, Y.; Poysa, V. (2005): Heat induced gelling properties of soy protein isolates prepared from different defatted soybean flours. *Food Research International*. 38 (4): 377–385 DOI: 10.1016/j.foodres.2004.10.006.
- Hyun, K.; Wilhelm, M.; Klein, C.O.; Cho, K.S.; Nam, J.G.; Ahn, K.H.; Lee, S.J.; Ewoldt, R.H.; McKinley, G.H. (2011): A review of nonlinear oscillatory shear tests: Analysis and application of large amplitude oscillatory shear (LAOS). *Progress in Polymer Science*. 36 (12): 1697–1753 DOI: 10.1016/j.progpolymsci.2011.02.002.

- Iametti, S.; Beatrice De Gregori; Giuseppe Vecchio; Bonomi, F. (1996): Modifications Occur at Different Structural Levels During the Heat Denaturation of  $\beta$  - Lactoglobulin. *European Journal of Biochemistry*. 237 (1): 106 – 112 DOI: 10.1111/j.1432-1033.1996.0106n.x.
- Job, N.; Théry, A.; Pirard, R.; Marien, J.; Kocon, L.; Rouzaud, J.-N.; Béguin, F.; Pirard, J.-P. (2005): Carbon aerogels, cryogels and xerogels: Influence of the drying method on the textural properties of porous carbon materials. *Carbon*. 43 (12): 2481–2494 DOI: 10.1016/j.carbon.2005.04.031.
- Jongsma, M.A.; Bolter, C. (1997): The adaptation of insects to plant protease inhibitors. *Journal of Insect Physiology*. 43 (10): 885–895 DOI: 10.1016/S0022-1910(97)00040-1.
- Jose, J.; Pouvreau, L.; Martin, A.H. (2016): Mixing whey and soy proteins: Consequences for the gel mechanical response and water holding. *Food Hydrocolloids*. 60: 216–224 DOI: 10.1016/j.foodhyd.2016.03.031.
- Judy, E.; Kishore, N. (2019): A look back at the molten globule state of proteins: thermodynamic aspects. *Biophysical Reviews*. 11 (3): 365–375 DOI: 10.1007/s12551-019-00527-0.
- Jung, J.-M.; Savin, G.; Pouzot, M.; Schmitt, C.; Mezzenga, R. (2008): Structure of heat-induced beta-lactoglobulin aggregates and their complexes with sodium-dodecyl sulfate. *Biomacromolecules*. 9 (9): 2477–2486 DOI: 10.1021/bm800502j.
- Kato, A.; Matsuda, T.; Matsudomi, N.; Kobayashi, K. (1984): Determination of protein hydrophobicity using sodium dodecyl sulfate binding method. *Journal of Agricultural and Food Chemistry*. 32 (2): 284–288 DOI: 10.1021/jf00122a027.
- Katzav, H.; Chirug, L.; Okun, Z.; Davidovich-Pinhas, M.; Shpigelman, A. (2020): Comparison of Thermal and High-Pressure Gelation of Potato Protein Isolates. *Foods*. 9 (8): 1041 DOI: 10.3390/foods9081041.
- Kavanagh, G.M.; Clark, A.H.; Ross-Murphy, S.B. (2000): Heat-Induced Gelation of Globular Proteins: 4. Gelation Kinetics of Low pH  $\beta$ -Lactoglobulin Gels. *Langmuir*. 16 (24): 9584–9594 DOI: 10.1021/la0004698.
- Keim, S. (2004): Hydrostatisch, thermisch, säure- und labinduzierte Casein- und Molkenprotein-Gele. Dissertation: Universität Hohenheim ISBN: 978-3-8322-4645-7:
- Keim, S.; Hinrichs, J. (2004): Influence of stabilizing bonds on the texture properties of high-pressure-induced whey protein gels. *International Dairy Journal*. 14 (4): 355–363 DOI: 10.1016/j.idairyj.2003.10.010.



- Keim, S.; Kulozik, U.; Hinrichs, J. (2006): Texture and stabilizing bonds in pressure-induced, heat-induced and rennet-induced milk protein gels. *Milchwissenschaft*. 61 (4): 363–366.
- Kleemann, C. (2021): Aerogels as a carrier system for sensitive substances - Protein based microcapsules with extreme inner adsorptive surfaces. Dissertation. München: Technische Universität München ISBN: 978-3843947879:
- Kleemann, C.; Schuster, R.; Rosenecker, E.; Selmer, I.; Smirnova, I.; Kulozik, U. (2020a): In-vitro-digestion and swelling kinetics of whey protein, egg white protein and sodium caseinate aerogels. *Food Hydrocolloids*. 101: 105534 DOI: 10.1016/j.foodhyd.2019.105534.
- Kleemann, C.; Selmer, I.; Smirnova, I.; Kulozik, U. (2018): Tailor made protein based aerogel particles from egg white protein, whey protein isolate and sodium caseinate. *Food Hydrocolloids*. 83: 365–374 DOI: 10.1016/j.foodhyd.2018.05.021.
- Kleemann, C.; Zink, J.; Selmer, I.; Smirnova, I.; Kulozik, U. (2020b): Effect of Ethanol on the Textural Properties of Whey Protein and Egg White Protein Hydrogels during Water-Ethanol Solvent Exchange. *Molecules*. 25 (19): 4417 DOI: 10.3390/molecules25194417.
- Kronberg, B. (2016): The hydrophobic effect. *Current Opinion in Colloid & Interface Science*. 22: 14–22 DOI: 10.1016/j.cocis.2016.02.001.
- Kurz, F.; Hengst, C.; Kulozik, U. (2020): RP-HPLC method for simultaneous quantification of free and total thiol groups in native and heat aggregated whey proteins. *MethodsX*: 101112 DOI: 10.1016/j.mex.2020.101112.
- Kurz, F.; Reitberger, V.; Hengst, C.; Bilke-Krause, C.; Kulozik, U.; Dombrowski, J. (2021): Correlation between Physico-Chemical Characteristics of Particulated  $\beta$ -Lactoglobulin and Its Behavior at Air/Water and Oil/Water Interfaces. *Foods*. 10 (6): 1426 DOI: 10.3390/foods10061426.
- Lan, H.; Liu, H.; Ye, Y.; Yin, Z. (2020): The Role of Surface Properties on Protein Aggregation Behavior in Aqueous Solution of Different pH Values. *AAPS PharmSciTech*. 21: 1–13 DOI: 10.1208/s12249-020-01663-7.
- Langton, M.; Hermansson, A.-M. (1992): Fine-stranded and particulate gels of  $\beta$ -lactoglobulin and whey protein at varying pH. *Food Hydrocolloids*. 5 (6): 523–539 DOI: 10.1016/S0268-005X(09)80122-7.
- Le Meste, M.; Roudaut, G.; Champion, D.; Blond, G.; Simatos, D. (2006): Interaction of water with food components. *FOOD SCIENCE AND TECHNOLOGY-NEW YORK-MARCEL DEKKER*. 154: 87.

- Leeb, E.; Haller, N.; Kulozik, U. (2018): Effect of pH on the reaction mechanism of thermal denaturation and aggregation of bovine  $\beta$ -lactoglobulin. *International Dairy Journal*. 78: 103–111 DOI: 10.1016/j.idairyj.2017.09.006.
- Li-Chan, E.C.Y. (1996): Macromolecular Interactions of Food Proteins Studied by Raman Spectroscopy. In: *ACS Symposium Series*: 15–36. Washington, DC: American Chemical Society DOI: 10.1021/bk-1996-0650.ch002.
- Liu, F.; Tang, C.-H. (2014): Emulsifying Properties of Soy Protein Nanoparticles: Influence of the Protein Concentration and/or Emulsification Process. *Journal of Agricultural and Food Chemistry*. 62 (12): 2644–2654 DOI: 10.1021/jf405348k.
- Løkra, S.; Helland, M.H.; Claussen, I.C.; Egelanddal, B.; Strætkevren, K.O. (2008): Chemical characterization and functional properties of a potato protein concentrate prepared by large-scale expanded bed adsorption chromatography. *LWT - Food Science and Technology*. 41 (6): 1089–1099 DOI: 10.1016/j.lwt.2007.07.006.
- Løkra, S.; Schüller, R.B.; Egelanddal, B.; Engebretsen, B.; Strætkevren, K.O. (2009): Comparison of composition, enzyme activity and selected functional properties of potato proteins isolated from potato juice with two different expanded bed resins. *LWT - Food Science and Technology*. 42 (4): 906–913 DOI: 10.1016/j.lwt.2008.11.011.
- Løkra, S.; Strætkevren, K.O. (2009): Industrial proteins from potato juice. A review. *Food*. 3 (Special Issue 1): 88–95.
- Loveday, S.M. (2016):  $\beta$ -Lactoglobulin heat denaturation. *International Dairy Journal*. 52: 92–100 DOI: 10.1016/j.idairyj.2015.08.001.
- Loveday, S.M.; Wang, X.L.; Rao, M.A.; Anema, S.G.; Creamer, L.K.; Singh, H. (2010): Tuning the properties of  $\beta$ -lactoglobulin nanofibrils with pH, NaCl and CaCl<sub>2</sub>. *International Dairy Journal*. 20 (9): 571–579 DOI: 10.1016/j.idairyj.2010.02.014.
- Lu, T.; Li, Q.; Chen, W.; Yu, H. (2014): Composite aerogels based on dialdehyde nanocellulose and collagen for potential applications as wound dressing and tissue engineering scaffold. *Composites Science and Technology*. 94: 132–138 DOI: 10.1016/j.compscitech.2014.01.020.
- Lukesh, J.C.; Palte, M.J.; Raines, R.T. (2012): A potent, versatile disulfide-reducing agent from aspartic acid. *Journal of the American Chemical Society*. 134 (9): 4057–4059 DOI: 10.1021/ja211931f.
- Lupano, C.E. (2000): Gelation of mixed systems whey protein concentrate–gluten in acidic conditions. *Food Research International*. 33 (8): 691–696 DOI: 10.1016/S0963-9969(00)00114-9.

- Ma, Y.; Zhao, Y.; Jiang, Y.; Chi, Y. (2019): Effect of dry heating on the aggregation behaviour and aggregate morphologies of ovalbumin. *Food chemistry*. 285: 296–304 DOI: 10.1016/j.foodchem.2019.01.170.
- Mandelbrot, B.B. (1983): *The fractal geometry of nature. Updated and augmented.* New York, NY: Freeman ISBN: 0716711869.
- Mark, J.E. (1981): Rubber elasticity. *Journal of Chemical Education*. 58 (11): 898 DOI: 10.1021/ed058p898.
- Martin, A.H.; Nieuwland, M.; Jong, G.A.H. de (2014): Characterization of heat-set gels from RuBisCO in comparison to those from other proteins. *Journal of Agricultural and Food Chemistry*. 62 (44): 10783–10791 DOI: 10.1021/jf502905g.
- Mehalebi, S.; Nicolai, T.; Durand, D. (2008): The influence of electrostatic interaction on the structure and the shear modulus of heat-set globular protein gels. *Soft Matter*. 4 (4): 893 DOI: 10.1039/b718640a.
- Mehling, T.; Smirnova, I.; Guenther, U.; Neubert, R. (2009): Polysaccharide-based aerogels as drug carriers. *Journal of Non-Crystalline Solids*. 355 (50-51): 2472–2479 DOI: 10.1016/j.jnoncrysol.2009.08.038.
- Melander, W.; Horváth, C. (1977): Salt effects on hydrophobic interactions in precipitation and chromatography of proteins: An interpretation of the lyotropic series. *Archives of biochemistry and biophysics*. 183 (1): 200–215 DOI: 10.1016/0003-9861(77)90434-9.
- Mercadé-Prieto, R.; Paterson, W.R.; Wilson, D.I. (2007): The pH threshold in the dissolution of beta-lactoglobulin gels and aggregates in alkali. *Biomacromolecules*. 8 (4): 1162–1170 DOI: 10.1021/bm061100l.
- Messens, W.; van de Walle, D.; Arevalo, J.; Dewettinck, K.; Huyghebaert, A. (2000): Rheological properties of high-pressure-treated Gouda cheese. *International Dairy Journal*. 10 (5): 359–367 DOI: 10.1016/S0958-6946(00)00066-2.
- Mezger, T. (2006): *Das Rheologie-Handbuch. 2., überarb. Aufl.* Hannover: Vincentz Network ISBN: 3-87870-175-6.
- Monahan, F.J.; German, J.B.; Kinsella, J.E. (1995): Effect of pH and temperature on protein unfolding and thiol/disulfide interchange reactions during heat-induced gelation of whey proteins. *Journal of Agricultural and Food Chemistry*. 43 (1): 46–52.
- Mounsey, J.S.; O’Kennedy, B.T. (2007): Conditions limiting the influence of thiol–disulphide interchange reactions on the heat-induced aggregation kinetics of  $\beta$ -lactoglobulin. *International Dairy Journal*. 17 (9): 1034–1042 DOI: 10.1016/j.idairyj.2006.12.008.

- Mulcahy, E.M.; Fargier-Lagrange, M.; Mulvihill, D.M.; O'Mahony, J.A. (2017): Characterisation of heat-induced protein aggregation in whey protein isolate and the influence of aggregation on the availability of amino groups as measured by the ortho-phthaldialdehyde (OPA) and trinitrobenzenesulfonic acid (TNBS) methods. *Food chemistry*. 229: 66–74 DOI: 10.1016/j.foodchem.2017.01.155.
- Nakai, S. (1988): *Hydrophobic interactions in food systems*. Boca Ratin, FL: CRC Press ISBN: 1351090216.
- Nicolai, T. (2019): Gelation of food protein-protein mixtures. *Advances in Colloid and Interface Science*. 270: 147–164 DOI: 10.1016/j.cis.2019.06.006.
- Nicolai, T.; Britten, M.; Schmitt, C. (2011):  $\beta$ -Lactoglobulin and WPI aggregates. *Food Hydrocolloids*. 25 (8): 1945–1962 DOI: 10.1016/j.foodhyd.2011.02.006.
- Nicolai, T.; Chassenieux, C. (2019): Heat-induced gelation of plant globulins. *Current Opinion in Food Science* DOI: 10.1016/j.cofs.2019.04.005.
- Nicolai, T.; Durand, D. (2007): Protein aggregation and gel formation studied with scattering methods and computer simulations. *Current Opinion in Colloid & Interface Science*. 12 (1): 23–28 DOI: 10.1016/j.cocis.2007.03.002.
- Nicolai, T.; Durand, D. (2013): Controlled food protein aggregation for new functionality. *Current Opinion in Colloid & Interface Science*. 18 (4): 249–256 DOI: 10.1016/j.cocis.2013.03.001.
- Nikolaidis, A.; Andreadis, M.; Moschakis, T. (2017): Effect of heat, pH, ultrasonication and ethanol on the denaturation of whey protein isolate using a newly developed approach in the analysis of difference-UV spectra. *Food chemistry*. 232: 425–433 DOI: 10.1016/j.foodchem.2017.04.022.
- Nikolaidis, A.; Moschakis, T. (2018): On the reversibility of ethanol-induced whey protein denaturation. *Food Hydrocolloids* DOI: 10.1016/j.foodhyd.2018.05.051.
- Okur, H.I.; Hladílková, J.; Rembert, K.B.; Cho, Y.; Heyda, J.; Dzubiella, J.; Cremer, P.S.; Jungwirth, P. (2017): Beyond the Hofmeister Series: Ion-Specific Effects on Proteins and Their Biological Functions. *The journal of physical chemistry. B*. 121 (9): 1997–2014 DOI: 10.1021/acs.jpcc.6b10797.
- Paulsson, M.; Hegg, P.-O.; Castberg, H.B. (1985): Thermal stability of whey proteins studied by differential scanning calorimetry. *Thermochimica Acta*. 95 (2): 435–440 DOI: 10.1016/0040-6031(85)85308-9.
- Pike, A.C.W.; Brew, K.; Acharya, K.R. (1996): Crystal structures of guinea-pig, goat and bovine  $\alpha$ -lactalbumin highlight the enhanced conformational flexibility of regions that are significant for its action in lactose synthase. *Structure*. 4 (6): 691–703 DOI: 10.1016/S0969-2126(96)00075-5.

- Plazzotta, S.; Calligaris, S.; Manzocco, L. (2020): Structural characterization of oleogels from whey protein aerogel particles. *Food Research International*. 132: 109099 DOI: 10.1016/j.foodres.2020.109099.
- Pots, A.M.; Grotenhuis, E. ten; Gruppen, H.; Voragen, A.G.J.; Kruif, K.G. de (1999a): Thermal Aggregation of Patatin Studied in Situ. *Journal of Agricultural and Food Chemistry*. 47 (11): 4600–4605 DOI: 10.1021/jf9901901.
- Pots, A.M.; Gruppen, H.; Hessing, M.; van Boekel, M.A.; Voragen, A.G. (1999b): Isolation and characterization of patatin isoforms. *Journal of Agricultural and Food Chemistry*. 47 (11): 4587–4592 DOI: 10.1021/jf981180n.
- Pots, A.M.; Gruppen, H.; Jongh, H.H.J. de; van Boekel, M.A.J.S.; Walstra, P.; Voragen, A.G.J. (1999c): Kinetic Modeling of the Thermal Aggregation of Patatin. *Journal of Agricultural and Food Chemistry*. 47 (11): 4593–4599 DOI: 10.1021/jf990191t.
- Pots, A.M.; Jongh, H.H.J. de; Gruppen, H.; Hamer, R.J.; Voragen, A.G.J. (1998a): Heat-induced conformational changes of patatin, the major potato tuber protein. *European Journal of Biochemistry*. 252 (1): 66–72 DOI: 10.1046/j.1432-1327.1998.2520066.x.
- Pots, A.M.; Jongh, H.H.J. de; Gruppen, H.; Hessing, M.; Voragen, A.G.J. (1998b): The pH Dependence of the Structural Stability of Patatin. *Journal of Agricultural and Food Chemistry*. 46 (7): 2546–2553 DOI: 10.1021/jf980034e.
- Pouvreau, L.; Gruppen, H.; Piersma, S.R.; van den Broek, L.A.M.; van Koningsveld, G.A.; Voragen, A.G.J. (2001): Relative Abundance and Inhibitory Distribution of Protease Inhibitors in Potato Juice from cv. Elkana. *Journal of Agricultural and Food Chemistry*. 49 (6): 2864–2874 DOI: 10.1021/jf010126v.
- Pouvreau, L.; Gruppen, H.; van Koningsveld, G.; van den Broek, L.A.M.; Voragen, A.G.J. (2005a): Conformational stability of the potato serine protease inhibitor group. *Journal of Agricultural and Food Chemistry*. 53 (8): 3191–3196 DOI: 10.1021/jf048353v.
- Pouvreau, L.; Kroef, T.; Gruppen, H.; van Koningsveld, G.; van den Broek, L.A.M.; Voragen, A.G.J. (2005b): Structure and stability of the potato cysteine protease inhibitor group (cv. Elkana). *Journal of Agricultural and Food Chemistry*. 53 (14): 5739–5746 DOI: 10.1021/jf050306v.
- Qi, X.L.; Holt, C.; McNulty, D.; Clarke, D.T.; Brownlow, S.; Jones, G.R. (1997): Effect of temperature on the secondary structure of  $\beta$ -lactoglobulin at pH 6.7, as determined by CD and IR spectroscopy. *Biochemical Journal*. 324 (1): 341–346 DOI: 10.1042/bj3240341.

- Qin, B.Y.; Bewley, M.C.; Creamer, L.K.; Baker, H.M.; Baker, E.N.; Jameson, G.B. (1998): Structural Basis of the Tanford Transition of Bovine  $\beta$ -Lactoglobulin. *Biochemistry*. 37 (40): 14014–14023 DOI: 10.1021/bi981016t.
- Racusen, D.; Foote, M. (1980): A major soluble Glycoprotein of potato tubers. *Journal of Food Biochemistry*. 4 (1): 43–52 DOI: 10.1111/j.1745-4514.1980.tb00876.x.
- Racusen, D.; Weller, D.L. (1984): Molecular weight of Patatin, a major potato tuber protein. *Journal of Food Biochemistry*. 8 (2): 103–107 DOI: 10.1111/j.1745-4514.1984.tb00318.x.
- Ralet, M.-C.; Guéguen, J. (2000): Fractionation of Potato Proteins. *LWT - Food Science and Technology*. 33 (5): 380–387 DOI: 10.1006/fstl.2000.0672.
- Rasheed, F.; Markgren, J.; Hedenqvist, M.; Johansson, E. (2020): Modeling to Understand Plant Protein Structure-Function Relationships-Implications for Seed Storage Proteins. *Molecules (Basel, Switzerland)*. 25 (4): 873 DOI: 10.3390/molecules25040873.
- Reithel, F.J.; Kelly, M.J. (1971): Thermodynamic analysis of the monomer-dimer association of  $\beta$ -lactoglobulin A at the isoelectric point. *Biochemistry*. 10 (13): 2639–2644.
- Relkin, P.; Eynard, L.; Launay, B. (1992): Thermodynamic parameters of  $\beta$ -lactoglobulin and  $\alpha$ -lactalbumin. A DSC study of denaturation by heating. *Thermochimica Acta*. 204 (1): 111–121 DOI: 10.1016/0040-6031(92)80320-V.
- Renard, D.; Lefebvre, J.; Robert, P.; Llamas, G.; Dufour, E. (1999): Structural investigation of  $\beta$ -lactoglobulin gelation in ethanol/water solutions. *International Journal of Biological Macromolecules*. 26 (1): 35–44 DOI: 10.1016/S0141-8130(99)00060-4.
- Reynolds, J.A.; Tanford, C. (1970): Binding of dodecyl sulfate to proteins at high binding ratios. Possible implications for the state of proteins in biological membranes. *Proceedings of the National Academy of Sciences of the United States of America*. 66 (3): 1002–1007 DOI: 10.1073/pnas.66.3.1002.
- Reynolds, J.G.; Coronado, P.R.; Hrubesh, L.W. (2001): Hydrophobic aerogels for oil-spill clean up – synthesis and characterization. *Journal of Non-Crystalline Solids*. 292 (1-3): 127–137 DOI: 10.1016/S0022-3093(01)00882-1.
- Richard, D.; Hallett, J.; Speck, T.; Royall, C.P. (2018): Coupling between criticality and gelation in "sticky" spheres: a structural analysis. *Soft Matter*. 14 (27): 5554–5564 DOI: 10.1039/C8SM00389K.

- Roefs, S.P.; Kruif, K.G. de (1994): A model for the denaturation and aggregation of  $\beta$  - lactoglobulin. *European Journal of Biochemistry*. 226 (3): 883 – 889 DOI: 10.1111/j.1432-1033.1994.00883.x.
- Roesch, R.R.; Corredig, M. (2005): Heat-induced soy-whey proteins interactions: formation of soluble and insoluble protein complexes. *Journal of Agricultural and Food Chemistry*. 53 (9): 3476–3482 DOI: 10.1021/jf048870d.
- Rombouts, I.; Lagrain, B.; Brunnbauer, M.; Koehler, P.; Brijs, K.; Delcour, J.A. (2011): Identification of Isopeptide Bonds in Heat-Treated Wheat Gluten Peptides. *Journal of Agricultural and Food Chemistry*. 59 (4): 1236–1243 DOI: 10.1021/jf103579u.
- Ruan, Q.; Chen, Y.; Kong, X.; Hua, Y. (2014): Heat-induced aggregation and sulphhydryl/disulphide reaction products of soy protein with different sulphhydryl contents. *Food chemistry*. 156: 14–22 DOI: 10.1016/j.foodchem.2014.01.083.
- Rydel, T.J.; Williams, J.M.; Krieger, E.; Moshiri, F.; Stallings, W.C.; Brown, S.M.; Pershing, J.C.; Purcell, J.P.; Alibhai, M.F. (2003): The crystal structure, mutagenesis, and activity studies reveal that patatin is a lipid acyl hydrolase with a Ser-Asp catalytic dyad. *Biochemistry*. 42 (22): 6696–6708 DOI: 10.1021/bi027156r.
- Sarkar, A.; Horne, D.S.; Singh, H. (2010): Interactions of milk protein-stabilized oil-in-water emulsions with bile salts in a simulated upper intestinal model. *Food Hydrocolloids*. 24 (2-3): 142–151 DOI: 10.1016/j.foodhyd.2009.08.012.
- Sava, N.; van der Plancken, I.; Claeys, W.; Hendrickx, M. (2005): The Kinetics of Heat-Induced Structural Changes of  $\beta$ -Lactoglobulin. *Journal of Dairy Science*. 88 (5): 1646–1653 DOI: 10.3168/jds.S0022-0302(05)72836-8.
- Schmidt, J.M.; Damgaard, H.; Greve-Poulsen, M.; Larsen, L.B.; Hammershøj, M. (2018): Foam and emulsion properties of potato protein isolate and purified fractions. *Food Hydrocolloids*. 74: 367–378 DOI: 10.1016/j.foodhyd.2017.07.032.
- Schmidt, J.M.; Damgaard, H.; Greve-Poulsen, M.; Sunds, A.V.; Larsen, L.B.; Hammershøj, M. (2019): Gel properties of potato protein and the isolated fractions of patatins and protease inhibitors – Impact of drying method, protein concentration, pH and ionic strength. *Food Hydrocolloids*. 96: 246–258 DOI: 10.1016/j.foodhyd.2019.05.022.
- Schokker, E.P.; Singh, H.; Creamer, L.K. (2000): Heat-induced aggregation of  $\beta$ -lactoglobulin A and B with  $\alpha$ -lactalbumin. *International Dairy Journal*. 10 (12): 843–853 DOI: 10.1016/S0958-6946(01)00022-X.
- Selmer, I.; Karnetzke, J.; Kleemann, C.; Lehtonen, M.; Mikkonen, K.S.; Kulozik, U.; Smirnova, I. (2019): Encapsulation of fish oil in protein aerogel micro-particles. *Journal of Food Engineering*. 260: 1–11 DOI: 10.1016/j.jfoodeng.2019.04.016.

- Selmer, I.; Kleemann, C.; Kulozik, U.; Heinrich, S.; Smirnova, I. (2015): Development of egg white protein aerogels as new matrix material for microencapsulation in food. *The Journal of Supercritical Fluids*. 106: 42–49 DOI: 10.1016/j.supflu.2015.05.023.
- Shih, W.-H.; Shih, W.Y.; Kim, S.-I.; Liu, J.; Aksay, I.A. (1990): Scaling behavior of the elastic properties of colloidal gels. *Physical Review A*. 42 (8): 4772–4779 DOI: 10.1103/PhysRevA.42.4772.
- Shimada, K.; Cheftel, J.C. (1988): Texture characteristics, protein solubility, and sulfhydryl group/disulfide bond contents of heat-induced gels of whey protein isolate. *Journal of Agricultural and Food Chemistry*. 36 (5): 1018–1025 DOI: 10.1021/jf00083a029.
- Shimada, K.; Cheftel, J.C. (1989): Sulfhydryl group/disulfide bond interchange reactions during heat-induced gelation of whey protein isolate. *Journal of Agricultural and Food Chemistry*. 37 (1): 161–168 DOI: 10.1021/jf00085a038.
- Shivu, B.; Seshadri, S.; Li, J.; Oberg, K.A.; Uversky, V.N.; Fink, A.L. (2013): Distinct  $\beta$ -sheet structure in protein aggregates determined by ATR-FTIR spectroscopy. *Biochemistry*. 52 (31): 5176–5183 DOI: 10.1021/bi400625v.
- Singh, J.; Kaur, L. (2016): *Advances in Potato Chemistry and Technology*. 2nd ed. s.l.: Elsevier Science ISBN: 9780128000021.
- Smirnova, I.; Gurikov, P. (2018): Aerogel production: Current status, research directions, and future opportunities. *The Journal of Supercritical Fluids*. 134: 228–233 DOI: 10.1016/j.supflu.2017.12.037.
- Stading, M.; Hermansson, A.-M. (1990): Viscoelastic behaviour of  $\beta$ -lactoglobulin gel structures. *Food Hydrocolloids*. 4 (2): 121–135 DOI: 10.1016/S0268-005X(09)80013-1.
- Stergar, J.; Maver, U. (2016): Review of aerogel-based materials in biomedical applications. *Journal of Sol-Gel Science and Technology*. 77 (3): 738–752 DOI: 10.1007/s10971-016-3968-5.
- Subrahmanyam, R.; Gurikov, P.; Dieringer, P.; Sun, M.; Smirnova, I. (2015): On the Road to Biopolymer Aerogels—Dealing with the Solvent. *Gels*. 1 (2): 291–313 DOI: 10.3390/gels1020291.
- Sun, X.D.; Arntfield, S.D. (2012): Molecular forces involved in heat-induced pea protein gelation: Effects of various reagents on the rheological properties of salt-extracted pea protein gels. *Food Hydrocolloids*. 28 (2): 325–332 DOI: 10.1016/j.foodhyd.2011.12.014.



- Takenaka, O.; Aizawa, S.; Tamaura, Y.; Hirano, J.; Inada, Y. (1972): Sodium dodecyl sulfate and hydrophobic regions in bovine serum albumin. *Biochimica et Biophysica Acta (BBA) - Protein Structure*. 263 (3): 696–703 DOI: 10.1016/0005-2795(72)90053-0.
- Takeshita, S.; Sadeghpour, A.; Malfait, W.J.; Konishi, A.; Otake, K.; Yoda, S. (2019): Formation of Nanofibrous Structure in Biopolymer Aerogel during Supercritical CO<sub>2</sub> Processing: The Case of Chitosan Aerogel. *Biomacromolecules*. 20 (5): 2051–2057 DOI: 10.1021/acs.biomac.9b00246.
- Tanford, C. (1968): Protein Denaturation. In: Anfinsen, C. B.; Anson, M. L.; Edsall, John T.; Richards, Frederic M., (Hrsg.). *Advances in Protein Chemistry*: 121–282: Academic Press DOI: 10.1016/S0065-3233(08)60401-5.
- Tanger, C.; Andlinger, D.; Brümmer-Rolf, A.; Engel, J.; Kulozik, U. (2021a): Quantification of protein-protein interactions in highly denatured whey and potato protein gels. *MethodsX*: 101243 DOI: 10.1016/j.mex.2021.101243.
- Tanger, C.; Engel, J.; Kulozik, U. (2020): Influence of extraction conditions on the conformational alteration of pea protein extracted from pea flour. *Food Hydrocolloids*. 107: 105949 DOI: 10.1016/j.foodhyd.2020.105949.
- Tanger, C.; Müller, M.; Andlinger, D.; Kulozik, U. (2021b): Influence of pH and ionic strength on the thermal gelation behaviour of pea protein. *Food Hydrocolloids*: 106903 DOI: 10.1016/j.foodhyd.2021.106903.
- Tanger, C.; Quintana Ramos, P.; Kulozik, U. (2021c): Comparative Assessment of Thermal Aggregation of Whey, Potato, and Pea Protein under Shear Stress for Microparticulation. *ACS Food Science & Technology* DOI: 10.1021/acsfoodscitech.1c00104.
- Tolkach, A.; Kulozik, U. (2007): Reaction kinetic pathway of reversible and irreversible thermal denaturation of  $\beta$ -lactoglobulin. *Le Lait*. 87 (4-5): 301–315 DOI: 10.1051/lait:2007012.
- Toro Sierra, J.P. (2016): On the separation, thermal and shear induced modification, and study of the functional properties of the major whey protein fractions.
- Udabage, P.; McKinnon, I.R.; Augustin, M.-A. (2000): Mineral and casein equilibria in milk: effects of added salts and calcium-chelating agents. *Journal of Dairy Research*. 67 (3): 361–370 DOI: 10.1017/S0022029900004271.
- Urbonaite, V.; van der Kaaij, S.; Jongh, H. de; Scholten, E.; Ako, K.; van der Linden, E.; Pouvreau, L. (2016): Relation between gel stiffness and water holding for coarse and fine-stranded protein gels. *Food Hydrocolloids*. 56: 334–343 DOI: 10.1016/j.foodhyd.2015.12.011.

- Uversky, V.N.; Narizhneva, N.V.; Kirschstein, S.O.; Winter, S.; Löber, G. (1997): Conformational transitions provoked by organic solvents in  $\beta$ -lactoglobulin. *Folding and Design*. 2 (3): 163–172 DOI: 10.1016/S1359-0278(97)00023-0.
- van Boekel, M. (1996): Statistical Aspects of Kinetic Modeling for Food Science Problems. *Journal of Food Science*. 61 (3): 477–486 DOI: 10.1111/j.1365-2621.1996.tb13138.x.
- van den Akker, C.C.; Engel, M.F.M.; Velikov, K.P.; Bonn, M.; Koenderink, G.H. (2011): Morphology and persistence length of amyloid fibrils are correlated to peptide molecular structure. *Journal of the American Chemical Society*. 133 (45): 18030–18033 DOI: 10.1021/ja206513r.
- Venkatesan, J.; Bhatnagar, I.; Manivasagan, P.; Kang, K.-H.; Kim, S.-K. (2015): Alginate composites for bone tissue engineering. *International Journal of Biological Macromolecules*. 72: 269–281 DOI: 10.1016/j.ijbiomac.2014.07.008.
- Vogtt, K.; Javid, N.; Alvarez, E.; Sefcik, J.; Bellissent-Funel, M.-C. (2011): Tracing nucleation pathways in protein aggregation by using small angle scattering methods. *Soft Matter*. 7 (8): 3906 DOI: 10.1039/c0sm00978d.
- Vries, A. de; Gomez, Y.L.; van der Linden, E.; Scholten, E. (2017): The effect of oil type on network formation by protein aggregates into oleogels. *RSC Advances*. 7 (19): 11803–11812 DOI: 10.1039/C7RA00396J.
- Vries, A. de; Hendriks, J.; van der Linden, E.; Scholten, E. (2015): Protein Oleogels from Protein Hydrogels via a Stepwise Solvent Exchange Route. *Langmuir : the ACS journal of surfaces and colloids*. 31 (51): 13850–13859 DOI: 10.1021/acs.langmuir.5b03993.
- Waglay, A.; Karboune, S.; Alli, I. (2014): Potato protein isolates: recovery and characterization of their properties. *Food chemistry*. 142: 373–382 DOI: 10.1016/j.foodchem.2013.07.060.
- Wagner, J.; Andreadis, M.; Nikolaidis, A.; Biliaderis, C.G.; Moschakis, T. (2020a): Effect of ethanol on the microstructure and rheological properties of whey proteins: acid-induced cold gelation. *LWT*: 110518 DOI: 10.1016/j.lwt.2020.110518.
- Wagner, J.; Biliaderis, C.G.; Moschakis, T. (2020b): Whey proteins: Musings on denaturation, aggregate formation and gelation. *Critical reviews in food science and nutrition*: 1–14 DOI: 10.1080/10408398.2019.1708263.
- Weijers, M.; van de Velde, F.; Stijnman, A.; van de Pijpekamp, A.; Visschers, R.W. (2006): Structure and rheological properties of acid-induced egg white protein gels. *Food Hydrocolloids*. 20 (2-3): 146–159 DOI: 10.1016/j.foodhyd.2005.02.013.

- Weitz; Huang; Lin; Sung (1985): Limits of the fractal dimension for irreversible kinetic aggregation of gold colloids. *Physical review letters*. 54 (13): 1416–1419 DOI: 10.1103/PhysRevLett.54.1416.
- Wensien, M.; Pappenheim, F.R. von; Funk, L.-M.; Kloskowski, P.; Curth, U.; Diederichsen, U.; Uranga, J.; Ye, J.; Fang, P.; Pan, K.-T.; Urlaub, H.; Mata, R.A.; Sautner, V.; Tittmann, K. (2021): A lysine-cysteine redox switch with an NOS bridge regulates enzyme function. *Nature*. 593 (7859): 460–464 DOI: 10.1038/s41586-021-03513-3.
- Wolz, M.; Kulozik, U. (2017): System parameters in a high moisture extrusion process for microparticulation of whey proteins. *Journal of Food Engineering*. 209: 12–17 DOI: 10.1016/j.jfoodeng.2017.04.010.
- Wu, C.; Hua, Y.; Chen, Y.; Kong, X.; Zhang, C. (2017): Effect of temperature, ionic strength and 11S ratio on the rheological properties of heat-induced soy protein gels in relation to network proteins content and aggregates size. *Food Hydrocolloids*. 66: 389–395 DOI: 10.1016/j.foodhyd.2016.12.007.
- Wu, H.; Morbidelli, M. (2001): A Model Relating Structure of Colloidal Gels to Their Elastic Properties. *Langmuir*. 17 (4): 1030–1036 DOI: 10.1021/la001121f.
- Xiong, Y.L.; Dawson, K.A.; Wan, L. (1993): Thermal Aggregation of  $\beta$ -Lactoglobulin: Effect of pH, Ionic Environment, and Thiol Reagent<sup>1</sup>. *Journal of Dairy Science*. 76 (1): 70–77 DOI: 10.3168/jds.S0022-0302(93)77324-5.
- Yan, Y.; Seeman, D.; Zheng, B.; Kizilay, E.; Xu, Y.; Dubin, P.L. (2013): pH-Dependent aggregation and disaggregation of native  $\beta$ -lactoglobulin in low salt. *Langmuir : the ACS journal of surfaces and colloids*. 29 (14): 4584–4593 DOI: 10.1021/la400258r.
- Yokogawa, H.; Yokoyama, M. (1995): Hydrophobic silica aerogels. *Journal of Non-Crystalline Solids*. 186: 23–29 DOI: 10.1016/0022-3093(95)00086-0.
- Yoshida, K.; Fukushima, Y.; Yamaguchi, T. (2014): A study of alcohol and temperature effects on aggregation of  $\beta$ -lactoglobulin by viscosity and small-angle X-ray scattering measurements. *Journal of Molecular Liquids*. 189: 1–8 DOI: 10.1016/j.molliq.2013.06.022.
- Yoshida, K.; Yamaguchi, T.; Osaka, N.; Endo, H.; Shibayama, M. (2010): A study of alcohol-induced gelation of beta-lactoglobulin with small-angle neutron scattering, neutron spin echo, and dynamic light scattering measurements. *Physical chemistry chemical physics : PCCP*. 12 (13): 3260–3269 DOI: 10.1039/b920187d.
- Zirbel, F.; Kinsella, J.E. (1988): Effects of thiol reagents and ethanol on strength of whey protein gels. *Food Hydrocolloids*. 2 (6): 467–475 DOI: 10.1016/S0268-005X(88)80046-8.

Zúñiga, R.N.; Tolkach, A.; Kulozik, U.; Aguilera, J.M. (2010): Kinetics of formation and physicochemical characterization of thermally-induced beta-lactoglobulin aggregates. *Journal of Food Science*. 75 (5): E261-8 DOI: 10.1111/j.1750-3841.2010.01617.x.

## 7 Appendix

### 7.1 Peer reviewed publications (included in this thesis)

Andlinger, David J.; Bornkeßel, Alina Claire; Jung, Isabella; Schröter, Baldur; Smirnova, Irina; Kulozik, Ulrich (2021a): Microstructures of potato protein hydrogels and aerogels produced by thermal crosslinking and supercritical drying. In: *Food Hydrocolloids* 112, S. 106305. DOI: 10.1016/j.foodhyd.2020.106305.

Andlinger, David J.; Rampp, Lena; Tanger, Caren; Kulozik, Ulrich (2021b): Viscoelasticity and Protein Interactions of Hybrid Gels Produced from Potato and Whey Protein Isolates. In: *ACS Food Science and Technology* 1 (7), S. 1304–1315. DOI: 10.1021/acsfoodscitech.1c00163.

Andlinger, David J.; Röscheisen, Pauline; Hengst, Claudia; Kulozik, Ulrich (2021c): Influence of pH, Temperature and Protease Inhibitors on Kinetics and Mechanism of Thermally Induced Aggregation of Potato Proteins. In: *Foods* 10 (4), S. 796. DOI: 10.3390/foods10040796.

Tanger, Caren; Andlinger, David; Brümmer-Rolf, Annette; Engel, Julia; Kulozik, Ulrich (2021a): Quantification of protein-protein interactions in highly denatured whey and potato protein gels. In: *MethodsX*, S. 101243. DOI: 10.1016/j.mex.2021.101243.

Andlinger, David J.; Bornkeßel, Alina Claire; Jung, Isabella; Schröter, Baldur; Smirnova, Irina; Kulozik, Ulrich (2021d): Hydro- and aerogels from ethanolic potato and whey protein solutions: Influence of temperature and ethanol concentration on viscoelastic properties, protein interactions, and microstructure. In: *Food Hydrocolloids* (Article accepted for publication 1 Dec 2021) DOI: 10.1016/j.foodhyd.2021.107424.

Andlinger, David J.; Schrempl, Ulrich; Hengst, Claudia; Kulozik, Ulrich (2021e): Heat-induced aggregation kinetics of potato protein - Investigated by reversed phase high pressure liquid chromatography, differential scanning calorimetry, and dynamic light scattering. Submitted to *Food Chemistry* on 02.09.2021, since then under review

### 7.2 Peer reviewed publications (not included in this thesis)

Tanger, Caren; Müller, Michaela; Andlinger, David; Kulozik, Ulrich (2021b): Influence of pH and ionic strength on the thermal gelation behaviour of pea protein. In: *Food Hydrocolloids*, S. 106903. DOI: 10.1016/j.foodhyd.2021.106903.

Weinberger, Maria E.; Andlinger, David J.; Kulozik, Ulrich (2021): A novel approach for characterisation of stabilising bonds in milk protein deposit layers on microfiltration membranes. In: *International Dairy Journal* 118, S. 105044. DOI: 10.1016/j.idairyj.2021.105044.

### 7.3 Oral & poster presentations

Andlinger, D.; Kuczynski, T.; Kulozik, U.; Smirnova, I. (2018). Oral: Aerogele aus Molken- und Kartoffelprotein in Partikel und Riegelform. Sitzung des Projektbegleitenden Ausschusses des AIF/FEI– Forschungsvorhabens AIF 19712 N, Freising/Germany 19.06.2012.

Andlinger, D.; Kuczynski, T.; Kulozik, U.; Smirnova, I. (2019). Oral: Aerogele aus Molken- und Kartoffelprotein in Partikel und Riegelform. Sitzung des Projektbegleitenden Ausschusses des AIF/FEI– Forschungsvorhabens AIF 19712 N, Freising/Germany 18.06.2019.

Andlinger, D.; Kuczynski, T.; Kulozik, U.; Smirnova, I. (2019). Poster: Development of an encapsulation system based on potato and whey protein. Jahrestreffen der ProcessNet-Fachgruppe Lebensmittelverfahrenstechnik, Nestlé Research Lausanne , Switzerland, 05.-07.03.2019.

Andlinger, D.; Kuczynski, T.; Kulozik, U.; Smirnova, I. (2020). Oral: Aerogele aus Molken- und Kartoffelprotein in Partikel und Riegelform. Sitzung des Projektbegleitenden Ausschusses des AIF/FEI– Forschungsvorhabens AIF 19712 N, Freising/Germany 30.10.2020.